AN ABSTRACT OF THE DISSERTATION OF

Taylor Dylan Harry for the degree of Doctor of Philosophy in Medical Physics presented on December 6, 2019.

Title: Linking Procedural Performance with Radiobiological Analysis in Radiation Therapy.

Abstract approved:

_____

Todd S. Palmer

Radiation therapy is a sophisticated complex process. Systematic methods are needed to quantitatively evaluate the quality of a complex process and hence radiation therapy treatments. An ideal result for a complex process must be established to determine if the complex process is completed acceptably. For radiation therapy, this can be accomplished through complication free tumor control probability functions. A theoretical mathematical function can be created from a treatment plan to represent its complication free tumor control probability quantitatively by exporting Dose Volume Histograms from treatment plans to create complication free tumor control probability functions. By creating a baseline treatment plan (or assuming an ideal course of treatment), a relative comparison can be performed to assess how variations in the tasks that contribute to the treatment plan affect the complication free tumor control probability. By creating a systematic method to outline how and when all tasks are performed, variations in complication free tumor control over the entire course of treatment can be established and analyzed as to their impact on the quality of treatment.

Linking Procedural Performance with Radiobiological Analysis in Radiation Therapy

by
Taylor Dylan Harry

A DISSERTATION

submitted to

Oregon State University

in partial fulfillment of
the requirements for the
degree of

Doctor of Philosophy

Presented December 6, 2019
Commencement June 2020

Doctor of Philosophy dissertation of Taylor Dylan Harry presented on December 6, 2019.

APPROVED:

_____

Major Professor, representing Medical Physics

_____

Head of the School of Nuclear Science and Engineering

_____

Dean of the Graduate School

I understand that my dissertation will become part of the permanent collection of Oregon State University libraries. My signature below authorizes release of my thesis to any reader upon request.

_____

Taylor Dylan Harry, Author

TABLE OF CONTENTS

Page

TABLE OF CONTENTS (Continued)

Page

LIST OF FIGURES

Figure Page

LIST OF FIGURES (Continued)

Figure Page

LIST OF FIGURES (Continued)

Figure Page

LIST OF FIGURES (Continued)

Figure Page

LIST OF FIGURES (Continued)

Figure Page

LIST OF FIGURES (Continued)

Figure Page

LIST OF FIGURES (Continued)

Figure Page

LIST OF FIGURES (Continued)

Figure Page

LIST OF TABLES

Table Page

LIST OF TABLES (Continued)

Table Page

LIST OF TABLES (Continued)

Table Page

LIST OF APPENDICES

LIST OF APPENDICES FIGURES

LIST OF ABBREVEATIONS

RT	Radiation Therapy
C	Consult
S	Simulation
TP	Treatment Planning
PR	Plan Review
Tx	Treatment
CT	Computed Tomography
CBCT	Cone Beam Computer Tomography
QMP	Qualified Medical Physicist
MD	Radiation Oncologist or Physician
RTT	Radiation Therapist
CMD	Certified Medical Dosimetrist
TCP	Tumor Control Probability
NTCP	Normal Tissue Complication Probability
CFTC	Complication Free Tumor Control
PRQ	Probability of Radiotherapy Quality
TPS	Treatment Planning System
DVH	Dose Volume Histogram
PTV	Planning Target Volume
CTV	Clinical Target Volume

QA Quality Assurance

AAPM American Association of Physicists in Medicine

TG Task Group

MPPG Medical Physics Practice Guideline

IMRT Intensity Modulated Radiation Therapy

EUD Equivalent Uniform Dose

SOE Sequence of Events

SEC Sequence of Events Chain

DEDICATION

This document along with the efforts behind it are here in dedicated to the human race, whose eternal struggle for knowledge has led to unbelievable explanations for the way nature behaves and methods to manipulate it for the best interests of life. Without the questions and mistakes of past conscious beings, we would still be just a bunch of particles floating around in a gravitational field. From the first creature that realized it could control its environment to the last living thing to inhabit the known universe, I thank thee for simply being. To know that there are other conscious entities is truly magical. To be alive is simply wonderful. To understand and solve a problem is utterly divine.

1. INTRODUCTION AND THEORY

The 20th century saw medicine evolve into a sophisticated complex system[1] and as such its quality, safety and procedural management strategies evolved. Over time, healthcare and radiation therapy continue to reconsider their approaches to quality, safety and procedural management as new information is learned and new tools are developed[1–22]. While striving to improve radiotherapy practices, many deficiencies can still be found as well as new problems created with emerging techniques and technologies in its processess[2,5,13,23–25]. Strategies have been adapted from other industries and professions, protocols and standards were developed from expert consensus, requirements increased to operate a radiotherapy clinic and continuing career education implemented to help achieve these improvements. Despite these efforts, the field still lacks a tool that can track quality quantitatively throughout an entire course of treatment to aid in decision making and to ensure the best treatments are provided. Reviewing a brief history of radiation therapy provides an understanding of how todays standard treatments developed and what is considered an acceptable quality treatment.

Radiation use in medicine began quickly following its discovery[26–28]. The first applications were simple and have since expanded as knowledge increased for its effects on living cells over the past 125 years. In an ideal world only diseased cells would receive dose while all other cells receive none[27,29]. Practically speaking, however, this is impossible and all steps in the radiation therapy process work towards achieving this ideal. The first administered exposures demonstrated what came to be the major limiting factor while delivering therapeutic radiation: damage to normal tissues. Procedures began to evolve in attempts to limit the doses that normal tissues received while still administering a high enough dose to eradicate diseased cells. These methods included collimating the radiation field, increasing the number fields used to deliver radiation, fractionation or increasing the number of exposures while decreasing the dose per exposure, better identifying diseased tissue locations and pinpointing the deposition of energy as radiation traverses matter (inorganic and organic)[26,27,30,31]. Hence more techniques, equipment, and individuals were needed to fulfill these goals to improve the efforts of therapeutic radiation by minimizing patient health complications from over dosing healthy cells or under dosing diseased cells.

1.1 Treatment Courses

Understanding the progression of techniques and equipment used in radiation therapy provides valuable insight into evaluating its quality. As it evolved, the advancements in radiation medicine replicate the steps of modern-day radiotherapy procedures. First, diseases that can be treated with radiation were identified[32]. Appropriate doses to eliminate these diseases while allowing surrounding tissues to survive were established. Properly localizing diseased and healthy cells came next in order to know where the radiation had to be deposited. Adequately collimating and directing radiation beams followed to ensure proper doses were deposited in tissues[30]. Finally, mechanisms to stabilize patients and coordinate anatomical and radiation locations were developed allowing therapeutic doses to be administered. Every task performed in radiotherapy works towards the ideal of providing a prescription dose to the diseased cells while providing limited dose to healthy cells. With technological and medical advances, the means with which to achieve the above-mentioned concepts increased in complexity creating the modern-day complex process of radiation therapy. This consists of five basic steps as shown in Figure 1: Consult, Simulation, Treatment Planning, Plan Review and Treatment.

1.1.1 Consult

Step by step information is gathered to provide the necessary criteria to properly treat a disease. As more information is acquired, the parameters involved in a course of treatment are defined and adjusted to provide a better-quality treatment. First, a disease must be identified which is accomplished during Consult. With technological and medical advances, more sophisticated mechanisms were developed to understand the inherent nature of a specific individual's disease, patterns of progression, ways to treat it, and side effects that occur[32]. Diseases are labeled in stages based on size and physiological characteristics observed in the cells. Different disease labels require additional information to be gathered and different techniques to be used in order to treat the disease to best standards. The Radiation Oncologist

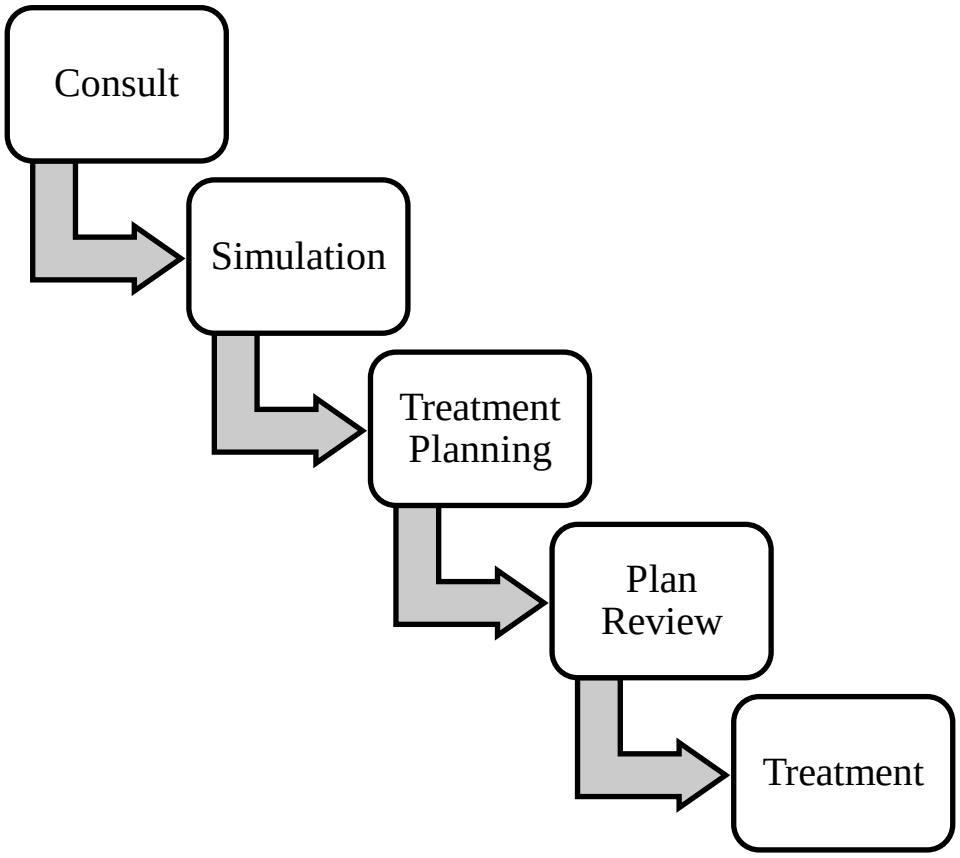

Figure 1. Flow chart for the basic steps of modern-day Radiation Therapy treatment process

uses the diagnosis, their training on the disease's behavior and progression, standard practice methods, colleague consensus, and patient conversations to move forward with a treatment by deciding the proceeding actions that must occur to eliminate diseased cells and preserve healthy cells.

1.1.2 Simulation

With a disease identified, defining its anatomical location and healthy cells location to a standardized coordinate system comes next[30]. Consider an analogy: radiation therapy is like shooting bullets at a moving target. A certain number of bullets must hit the bull's-eye. The clearer the bull's-eye and path to it are, the better chances there are to hit it. Initially, anatomical knowledge provides the information to localize the disease. For example, the lower pelvis is the region of interest for prostate cancer. Without any medical imaging a field can be focused on this area that will, without a doubt, include the entire prostate volume, but the target is very blurry. There of course are other organs in the area that must be avoided such as the bladder, rectum, and

gonads. As medical imaging advanced, a single x-ray provided 2-dimensional information that began to outline where all these organs were located allowing more clarity as to the target's location and direct paths to it. With multiple x-rays and eventually computed tomography (CT), 3-dimensonal information can be acquired allowing complete volumes of all organs in the region of interest to be determined[28,33,34]. With 3D information, all points in a medical image can be linked to a coordinate system which further clarifies the bull's-eye and allows mathematical representations of positions and path lengths to those positions that make up organs in the region of interest. Thus, if the bull's-eye or target moves around, it can be tracked with high precision and accuracy.

This of course represents the simulation portion of modern-day radiation therapy. CT scans, as well as other imaging modalities, provide volumetric information[33] to be used for defining the locations of organs and coordinating them with radiation fields to allow the proper deposition of dose. CT scans also provided electron density information that is used to calculate how radiation traverses the patient and where energy is deposited delivering dose[27,30,33]. By localizing everything to a coordinate system, positions can be replicated to clearly identify the target to ensure the radiation can hit it. Various devices are then used to aid in positioning the patient within the coordinate system and minimize movement. Replicating a given position and stabilizing the target makes it easier to shoot at. A Radiation Therapist, based on the Radiation Oncologist's directions, works to position and stabilize the patient position comfortably, produce markers and indicators for easy positional replication and acquire a CT scan to include desired organs in the image necessary to complete the remaining steps in the process.

1.1.3 Treatment Planning

Knowing what the disease is and having volumetric information to clearly locate the target and a path to it, planning how to get radiation dose to the tumor comes next. A Radiation Oncologist and Certified Medical Dosimetrist begin outlining the tumor and surrounding healthy organs on the CT scan. Sophisticated software applications then link the CT scan and these contours to a calculation engine for radiation transport. The calculation engine incorporates a model of the physical machine used to produce the radiation to estimate the dose cells would receive given set parameters[27,30,32,35]. The Dosimetrist adjusts these parameters (field sizes, beam

angles, distance to source, x-ray energy, fluence, etc.) until dosimetric constraints are achieved. The constraints have previously been determined through numerous studies over the history of radiotherapy that determined appropriate tumor prescription doses and tolerance doses for healthy organs. After many iterations of parameter adjustments, the dosimetrist and physician decide on and finalize a plan to be used to treat a particular patient where the dosimetric constraints are best met. The general descriptions of these actions are incorporated in the treatment planning portion of radiation therapy. It is here that the ideas for treating a patient become a reality as physical characteristics are established to produce a radiation dose distribution that conforms to a tumor.

1.1.4 Plan Review

Reviewing the decided upon plan comes next to ensure all aspects meet the intended goals and the treatment can be physically carried out to treat the patient with the best possible quality. A Qualified Medical Physicist performs an independent check on the majority of the parameters to be used in the treatment plan. While the main goal is to verify that dosimetric constraints are met and the physical parameters used in the production and delivery of radiation are appropriate, many documentation parameters must also be verified. Numerous interlocks exist in the devices used and non-congruent occurrences between all software and devices used through the entire process will prevent treatment. Radiation Therapists perform tasks in preparation for a treatment to confirm they have the materials needed. Similarly, Radiation Oncologists perform an independent review of the plan to form a consensus that the theoretical reasoning for a treatment is suitable for a given patient. A formal meeting exists for this purpose, but informal conversations also occur. Ideally all tasks performed up to this point in the process are reviewed and verified to allow the delivery of a plan to the highest achievable quality.

1.1.5 Treatment

With a plan developed and verified, it comes time to carry out the actions to deliver the radiation to the patient. The treatment plan, which contains imaging position techniques, is loaded onto the treatment console and machine. Next the Radiation Therapists work to help the patient lay on the treatment table and replicate the position they were in during their simulation CT scan. Various imaging techniques in the treatment room are used to align external and internal patient landmarks to match the tumor’s and radiation’s centralized point or isocenter. Radiation

Therapists, Radiation Oncologists and Qualified Medical Physicists all, at some point, verify that patient positioning and alignment are acceptable for treatment. With the patient position approved, treatment begins, and radiation is delivered. While radiation is delivered the patient is monitored to ensure there is minimal movement through the remainder of the delivery that will affect planned dose. Once the fraction's dose is delivered, the patient is helped down from the treatment table and treatment information is logged. With treatment information logged, further review is conducted to verify that the treatment is being delivered as planned for the remainder of fractions. Upon completion a final review is performed to once again verify that the treatment occurred as planned.

While this provides a brief summary of the work involved for treating a patient with radiation, details for the specific tasks all individuals perform over the entire process are cumbersome to write out with large variations (between institutions and individuals). Monitoring these tasks is a complex process with many industries supplying studies on the best methods to evaluate procedures that create these complex systems. In the modern day, quality, safety and procedural management practices help organizations achieve their goals by maximizing the quality of their products while minimizing costs (material and personal). Sophisticated outlines for the tasks involved within a complex process are developed to aid in identifying potential areas of risk to help mitigate an undesired event or product from occurring. Many fields striving to improve their quality, safety and procedural management practices have produced much in the literature[23,36–49]. An article published in 2013 discussed the lack of systematic research involved in evaluating and implementing these strategies[36]. Specifically, the article focused on a zero-accident vision strategy adopted by several companies that have achieved low rates of severe accidents or losses while achieving their goals. Challenges with current management practices, due to a lack of detailed evaluation of those strategies, lead the authors to call on the community to produce more scientific evidence to support conclusions on the successes and failures of strategies implemented. This is interesting in that organizations striving for zero accidents that have already achieved infrequent accidents recognized there was little scientific evidence to support the methods used to achieve their goals. When considering radiation therapy quality, safety and management practices, systematically understanding the many aspects that comprise a course of treatment are necessary to quantitatively evaluate the successes and failures of strategies

implemented. Reviewing complex systems and methods to evaluate them helps to understand the radiotherapy process.

1.2 Complex Systems

Complex systems arise as humanity attempts to understand and solve problems. Over time more difficult problems have been addressed with more sophisticated methods. By focusing on individual mechanisms to determine cause and effect relationships[50], science allows us to predict behavior in nature by creating laws aiding in future applications. However, these laws have constraints and one must know when and how to employ a specific law. As a system continues to include more mechanisms the laws and their constraints become distorted and adjustments must be made. An example of this can be seen from a sample problem worked in Tips On Physics: A Problem-Solving Supplement To The Feynman Lectures On Physics by Richard Feynman[51]. Here the importance of working and thinking circularly instead of linearly are emphasized.

Feynman works through a simple problem to achieve an answer. The answer acquired with universally accepted laws of physics does not match the reality of a measurement. By reevaluating the problem, Feynman shows us how the initial problem was a simplification of the physical phenomena. He then reworks the problem with an added constraint (a neglected force) achieving a different answer. This step is then repeated multiple times until the theoretical answer "matches" the actual measurement. Each time the problem was worked previous information that was neglected, or unknown prior, was then used to produce a more exact answer. Furthermore, constraints that were used in the initial problem changed as more information was incorporated into later problems. This underlines the behavior of modern complex systems: each time a problem is worked information may or may not be included, which then varies the constraints that are used. Consequently, the detail desired by the observer dictates the degree to which the outcome of theoretical predictions is contrary to physical measurements.

Knowing when and which laws and constraints to use is crucial to achieve a complete quantitative evaluation of a complex system and problem. Weinberg created three categories for the types of complex systems that can exist or develop: Organized Simplicity, Unorganized Complexity, and Organized Complexity[50] as seen in Figure 2. Organized Simplicity and Unorganized Complexity include systems with very few or an extremely large number of

components. Here measurements provide results that are close to predicted values. Modern human systems fall into the organized complexity category. Here systems are “too complex for analysis and too organized for statistics”. These systems follow what Weinberg defines as the law of medium numbers in which large fluctuations, irregularities and discrepancies with any theory occur regularly when attempting to analyze the system in question. These systems include exceptions to the laws and constraints that are currently used to evaluate system behavior. To provide a systematic evaluation of a system, one must be able to account for large fluctuations, irregularities and discrepancies within the context of the laws and constraints established.

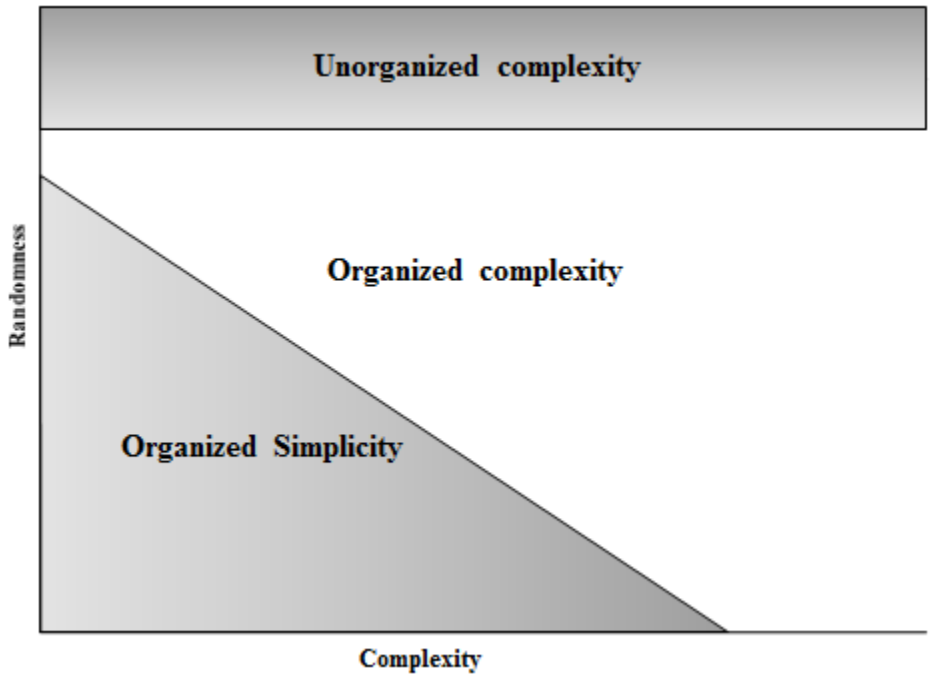

Figure 2. Weinberg’s graph for the types of systems that can exist as complexity and randomness increase in complex systems

Quality, safety and procedural management evaluations have come to include the development of process maps and diagrams, mathematical calculations from physical measurements, and philosophies for relationships between the two to help understand how the many aspects involved in a process help achieve the ideal goal. Two of the more prominent philosophies are Heinrich’s domino model[43] and Reason’s swiss cheese model[44]. The ideas of a root cause event responsible for an undesired result and subsequent probabilistic calculation of their occurrence can be found in a vast majority of evaluations. With these, focus is placed on

individual events leading to deficiencies in factors related to component relationships and human interactions as described by Leveson[45]. Capturing these individual events and understanding cause and effect relationships between them allow the complete evaluation of a complex system.

1.2.1 Control Loops

Leveson proposed representing component functions, relationships and human interactions for a process visually through engineering control loop diagrams[45]. A manual process consists of an operator or controller, the controls or equipment used and display or feedback mechanisms for the process. The operator uses controls to perform a process and receives feedback thru display mechanisms to gauge how the process is progressing. For an automated process an extra component is added or a device that now performs tasks humans would have previously performed. The device, or an actuator, performs the task mechanically, electromechanically or computationally via hardware and software. This device has its own sensors to relay feedback for its performance. Figure 3 displays two simple control loops for a manual and automated process.

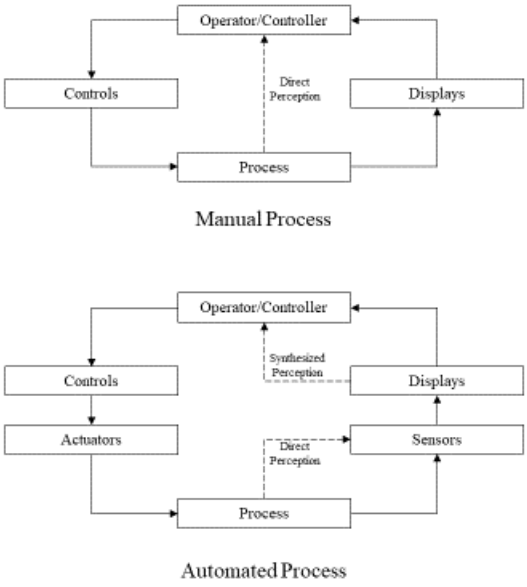

Figure 3. Simple control loops for a manual and automated process. For the manual process the operator's physical senses provide feedback for how the process is progressing, or direct perception. In the automated process all feedback is dependent on a mechanical or electromechanical system to provide feedback, or synthesized perception.

An example in radiation therapy would be the positioning of the linac treatment couch. Manually, a Radiation Therapist (operator) presses the unlock switch on the couch allowing it to be manually pushed (controls) into a desired position (process). Monitors display translational positions of the couch; the Radiation Therapist can visually see the position of the couch and feel resistance as they move the couch into position (displays). An automated approach includes a mechanical system that physically moves the couch by pressing buttons. Here the Therapist pushes a button to move the couch in a desired direction. The physical aspect has been removed and is now reliant on the mechanical system. Some physical senses of the operator have also been removed and accurate information about how the process is progressing is provided by the automated system.

While completing a process, control loops help describe the actions taken and the order in which they occur. Details can be documented based on the operator, controls and sensory information used to complete a given process or task. As processes become more complex, additional operators, controls, and sensory displays are incorporated creating sub-processes which in themselves are considered complex processes. This creates control loops inside of control loops, or descriptive mechanisms for specific tasks within generalized tasks. An overall complex process is broken down into multiple sub-processes necessitating multiple control loops to describe the various functions, relationships and interactions that take place. As complexity increases results of sub-processes rely on results from other sub-processes even though there may never be direct interaction. Here hierarchal levels help maintain organization as process complexity increases.

1.2.2 Process Hierarchy

Using a top-down approach, generalized tasks are first defined that must be performed in order to achieve the goal of the complex process. A control loop can be generated for each generalized task that is defined. This establishes the first hierarchal level for radiotherapy, where the basic steps are defined necessary to achieve the goal of the complex process. For radiotherapy and this study these are defined as Consult, Simulation, Treatment Planning, Plan Review and Treatment (as described earlier). At this level the generalized tasks include all individuals, equipment and steps involved without specific information as to how they are performed. The second hierarchal level defines the basic steps needed to complete the generalized tasks in the

previous level, once again with each one generating an additional control loop. This begins to outline the individuals involved in each generalized task and provide more descriptive actions that are performed to complete the higher-level tasks. Further decompressing the tasks individuals perform begins to outline the specific protocols for equipment used during tasks capturing information about the progression of actions with the actuators and sensors involved. At some point, enough hierarchal levels are defined to include all actions that can occur during the complex process. This allows a complete sequence of events to be documented describing and linking all actions and the individuals that perform them to the first hierarchal level of tasks.

Processes are designed to operate in a specific manner with a chronological order in which tasks are to be completed creating an ideal process progression. If one can document all actions that occur during a process, these actions can be compared to the ideal process operation to identify deviations that cause an undesired final product. These deviations include any chronological differences as well as any variation in the quality for the performance of each task leading to a sub-quality product. This information allows evaluations of how and when mistakes occur and their effect on the overall quality. Additional steps are generally put into place to ensure processes operate as intended and indicators provided to identify if an undesired event occurs requiring a form of intervention to take place. Ideally an evaluation system can monitor in real time the process operations to provide feedback on how and why a task is sub-optimal so the issues can be addressed and normal operations resumed.

1.2.3 Complex System Evaluations

Evaluations of processes rely on analytical reduction techniques to organize large systems into distinct components or subsystems for independent analysis[45,50,52]. Typically, general evaluations are all that is needed or desired for routine and general operations and only in special circumstances do evaluations begin to address the specifics causing an undesired event. As sequences of events take place chronologically, the overall quality of the final product of the process fluctuates[53]. If the ideal final product is represented by 100% quality, any point in time during the sequence of events represents a percentage of that quality. A simple example would be an equally weighted interpretation where when half of the process's tasks are completed ideally the quality of the overall product is 50%. Metrics that are collected, or could be collected, during

a process can be represented as terms in an equation for the quality of the product. With the process maps mentioned earlier and the interactions of all components (material and human), sequences of events can be generated describing what took or takes place and linked to a quantitative representation of the goals or the quality of a process at any given time.

The constraints imposed on a process verify that the process is progressing acceptably or that the terms in the equation provide the correct result[45,52]. These include safety constraints to ensure individuals are not harmed during the process and quality constraints to minimize physical, temporal and economic losses. Taguchi demonstrated that not completing procedural tasks to 100% quality can affect the overall outcome regardless of the variation accepted for satisfying the constraints[53]. Understanding global and local effects in the overall process is necessary as not all events have a large global component. In other words, each task has a component that can affect the quality at that particular event and the overall quality of the process. Accounting for exceptions means having the ability to calculate the effect the exception has both locally and globally. Identifying when and how non-ideal completion of procedural tasks occur during operation and whether they are acceptable for achieving the complex process's goals contributes to understanding what the true quality of the final product is at any given point in time.

Theoretically, a mathematical function exists that represents the level of quality vs. time for a process. As each task is performed the quality of the product ideally increases with the completion of the final task resulting in 100% quality. This function is comprised of the components and operations involved which includes the individuals, task performance, task importance, previous task dependencies and time. For radiotherapy this includes all the steps and tasks involved in the generalized tasks outlined. As each task is completed the treatment plan parameters incrementally close in on their ideals. All these tasks in some manner work towards achieving the ideal dose for each cell (healthy cells receiving no dose while diseased cells receiving the prescription dose), properly localizing each cell in the radiation field to receive that planned dose or a combination of the two.

1.2.4 Evaluating Radiation Therapy

Essentially all tasks are linked to the quality of a treatment plan by their contribution to the dosimetric and geometric components of the ideal plan. As the tasks for radiotherapy progress the

radiation field is adjusted and conforms to the diseased cells, or tissue, while avoiding healthy tissues and tissues are localized to the radiations coordinate system. While it is difficult to demonstrate exactly how every task contributes to these components mathematically, hypothetical examples do provide valuable information. As tasks are completed, tissues are more clearly defined and localized to the radiation field coordinate system and the size and shape of the radiation field conforms better to the diseased tissue. In terms of a treatment plan, this means more beam angles are being added, field collimation is shrinking to fit the diseased tissue, and the diseased tissues isocenter is better aligned with the radiation field isocenter so, as radiation transverses matter, proper dose is deposited in the diseased tissue. The dose deposited to all tissues can then be used to calculate the quality of the radiotherapy process.

Dosimetric and radiobiological analysis has aided in determining how radiation can be used to eliminate diseased cells while allowing healthy cells to survive[29]. Theoretically, the effect radiation has on diseased cells and healthy cells are represented via Tumor Control Probabilities (TCPs) and Normal Tissue Complication Probabilities (NTCPs). This is coordinated with the volumes of cells receiving doses. With advancements in technology, the TCPs and NTCPs can be constructed from treatment planning systems with low costs (physical and temporal)[54] where diseased and healthy cells equate to the tissues contoured for a given treatment plan. These methods relate dose-volume data with control and complication probabilities. Ideally tumor cells (or the voxels containing tumor cells) receive the prescription dose while healthy cells (or voxels containing healthy cells) receive no dose. Realistically all cells receive dose and the amount of dose each cell receives impacts the calculation of the TCP and NTCP functions. A theoretical function can be calculated for a course of treatment corresponding to TCPs and NTCPs generated from treatment planning systems (TPS) in the form of Complication Free Tumor Control (CFTC) probabilities. CFTC can then represent a probability of radiotherapy quality (PRQ) and used to define the ideal goal for the Radiation Therapy complex process.

With the ability to create a function for the quality of a treatment based on the ideal dose tissues receive, a benchmark can be set to compare non-ideal plans to. With the knowledge that all tasks relate to the dosimetric and geometric components, non-ideal plans can be created by varying the dosimetric and geometric parameters of a treatment plan. Working backward, starting from the

completion of the last task, each previous task should have a slight deviation from the ideal plan's dosimetric and/or geometric components. Treatment plans can be created for these slight deviations and a quality function generated for each. Continuing back to the beginning of the process, quality functions can be created for each task and the rise in quality over time for the entire process can be determined. The goal of this work is to develop relationships for the rise in quality to the tasks outlined over the course of the radiotherapy process.

1.3 Research Objectives

The first objective for this work is to investigate how incremental variations of geometric and dosimetric parameters alter the complication free tumor control probabilistic functions from an ideal treatment plan. This phase will contain the majority of this thesis. All tasks in the course of a radiotherapy treatment work towards either: adjusting the locations and borders of delineated structures to more accurately and precisely define diseased and healthy tissues, adjusting radiation field collimation and entrance angles to better conform to the defined diseased tissue while avoiding defined healthy tissues, or ensuring acceptable doses are delivered to diseased and healthy tissues. Geometric parameters encompass tasks involved with establishing the specific location of all tissues with relation to the radiation isocenter as well as determining ideal radiation field sizes and angles. Dosimetric parameters encompass tasks involved to deliver prescription doses to the diseased tissue while minimizing doses to healthy tissue. Due to the nature of radiation the two are heavily coupled as geometric variations alter dose based on scatter and beam penetration.

The second objective for this work is to estimate a possible quality vs. time plot based on how geometric and dosimetric treatment parameters approach their ideal values as tasks are completed. This portion of the thesis is a proof of concept due to the large number of variations that can occur while performing tasks, the numerous interpretations of how geometric and dosimetric parameters can be impacted and the large number of hypothetical scenarios generated to produce deviations. This objective serves as nothing more than a demonstration that realistic estimates of quality vs. time can be generated and supported with reasonable logic. It builds the framework for future work to be considering given the results of this dissertation.

2. METHODS

An assumption will be made that a previously treated patient's plan was ideal consisting of ideal treatment parameters (contours, field collimation, patient setup, etc) leading to an ideal course of treatment. Thus, all information that was gathered or reviewed was 100% accurate and all tasks performed by all individuals during the course of treatment were completed perfectly. It will be shown that a single function can be generated for a given treatment plan based on dosimetric data. With an ideal plan carried out to perfection and a corresponding function, relative comparisons can be made to functions generated from non-ideal plans and/or performances. Non-ideal functions for plans and treatments can be hypothetically generated by varying the treatment parameters from the ideal plan. This allows a relative quantitative assessment for the quality of treatments that could occur due to variations from uncertainties and sub-par task performance.

2.1 Probability of Radiotherapy Quality

Treatment planning systems (TPS) have been used routinely for several decades now (commercial and institutionally developed)[35]. The TPS calculation of the dose a voxel receives is coordinated with anatomical structures delineated to determine acceptable treatment plans. This information can be exported in the form of Dose Volume Histograms (DVH) to be used for dosimetric and subsequent radiobiological analysis using TCP and NTCPs for a given treatment plan. Over time treatment techniques have changed and these changes can be used to demonstrate how complication free tumor control probability and the probability of radiotherapy quality are affected due to different courses of treatment using modern TPS data. For example, the treatment for prostate cancer transitioned from a 3D conformal 4-field box method to a multiple field Intensity Modulated Radiation Therapy (IMRT) technique and eventually to volume modulated arc therapy.

2.1.1 PRQ Parameters

Using the method provided by Gay *et al.*[54], MATLAB code was created to generate TCP and NTCPs for prostate cancer patients based on DVHs from the TPS using Eclipse version 13 (Varian Inc.). Delineated structures for prostate treatments included the prostate CTV (TCP), bladder, and rectum (NTCPs). Femoral heads were used in the initial modality example but were excluded for the remainder of the work due to low doses they receive in IMRT treatment plans. The radiobiological parameters used for calculations are displayed in Table 1.

Table 1. Radiobiological parameters for prostate CTV TCP, bladder, and rectum NTCPs.

	Radiobiological Parameters				
	a	γ_{50}	TCD_{50}	TD_{50}	α/β
Prostate	-10	1.5	65	–	1.5
Rectum	11.11	3.1	–	76.9	3
Bladder	2	3.6	–	80	3

γ_{50} is a structure model parameter relating to the slope of the complication probability vs. dose-response curve, TCD_{50} and TD_{50} are the tolerance doses for a 50% control or complication rate, α/β is the alpha beta ratio where components of the linear and quadratic portion of the curve are equal, and *a* is a structure model parameter for the volume dependence of the complication probability[29,55–57]. Prostate CTV parameters were selected to conservatively represent low to intermediate risk patients[58–60]. Bladder parameters were determined based on evaluation of the QUNATEC organ specific publication and Burmans analysis[57,61]. Rectum parameters were selected based on the QUANTEC organ specific publication[62].

Equivalent Uniform Dose (EUD) was calculated using equation 1 where v_i is the partial volume that receives dose D_i.

$$EUD = [\sum_{i=1}(v_i D_i^a)]^{1/a} \quad (eq\ 1)$$

TCP and NTCPs were calculated using the calculated EUD with equations 2 and 3:

$$TCP = [1 + (TCD_{50}/EUD)^{4\gamma 50}]^{-1} \quad (eq\ 2)$$

$$NTCP = [1 + (TD_{50}/EUD)^{4\gamma 50}]^{-1} \quad (eq\ 3)$$

20 patients were selected that completed treatment for prostate cancer using an IMRT technique. For each patient, a 3D conformal 4-field box plan was created using Anterior, Posterior, Right and Left Lateral fields for the same structures used with the IMRT plans. The planning followed normal clinical routines and was approved by treating physicians (assuming they would treat with the 4-field plans). DVHs for all patients and plans were exported for offline analysis with the created MATLAB code. Subsequent TCPs and NTCPs were calculated for all patients and delineated structures.

From the TCP and NTCPs, a function was generated to represent the probability of radiotherapy quality for a planned course treatment based on complication free tumor control probabilities[56,63] using equation 4:

$$PRQ = TCP \cdot \prod_i (1 - NTCP_i) \ (eq\ 4)$$

This has been described as a complication free tumor control probability (P+) but for this study will represent the plan quality achievable (aka PRQ)[56,63]. It is assumed that a complication free tumor control probability becomes a PRQ when it is associated with a specific scenario or circumstance. This provides a single quantitative function to represent treatment plans. While it is recognized that more information is needed as to the physical meaning of this function and appropriate use for clinical purposes, it does provide a relative measure to assess cause and effect relationships between variations in treatment plans. Specifically, Boyer used a version of complication free tumor control probability in the late 80's to understand how uncertainties in the treatment process could affect treatment outcomes[63]. This demonstrates its ability to be used to understand quantitatively how treatment outcomes vary under specified circumstances.

2.1.2 Modality Example

The PRQs for the IMRT plans were averaged and the same was done for the 3D conformal plans. The PRQ functions for both are plotted with the complication free tumor control probability (%) on the y-axis and the percentage of the prescription dose on the x-axis as seen in Figure 4.

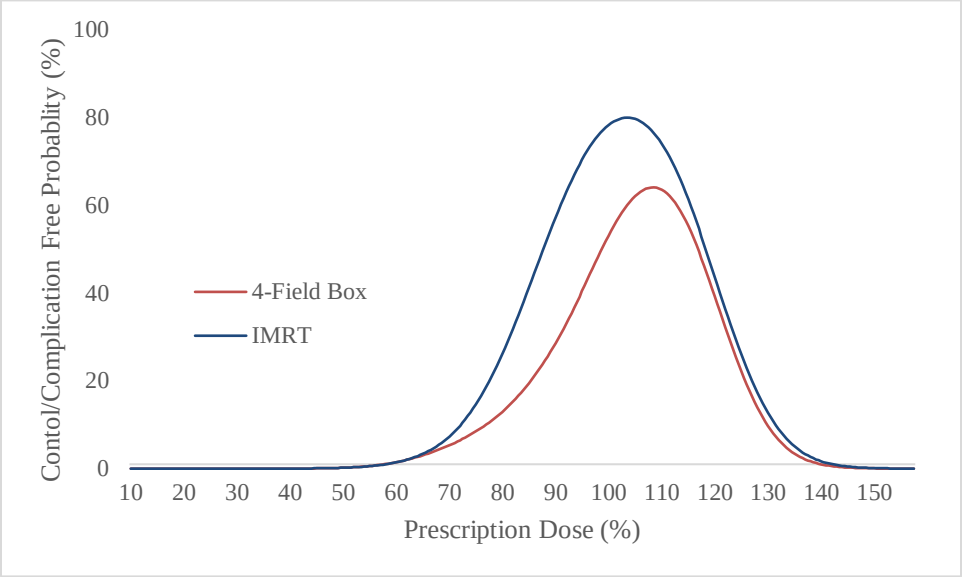

Figure 4. Probability of Radiotherapy Quality between IMRT and 4 field box techniques plotted against a percentage of the prescription dose

To further demonstrate the difference between the treatment techniques Figure 5 displays the TCP, NTCPs and PRQs for each technique with Figure 6 displaying the dose distributions. The differences between the two techniques are easily visualized in these three figures. The peak of the PRQ represents an optimal point where the TCP is maximized and the NTCPs are minimized. The reason for this is the variation of the dose distributions between the techniques. The TCP and NTCPs sigmoidal curves are closer for the 4-field box technique as the normal tissues receive higher doses resulting in a higher complication possibility. A subtle difference in the slope of the curves can also be seen when comparing the two treatment techniques. As the TCP or NTCPs are altered for any reason a unique PRQ can be generated due to the change in dose tissues or voxels receive.

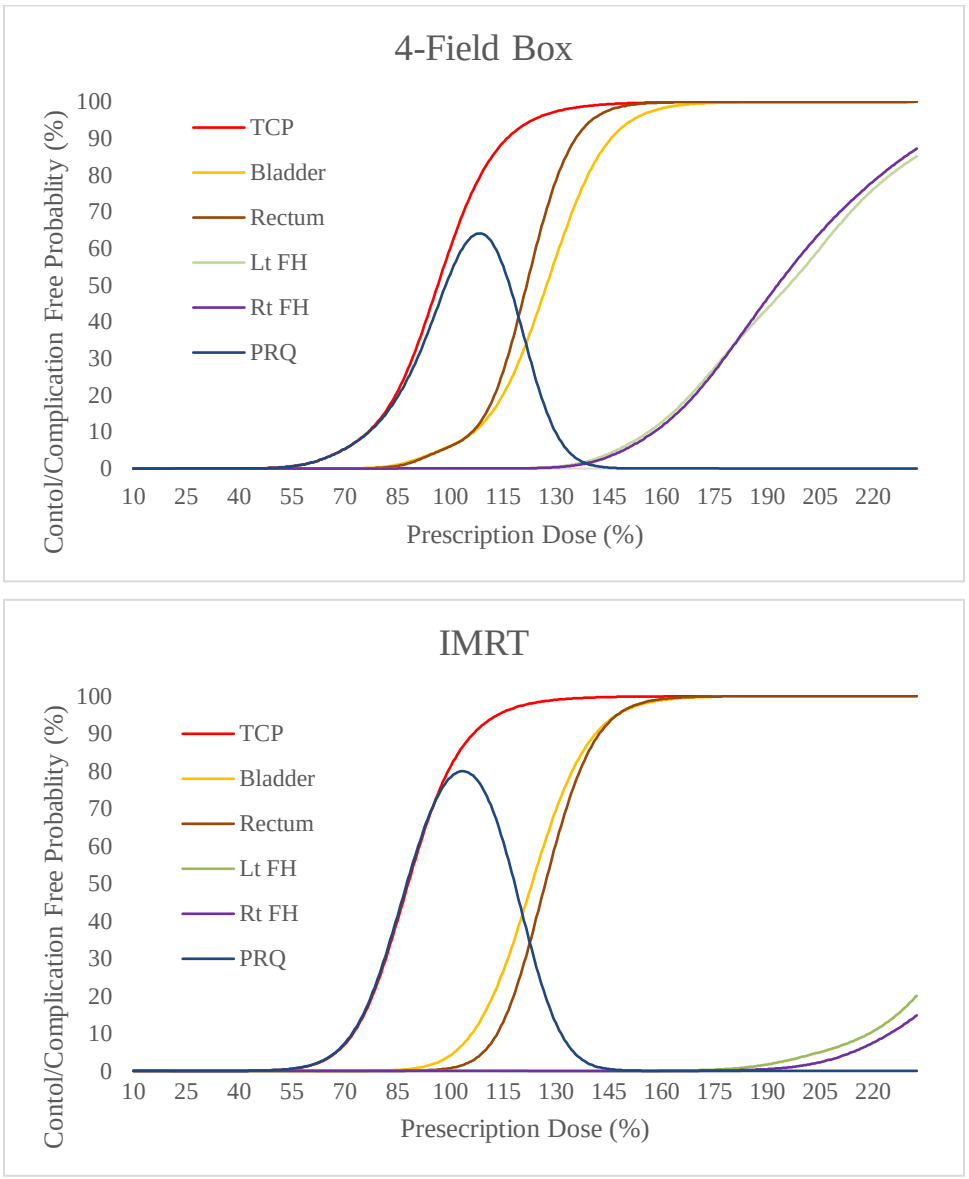

Figure 5. The TCP, NTCPs and PRQs for the two treatment techniques.

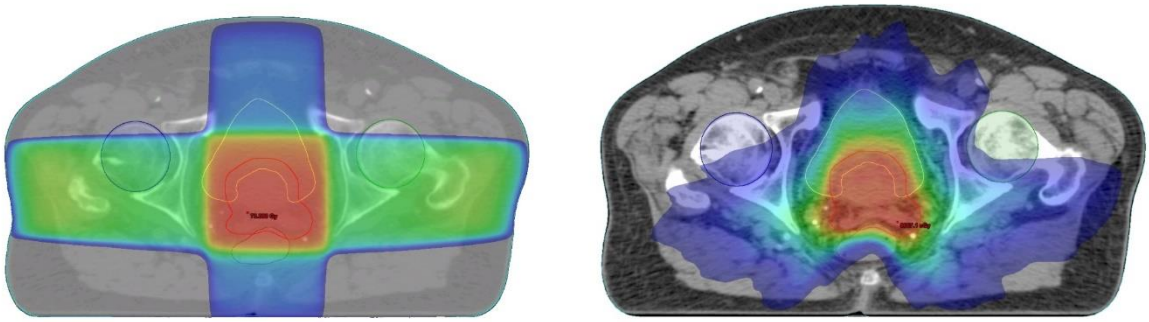

Figure 6. The dose distributions for the 4-Field Box (left) and IMRT (right) plans

Variations in delineating anatomical structures, production of radiation, localization of radiation, and geometric localization cause the deviations in doses voxels receive for any given course of treatment. Theoretically one can alter the TCP and NTCPs (or voxel doses directly) to create a range of PRQs for all possible courses of treatment. These functions represent scenarios where a task (or many tasks) in the course of treatment were substandard leading to a deviation from the ideal voxel doses. For example, a plan used the incorrect rectum contour and the true rectum received high doses. The rectum NTCP shifts left (receives higher doses) affecting the PRQ creating a constricted and smaller function. Similarly, there could have been a poor CT scan causing the drawn volumes to be smaller than true volumes. Regardless of the situation, generic plans can be generated that include possible PRQs for any scenario. Multiple scenarios or situations can be represented by a single PRQ. Likewise, a library of PRQs can be created to sample from when a specific scenario does occur or is theoretically identified.

The first objective for this work is to investigate how incremental variations of geometric and dosimetric parameters alter the complication free tumor control probabilistic functions from an ideal treatment plan. This phase will contain the majority of this thesis. All tasks in the course of a radiotherapy treatment work towards either: adjusting the locations and borders of delineated structures to more accurately and precisely define diseased and healthy tissues, adjusting radiation field collimation and entrance angles to better conform to the defined diseased tissue while avoiding defined healthy tissues, or ensuring acceptable doses are delivered to diseased and healthy tissues. Geometric parameters encompass tasks involved with establishing the specific location of all tissues with relation to the radiation isocenter as well as determining ideal radiation

field sizes and angles. Dosimetric parameters encompass tasks involved to deliver prescription doses to the diseased tissue while minimizing doses to healthy tissue. Due to the nature of radiation the two are heavily coupled as geometric variations alter dose based on scatter and beam penetration.

With the ability to generate a relative quantitative function (PRQ) for an ideal course of treatment and with a model to systematically generate the sequence of events that occurred to produce that treatment (as outlined in section 1.2 Complex Systems), one can now generate sequences of events that lead to quantitative functions (PRQs) diverting from the ideal. The first portion of this work will outline the various PRQs that occur as dosimetric and geometric components vary from their ideal counterparts. No matter what happens during a treatment course task the result will affect the dosimetric and geometric components for a given course of treatment. By systematically varying the parameters from an ideal treatment plan a library of PRQs can be created that encompass the dosimetric and geometric variations that occur due to errors and uncertainties while performing tasks. This library can then be used to estimate the PRQ whenever an error or uncertainty in a task is identified, realistically or hypothetically.

2.1.3 Dosimetric Deviations

First, an ideal treatment plan will be established for a patient with prostate cancer. It will be assumed that physician approved delineated structures are true representations of the actual volumes they possess. It will be assumed that all tasks and treatment delivery were completed perfectly leading to the ideal dose distribution and treatment plan providing the 100% PRQ. This provides a benchmark for comparison. Plans will be created that vary dosimetrically for increments of 1% for plus or minus 10% (20 PRQs) by changing the prescription dose and reperforming the dose calculation. The TCP, NTCPs and subsequent PRQs will be calculated using the original prescription dose in the calculation while using the DVH information from the plan with the varied dose.

2.1.4 Delineation Deviations

Next, new structures will be created by symmetrically deviating all delineated structures in 1 mm increments. DVHs for these structures will be calculated and exported to generate corresponding TCP, NTCPs and PRQs. First all structures will be contracted and expanded 5 mm

and corresponding PRQs calculated (10 PRQs). To provide more realistic PRQs for errors in delineation, PRQs will be generated with only one structure deviating while the remaining structures true volume DVHs are used in the PRQ calculation. PRQs with varying size CTVs will be generated with a 5 mm contraction and 10 mm expansion to account for extreme cases where PTV margins fail to encompass the tumor (15 PRQs). PRQs for varying size bladders will be generated with 5 mm contraction and expansions (10 PRQs). Additional bladder volumes will be generated where the contraction and expansion only occur in the direction proximal to the tumor (10 PRQs). PRQs with varying Rectum sizes will be generated with 5 mm contraction and expansions (10 PRQs). Additional rectum volumes will be generated where the contraction and expansion only occur in the direction proximal to the tumor (10 PRQs). Femoral Heads will be excluded as their contribution is minimal as seen in the IMRT PRQ example.

2.1.5 Geometric Deviations

PRQs for geometric deviations will be the final sets generated. In a 3D coordinate system, geometric deviations will be applied in the cardinal directions (6) and in the interplanar directions (20), or directions that split all planes. This results in 26 geometric deviations originating from the origin extending 10 mm out in 1 mm increments. Cardinal direction geometric deviations that will be applied include: the left and right directions (20 PRQs), the anterior and posterior directions (20 PRQs) and the superior and inferior directions (20 PRQs). The remaining geometric deviations involve combinations of the cardinal direction's deviations applied simultaneously. These deviations include: the right/posterior/superior and left/anterior/inferior directions (20 PRQs), the right/anterior/inferior and left/posterior/superior directions (20 PRQs), the right/posterior/inferior and left/anterior/superior directions (20 PRQs), the left/posterior/inferior and right/anterior/superior directions (20 PRQs), the left/anterior and right/posterior directions (20 PRQs), the left/inferior and right/superior directions (20 PRQs), the anterior/inferior and posterior/superior directions (20 PRQs), the left/posterior and right/anterior directions (20 PRQs), the left/superior and right/inferior directions (20 PRQs), and the anterior/superior and posterior/inferior directions (20 PRQs).

The above mentioned deviations will create the PRQ library that treatment course errors and uncertainties can produce creating deviations from ideal parameters. In total the library will

consist of 345 PRQs that represent non-ideal treatment courses from dosimetric and geometric deviations. In theory, increases in normal tissue doses will cause higher probabilities of complication which will decrease PRQs. Similarly, decreases in tumor doses will cause lower probabilities of tumor control decreasing PRQs. As deviations continue to increase the PRQs will decrease serving as a verification that this approach quantitatively captures the impact dosimetric and geometric parameters have on complication free tumor control probabilities and hence the probability of radiotherapy quality.

2.2 Defining The Radiation Therapy Process

With a method to establish a single quantitative function associated with a course of treatment, determining exactly how the course of treatment occurs to produce this quantity follows. Next begins creation of a framework for a systematic model to identify all events that take place during the treatment process, how and when. This involves outlining the process to identify and label all actions and reactions that occur from start to finish. Theoretically, if the capabilities existed, every action and reaction could be measured, documented and analyzed and the model must incorporate this concept. First generalized tasks for radiotherapy treatment courses were defined: Consult (C), Simulation (S), Treatment Planning (TP), Planning Review (PR), Treatment (Tx). These define the higher-level hierarchal tasks that all actions and reactions will occur within. Numerous professionals are involved in the completion of the above-mentioned tasks and for this study are identified as Radiation Oncologists or Physicians (MD), Qualified Medical Physicists (QMP), Certified Medical Dosimetrists (CMD) and Radiation Therapists (RTT). Each higher-level task may have numerous individuals complete various subtasks as the course of treatment progresses which is the next step in outlining the process.

2.2.1 Radiation Therapy Control Loops

Here the use of control loops to identify the individuals and tasks performed helps organize the events that take place and bin them according to the level of detail needed for an evaluation. Individuals involved in the completion of the defined higher-level tasks were identified. Figure 7 shows which individuals are involved in the Simulation (Sim) portion of the course of treatment.

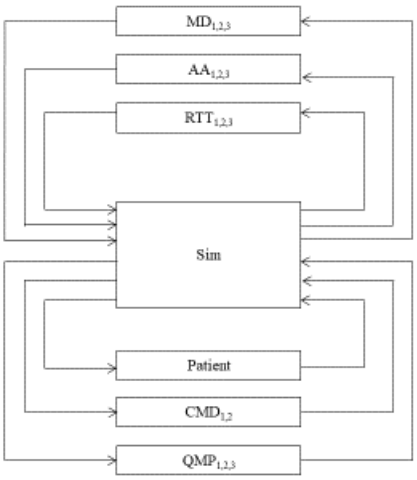

Figure 7. A control loop for all individuals that interact with the simulation process.

A control loop for each individual that interacts with the Simulation phase must be generated to describe the tasks they perform. Similar to the higher-level tasks for the entire course of treatment, generalized higher-level tasks for each individual were determined for Consult, Simulation, Treatment Planning, Plan Review and Treatment. This defines the next hierarchal level in the course of treatment which are the generalized tasks individuals perform to complete Consult, Simulation, Treatment Planning, Plan Review and Treatment for a course of treatment. Figure 8 displays the generalized tasks a RTT performs during Simulation. To perform these tasks various devices and sensors are used by the RTT. These are represented by the lined boxes in the control loops. The vertical lined boxes on the left represent actuators, or the devices the RTT uses to complete Sim Prep, Immobilization, Sim Scan and Documentation. These devices include computers, software, cameras, CT couch attachments, head cushions, vacuum lock bags and so forth. The diagonal lined boxes represent the sensors that supply feedback to the RTT. These include computer monitors, digital displays, RTT physical senses (sight, touch, sound), audio alerts and so forth. As more hierarchal levels are defined the specifics for performing a task are defined which eventually become dependent on the equipment that is used.

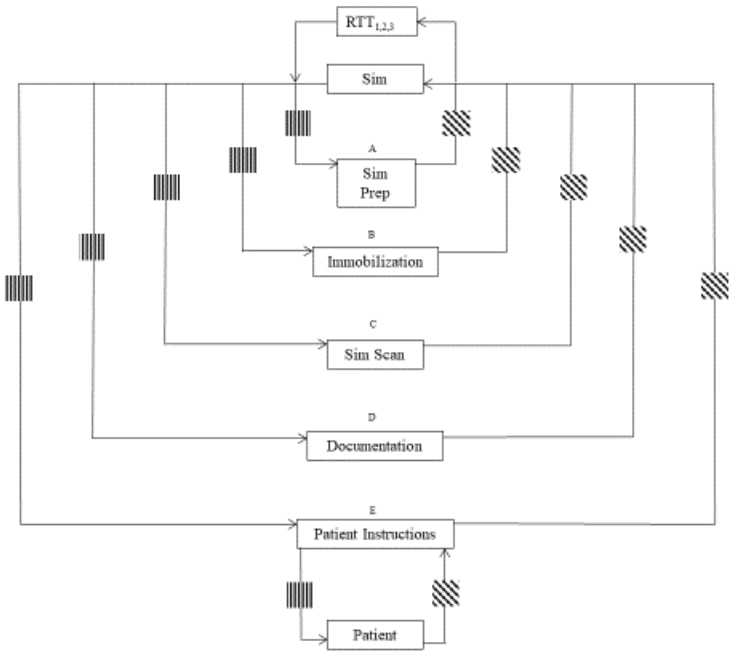

Figure 8. Control loops for the generalized tasks a Radiation Therapist performs during Simulation. Actuators are represented by the vertical line boxes on the left while sensory feedback is represented by the diagonal lined boxes on the right

Continuing in the same manner, the next hierarchal level defines more specific tasks for the generalized tasks individuals perform to complete Consult, Simulation, Treatment Planning, Plan Review and Treatment for a course of treatment. There is a pattern here associated with how generalized tasks are defined and subsequent specific tasks follow. As more specific tasks become defined, the devices used to complete the tasks become involved. Institution specific protocols outline which devices are used as the steps for completing those tasks are dependent on inherent device properties. Similarly, the feedback mechanisms used to verify proper task completion are dependent on inherent device properties. While the RTT is performing the Immobilization task, a specific step within the Sim Immobilization control loop would be to "Place a Vendor A Thermo Plastic mask in the hot water bath". Many companies supply Thermo Plastic masks and a clinic could use masks from multiple companies as well as different types of Thermo Plastic masks. All devices that could be used to complete a task can be identified in an actuator list. In the lowest-level control loops, the specific steps to complete a task are dependent on the equipment used and a loop for each piece of equipment can be generated.

Figures 9-12 demonstrate the further decompression of generalized tasks that a RTT performs during Simulation. The further one decompresses generalized tasks the more one describes the specific details a given institution uses to complete all tasks for their course of treatment. A large amount of time and effort is needed to define every hierarchal level and all tasks involved for a given institution. This incorporates all equipment available and protocols for how to use them. Regardless of the specifics, however, with the pattern a theoretical decompression can be outlined for all tasks. While specifics may vary, it can be assumed that simply labeling lower level hierarchal tasks will capture the numerous possibilities that explicit details in the lowest level tasks could encompass. In actual implementation similar mentalities follow for defining tasks in lower levels and the mechanisms in which they contribute to the overall quality of the course of treatment. Example control loop diagrams can be found in Appendix B: Radiation Therapy Control Loops.

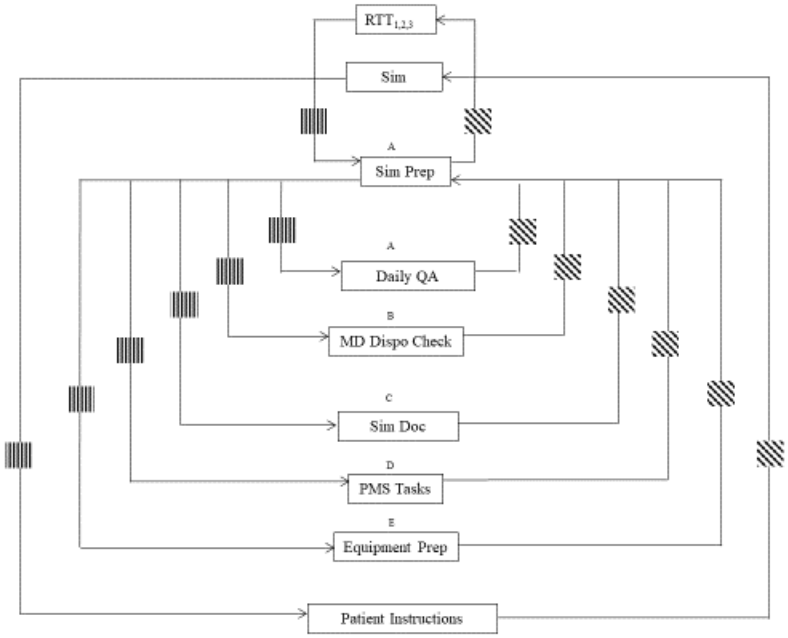

Figure 9. Control loops for the tasks a Radiation Therapist performs for the Sim Prep portion of Simulation.

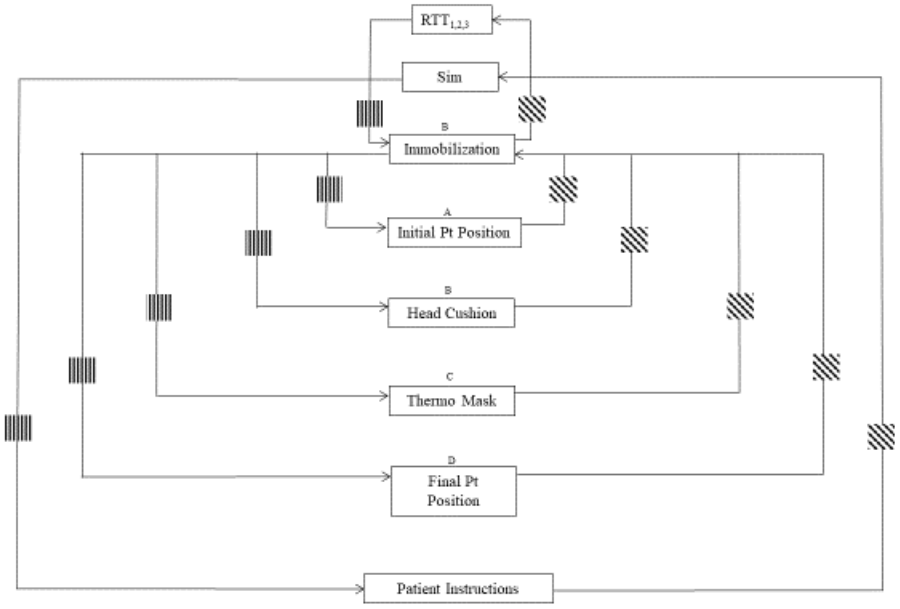

Figure 10. Control loops for the tasks a Radiation Therapist performs during the Immobilization portion of Simulation.

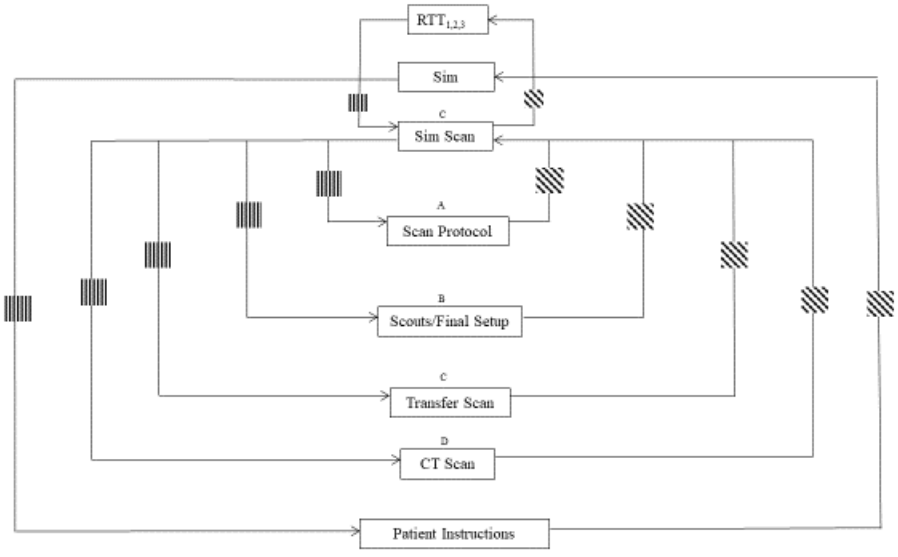

Figure 11. Control loops for the tasks a Radiation Therapist performs during the CT Scan of the Simulation.

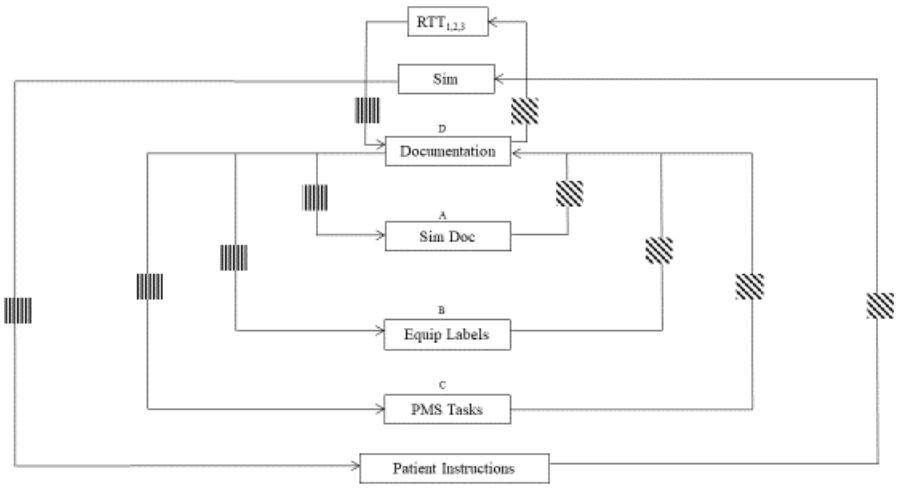

Figure 12. Control loops for the tasks a Radiation Therapist performs while documenting the Simulation Portion.

2.2.2 Radiation Therapy Process Quality

As tasks are defined and control loops generated, the ideal level of quality for the process can also be established. Starting with the initial generalized tasks, the level of quality that ideally is achieved after completing them can be determined or estimated. As lower level tasks are defined for the higher-level tasks, these too can be associated with an ideal level of quality that should be achieved upon their completion. Continuing forward, as tasks are defined while decompressing higher-level tasks, ideal levels of quality can be determined for each task and control loops that are defined. The equally weighted example demonstrates this concept. At first there are 5 higher level tasks defined. After completing each task, the process's quality increases 20%. Next, assume that each higher-level task was decompressed into 4 lower level tasks now equating to a total of 20 overall tasks, all equally weighted in terms of their contribution to the final process's quality. Now with every task's completion the process's quality increases 5%. For this example, as more tasks are defined while decompressing higher level tasks, the rise in quality would be equal to the number of tasks defined. At first a step function represents the rise in quality, but as more tasks are added the step function smooths out and eventually can be represented by a straight line with a slope of one.

The reality, of course, is that tasks are not equally weighted and their contribution to the overall quality is comprised of many factors. Each task can be thought of as a function with many variables that provides the quality for said task. For Radiotherapy, possible variables are accuracy and reliability of equipment used, using equipment properly and as intended, expertise and competency of the individual performing the task, the importance of the task or its contribution to the final quality, dependences on other tasks, previous task performance and temporal effects. The overall quality function is then a compilation of all task functions for the process. Determining the ideal quality for each task is difficult, however. The capabilities do not exist to measure and analyze all variables involved in a complex process to establish ideal qualities for every task. Furthermore, even though there is a chronological order tasks should be completed in, numerous tasks are capable of being performed out of order with no deterioration of the final quality. Determining variables to calculate the quality for every task may be unachievable but understanding that each task relates to the quality mathematically can provide valuable information as to how quality changes over time for radiotherapy.

Triage scenarios help to begin estimating how the quality increases after each task's completion. Starting with the generalized tasks, assume that after each task is completed the patient must be treated as is. If a patient arrives and must be treated, but the disease and its location are completely unknown, the result will be of poor quality due to large deviations in the treatment parameters that would be achieved if all tasks were completed. If the patient arrives and goes through consult, the quality of treatment that can be provided increases. For prostate cases, even without knowing exactly where the tumor and normal tissues lay, a treatment can be provided that eradicates the tumor. A 4-field box style technique could be set up reminiscent of older radiotherapy methods from the past or another patient's plan with a similar disease, physical size and demographics could be used to provide a decent treatment. Without performing the remaining 4 generalized tasks, there is still enough knowledge and expertise to treat the patient if it was absolutely necessary with some degree of success. Moving forward, as tasks are completed treatment parameters approach ideal values. In other words, treatment parameters deviations from their ideals decrease as tasks are completed.

While the variables may be unknown to directly calculate the quality, functions related to lower level tasks and the process, hypothesized levels of quality can still be estimated by assuming treatment will occur immediately following the completion of any given lower level task. Without knowing the "function variables", exactly what happened during the task, or where the treatment parameters were related to their ideals are after said task, calculating a PRQ for each task cannot be done with high accuracy. The first portion of this work, however, provides a solution to this issue to allow accurate estimates of PRQs that could be calculated following the completion of any task at any time during the entire process. If the ideal quality is achieved after the final task is complete, all previous tasks must have an inferior quality. In other words, working backwards, each previous task's quality is less than the proceeding task's quality and something during that task occurred to narrow treatment parameter values towards their ideals. It can be assumed then, that after each task's completion there was a deviation in treatment parameters as outlined in the pre-calculated PRQs generated. After the median task for treatment planning was completed, pretend that there was a tumor contour deviation and/or a field size deviation of 3-4 millimeters. Without knowing exactly how this occurred but omnisciently assuming there was a 3-4 millimeter deviation, a pre-calculated PRQ can be used to determine the quality for this point during the radiotherapy process. Thus, working backward from the final task, it can be assumed that treatment parameters deviate from their ideals with larger deviations occurring earlier in the process.

2.2.3 Radiation Therapy Sequence of Events

Tasks either directly or indirectly affect treatment parameters. A task that indirectly affects treatment parameters can be grouped with several other tasks to provide information or an action that allows another task in that group to directly alter a treatment parameter. As tasks are performed a specific sequence of events takes place that are directly coordinated with time. As time and the process progresses the detailed sequence of events gives rise to the percentage of quality that was achieved based on the deviations from treatment parameters ideals. This can be visualized by plotting the order that tasks should or could occur on an x-axis vs. their "ideal" quality after completion. A hypothetical plot is displayed in Figure 13 to demonstrate this.

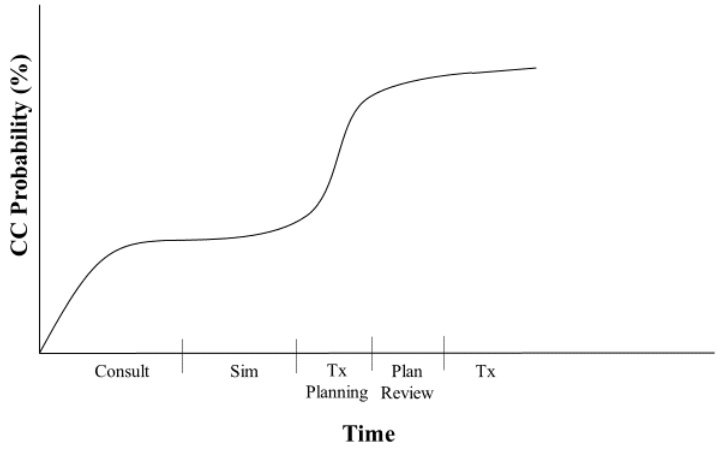

Figure 13. Example for PRQ plotted against an ideal chronological process. Time is on the x-axis while hypothetical PRQ values are on the y-axis.

The x-axis represents all actions and reactions that take place as outlined in the control loops for tasks with Figure 13 displaying the higher-level tasks for a course of treatment. As more hierarchal level tasks are defined, further temporal increments can be displayed in this graphical representation of the course of treatment. The lower-level tasks defined for Consult in which individuals perform to complete Consult can be input into the x-axis. Figure 14 displays the Consult tasks expanded while Figure 15 displays Treatment Planning tasks expanded. Ideally, certain individuals complete some of their tasks before the other individuals complete some of theirs and several tasks are iterative in nature, meaning they are repeated in order to narrow treatment parameters to more ideal values. Incorporating lower-level tasks then creates a long cumbersome list of actions and reactions, or tasks that occur during the radiotherapy complex process.

To consolidate the long list of tasks generated and the order in which they occur, a notation was incorporated to capture all the tasks defined in hierarchal level control loops. The first letter represents the generalized task in a course of treatment with the subscripts representing the individual performing a task. C_{MD} represents the Physicians tasks. A slash (\) represents the hierarchal levels for the tasks that individuals perform, representing the decompressed control loops constructed earlier describing more details for how higher-level tasks are performed. While referencing the control loops previously generated, C_{MD}\A\A\1…N thus represents the Physician

performing a very specific task. C_{MD}\A represents the Physician performing a disease overview for a patient. C_{MD}\A\A represents the Physician performing the patient referral review for the disease overview. The C_{MD}\A\A\4 would then represent the institution or physician specific 4th task in the patient referral review for the disease overview. As tasks are performed, they can be labeled and sequentially ordered to demonstrate what was done, who did it, how they did it and what they did it with.

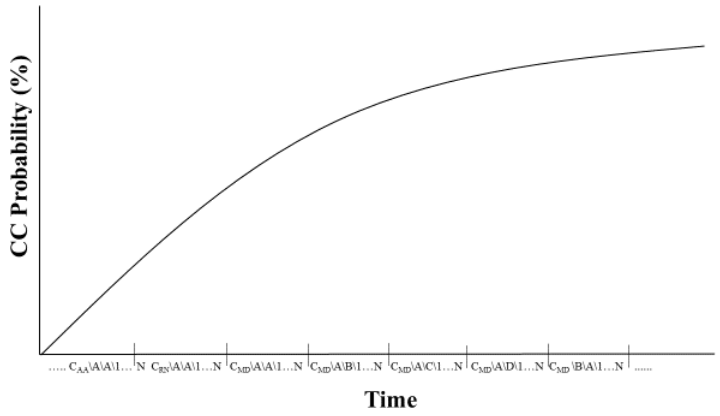

Figure 14. Portion of the PRQ vs. Time plot zoomed in to show the numerous tasks involved for completing consult. The values on the x-axis are found in Appendix A which outlines hypothetical tasks for a course of treatment for radiotherapy.

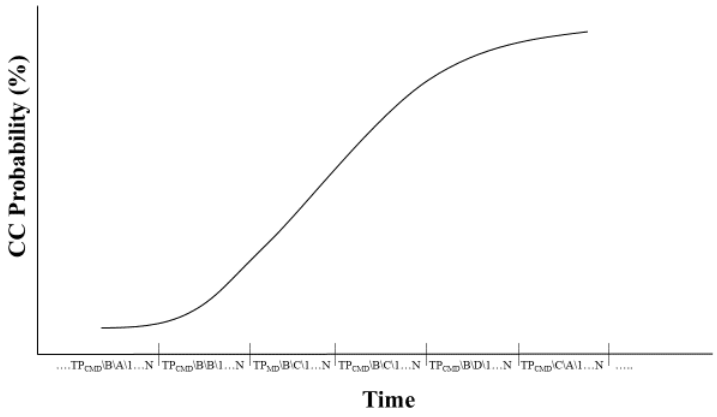

Figure 15. PRQ vs. Time plot zoomed in to show a portion of the treatment planning tasks. Appendix A includes the values on the x-axis.

All tasks identified, labeled and ordered in a course of treatment create a complete sequence of events chain (SEC). A hypothetical (ideal) SEC can be found in Appendix A which can be used to begin estimating a quality vs. time relationship for the entire process. Each SEC will affect the quality vs. time as tasks or groups of tasks work to alter treatment parameter values towards their ideals. Identifying which treatment parameters are affected by each task and the degree to which they are affected must be established in order to link a realistic estimate for possible PRQs associated with the completion of each task. The second portion of this work is to analyze outlined task control loops to determine which treatment parameters tasks impact, realistic degrees these parameters can vary as tasks are performed, and associate appropriate PRQs with tasks to estimate a quality vs time relationship for the radiotherapy process.

2.2.4 Quality, Time, and Sequences of Events

The second objective for this work is to estimate a possible quality vs. time plot based on how geometric and dosimetric treatment parameters approach their ideal values as tasks are completed. This portion of the thesis is a proof of concept due to the large number of variations that can occur while performing tasks, the numerous interpretations of how geometric and dosimetric parameters can be impacted and the large amount of hypothetical scenarios generated to produce deviations. This objective serves as nothing more than a demonstration that realistic estimates of quality vs. time can be generated and supported with reasonable logic.

Essentially, the beginning of the process's quality is represented by a PRQ with very large deviations and as each task is performed the deviations decrease. The generalized tasks outline the basic points where adequate information was acquired or actions performed to achieve ideal parameters. This begins to establish possible limits for the PRQ values before and after each generalized task. Consult determines the disease and treatment options, Simulation produces the planning scan used to delineate structures and calculate dose, Treatment Planning physically delineates structures, sets radiation field parameters and calculates dose, Plan Review verifies that parameters within the first three generalized tasks are correct, and Treatment physically carries out the treatment plan to deliver the prescribed dose. A PRQ can be calculated from a generic treatment plan template for which as tasks are completed becomes more specific to the patient eventually reaching their ideal plan. As information is acquired during the process an appropriate dose can be

determined, the radiation beams become centralized on the disease and the radiation fields conform to the tumor's shape. With the completion of each task, the generic plan becomes more specific and the quality ideally increases. This increase can then be plotted against time or the order with which tasks are performed. First, possible limits for PRQ values that can be achieved will be hypothesized for the 5 generalized tasks. Second, estimates for the increase of quality for the 22 specific tasks outlined will be generated.

To generate possible PRQ limits focus will be placed on the magnitude of deviations used for evaluation and the max values for the PRQs generated. The largest deviations PRQs will be averaged and their PRQ max values used for the quality achieved through consult with incrementally smaller deviations used for each additional generalized task identified. Initially with five generalized tasks identified 2 sets of deviations will be used to sample PRQs for each task; 9-10 mm deviations average PRQs will be sampled for consult, 7-8 mm for simulation, 5-6 mm for treatment planning, 3-4 mm for plan review and 1-2 mm for treatment. Next the assumption will be made that treatment planning has larger deviation decreases then other tasks. 10 mm deviations average PRQs will be used for consult, 9 mm deviations used for simulation, 5-8 mm for treatment planning, 3-4 mm plan review and 1-2 mm used for treatment. Finally, PRQ max values will be selected to represent the quality for generalized tasks for an equally weighted approach. As seen in the modality example, the IMRT PRQ does not reach 100 %. Based on the ideal PRQ max value calculated for the case to be evaluated, PRQs will be sampled for the generalized tasks with an evenly distributed approach.

With limits hypothesized for generalized task PRQ values, evaluation of the increase of quality within the generalized tasks will be estimated. A quick mockup of this concept was used to generate Figure 13. While numerous individuals perform tasks within the generalized tasks, focus will be placed on the main individuals that perform each generalized task. These are the MD for Consult, the RTT for Simulation, the CMD for Treatment Planning, the QMP for Plan Review and the RTT for Treatment. Within the 5 generalized tasks, an additional 22 tasks were defined for the second hierarchal level. These tasks are outlined in Appendix B which includes 4 tasks for Consult, 4 tasks for Simulation, 5 tasks for Treatment planning, 5 tasks for Plan Review and 5 tasks for treatment. From the evaluation, appropriate treatment parameter deviations for each task

can be estimated and corresponding PRQs linked. With this, complete realistic PRQ value estimates can be associated with Figure 13 to provide a reasonable idea of how the quality increases throughout the entire course of treatment for radiation therapy.

3. RESULTS

3.1 Treatment Parameter Variations

Patient anatomy for the treatment plan used consisted of an origin set at the right, posterior, and inferior region of the prostate CTV. The bladder was located anterior to the prostate CTV with the rectum directly posterior. This case was chosen due to the bladder and rectum locations aligned on the y-axis, or longitudinally consistent, to minimize variables for validation and verification purposes. The coordinate system labeled the longitudinal axis (right/left) as x with +x being the patient's right and -x being the patient's left. The longitudinal axis (superior/inferior) was labeled z with +z being the patient's superior and -z being the patient's inferior. The vertical axis (anterior/posterior) was labeled y with +y being the patient's posterior and -y being the patient's anterior. Figure 16 and Figure 17 display screenshots of the TPS graphical user interface (GUI) centered on the origin to provide context for the treatment parameter variations that were evaluated. The plan that was treated used a prescription dose of 78 Gy delivered in 39, 2 Gy fractions using a 9 field IMRT method.

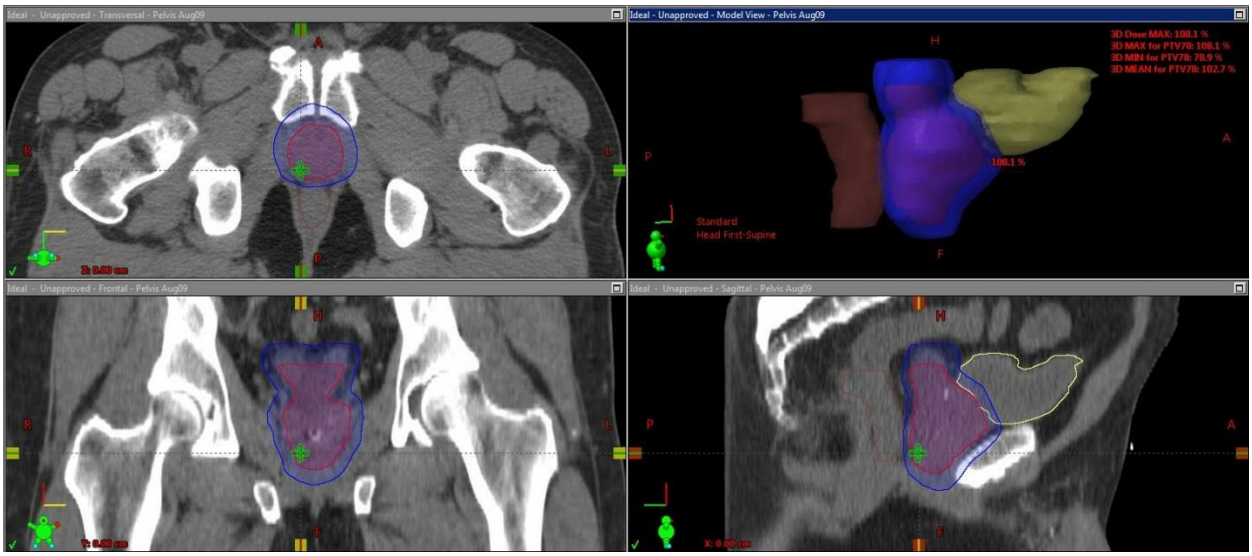

Figure 16. Patient anatomy used for plan evaluations. The Rectum (brown), Bladder (yellow), CTV (red), and PTV (blue) are displayed with the planes centered on the coordinate systems origin.

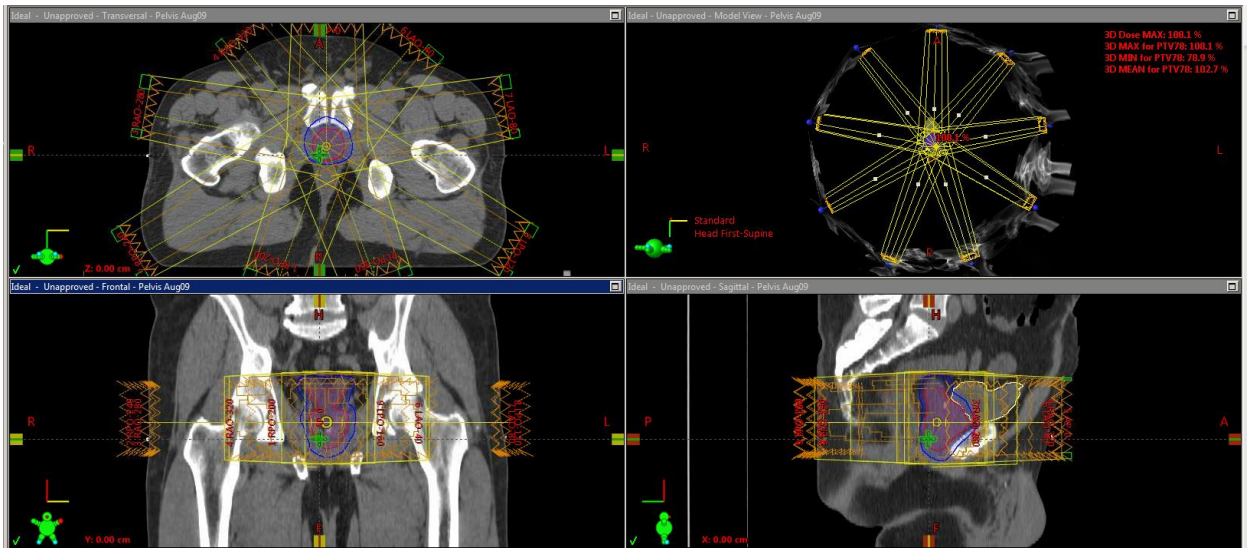

Figure 17. Fields for the treatment plan used for plan evaluations. A 9 field IMRT plan with dynamic MLCs was used.

The ideal PRQ calculated for this case is shown in Figure 18. Figure 19 displays the ideal TCP and NTCPs calculated and Figure 20 shows the DVHs for the ideal plan. For the PRQ and TCP/NTCP graphs, the x-axis consists of dose in gray (Gy) and the y-axis consists of the Control/Complication Probability in percent (%). For the DVH graph the x-axis is the dose in Gy and the y-axis is the structure volume in percent. Table 2 displays 5 additional metrics calculated for the PRQ curve. The first metric is the Control/Complication probability value (%) at the peak of the curve which was 82.99 %. The second metric is the dose the peak occurs at which was 83.85 Gy. The third metric is the value of the PRQ curve that occurs at the prescription dose (78 Gy) used for the treatment plan which was 77.70 %. The fourth metric is the full width half max (FWHM) for the curve which was 33.15 Gy. The fifth metric is the area under the curve (AUC) which was 29.50 kGy%. Table 3 displays 6 additional metrics calculated for the TCP and NTCP curves. There are two metrics for each structure for any deviation. The first is the dose (x-axis value) at the 50 % Control/Complication probability. The second in the slope calculated between the 80 % and 20 % Control/Complication. These two graphs and 11 metrics represent the baseline plan that all other plan PRQs are compared with.

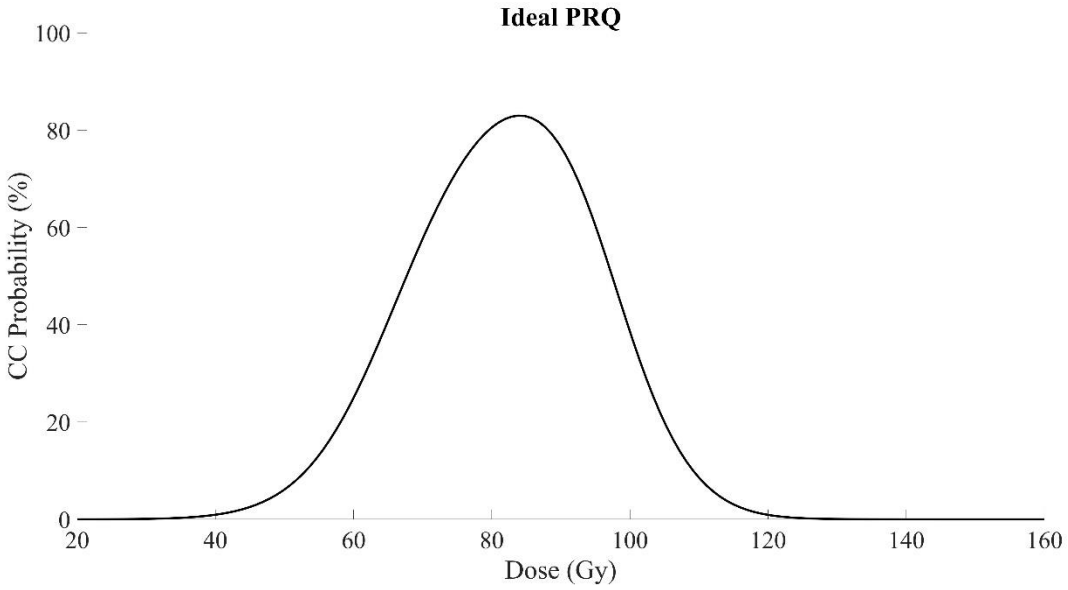

Figure 18. The Complication Free Tumor Control Probability Function calculated for an assumed Ideal Plans Dose Volume Histograms. This function represents the Ideal PRQ for the course of treatment.

Table 2. PRQ metrics calculated for the Ideal Treatment Plan.

Max	Dose @ Max	Rx Dose	FWHM	AUC
(%)	(Gy)	(%)	(Gy)	(kGy%)
82.99	83.85	77.70	33.15	29.50

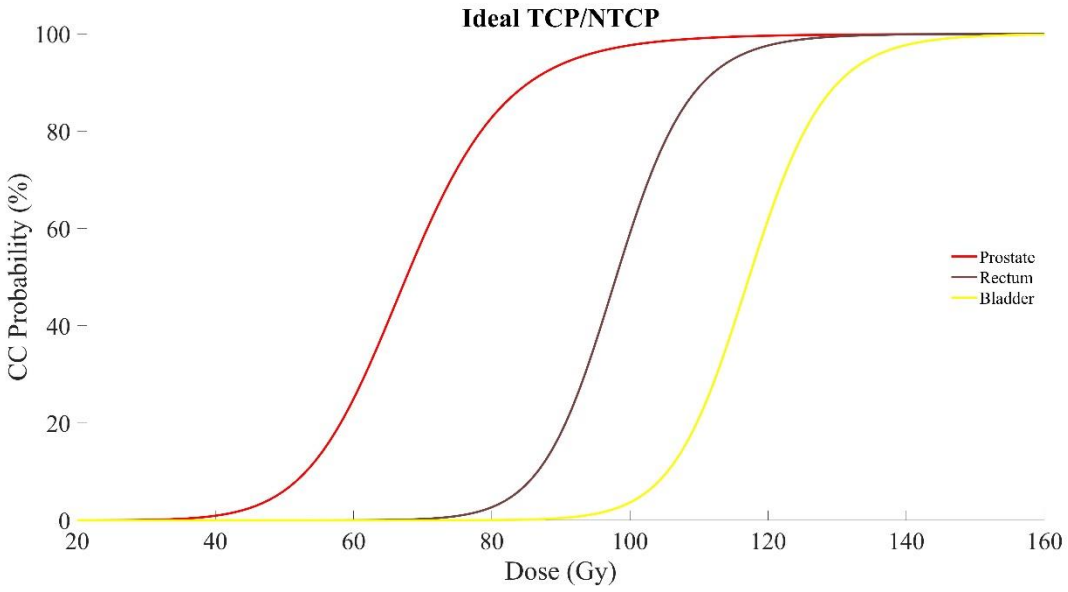

Figure 19. The TCP and NTCP functions generated from the ideal plan.

Table 3. TCP and NTCP metrics calculated from the ideal plan.

Prostate CTV		Bladder		Rectum	
50% Dose	80/20 Slope	50% Dose	80/20 Slope	50% Dose	80/20 Slope
67.76	2.93	117.49	3.85	97.99	4.10

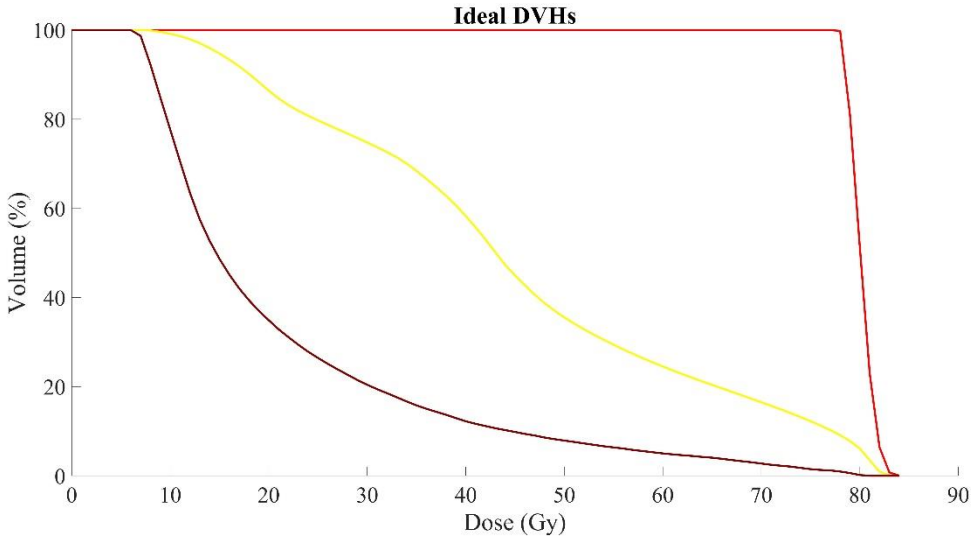

Figure 20. DVHs for CTV (red), bladder (yellow) and rectum (brown) for the ideal plan.

345 total PRQs were generated to form the sampling library. As deviation PRQs were calculated the following mechanisms were employed in displaying the graphs. For PRQ graphical displays, as deviation increments increase, plots are colored in the order of the visual spectrum or a rainbow color scheme. The first plot for all deviations is red, the second dark orange, orange, yellow, dark green and so forth. Deviations that involve "minus" treatment parameters are represented by dashed lines while deviations that involve "plus" treatment parameters are represented by dotted-dashed lines. Labeling is done to represent patient anatomy, however, which provides a more realistic reference for clinical scenarios. For TCP and NTCP plots, shading is used to differentiate between curves. As deviations increase all shades grow darker. TCPs are colored red with light red being the smallest deviation and dark red being the largest deviation. Bladder NTCPs are colored yellow with light yellow being the smallest deviation and dark yellow being the largest. Rectum NTCPs are colored brown with light brown being the smallest deviation and dark brown the largest.

3.1.1 Dosimetric Deviation PRQs

The first set of treatment parameter variations evaluated were dosimetric deviations in ±1% increments of the prescription dose. For each set of deviations first the PRQs are plotted followed by a table for the PRQ metrics. Next a plot of the TCPs and NTCPs is displayed followed by a table for additional TCP/NTCP metrics. Finally plots of the DVHs are displayed. There was very little variation of the value the max occurred at for both ± percentages of the prescription dose revolving around 83%. For minus percentages of the prescription dose, the PRQs shift right on Figure 21 or simply increase in dose. For plus percentages of the prescription dose, the PRQs shift left on the graph or simply decreases in dose. This can visually be seen in the two graphs as well as seen in the dose at which the PRQ max occurs and the PRQ value at the prescription dose in the subsequent tables. For minus percentages of the prescription dose, the dose at which the max occurs steadily increases with the PRQ value at the prescription steadily decreasing. For plus percentages of the prescription dose, the dose at which the max occurs steadily decreases. Here the PRQ value at the prescription dose starts on the left side of the curves for lower percentages of the prescription dose deviations and slides along the curves reaching the max value then decreases as it slides down the right side of the curves.

As dose is decreased in 1% increments the FWHM slightly increases which also leads to a slight increase in the AUC values. As dose is increased in 1% increments the FWHM slightly decreases which also leads to a slight decrease in the AUC values. The TCPs and NTCPs calculated as the dose is decreased shift right while the TCPs and NTCPs calculated as the dose is increased shift left.

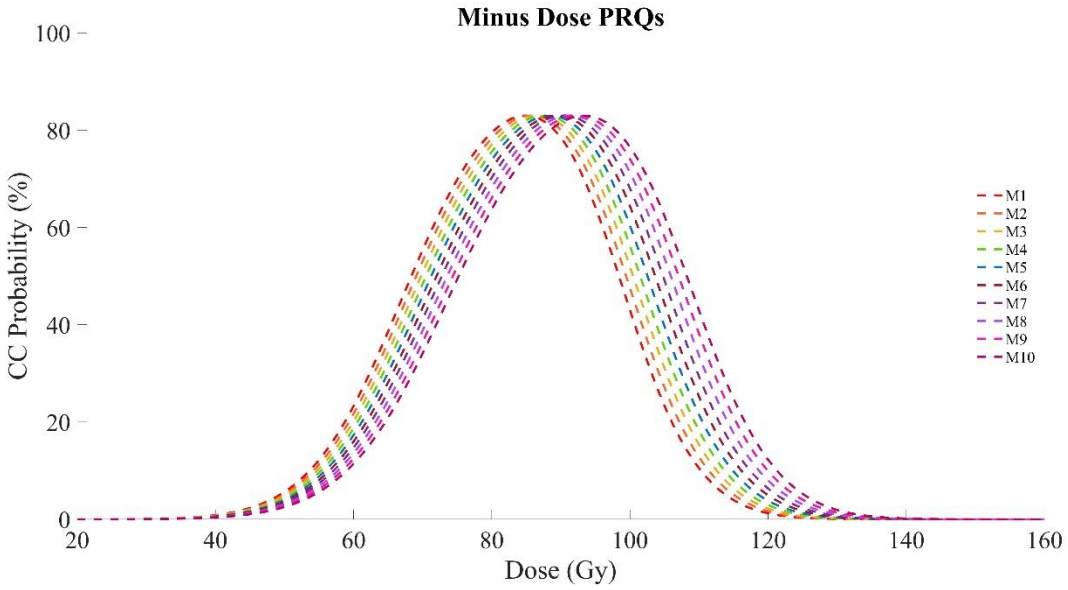

Figure 21. PRQs calculated for Dosimetric Deviations in Minus 1 percent increments of the prescription dose.

Table 4. PRQ metrics for Dosimetric Variations in Minus 1 percent increments of the prescription dose.

	Max	Dose @ Max	Rx Dose	FWHM	AUC
MD1	83.00	84.83	76.32	33.15	29.81
MD2	83.02	85.80	74.82	33.15	30.14
MD3	83.03	86.78	73.19	35.10	30.45
MD4	83.00	87.75	71.41	35.10	30.75
MD5	82.98	88.73	69.48	35.10	31.05
MD6	82.99	89.70	67.45	35.10	31.40
MD7	83.01	90.68	65.33	36.08	31.76
MD8	83.02	91.65	63.10	36.08	32.11
MD9	82.98	92.63	60.74	36.08	32.42
MD10	82.97	93.60	58.28	37.05	32.77

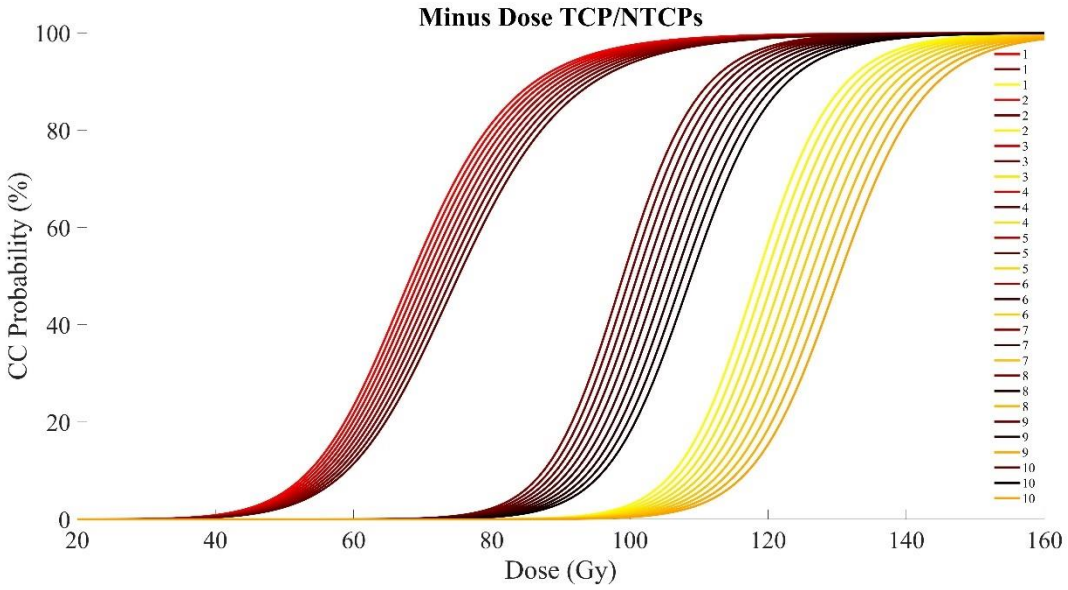

Figure 22. TCP and NTCPs calculated as dose varied with Minus 1 percent increments of the prescription dose. Lighter shades indicate smaller deviations while darker shades represent larger deviations.

Table 5. TCP and NTCP metrics calculated from dosimetric decreases.

	Prostate CTV		Bladder		Rectum	
	50% Dose	80/20 Slope	50% Dose	80/20 Slope	50% Dose	80/20 Slope
MD1	68.74	2.49	118.46	3.28	98.96	3.28
MD 2	68.74	2.41	119.44	3.16	99.94	3.28
MD3	69.71	2.41	121.39	3.16	100.91	3.28
MD4	70.69	2.34	122.36	3.04	101.89	3.16
MD5	71.66	2.34	123.34	3.04	102.86	3.16
MD6	71.66	2.28	124.31	3.04	103.84	3.16
MD7	72.64	2.28	126.26	3.04	105.79	3.04
MD8	73.61	2.28	127.24	2.93	106.76	3.04
MD9	74.59	2.22	129.19	2.93	107.74	3.04
MD10	75.56	2.22	130.16	2.93	108.71	2.93

Plots of the DVHs for plans with variation in dose are displayed in Figure 23 and Figure 26. Similarly, minus percentages of the prescription dose deviation plans caused the DVHs to shift left as structure volumes received less dose. Plus percentages of the prescription dose deviation plans caused the DVHs to shift right as structure volumes received more dose. The DVH graphs are placed throughout the results section for more of a qualitative reference. A thorough quantitative analysis of the DVHs will not be part of this work and is left for future projects. The importance of the DVHs displayed in the results section is to give the reader a general sense of their behavior in relation to the deviations, the limits they approach, and the relationship they have

with TCPs/NTCPs as well as PRQs. This provides a full walk through as to how the physical changes in plans manifest themselves in complication free tumor controls or PRQs. Changes to the PRQs, TCPs, NTCPs, and DVHs from deviations can all be viewed to help better understand how the deviations impact the quality from any given deviation.

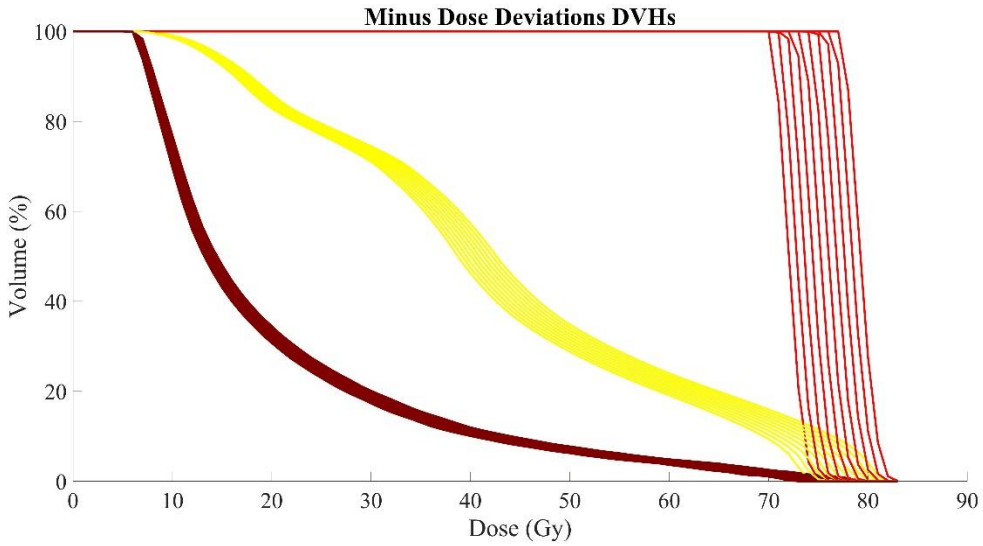

Figure 23. DVHs for Prostate CTV (red), Bladder (yellow), and Rectum (brown) for plans calculated with minus 1% increments of the prescription dose. All DVHs shift left.

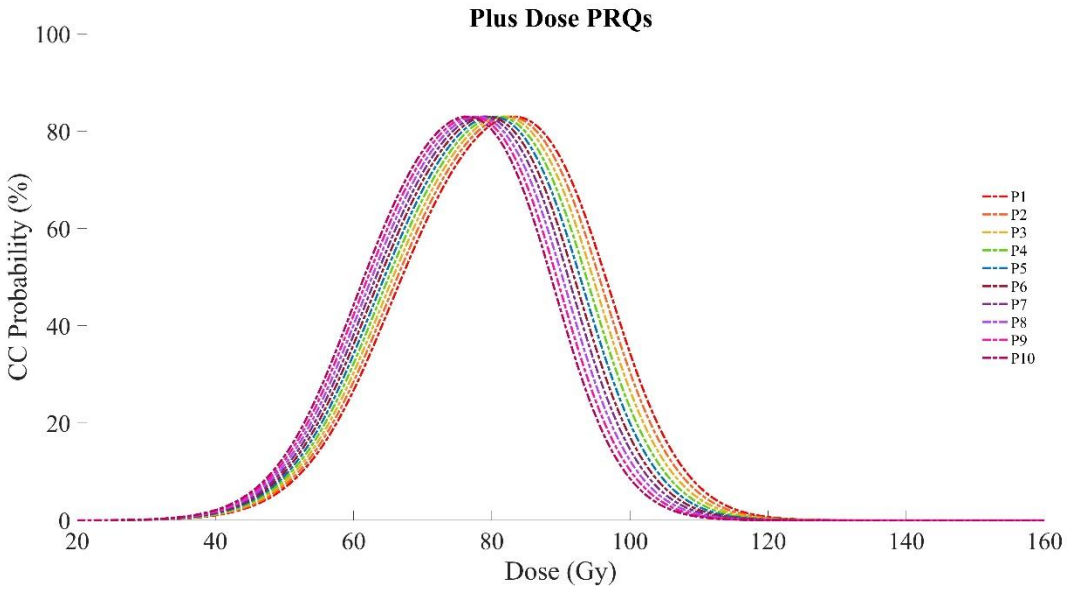

Figure 24. PRQs calculated for Dosimetric Deviations in Plus 1 percent increments of the prescription dose.

Table 6: PRQ metrics for Dosimetric Variations in Plus 1 percent increments of the prescription dose.

	Max	Dose @ Max	Rx Dose	FWHM	AUC
PD1	82.99	82.88	78.94	32.18	29.23
PD2	82.99	82.88	80.02	32.18	28.95
PD3	83.01	81.90	80.93	32.18	28.67
PD4	83.00	80.93	81.68	31.20	28.38
PD5	83.00	79.95	82.28	32.18	28.11
PD6	83.00	78.98	82.72	31.20	27.86
PD7	82.99	78.98	82.96	31.20	27.60
PD8	83.00	78.00	83.00	31.20	27.33
PD9	83.00	77.03	82.85	30.23	27.08
PD10	82.99	76.05	82.52	30.23	26.84

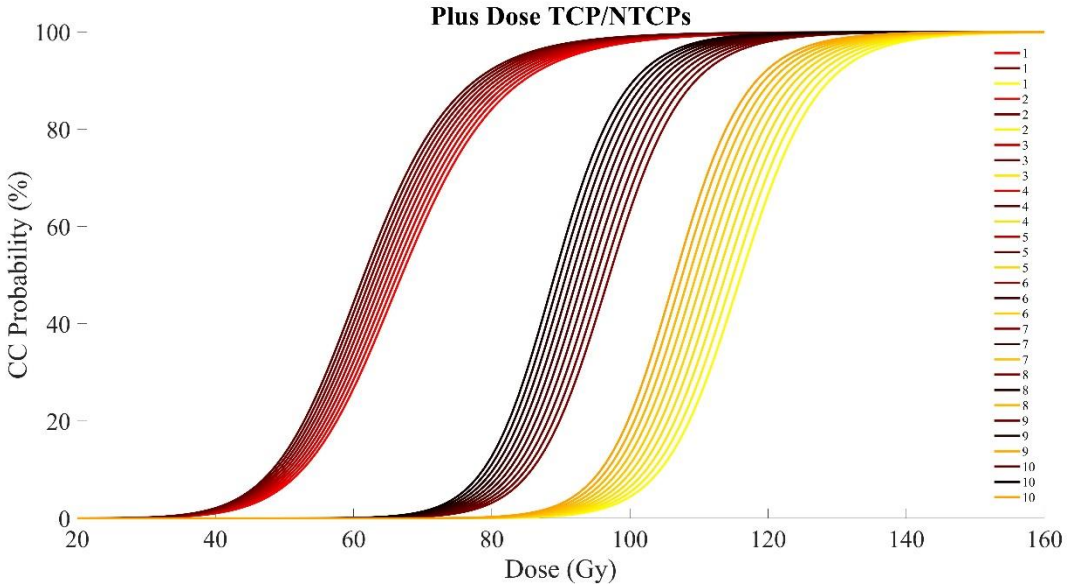

Figure 25. TCP and NTCPs calculated as dose varied with Plus 1 percent increments of the prescription dose. Lighter shades indicate smaller deviations while darker shades represent larger deviations.

Table 7. TCP and NTCP metrics calculated from dosimetric increases.

	Prostate CTV		Bladder		Rectum	
	50% Dose	80/20 Slope	50% Dose	80/20 Slope	50% Dose	80/20 Slope
PD1	66.79	2.49	116.51	3.28	97.01	3.28
PD2	66.79	2.56	114.56	3.42	96.04	3.42
PD3	65.81	2.49	113.59	3.28	95.06	3.42
PD4	64.84	2.56	112.61	3.28	94.09	3.42
PD5	64.84	2.56	111.64	3.28	93.11	3.42
PD6	63.86	2.65	110.66	3.57	92.14	3.42
PD7	62.89	2.65	109.69	3.57	91.16	3.57
PD8	62.89	2.65	108.71	3.57	91.16	3.57
PD9	61.91	2.65	107.74	3.57	90.19	3.57
PD10	61.91	2.74	106.76	3.57	89.21	3.57

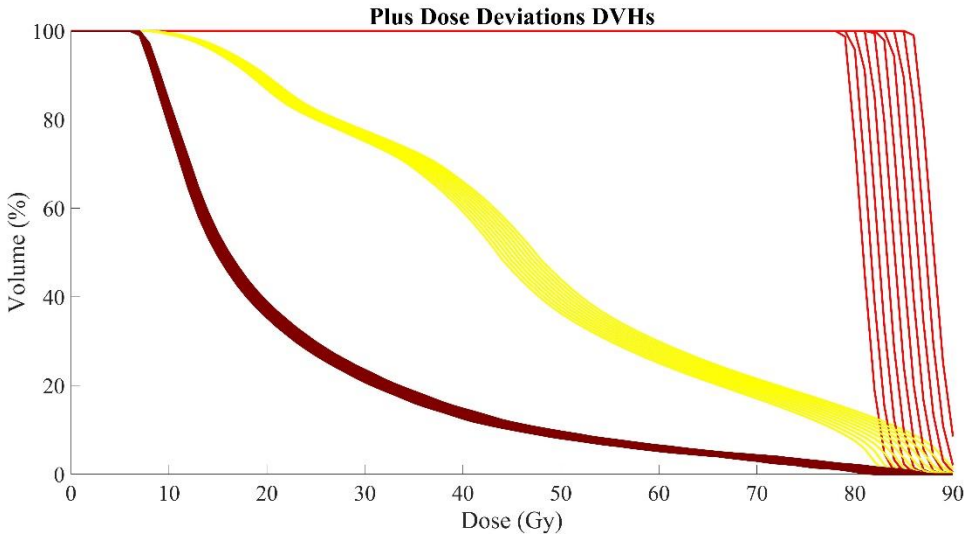

Figure 26. DVHs for Prostate CTV (red), Bladder (yellow), and Rectum (brown) for plans calculated with plus 1% increments of the prescription dose. All DVHs shift right.

3.1.2 Delineation Deviation PRQs

The second set of treatment parameter deviations evaluated consisted of delineation deviations that occur while outlining and defining all structures of interest, which were the prostate CTV, bladder and rectum for this study. As structures were isotopically contracted, this was considered a minus deviation and when they were expanded this was considered a plus deviation. Thus, all PRQ graphs are represented by dashed lines for M# mm deviations and dotted-dashed lines for P# mm deviations.

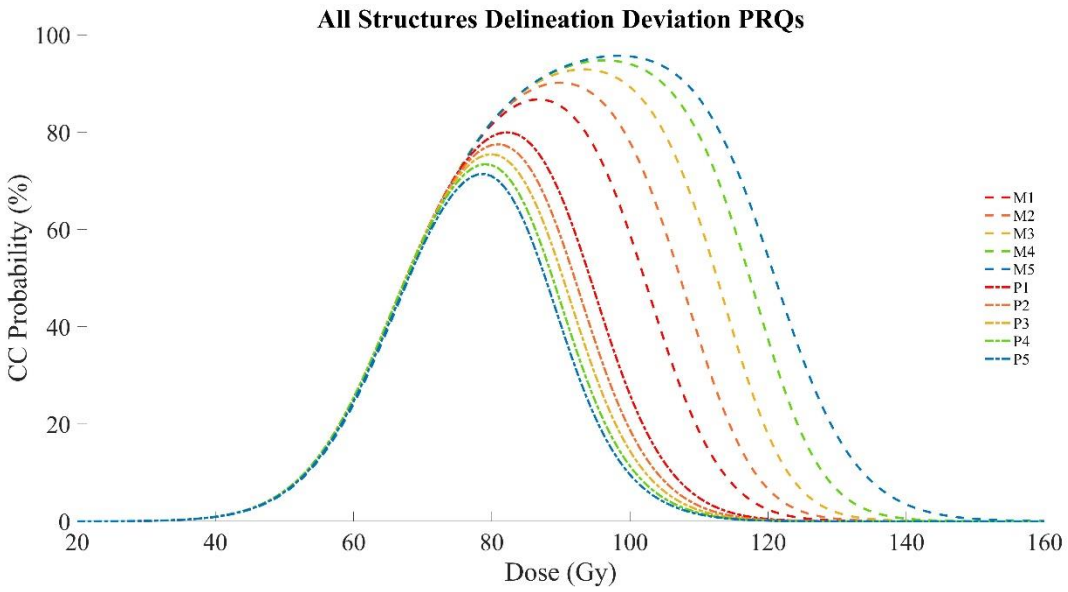

Figure 27. PRQs calculated when expanding and contracting all structures in 1 mm increments.

Table 8: PRQ metrics as all structures are contracted and expanded in 1 mm increments.

	Max	Dose @ Max	Rx Dose	FWHM	AUC
M1	86.74	86.78	78.19	37.05	33.60
M2	90.16	89.70	78.40	40.95	38.34
M3	92.91	93.60	78.43	45.83	43.37
M4	94.75	96.53	78.34	49.73	48.08
M5	95.70	98.48	78.25	52.65	52.13
P1	79.96	81.90	76.93	30.23	26.80
P2	77.50	80.93	75.86	29.25	24.88
P3	75.47	79.95	74.66	28.28	23.46
P4	73.42	78.98	73.14	27.30	22.17
P5	71.39	78.98	71.31	26.33	21.07

As all structures were contracted the max PRQ values increased from 86.74 % to 95.70 % with the dose at which the max occurred at increasing too beginning at 86.78 Gy and finishing at 98.48 Gy. The PRQ value at the prescription dose had little change with an average value of 78.32 ± 0.1%. The FWHM increased starting at 37.05 Gy and finishing at 52.65 Gy. The AUC also increased from 33.60 Gy% to 52.13 Gy%. As all structures were expanded the max PRQ values decreased from 79.96 % to 71.39 % with the dose at which the max occurred decreasing beginning at 81.90 Gy and finishing at 78.98 Gy. The PRQ value at the prescription dose decreased with expansions starting at 76.93 % and ending at 71.31 %. The FWHM decreased with expansions

beginning at 30.23 Gy and finishing at 26.33 Gy. The AUC also decreased from 26.80 kGy% to 21.07 kGy%.

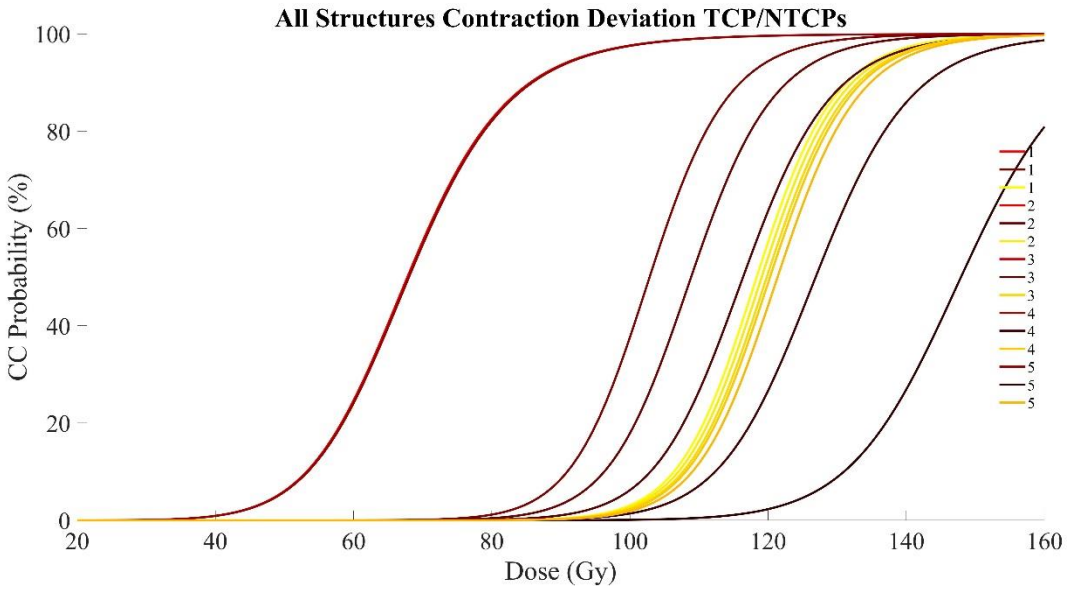

Figure 28. TCPs and NTCPs as all structures are contracted in 1 mm increments.

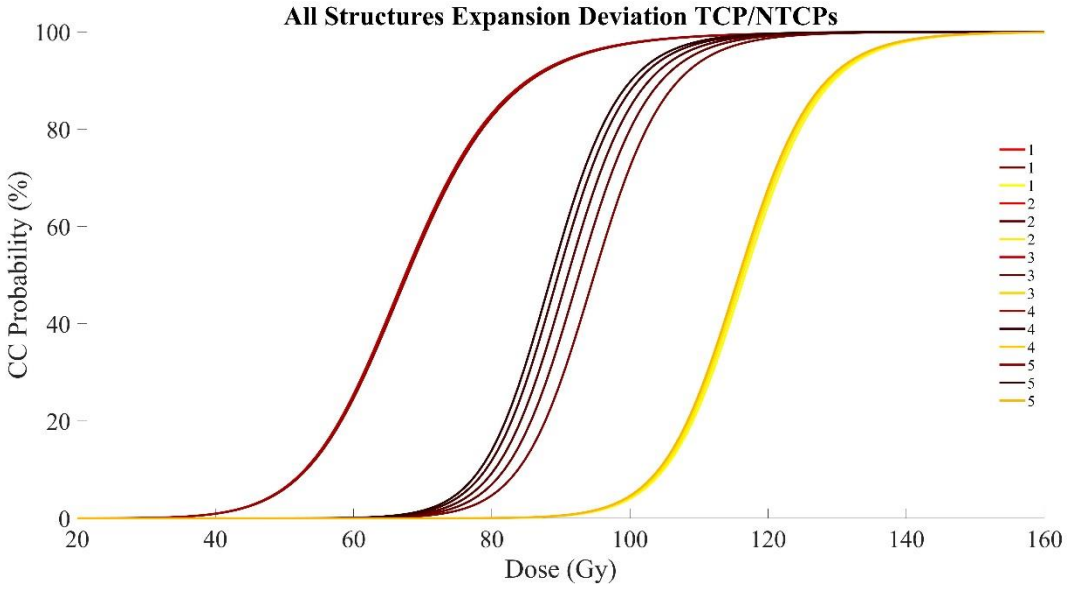

Figure 29. TCPs and NTCPs as all structures are expanded in 1 mm increments.

Table 9. TCP and NTCP metrics calculated from all structure isotropic contractions and expansions.

	Prostate CTV		Bladder		Rectum	
	50% Dose	80/20 Slope	50% Dose	80/20 Slope	50% Dose	80/20 Slope
M1	67.76	2.49	118.46	3.28	102.86	3.28
M2	67.76	2.49	119.44	3.16	108.71	3.04
M3	67.76	2.49	119.44	3.16	116.51	2.83
M4	67.76	2.41	120.41	3.04	127.24	2.65
M5	67.76	2.41	121.39	3.04	147.71	2.28
P1	67.76	2.49	116.51	3.28	95.06	3.42
P2	67.76	2.49	116.51	3.28	93.11	3.42
P3	67.76	2.49	115.54	3.28	91.16	3.57
P4	67.76	2.49	115.54	3.28	89.21	3.73
P5	67.76	2.49	115.54	3.28	88.24	3.73

The TCP curves for the prostate CTV for both contractions and expansions of all structures remained unchanged in the ±5 mm range. The bladder experienced small changes in its NTCP curves with a larger shift right as structures were contracted compared to the shift left from expansions. The rectum experienced the greatest change in its NTCP curves. As the rectum was contracted there was a larger shift in the curves to the right with a slight decrease in slope by the largest contraction. The shifts right became larger with each additional mm contraction. The shifts left became smaller with each additional mm expansion. Figure 30 displays the DVHs for all structures with isotropic delineation deviations for ± 5 mm. There are inflection points for the bladder and rectum DVHs at around 53 Gy and 14 Gy respectively. For contraction deviations the DVHs are above the ideal DVHs left of the inflection point and below the ideal DVHs right of the inflection point.

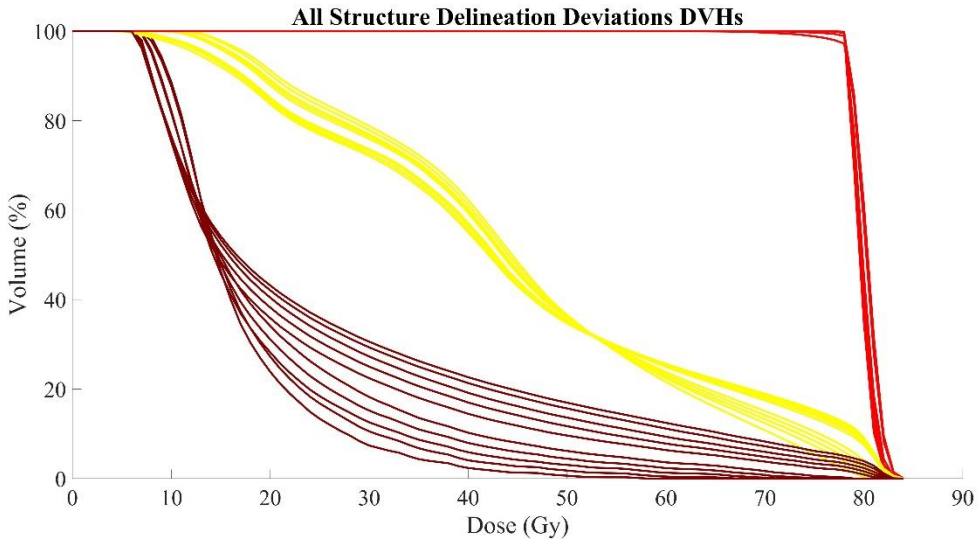

Figure 30. DVHs for all structures as they are contracted and expanded. For bladder and rectum contraction DVHs first appear above the initial line then inflect and appear below the initial line around 14 Gy for the rectum and 53 Gy for the bladder.

Next PRQs were calculated with just contractions and expansions of the bladder. There was minimal change in the PRQs with bladder delineation deviations with small changes between 105 Gy and 120 Gy. The max PRQ value for bladder contraction deviations was 83.02 ± 0.01 % with 82.97 ± 0.01 % for expansion deviations. The dose the max values occurred at was 83.85 Gy for both contractions and expansions. The PRQ value at the prescription dose was 77.71 % for bladder contractions and 77.70 % for expansions. The FWHM was 33.54 ± 0.53 % for contractions and 33.15 % for expansions. The AUC for contractions was 29.66 ±0.06 kGy% and 29.41 ± 0.03 kGy% for expansions.

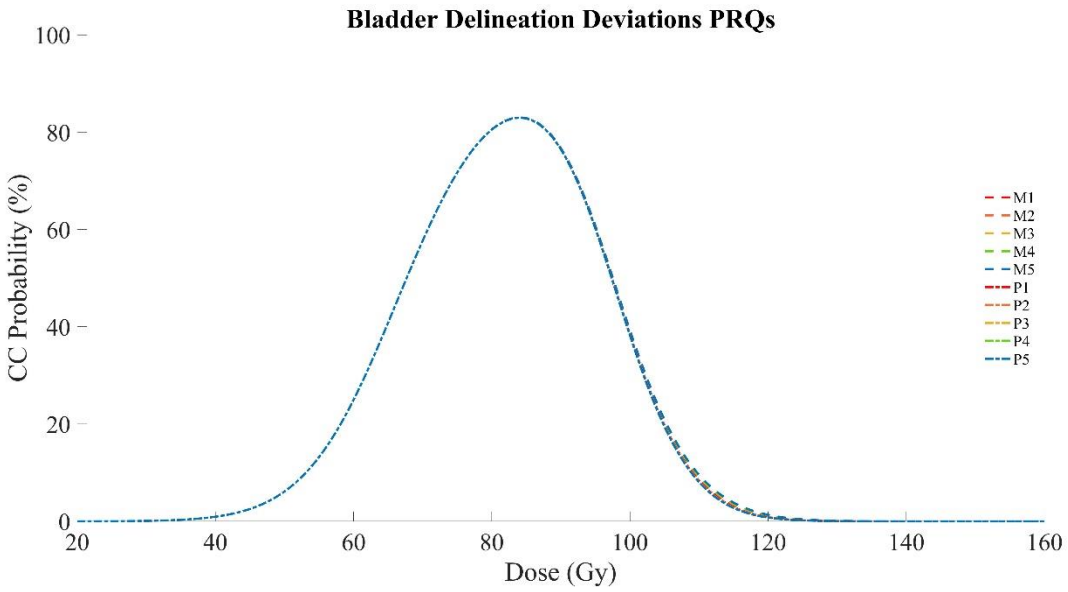

Figure 31. PRQs calculated when the Bladder is contracted and expanded in 1 mm increments.

Table 10: PRQ metrics as the Bladder is contracted and expanded in 1 mm increments.

	Max	Dose @ Max	Rx Dose	FWHM	AUC
M1	83.00	83.85	77.71	33.15	29.58
M2	83.01	83.85	77.71	33.15	29.62
M3	83.02	83.85	77.71	33.15	29.66
M4	83.02	83.85	77.71	34.13	29.69
M5	83.03	83.85	77.71	34.13	29.74
P1	82.98	83.85	77.70	33.15	29.46
P2	82.97	83.85	77.70	33.15	29.43
P3	82.96	83.85	77.70	33.15	29.40
P4	82.96	83.85	77.70	33.15	29.39
P5	82.96	83.85	77.70	33.15	29.39

The NTCP curves for the bladder contractions and expansions are the same as displayed in Figure 28 and Figure 29. Figure 32 and Figure 33 plot the bladder delineation deviations with the rectum NTCPs and prostate CTV TCPs unchanged.

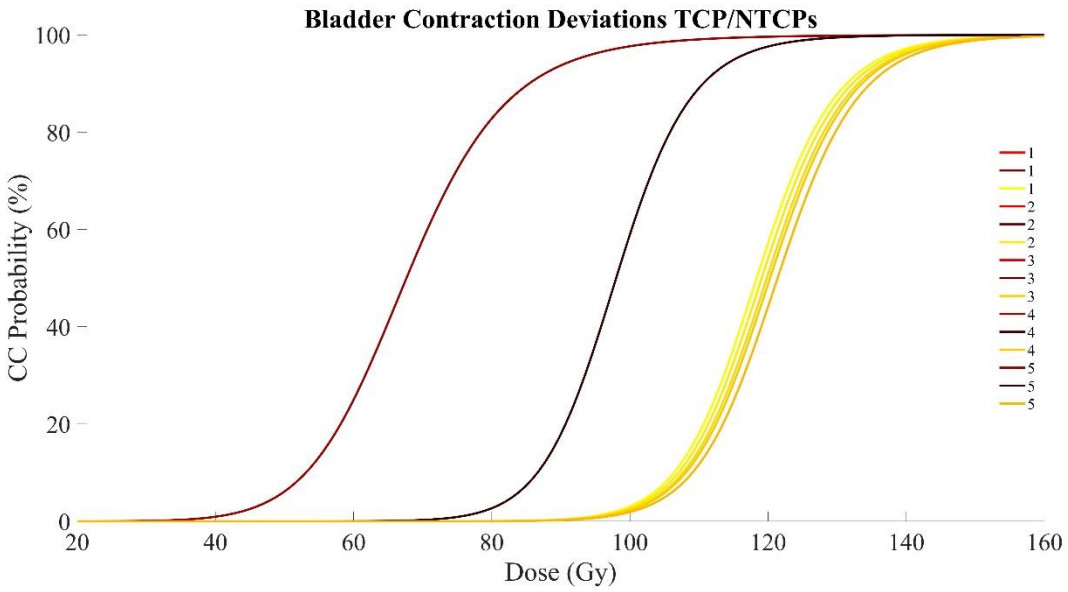

Figure 32. TCPs and NTCPs as the Bladder in contracted in 1 mm increments.

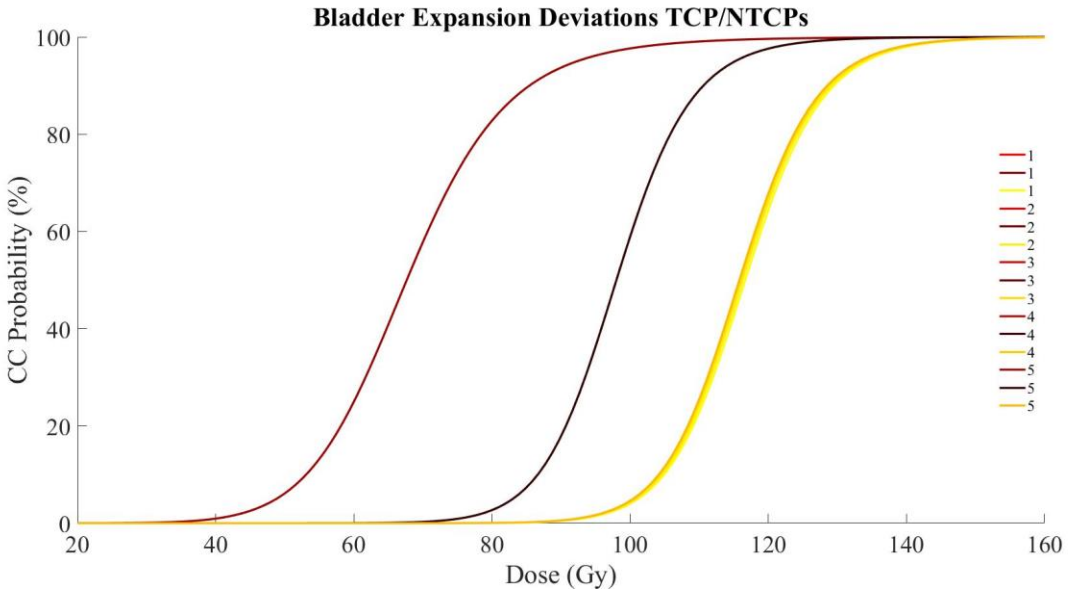

Figure 33. TCPs and NTCPs as the Bladder is expanded in 1 mm increments.

Table 11. TCP and NTCP metrics calculated from bladder isotropic contractions and expansions.

	Prostate CTV		Bladder		Rectum	
	50% Dose	80/20 Slope	50% Dose	80/20 Slope	50% Dose	80/20 Slope
M1	67.76	2.49	118.46	3.28	97.99	3.28
M2	67.76	2.49	119.44	3.16	97.99	3.28
M3	67.76	2.49	119.44	3.16	97.99	3.28
M4	67.76	2.49	120.41	3.04	97.99	3.28
M5	67.76	2.49	121.39	3.04	97.99	3.28
P1	67.76	2.49	116.51	3.28	97.99	3.28
P2	67.76	2.49	116.51	3.28	97.99	3.28
P3	67.76	2.49	115.54	3.28	97.99	3.28
P4	67.76	2.49	115.54	3.28	97.99	3.28
P5	67.76	2.49	115.54	3.28	97.99	3.28

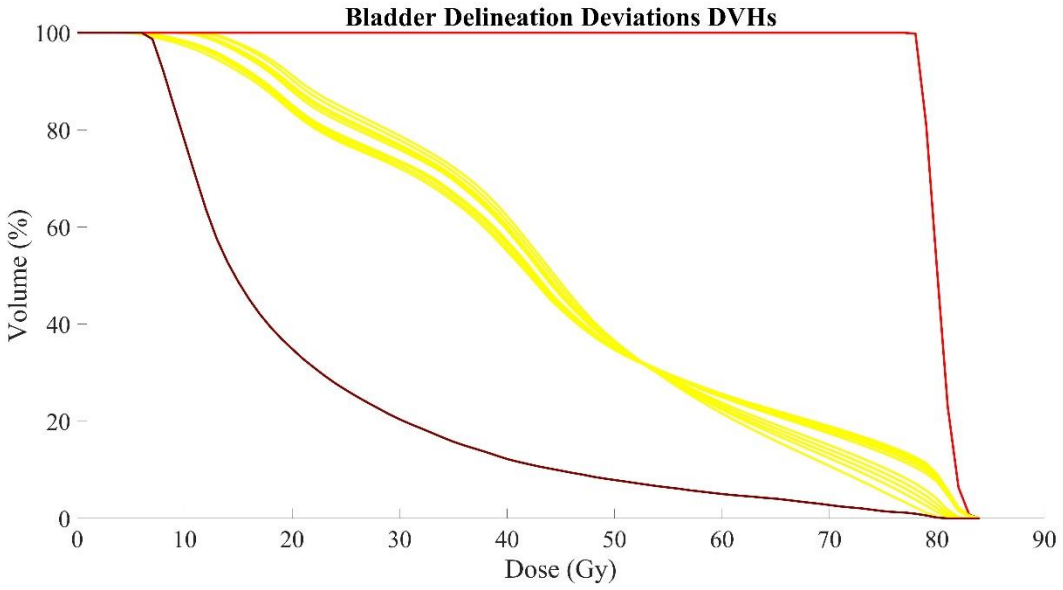

Figure 34. DVHs for contraction and expansion of the bladder in 1 mm increments.

Next the bladder was contracted and expand only in the direction proximal to the tumor, or posteriorly in the +y coordinate direction and inferiorly in the –z direction. There was still a small change in PRQs, but a larger change than when the entire bladder was contracted and expanded. Visually the difference can be seen on the right side of Figure 35 between 100 Gy and 120 Gy.

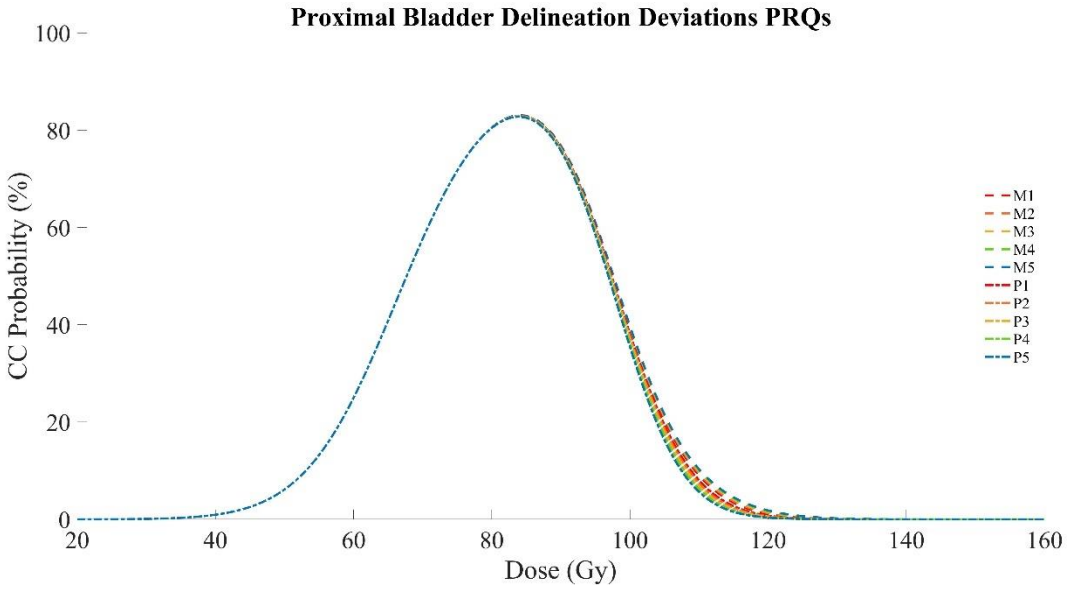

Figure 35. PRQs calculated when the Bladder is contracted and expanded in the directions proximal to the tumor in 1 mm increments.

Table 12. PRQ metrics as the Bladder is contracted and expanded in the directions proximal to the tumor in 1 mm increments.

	Max	Dose @ Max	Rx Dose	FWHM	AUC
M1	83.01	83.85	77.71	33.15	29.62
M2	83.03	83.85	77.71	34.13	29.72
M3	83.04	83.85	77.72	34.13	29.80
M4	83.05	83.85	77.72	34.13	29.87
M5	83.06	83.85	77.72	34.13	29.93
P1	82.96	83.85	77.70	33.15	29.38
P2	82.92	83.85	77.69	33.15	29.24
P3	82.88	83.85	77.68	33.15	29.09
P4	82.83	83.85	77.67	33.15	28.92
P5	82.77	83.85	77.66	33.15	28.75

The PRQ max values on average were 83.04 ± 0.02 % when the bladder was contracted away from the prostate CTV and 82.87 ± 0.07 % when expanded towards the prostate CTV. The dose where the max value occurred did not change for any proximal bladder contractions or expansions with a value of 83.85 Gy. Bladder proximal contractions FWHM were 33.15 Gy for the 1 mm contraction and 34.13 Gy for all others. Bladder proximal expansions FWHM were 33.15 Gy for all. The AUC slightly increased with proximal contractions beginning at 29.62 kGy% for 1 mm contraction and ending at 29.93 kGy% for 5 mm contraction. The AUC slightly decreased from

29.38 kGy% to 28.78 kGy%. The bladder NTCP curves experienced a greater shift right with proximal contractions than shifts left from bladder expansions.

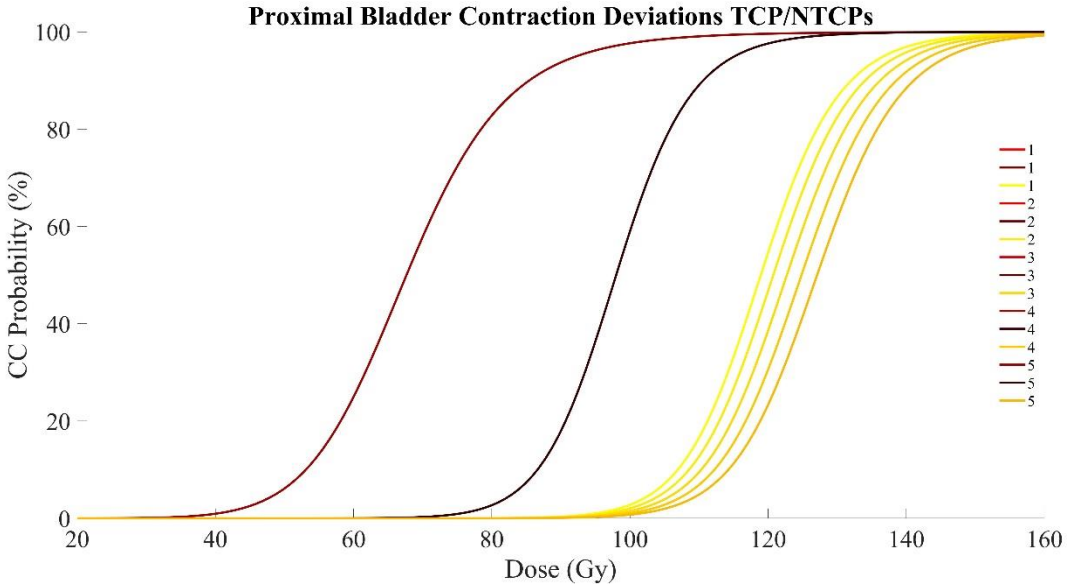

Figure 36. TCPs and NTCPs calculated when the Bladder is contracted in the directions proximal to the tumor in 1 mm increments.

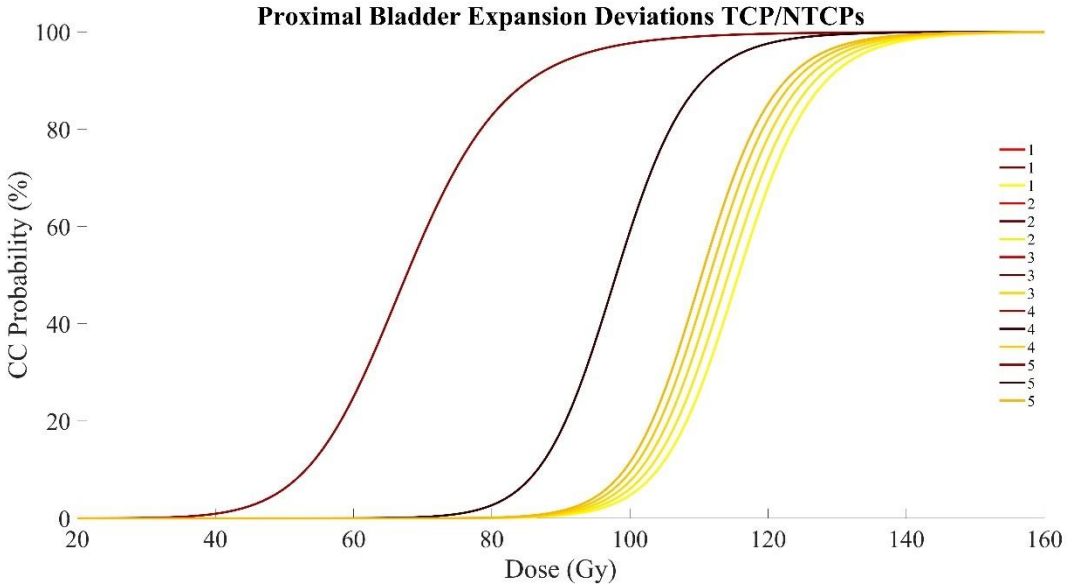

Figure 37. TCPs and NTCPs calculated when the Bladder is expanded in the directions proximal to the tumor in 1 mm increments.

Table 13. TCP and NTCP metrics calculated from bladder contractions and expansion in directions proximal to the tumor.

	Prostate CTV		Bladder		Rectum	
	50% Dose	80/20 Slope	50% Dose	80/20 Slope	50% Dose	80/20 Slope
M1	67.76	2.49	118.46	3.16	97.99	3.28
M2	67.76	2.49	120.41	3.16	97.99	3.28
M3	67.76	2.49	122.36	3.16	97.99	3.28
M4	67.76	2.49	125.29	3.04	97.99	3.28
M5	67.76	2.49	127.24	3.04	97.99	3.28
P1	67.76	2.49	115.54	3.28	97.99	3.28
P2	67.76	2.49	114.56	3.28	97.99	3.28
P3	67.76	2.49	112.61	3.42	97.99	3.28
P4	67.76	2.49	111.64	3.28	97.99	3.28
P5	67.76	2.49	110.66	3.42	97.99	3.28

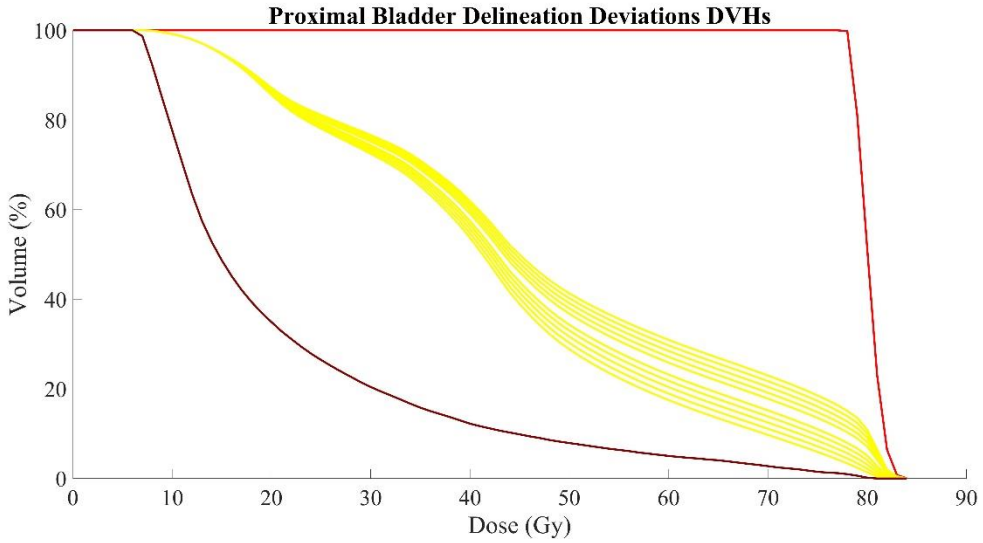

Figure 38. DVHs for contractions and expansions of the bladder direction proximal to the tumor.

The rectum delineation deviations change in PRQs was similar to the PRQs for all structure delineation deviations. For rectum contractions the PRQs grew in max value and widened with the right side of the PRQs expanding. For rectum expansions the PRQs decreased in max value and contracted with the right side of the PRQs contracting. PRQ max's for rectum contractions began at 86.85 % for 1 mm contractions rising to 94.90 % for 5 mm contractions. PRQ max's decreased for expansions starting at 79.76 % dropping to 71.67 %. The dose the max value occurred at increased for contractions from 86.78 Gy to 95.55 Gy and decreased for expansions from 81.90

Gy to 78.98 Gy. FWHMs increased for contractions beginning at 37.05 Gy growing to 49.73 Gy and decreased for expansions starting at 31.20 Gy dropping to 26.33 Gy. The AUC increased from 33.59 kGy% to 48.63 kGy% for contractions and decreased starting at 26.71 kGy% to 21.21 kGy% for expansions.

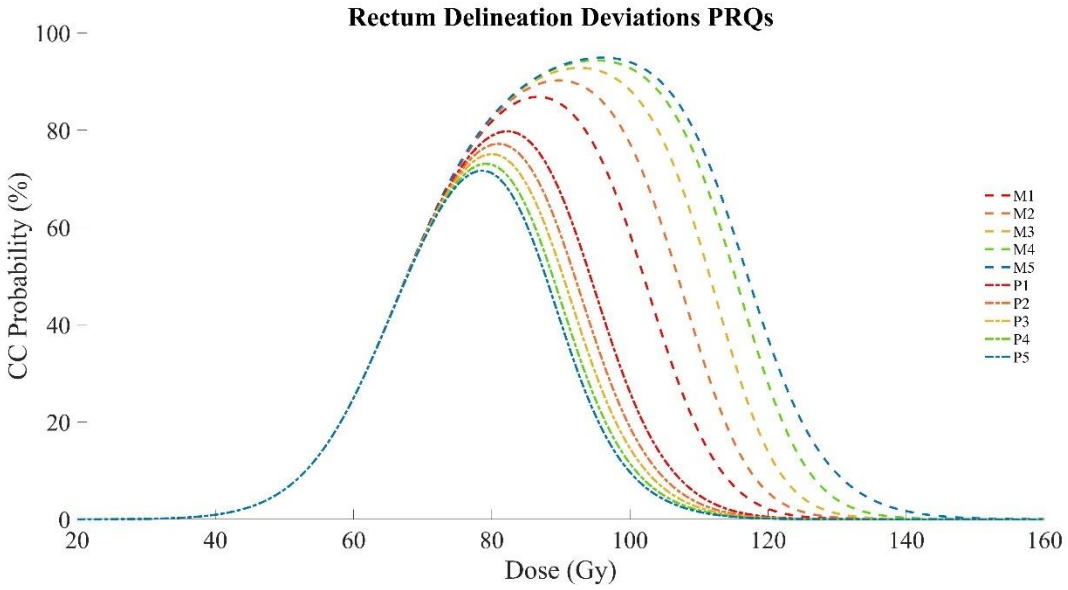

Figure 39. PRQs calculated when the Rectum is contracted and expanded in 1 mm increments.

Table 14. PRQ metrics as the Rectum is contracted and expanded in 1 mm increments.

	Max	Dose @ Max	Rx Dose	FWHM	AUC
M1	86.85	86.78	78.49	37.05	33.59
M2	90.24	89.70	78.86	40.95	38.12
M3	92.80	92.63	79.02	44.85	42.58
M4	94.34	94.58	79.07	47.78	46.35
M5	94.90	95.55	79.08	49.73	48.63
P1	79.76	81.90	76.65	31.20	26.71
P2	77.19	80.93	75.46	29.25	24.74
P3	75.10	79.95	74.22	28.28	23.31
P4	73.10	78.98	72.79	27.30	22.05
P5	71.67	78.98	71.61	26.33	21.21

The rectum NTCPs for contractions had a large shift to the right and a decrease in slope by the 5 mm contraction NTCP. With each mm contraction the shift right increased in magnitude. For expansions there was a small shift left. With each mm expansion the shift left decreased in magnitude.

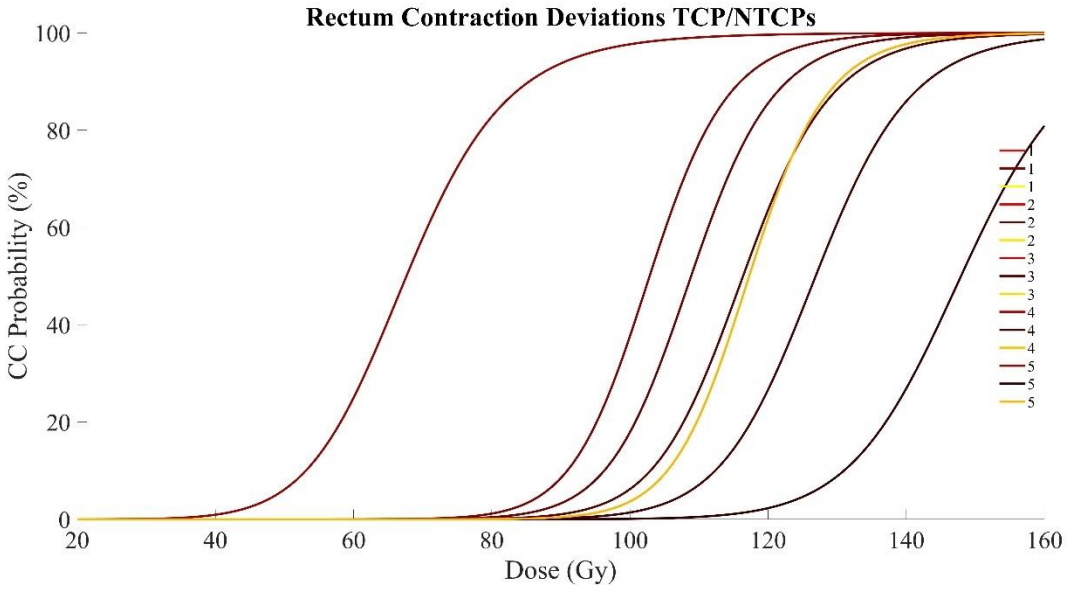

Figure 40. TCPs and NTCPs calculated when the Rectum is contracted in 1 mm increments.

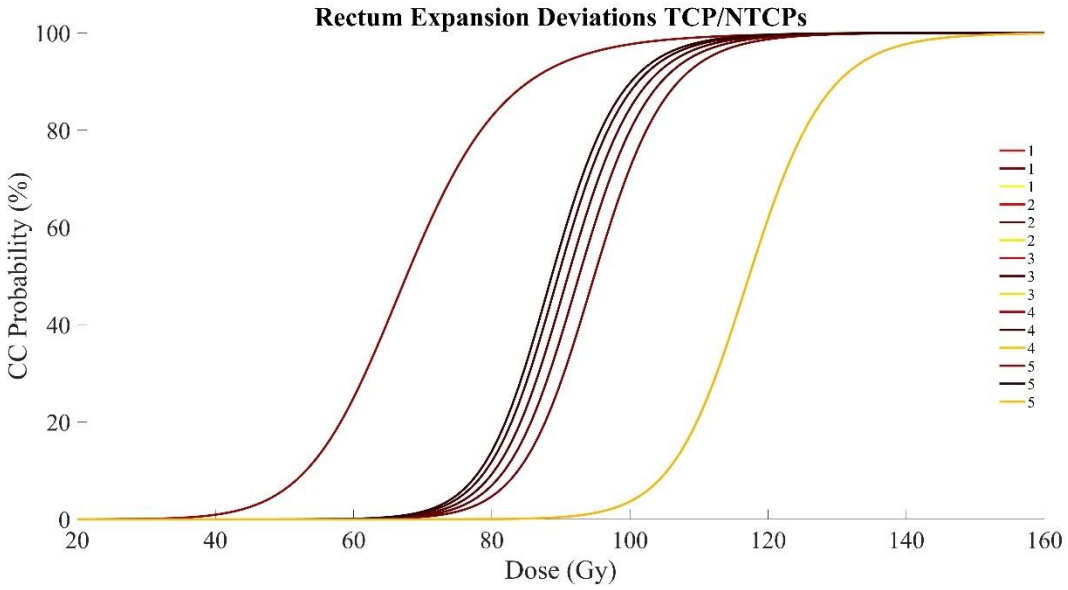

Figure 41. TCPs and NTCPs calculated when the Rectum is expanded in 1 mm increments.

Table 15. TCP and NTCP metrics calculated from rectum contractions and expansions.

	Prostate CTV		Bladder		Rectum	
	50% Dose	80/20 Slope	50% Dose	80/20 Slope	50% Dose	80/20 Slope
M1	67.76	2.49	117.49	3.28	102.86	3.28
M2	67.76	2.49	117.49	3.28	108.71	3.04
M3	67.76	2.49	117.49	3.28	116.51	2.83
M4	67.76	2.49	117.49	3.28	127.24	2.65
M5	67.76	2.49	117.49	3.28	147.71	2.28
P1	67.76	2.49	117.49	3.28	95.06	3.42
P2	67.76	2.49	117.49	3.28	93.11	3.42
P3	67.76	2.49	117.49	3.28	91.16	3.57
P4	67.76	2.49	117.49	3.28	89.21	3.73
P5	67.76	2.49	117.49	3.28	88.24	3.73

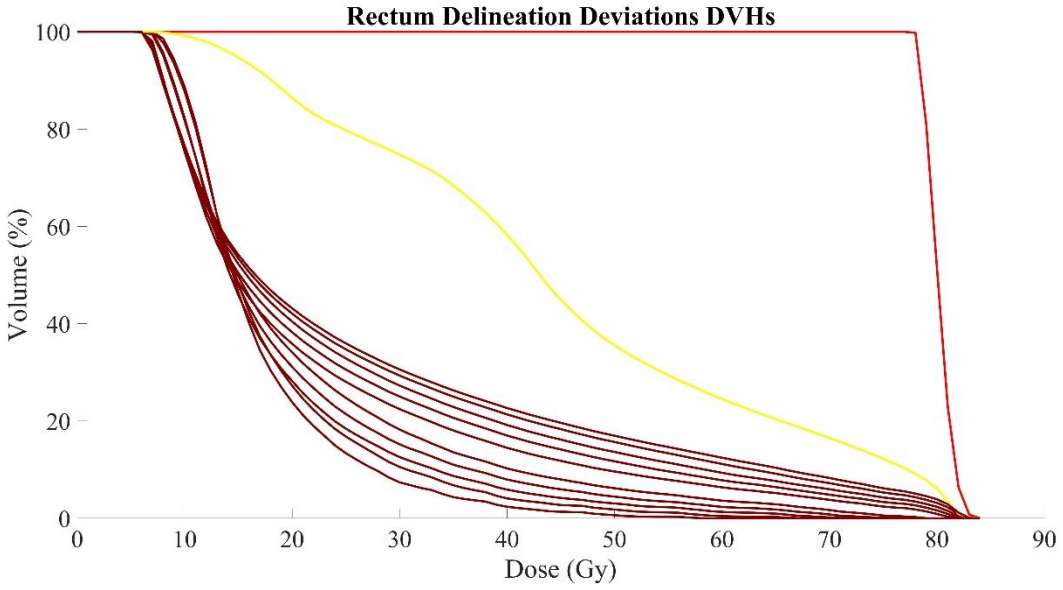

Figure 42. DVHs for contractions and expansions of the rectum in 1 mm increments.

For proximal rectum delineation deviations, the PRQs experienced similar behavior with the contraction PRQs growing in size and expansion PRQs shrinking in size. The max PRQ values increased from 86.51 % rising to 94.87 % with contractions and decreased from 76.65 % to 69.04 %. The dose the max occurred at increased with contractions beginning at 86.78 Gy rising to 95.55

Gy and decreased with expansion beginning at 81.90 Gy falling to 78.00 Gy. The PRQ value at the prescription dose slightly increased with contractions from 78.44 % to 79.08 % while it decreased for expansion from 76.60 % to 69.04 %. The FWHMs increased from 36.08 Gy to 49.73 Gy with contractions and decreased from 30.23 Gy to 25.35 Gy. The AUC increased with contractions from 33.19 kGy% to 48.39 kGy% and decreased from 26.62 kGy% to 19.76 kGy% with rectum proximal expansions.

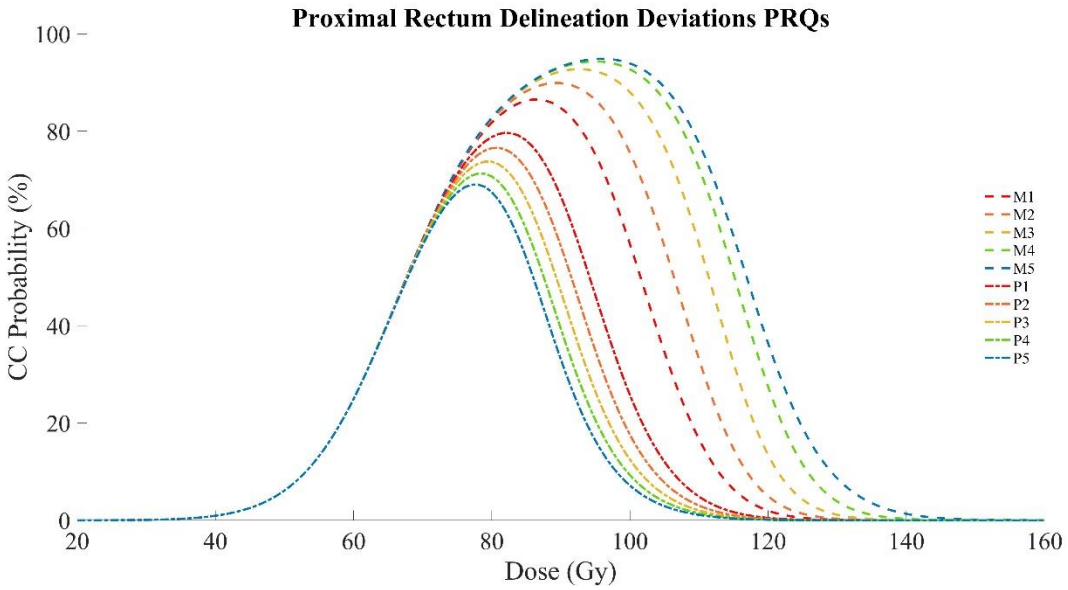

Figure 43. PRQs calculated when the Rectum is contracted and expanded in the directions proximal to the tumor in 1 mm increments.

Table 16. PRQ metrics as the Rectum is contracted and expanded in the directions proximal to the tumor in 1 mm increments.

	Max	Dose @ Max	Rx Dose	FWHM	AUC
M1	86.51	86.78	78.44	36.08	33.19
M2	89.91	89.70	78.84	40.95	37.62
M3	92.74	92.63	79.01	44.85	42.44
M4	94.32	94.58	79.07	47.78	46.26
M5	94.87	95.55	79.08	49.73	48.39
P1	79.65	81.90	76.60	30.23	26.62
P2	76.58	80.93	75.13	29.25	24.33
P3	73.73	78.98	73.30	27.30	22.47
P4	71.27	78.00	71.27	26.33	21.00
P5	69.04	78.00	69.04	25.35	19.76

The NTCPs for the rectum when it is contracted in the direction proximal to the tumor have a large shift right on the graph with an eventual decrease in slope by the 5 mm contraction rectum

NTCP. For each mm contraction the magnitude of the shift right increases. For proximal expansions NTCPs shift left on the graph with a decrease in the magnitude of the shift with each additional mm expansion.

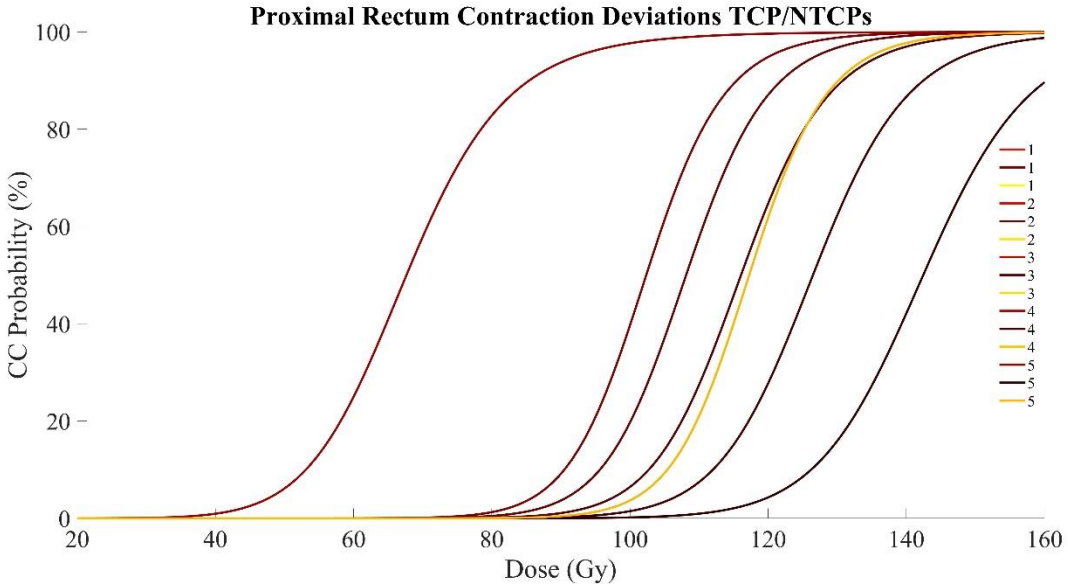

Figure 44. TCPs and NTCPs calculated as the Rectum is contracted in the directions proximal to the tumor in 1 mm increments.

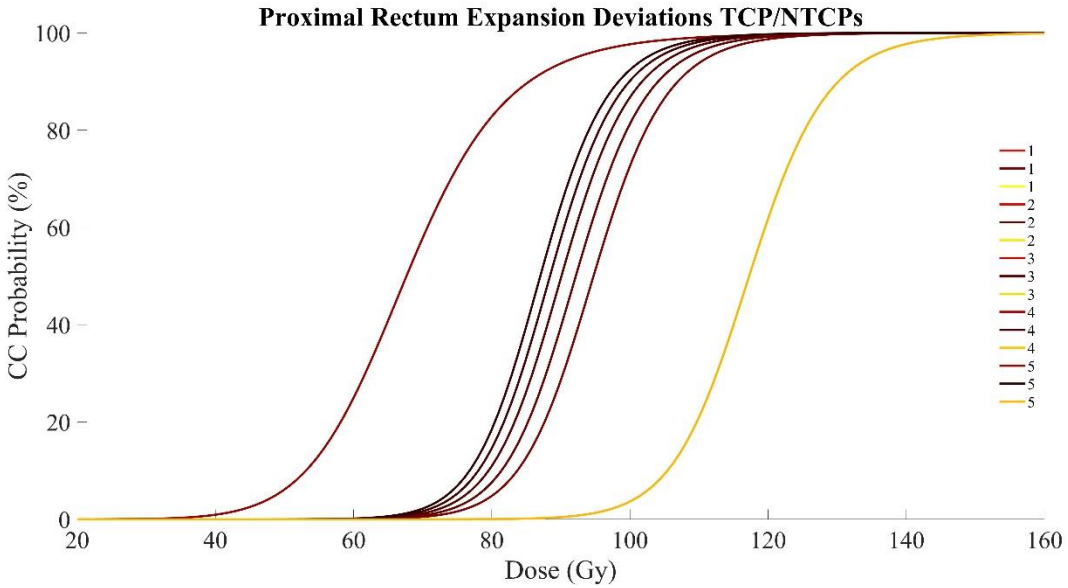

Figure 45. TCPs and NTCPs calculated as the Rectum is expanded in the directions proximal to the tumor in 1 mm increments.

Table 17. TCP and NTCP metrics calculated from rectum contractions and expansions in directions proximal to the tumor.

	Prostate CTV		Bladder		Rectum	
	50% Dose	80/20 Slope	50% Dose	80/20 Slope	50% Dose	80/20 Slope
M1	67.76	2.49	117.49	3.28	101.89	3.16
M2	67.76	2.49	117.49	3.28	107.74	3.04
M3	67.76	2.49	117.49	3.28	116.51	2.83
M4	67.76	2.49	117.49	3.28	126.26	2.56
M5	67.76	2.49	117.49	3.28	142.84	2.34
P1	67.76	2.49	117.49	3.28	95.06	3.42
P2	67.76	2.49	117.49	3.28	92.14	3.57
P3	67.76	2.49	117.49	3.28	90.19	3.57
P4	67.76	2.49	117.49	3.28	88.24	3.73
P5	67.76	2.49	117.49	3.28	87.26	3.73

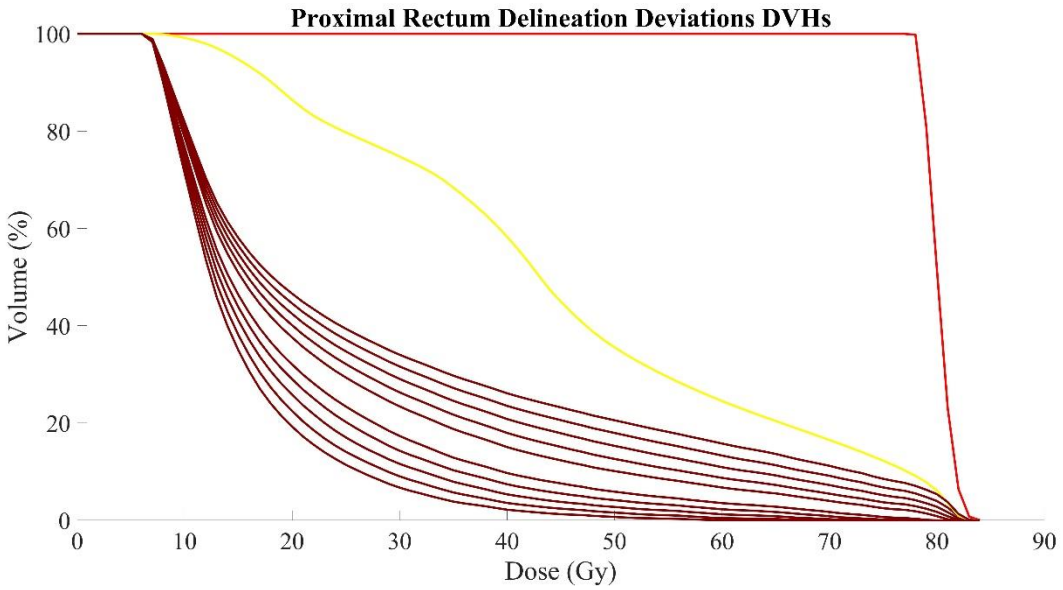

Figure 46. DVHs for contractions and expansions for the rectum in the direction proximal to the tumor.

Finally, the prostate CTV contours were contracted and expanded to calculate corresponding PRQs. An additional 5 mm expansion was applied making the largest prostate CTV expansion 10 mm. There was little change in PRQs with all contraction and expansions within ±5 mm. For 6 mm to 10 mm expansions however the PRQs effectively collapsed. The PRQ max values had an average of 82.64 ± 0.13 % for contractions. For 1 mm to 5 mm expansions PRQs max average was 83.13 ± 0.20 % and decreased from 80.92 % to 3.33 % for 6 mm to 10 mm expansions. The dose at which the max occurred was the same for all prostate CTV delineation

deviations within ±5 mm with a value of 83.85 Gy. The dose the max occurred at increased from 84.83 Gy to 95.55 Gy for 6 mm to 10 mm expansions. The PRQ value at the prescription dose slightly decreased with contractions from 77.41 % to 76.88 %. For expansions the values first slightly increased but then decreased from the 4 mm expansion on to 1.14 %. The FWHM for contractions was 33.15 Gy for the 1 mm contraction and 32.18 Gy for the rest. For expansions the FWHM values were 33.15 Gy for the first 6 expansions then decreased to 24.38 Gy for the last 3 expansions. The AUC slightly decreased for contractions from 29.38 kGy% to 29.16 kGy%. For expansions the AUC slightly increased but began to slightly decrease with the 4 mm expansion PRQ falling to 0.96 kGy%.

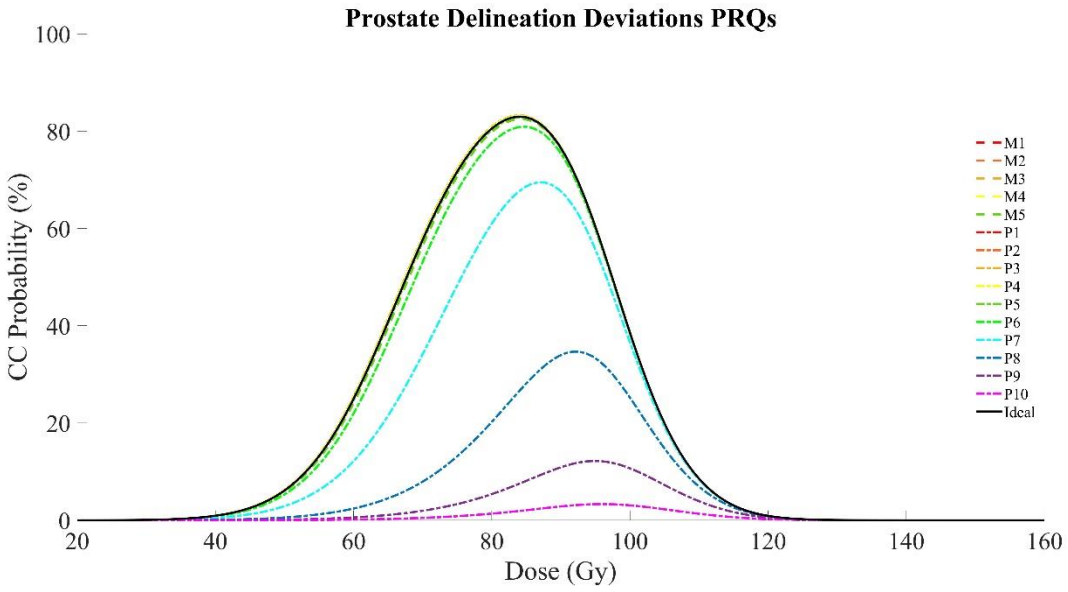

Figure 47. PRQs calculated when the Prostate CTV is contracted and expanded in 1 mm increments.

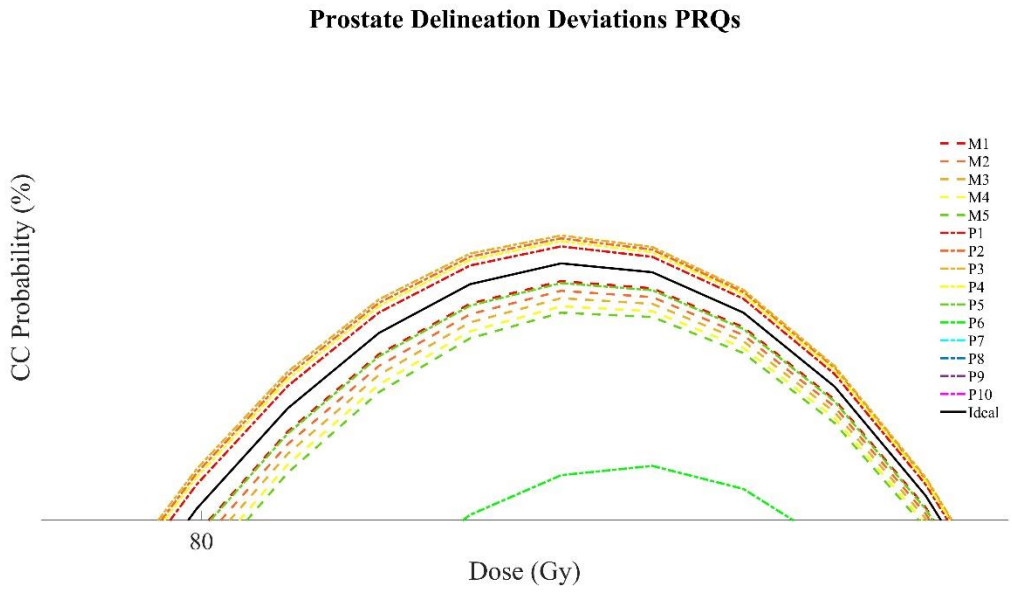

Figure 48. Magnified view of Prostate CTV delineation deviations PRQs.

Table 18. PRQ metrics as the Prostate CTV is contracted and expanded in 1 mm increments.

	Max	Dose @ Max	Rx Dose	FWHM	AUC
M1	82.81	83.85	77.41	33.15	29.38
M2	82.71	83.85	77.24	32.18	29.31
M3	82.63	83.85	77.12	32.18	29.26
M4	82.55	83.85	76.98	32.18	29.21
M5	82.48	83.85	76.88	32.18	29.16
P1	83.16	83.85	77.99	33.15	29.63
P2	83.24	83.85	78.13	33.15	29.68
P3	83.27	83.85	78.18	33.15	29.70
P4	83.21	83.85	78.08	33.15	29.66
P5	82.79	83.85	77.39	33.15	29.38
P6	80.92	84.83	74.32	33.15	28.22
P7	69.49	86.78	56.31	29.25	22.43
P8	34.66	92.63	17.20	24.38	9.83
P9	12.19	94.58	4.48	24.38	3.43
P10	3.33	95.55	1.14	24.38	0.96

TCPs for contractions were effectively unchanged meaning Figure 49 is similar to the ideal TCP and NTCP plot (Figure 19). For prostate CTV expansions up to 5 mm the TCPs remained effectively unchanged. From the 6 mm expansion on the TCPs experience larger shifts right with a decrease in slope.

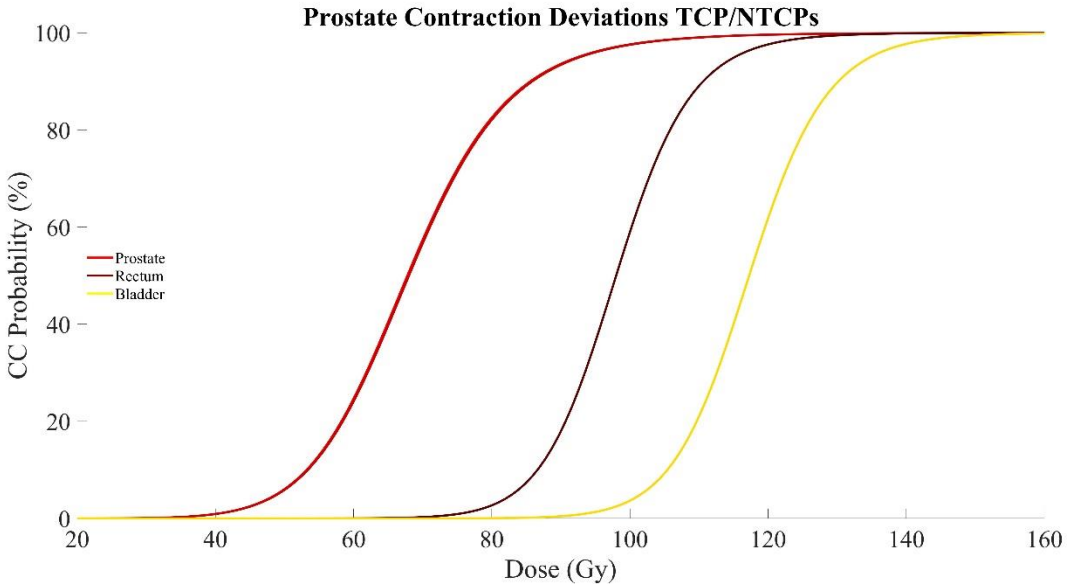

Figure 49. TCPs and NTCPs calculated as the Prostate CTV is contracted in 1 mm increments.

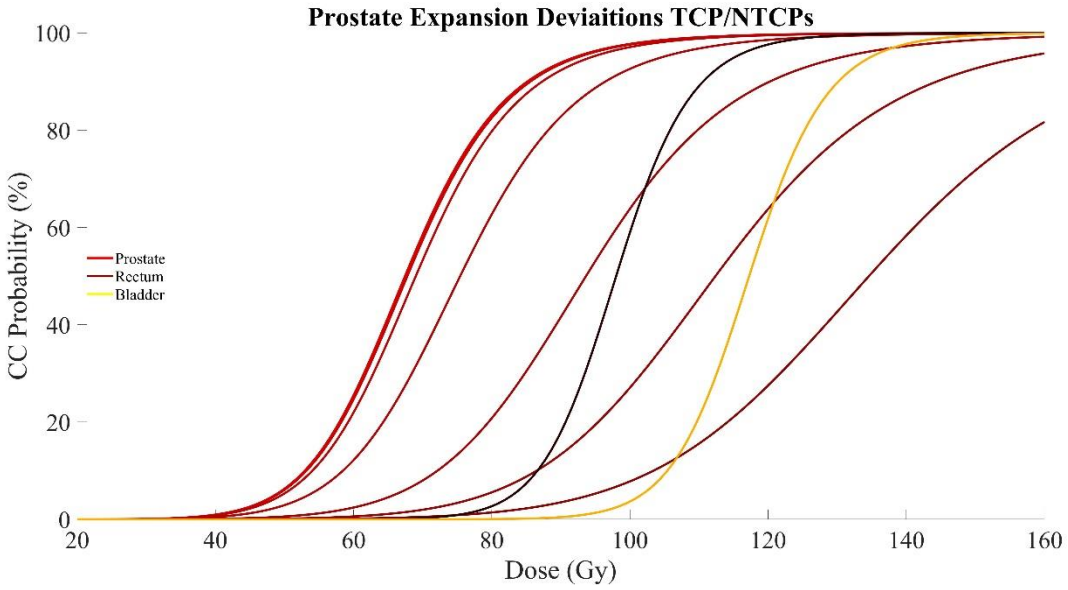

Figure 50. TCPs and NTCPs calculated as the Prostate CTV is expanded in 1 mm increments.

Table 19. TCP and NTCP metrics calculated from prostate CTV contractions and expansions.

	Prostate CTV		Bladder		Rectum	
	50% Dose	80/20 Slope	50% Dose	80/20 Slope	50% Dose	80/20 Slope
M1	67.76	2.49	117.49	3.28	97.99	3.28
M2	67.76	2.49	117.49	3.28	97.99	3.28
M3	67.76	2.49	117.49	3.28	97.99	3.28
M4	67.76	2.41	117.49	3.28	97.99	3.28
M5	67.76	2.41	117.49	3.28	97.99	3.28
P1	67.76	2.49	117.49	3.28	97.99	3.28
P2	67.76	2.49	117.49	3.28	97.99	3.28
P3	67.76	2.49	117.49	3.28	97.99	3.28
P4	67.76	2.49	117.49	3.28	97.99	3.28
P5	67.76	2.49	117.49	3.28	97.99	3.28
P6	68.74	2.41	117.49	3.28	97.99	3.28
P7	75.56	2.10	117.49	3.28	97.99	3.28
P8	94.09	1.64	117.49	3.28	97.99	3.28
P9	112.61	1.37	117.49	3.28	97.99	3.28
P10	135.04	1.16	117.49	3.28	97.99	3.28

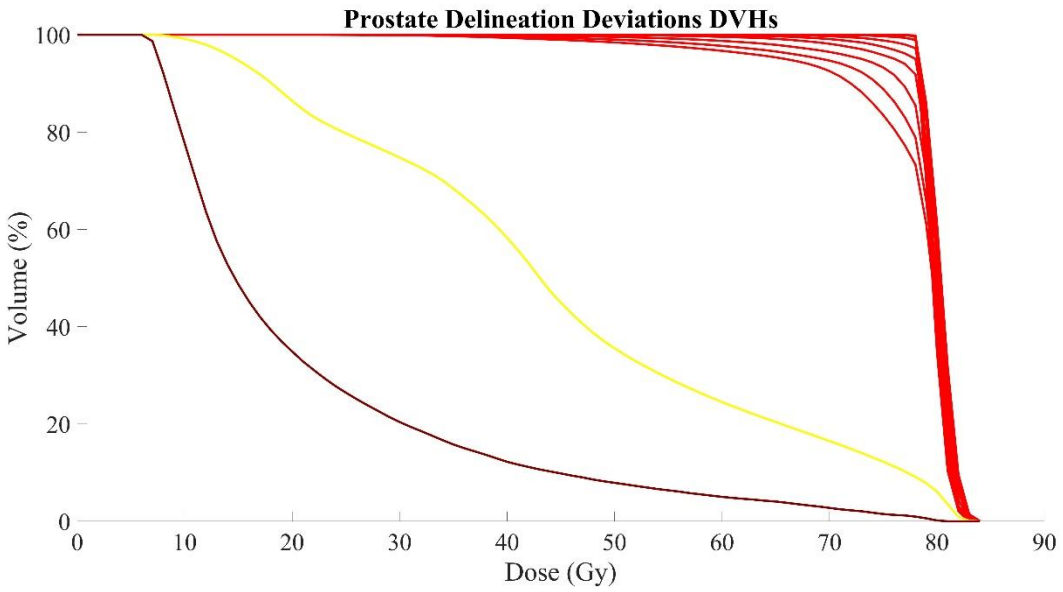

Figure 51. DVHs for contractions and expansions for the prostate CTV in 1 mm increments.

3.1.3 Geometric Deviation PRQs

Geometric deviations were the next set of treatment parameters variations evaluated. 26 directions were evaluated to include all cardinal direction “vectors” and interplanar “vectors”.

These are displayed in 13 sets of graphs as plots display shifts in equal and opposite directions. The first shifts are in the lateral direction (±x or patient right/left) and PRQs are plotted in mm increments for left and rights shifts. Left shifts are denoted by dashed lines while right shifts are denoted by dashed and dotted lines. For left and right shifts there are small differences in the PRQs which visually can be seen on the right side of the plot in Figure 52. Both sets of shifts PRQ max values decreases slightly as shifts increased with left shifts beginning at 82.91 % and finishing at 79.85 % while right shifts began at 83.02 % and ended at 82.22 %. The PRQ max occurred at 83.85 Gy for the first 5 deviations left and 82.88 Gy for the last 5 deviations left. The PRQ max occurred at 83.85 Gy for all right shifts. The PRQ value at the prescription dose also decreased slightly from 77.68 % to 76.33 % for left shifts and 77.72 % to 77.20 % for right shifts. The FWHM decreased for left shifts from 33.15 Gy to 31.20 Gy. The FWHM was 33.15 Gy for all rights shifts. The AUC slightly decreased for all shifts dropping from 29.42 kGy% to 26.92 kGy% for left shifts and 29.54 kGy% to 29.05 kGy% for right shifts.

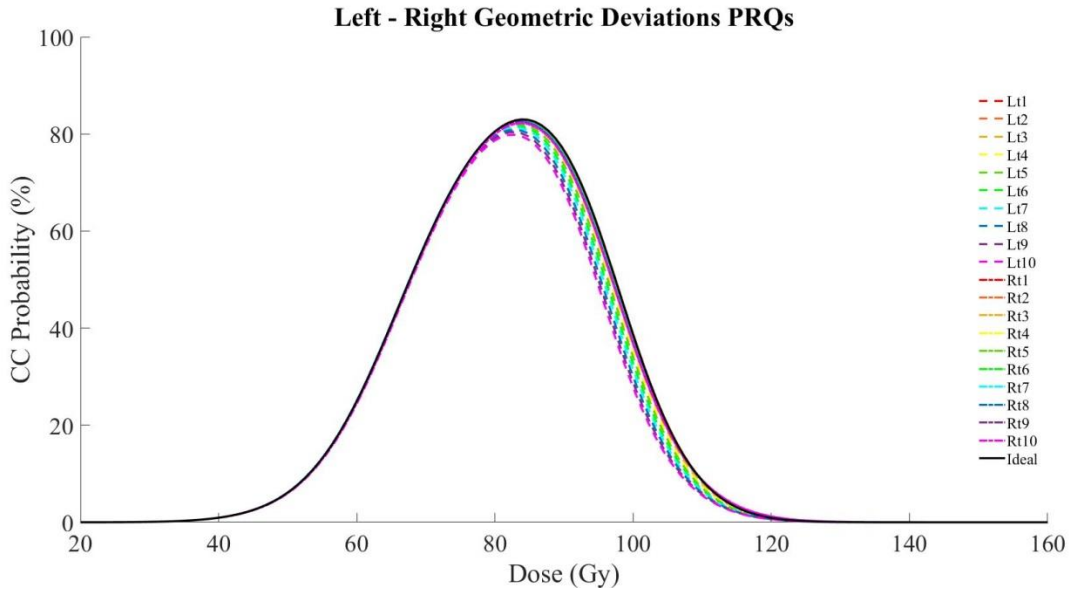

Figure 52. PRQs calculated for geometric deviations in the right and left directions in 1 mm increments.

Table 20. PRQ metrics for geometric deviations in the right and left directions in 1 mm increments.

	Max	Dose @ Max	Rx Dose	FWHM	AUC
L1	82.91	83.85	77.68	33.15	29.42
L2	82.79	83.85	77.66	33.15	29.31
L3	82.56	83.85	77.62	33.15	29.09
L4	82.29	83.85	77.58	33.15	28.84
L5	81.97	83.85	77.51	32.18	28.58
L6	81.65	82.88	77.42	32.18	28.29
L7	81.31	82.88	77.28	32.18	27.99
L8	80.87	82.88	77.08	31.20	27.64
L9	80.39	82.88	76.79	31.20	27.29
L10	79.85	82.88	76.33	31.20	26.92
R1	83.02	83.85	77.72	33.15	29.54
R2	82.99	83.85	77.72	33.15	29.53
R3	82.95	83.85	77.71	33.15	29.50
R4	82.86	83.85	77.70	33.15	29.43
R5	82.78	83.85	77.69	33.15	29.37
R6	82.69	83.85	77.69	33.15	29.31
R7	82.63	83.85	77.68	33.15	29.28
R8	82.54	83.85	77.62	33.15	29.23
R9	82.40	83.85	77.48	33.15	29.15
R10	82.22	83.85	77.20	33.15	29.05

The prostate CTV TCP is unchanged for lateral shifts of ±10 mm. For left shift deviations the bladder NTCP experiences a small shift right while the rectum NTCPs shift left. For right shift deviations the bladder NTCPs experiences a right shift while the rectum NTCPs have a tiny left shift.

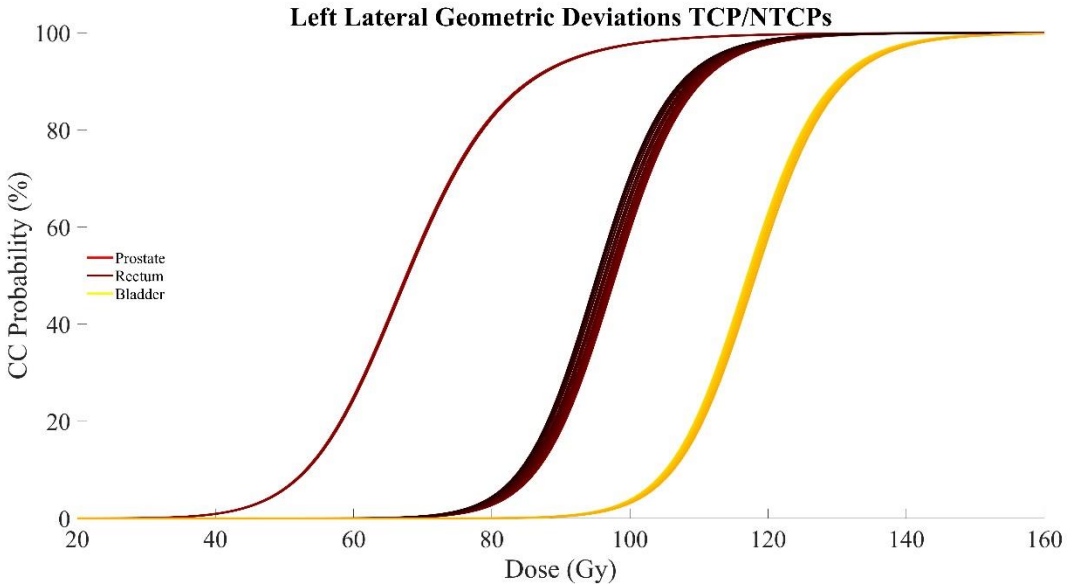

Figure 53. TCPs and NTCPs calculated for geometric deviations shifted right in 1 mm increments.

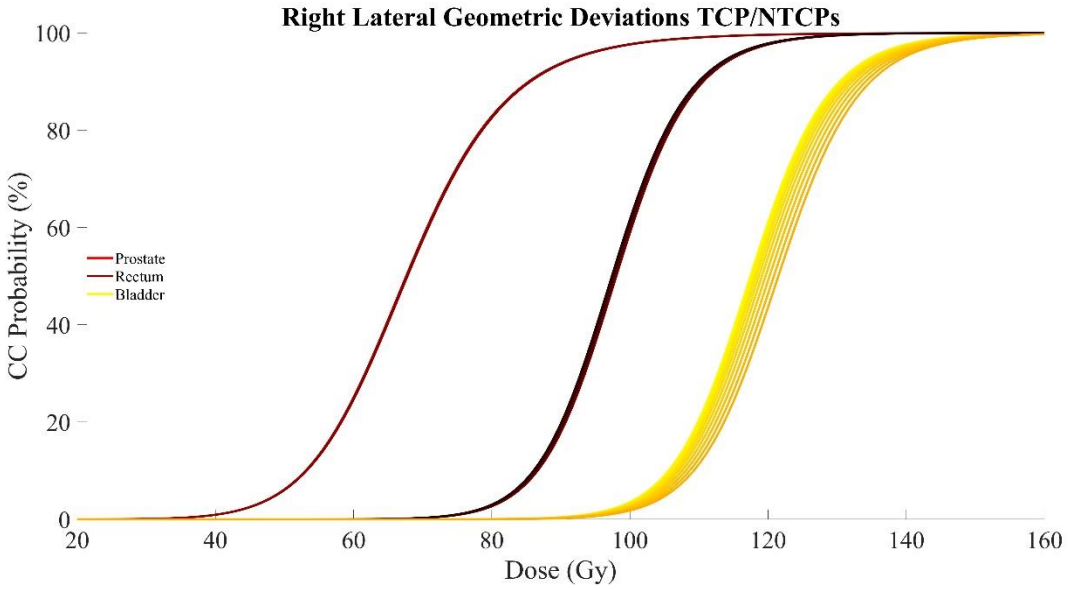

Figure 54. TCPs and NTCPs calculated for geometric deviations shifted left in 1 mm increments.

Table 21. TCP and NTCP metrics calculated from Left and Right geometric deviations.

	Prostate CTV		Bladder		Rectum	
	50% Dose	80/20 Slope	50% Dose	80/20 Slope	50% Dose	80/20 Slope
L1	67.76	2.49	117.49	3.28	97.99	3.28
L2	67.76	2.49	117.49	3.16	97.99	3.28
L3	67.76	2.49	117.49	3.16	97.99	3.42
L4	67.76	2.49	117.49	3.16	97.01	3.42
L5	67.76	2.49	117.49	3.16	97.01	3.28
L6	67.76	2.49	117.49	3.28	97.01	3.42
L7	67.76	2.49	117.49	3.28	96.04	3.42
L8	67.76	2.49	117.49	3.28	96.04	3.42
L9	67.76	2.49	117.49	3.16	95.06	3.42
L10	67.76	2.49	118.46	3.16	95.06	3.42
R1	67.76	2.49	117.49	3.28	97.99	3.28
R2	67.76	2.49	117.49	3.28	97.99	3.28
R3	67.76	2.49	117.49	3.16	97.99	3.28
R4	67.76	2.49	118.46	3.28	97.99	3.28
R5	67.76	2.49	118.46	3.16	97.99	3.28
R6	67.76	2.49	119.44	3.16	97.99	3.42
R7	67.76	2.49	119.44	3.16	97.99	3.42
R8	67.76	2.49	120.41	3.16	97.01	3.42
R9	67.76	2.49	120.41	3.16	97.01	3.42
R10	67.76	2.49	121.39	3.16	97.01	3.42

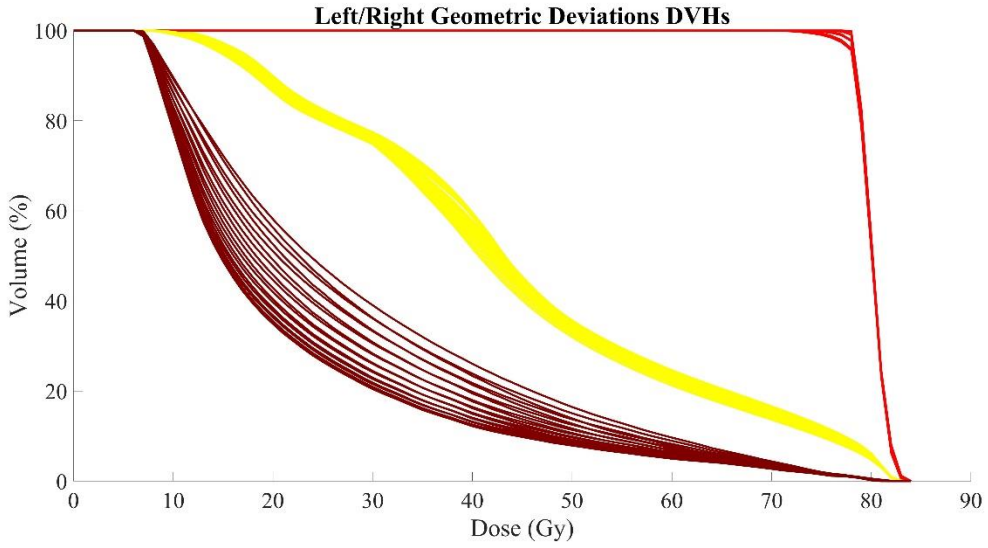

Figure 55. DVHs for left and right geometric deviations.

Next geometric deviations in the vertical direction (±y or patient anterior/posterior) were evaluated. Shifts in the anterior direction are represented by the dashed lines while posterior shifts are represented by dashed and dotted lines. Anterior shift deviation PRQs max value increased for

the first 3 mm than decreased from 4 mm on. The other 4 PRQ metrics followed similar behavior for anterior shift deviations. Please refer to Table 22 for quantitative specifics. Posterior shift PRQs

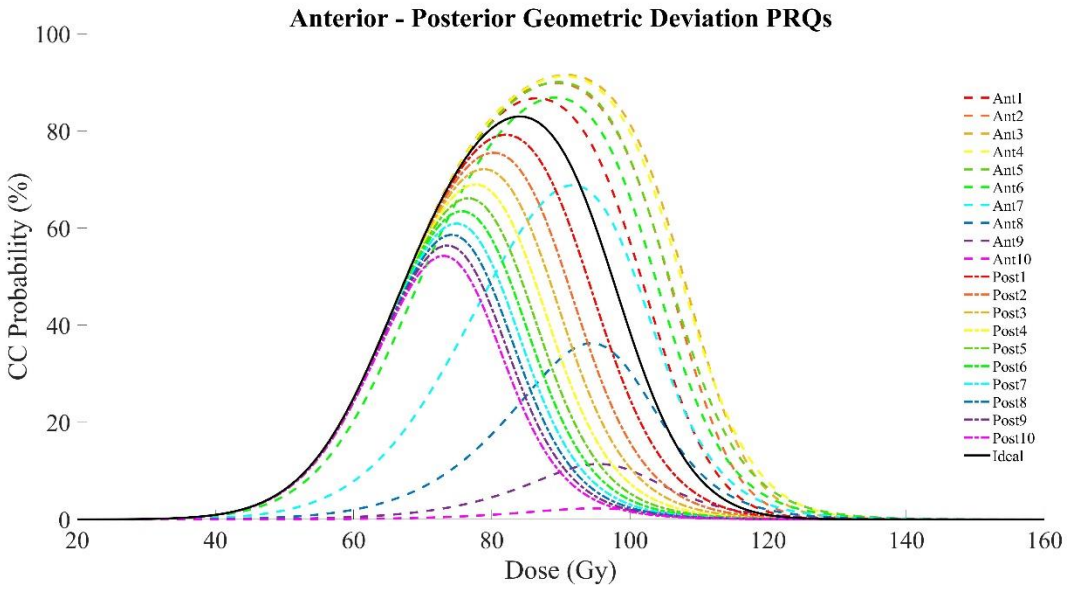

Figure 56. PRQs calculated for geometric deviations in the anterior and posterior directions in 1 mm increments.

Table 22. PRQ metrics geometric deviations in the anterior and posterior directions in 1 mm increments.

	Max	Dose @ Max	Rx Dose	FWHM	AUC
A1	86.73	86.78	78.52	36.08	33.15
A2	89.89	89.70	78.94	39.98	36.77
A3	91.52	90.68	79.07	40.95	39.06
A4	91.29	90.68	78.90	40.95	38.96
A5	90.07	89.70	78.04	39.00	37.17
A6	86.86	89.70	73.32	36.08	33.58
A7	68.84	91.65	43.94	29.25	22.43
A8	36.30	94.58	14.73	24.38	10.27
A9	11.42	95.55	3.77	23.40	3.18
A10	2.26	94.58	0.79	23.40	0.65
P1	79.23	81.90	76.39	30.23	26.37
P2	75.51	79.95	74.45	28.28	23.71
P3	72.16	78.98	71.99	26.33	21.59
P4	68.98	78.00	68.98	25.35	19.81
P5	66.11	77.03	65.60	24.38	18.34
P6	63.45	76.05	61.86	24.38	17.08
P7	60.95	75.08	57.87	23.40	15.96
P8	58.64	74.10	53.91	22.43	15.01
P9	56.39	73.13	50.02	22.43	14.16
P10	54.30	73.13	46.27	21.45	13.37

max values gradually decreased beginning at 79.23 % and ending at 54.30 %. The dose at the max value decreased from 81.90 Gy to 73.13 Gy. The PRQ value at the prescription dose decreased from 76.39 % to 46.27 %. The FWHM decreased from 30.23 Gy to 21.45 Gy while the AUC decreases as well from 26.37 kGy% to 13.37 kGy%.

TCPs for anterior shift deviations begin to shift right at 6 mm. They then experience large right shifts and decrease in slope. The bladder NTCPs experience a shift left with increased anterior deviations. The rectum NTCPs experience larger shifts right and decrease in slope with increased anterior deviations. For Posterior deviations the TCP is unchanged. The bladder NTCPs shift right as posterior deviations increase. The rectum NTCPs experience a smaller shift left decreasing in magnitude with increased posterior deviations.

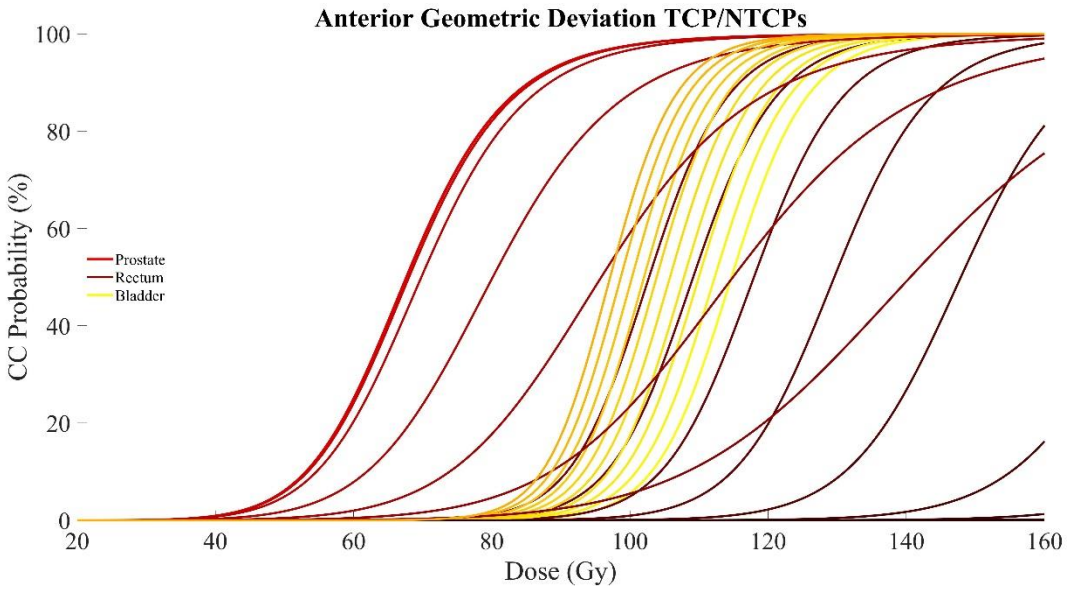

Figure 57. TCPs and NTCPs calculated for geometric deviations shifted anteriorly in 1 mm increments.

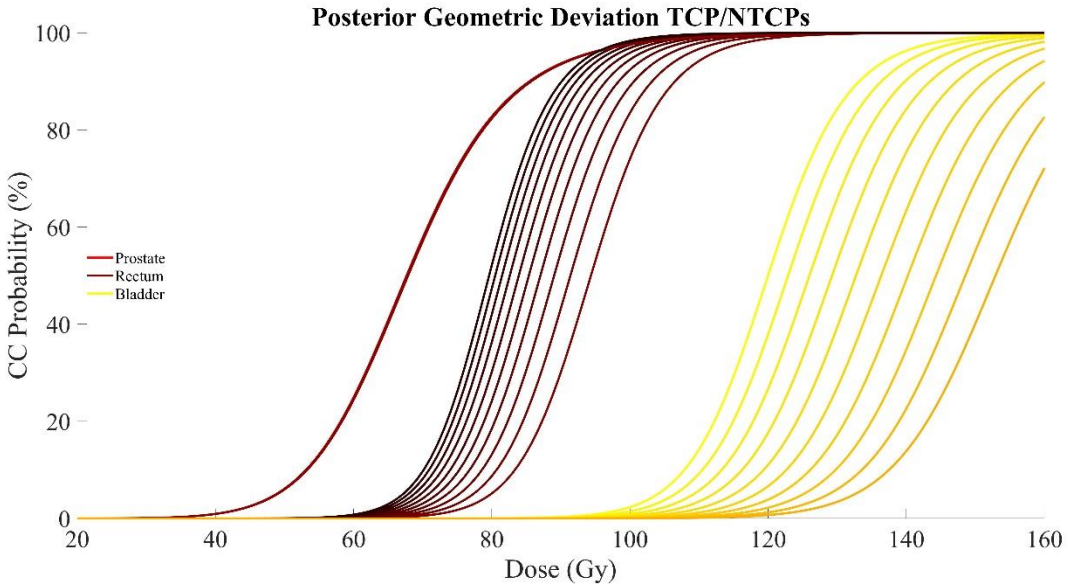

Figure 58. TCPs and NTCPs calculated for geometric deviations shifted posteriorly in 1 mm increments.

Table 23. TCP and NTCP metrics calculated from Anterior and Posterior geometric deviations.

	Prostate CTV		Bladder		Rectum	
	50% Dose	80/20 Slope	50% Dose	80/20 Slope	50% Dose	80/20 Slope
A1	67.76	2.49	114.56	3.28	102.86	3.28
A2	67.76	2.49	112.61	3.42	108.71	3.04
A3	67.76	2.49	109.69	3.42	117.49	2.83
A4	67.76	2.49	107.74	3.57	129.19	2.56
A5	67.76	2.41	105.79	3.57	147.71	2.28
A6	69.71	2.41	103.84	3.57	175.01	0.00
A7	80.44	1.95	101.89	3.73	0.00	0.00
A8	96.04	1.61	99.94	3.73	0.00	0.00
A9	114.56	1.35	98.96	3.73	0.00	0.00
A10	140.89	1.11	97.01	3.91	0.00	0.00
P1	67.76	2.49	120.41	3.16	94.09	3.42
P2	67.76	2.49	123.34	3.16	91.16	3.57
P3	67.76	2.49	126.26	3.04	89.21	3.57
P4	67.76	2.49	129.19	2.93	87.26	3.73
P5	67.76	2.49	133.09	2.83	85.31	3.91
P6	67.76	2.49	136.01	2.74	84.34	3.73
P7	67.76	2.49	139.91	2.74	82.39	3.91
P8	67.76	2.49	144.79	2.65	81.41	3.91
P9	67.76	2.49	148.69	2.56	80.44	3.91
P10	67.76	2.49	152.59	2.49	79.46	3.91

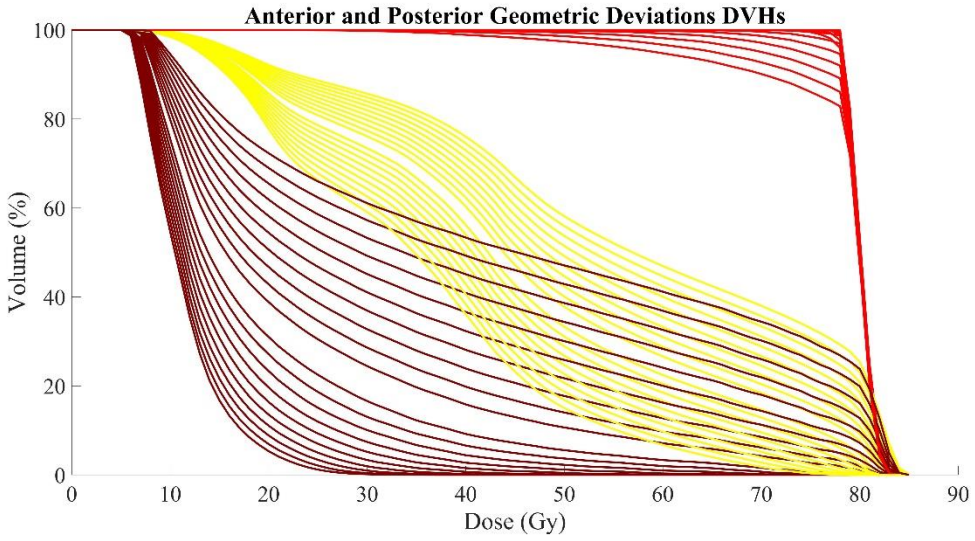

Figure 59. DVHs for anterior and posterior geometric deviations.

Longitudinal geometric deviations (±z or patient superior/inferior) evaluations followed. There was a subtle change in PRQs expect for the 8 mm to 10 mm superior deviations as can be seen in Figure 60. Inferior shifts are represented by dashed lines while superior shifts are represented by dashed and dotted lines. The PRQ max values for inferior deviations slightly decreased from 82.78 % to 82.00 %. Superior deviations PRQ max values had a small increase for the first 3 mm deviations then continued to decrease from there. At the 8 mm superior deviation the max dropped to 79.80 % falling to 19.79 % for the 10 mm deviation PRQ. The dose the max occurred at was 83.85 Gy for the first 6 and last deviation PRQS for inferior deviations. For superior deviations the dose the max occurred at was 83.85 Gy for the first 7 deviations then increased to 93.60 Gy. There was a minimal decrease then increase in PRQ value at the prescription dose for inferior deviations with an average value of 77.63 ± 0.03 %. The same behavior occurred for the first 7 superior deviations with the PRQ values at the prescription dose being 77.65 ± 0.16 %. From 8 mm to 10 mm the value dropped from 72.42 % to 8.17 %. The FWHM for inferior deviations was 33.15 Gy for the first 6 and 32.18 Gy to the remaining 4. The AUC slightly decreased for inferior deviations from 29.39 kGy% to 28.96 kGy%. For superior deviations the AUC decreased from 29.48 kGy% to 5.05 kGy% with the majority of the decreasing occurring from the 8 mm to 10 mm deviations.

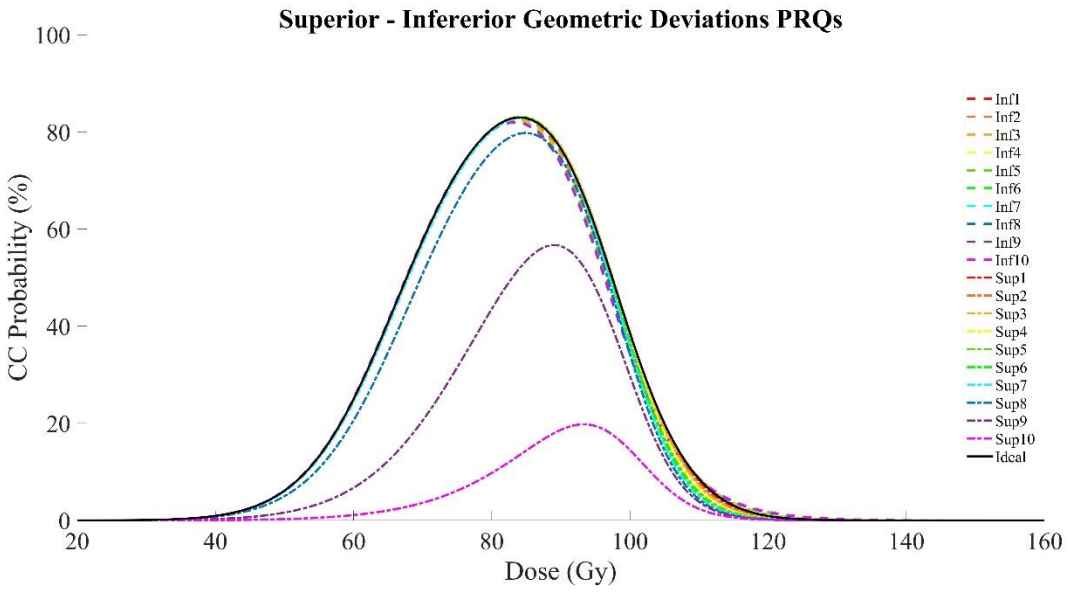

Figure 60. PRQs calculated for geometric deviations in the superior and inferior directions in 1 mm increments.

Table 24. PRQ metrics for geometric deviations in the superior and inferior directions in 1 mm increments.

	Max	Dose @ Max	Rx Dose	FWHM	AUC
I1	82.78	83.85	77.67	33.15	29.39
I2	82.67	83.85	77.67	33.15	29.34
I3	82.50	83.85	77.66	33.15	29.25
I4	82.24	83.85	77.61	33.15	29.05
I5	82.17	83.85	77.62	33.15	29.02
I6	82.04	83.85	77.61	33.15	28.93
I7	81.91	82.88	77.60	32.18	28.82
I8	81.96	82.88	77.62	32.18	28.88
I9	81.97	82.88	77.61	32.18	28.91
I10	82.00	83.85	77.61	32.18	28.96
S1	83.06	83.85	77.71	33.15	29.48
S2	83.05	83.85	77.68	33.15	29.37
S3	83.17	83.85	77.70	33.15	29.36
S4	83.11	83.85	77.66	33.15	29.17
S5	83.01	83.85	77.60	33.15	28.95
S6	83.02	83.85	77.55	33.15	28.84
S7	82.81	83.85	77.24	32.18	28.56
S8	79.80	84.83	72.42	31.20	26.65
S9	56.71	88.73	38.75	25.35	16.31
S10	19.79	93.60	8.17	21.45	5.05

There was no change in TCPs for inferior shifts. At the 8 mm superior deviation the TCPs shifted right with a decrease in slope. Bladder NTCPs experienced a shift right for inferior

deviations and a smaller shift left for superior deviations. For rectum NTCPs there was a small shift left for inferior deviations and a small shift right for superior deviations.

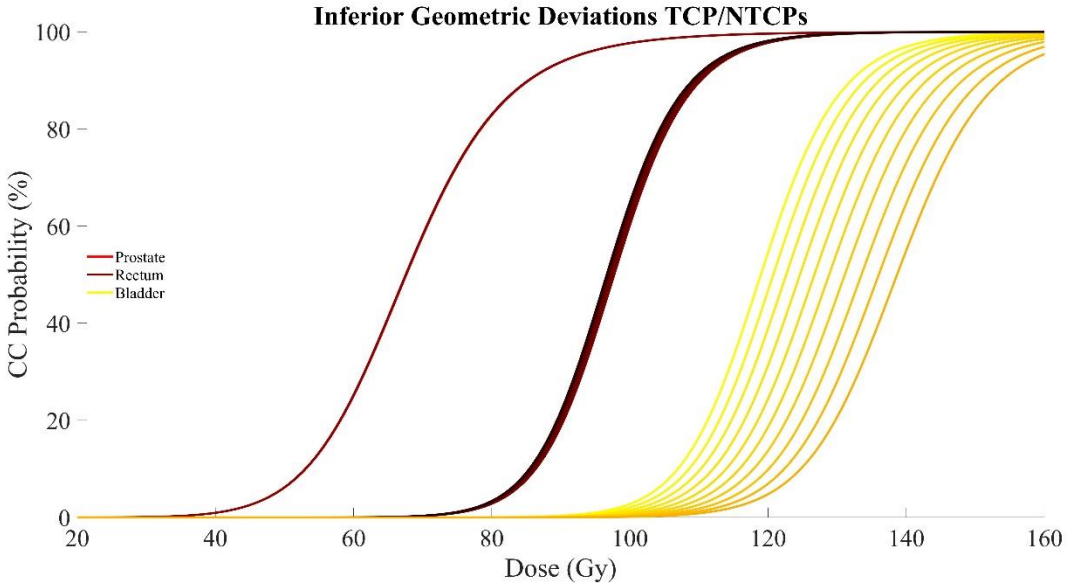

Figure 61. TCPs and NTCPs calculated for inferior geometric deviations in 1 mm increments.

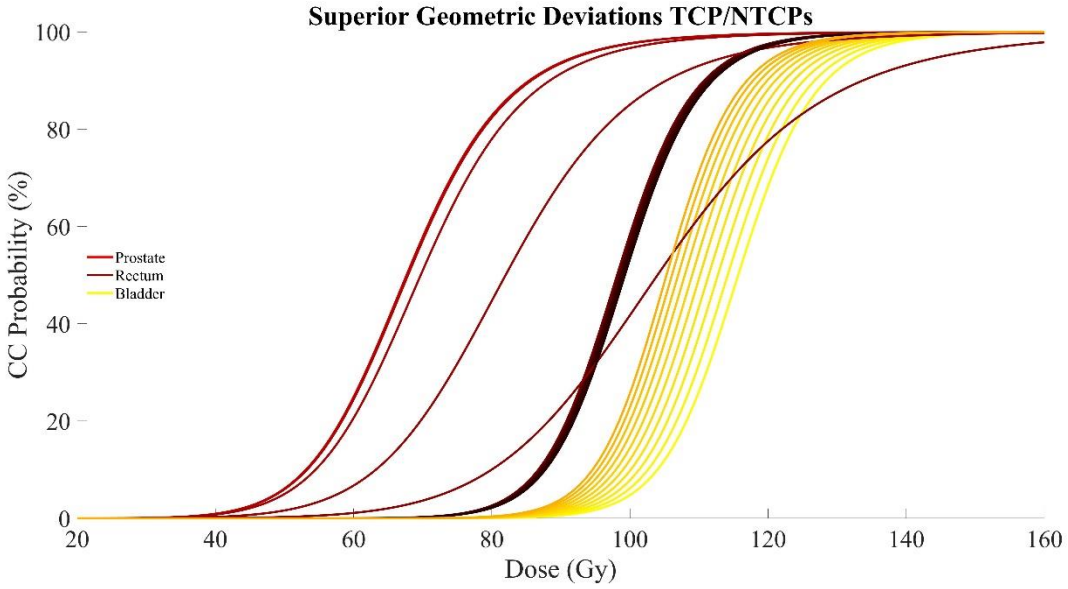

Figure 62. TCPs and NTCPs calculated for superior geometric deviations in 1 mm increments.

Table 25. TCP and NTCP metrics calculated from Superior and Inferior geometric deviations.

	Prostate CTV		Bladder		Rectum	
	50% Dose	80/20 Slope	50% Dose	80/20 Slope	50% Dose	80/20 Slope
I1	67.76	2.49	119.44	3.16	97.99	3.28
I2	67.76	2.49	120.41	3.16	97.99	3.42
I3	67.76	2.49	122.36	3.16	97.01	3.42
I4	67.76	2.49	124.31	3.04	97.01	3.28
I5	67.76	2.49	126.26	2.93	97.01	3.28
I6	67.76	2.49	129.19	2.93	97.01	3.28
I7	67.76	2.49	131.14	2.83	97.01	3.42
I8	67.76	2.49	133.09	2.93	97.01	3.42
I9	67.76	2.49	136.01	2.83	97.01	3.42
I10	67.76	2.49	138.94	2.74	97.01	3.42
S1	67.76	2.49	115.54	3.28	97.99	3.28
S2	67.76	2.49	114.56	3.42	97.99	3.42
S3	67.76	2.49	112.61	3.28	97.99	3.42
S4	67.76	2.49	111.64	3.42	97.99	3.42
S5	67.76	2.49	109.69	3.42	97.99	3.42
S6	67.76	2.49	108.71	3.42	98.96	3.28
S7	67.76	2.49	107.74	3.57	98.96	3.28
S8	69.71	2.34	106.76	3.57	98.96	3.28
S9	82.39	1.91	105.79	3.57	98.96	3.28
S10	103.84	1.49	104.81	3.73	98.96	3.42

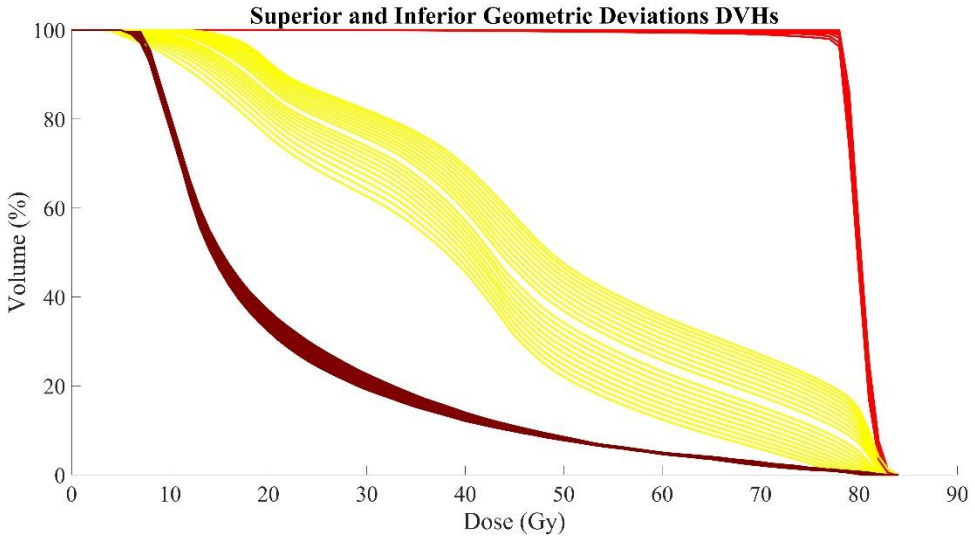

Figure 63. DVHs for superior and inferior geometric deviations.

Next shifts were applied in all directions simultaneously in 1 mm increments. This corresponded to equal magnitude shifts in the left, anterior, and inferior directions (Lt/Ant/Inf) and in the right, posterior, and superior directions (Rt/Post/Sup). The Lt/Ant/Inf shifts are denoted by dashed lines while the Rt/Post/Sup shifts are denoted by dashed and dotted lines. This is the first geometric deviation with a visual difference on the left side of the PRQ curves shown in Figure 64. The Lt/Ant/Inf PRQs experienced a reversal in behavior at the 5 mm deviation on. The PRQ max first increases from 86.46 % to 92.66 % then decreases to 22.41 % for Lt/Ant/Inf geometric deviations. The Rt/Post/Sup deviations PRQ max's decreased from 79.31 % to 0.65 %. The dose the max occurred at for Lt/Ant/Inf deviations increased from 86.78 Gy to 104.33 Gy. For Rt/Post/Sup deviations the dose the max occurred at decreased for the first 7 deviations (81.90 Gy to 76.05 Gy) then increased to 79.95 Gy. The FWHM for Lt/Ant/Inf deviations increase for the first mm deviations (36.08 Gy to 43.88 Gy) then decreased to 25.35 Gy. For Rt/Post/Sup deviations the FWHM decreased from 30.23 Gy to 21.45 Gy by the 9 mm deviation and was 23.40 Gy for the 10 mm deviation. The AUC increased from 33.01 kGy% to 41.87 kGy% for the first 5 Lt/Ant/Inf deviations then decreased to 6.68 kGy%. Rt/Post/Sup deviations AUC decreased from 26.40 kGy% to 0.18 kGy%.

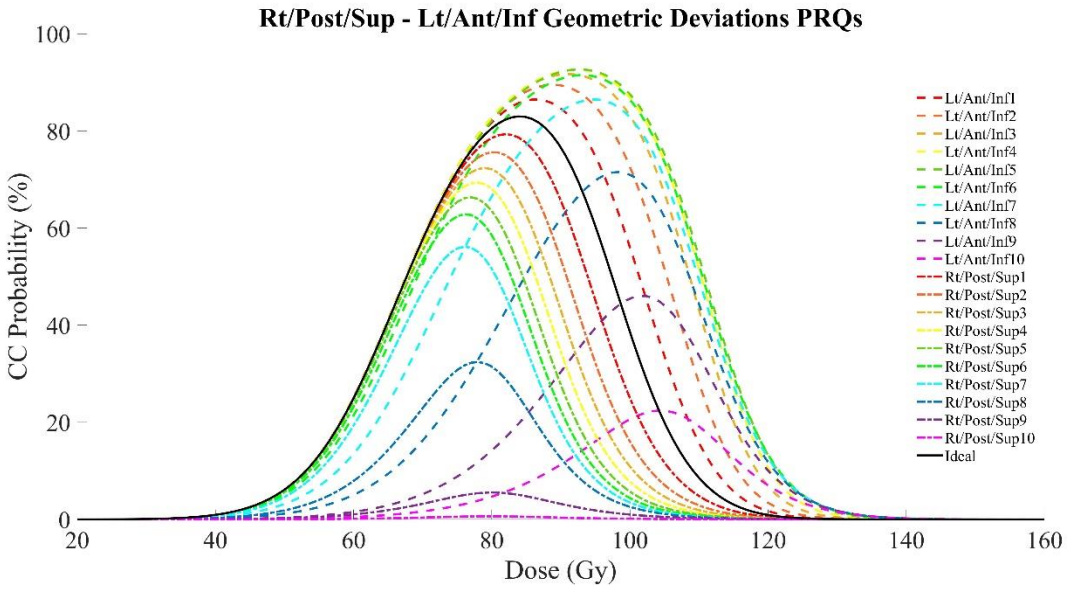

Figure 64. PRQs calculated for geometric deviations in the Right/Posterior/Superior and Left/Anterior/Inferior directions in 1 mm increments.

Table 26. PRQ metrics for geometric deviations in the Right/Posterior/Superior and Left/Anterior/Inferior directions in 1 mm increments.

	Max	Dose @ Max	Rx Dose	FWHM	AUC
L/A/I1	86.46	86.78	78.51	36.08	33.01
L/A/I2	89.51	88.73	78.99	39.98	36.66
L/A/I3	91.68	90.68	79.20	41.93	39.86
L/A/I4	92.60	92.63	79.12	42.90	41.51
L/A/I5	92.66	92.63	78.37	43.88	41.87
L/A/I6	91.47	92.63	74.97	42.90	40.36
L/A/I7	86.47	94.58	61.29	39.00	35.22
L/A/I8	71.53	98.48	32.83	31.20	25.17
L/A/I9	46.02	101.40	11.82	26.33	14.31
L/A/I10	22.41	104.33	3.85	25.35	6.68
R/P/S1	79.31	81.90	76.41	30.23	26.40
R/P/S2	75.60	79.95	74.49	29.25	23.74
R/P/S3	72.36	78.98	72.14	26.33	21.68
R/P/S4	69.36	78.00	69.36	26.33	20.00
R/P/S5	66.34	77.03	66.00	24.38	18.47
R/P/S6	62.85	76.05	61.91	23.40	16.95
R/P/S7	56.16	76.05	55.11	22.43	14.58
R/P/S8	32.42	78.00	32.42	21.45	8.03
R/P/S9	5.54	79.95	5.40	21.45	1.46
R/P/S10	0.65	79.95	0.63	23.40	0.18

Lt/Ant/Inf deviations TCPs experienced a large shift right with a decrease in slope from the 6 mm deviation on. The same behavior was seen for the Rt/Post/Sup deviations but the Lt/Ant/Inf deviations shift was more constant while the Rt/Post/Sup deviations shift increased in magnitude. The bladder NTCPs experienced a shift left for Lt/Ant/Inf deviations and a larger shift right with Rt/Post/Sup deviations. The rectum NTCPs experienced a shift right for Lt/Ant/Inf deviations and a shift left for Rt/Post/Sup deviations.

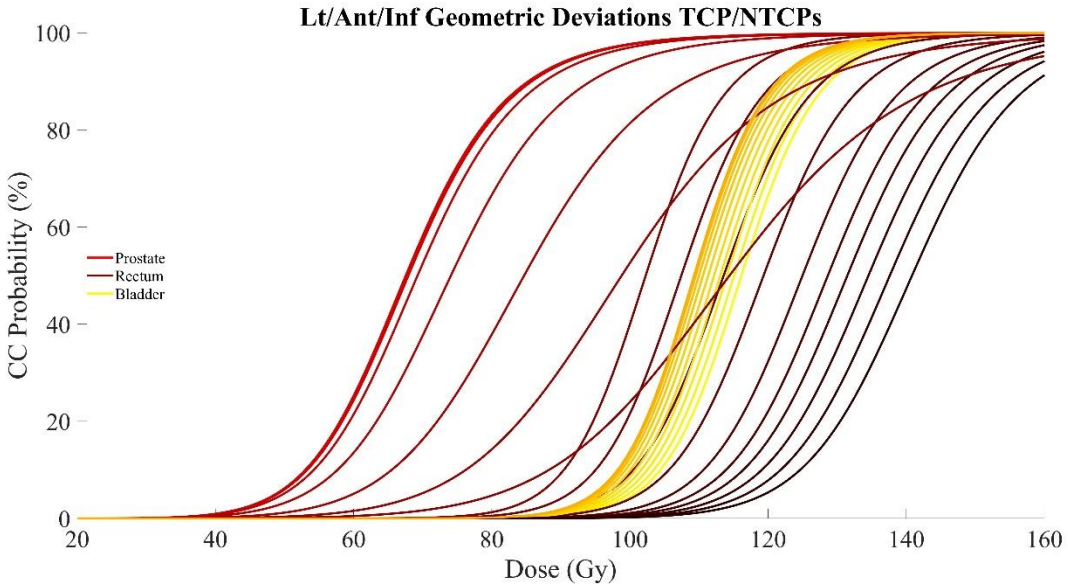

Figure 65. TCPs and NTCPs calculated for geometric deviations applied in negative directions of 1 mm increments.

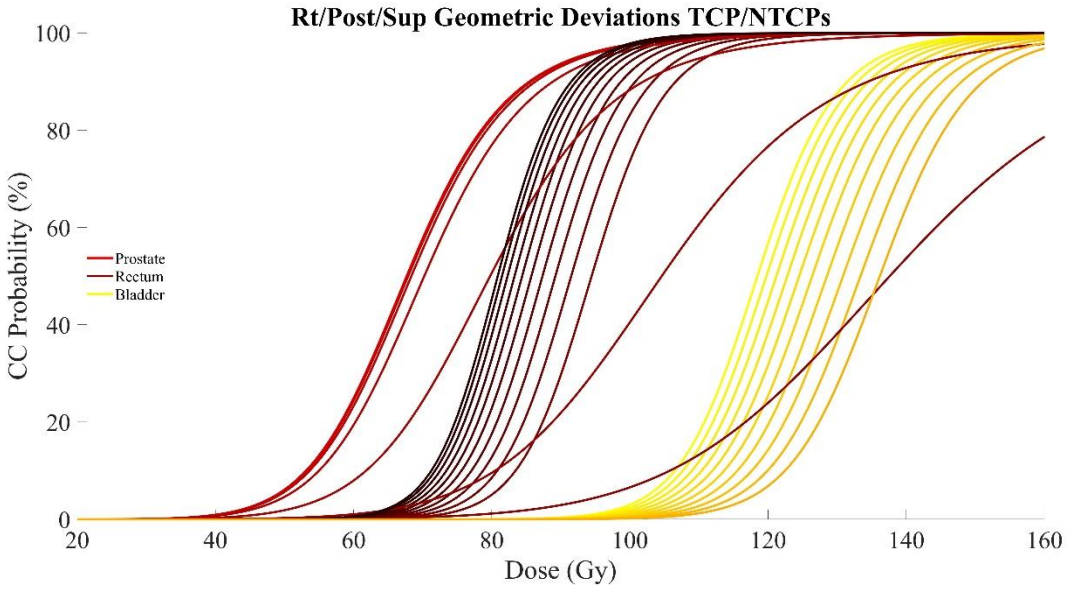

Figure 66. TCPs and NTCPs calculated for geometric deviations applied in positive direction of 1 mm increments.

Table 27. TCP and NTCP metrics calculated from Left/Anterior/Inferior and Right/Posterior/Superior geometric deviations.

	Prostate CTV		Bladder		Rectum	
	50% Dose	80/20 Slope	50% Dose	80/20 Slope	50% Dose	80/20 Slope
L/A/I1	67.76	2.49	116.51	3.28	101.89	3.16
L/A/I2	67.76	2.49	115.54	3.28	107.74	3.04
L/A/I3	67.76	2.49	113.59	3.42	113.59	2.93
L/A/I4	67.76	2.49	112.61	3.42	119.44	2.83
L/A/I5	67.76	2.49	112.61	3.42	125.29	2.65
L/A/I6	69.71	2.41	111.64	3.42	128.21	2.56
L/A/I7	73.61	2.22	110.66	3.42	131.14	2.56
L/A/I8	84.34	1.86	109.69	3.42	134.06	2.49
L/A/I9	98.96	1.61	109.69	3.42	137.96	2.34
L/A/I10	114.56	1.37	109.69	3.42	140.89	2.34
R/P/S1	67.76	2.49	118.46	3.28	94.09	3.42
R/P/S2	67.76	2.49	119.44	3.16	91.16	3.57
R/P/S3	67.76	2.49	121.39	3.16	89.21	3.57
R/P/S4	67.76	2.49	122.36	3.16	87.26	3.73
R/P/S5	67.76	2.49	124.31	3.04	85.31	3.73
R/P/S6	68.74	2.49	126.26	3.04	84.34	3.91
R/P/S7	70.69	2.34	128.21	2.93	83.36	3.91
R/P/S8	79.46	2.00	131.14	2.93	82.39	3.91
R/P/S9	104.81	1.49	133.09	2.93	81.41	3.91
R/P/S10	137.96	1.12	136.01	2.74	80.44	4.10

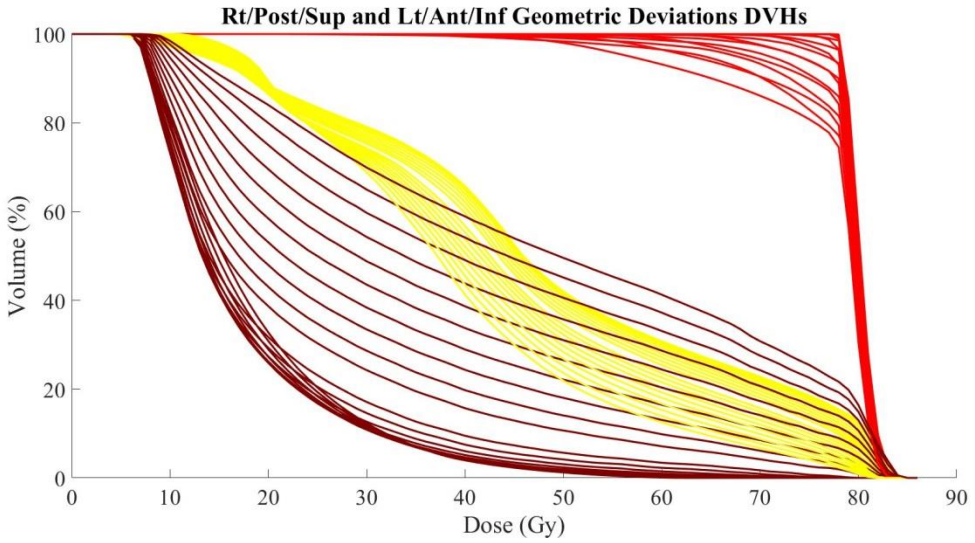

Figure 67. DVHs for Rt/Post/Sup and Lt/Ant/Inf geometric deviations.

The next set of geometric deviations evaluated consisted of shifts in 1 mm increments in the right, anterior, and inferior (Rt/Ant/Inf) direction and in the left, posterior, and superior (Lt/Post/Sup) direction. Lt/Post/Sup deviations are denoted by dashed lines while Rt/Ant/Inf

deviations are denoted by dashed and dotted lines. Similar behavior was observed as seen in the previous geometric deviations previously. Lt/Post/Sup deviation PRQ max values decreased from 79.20 % to 0.22 %. Rt/Ant/Inf deviations PRQs experienced a reversal in behavior from the 5 mm deviation on. The max values increased from 86.58 % to 93.57 % before decreasing to 3.40 %. The dose the max occurred at for Lt/Post/Sup deviations decreased for the first 6 deviations then increased for the remainder. For quantitative specifics please see Table 28. The dose the max occurred at for Rt/Ant/Inf deviations increased from 86.78 Gy to 109.20 Gy. The PRQ values at the prescription dose for Lt/Post/Sup deviations decreased from 76.36 % to 0.22 %. The PRQ values at the prescription dose for Rt/Ant/Inf deviations slightly increased for the first 3 deviations (78.53 % to 79.18 %) then decreased to 0.41 %. The FWHM for Lt/Post/Sup decreased from 30.23 Gy to 22.43 Gy. Rt/Ant/Inf deviations FWHMs increased for the first 5 deviations (36.08 Gy to 45.83 Gy) then decreased to 27.30 Gy. The AUC for Lt/Post/Sup deviations decreased from 26.30 kGy% to 0.06 kGy%. Rt/Ant/Inf deviations AUCs increased for the first 4 deviations (33.17 kGy% to 44.05 kGy%) then decreased to 1.11 kGy%.

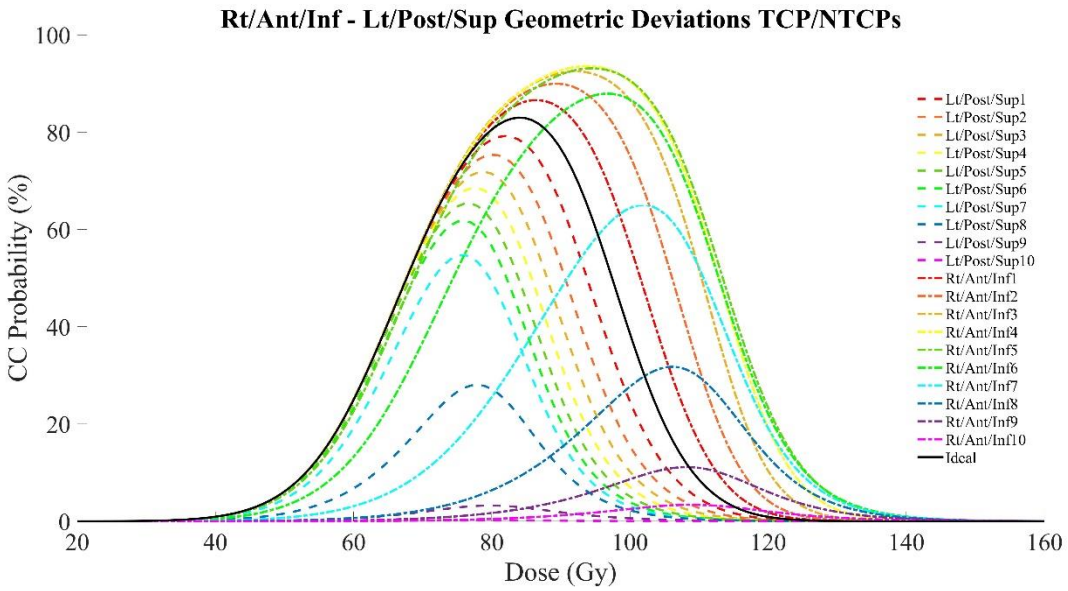

Figure 68. PRQs calculated for geometric deviations in the Right/Anterior/Inferior and Left/Posterior/Superior directions in 1mm increments.

Table 28. PRQ metrics for geometric deviations in the Right/Anterior/Inferior and Left/Posterior/Superior directions 1 mm increments.

	Max	Dose @ Max	Rx Dose	FWHM	AUC
R/A/I1	79.20	81.90	76.36	30.23	26.30
R/A/I2	75.35	79.95	74.33	28.28	23.55
R/A/I3	71.84	78.98	71.71	26.33	21.37
R/A/I4	68.49	78.00	68.49	25.35	19.55
R/A/I5	65.31	77.03	64.76	24.38	17.99
R/A/I6	61.80	76.05	60.43	23.40	16.47
R/A/I7	54.73	76.05	53.23	22.43	14.05
R/A/I8	28.05	78.00	28.05	21.45	6.92
R/A/I9	3.25	79.95	3.18	22.43	0.87
R/A/I10	0.22	78.98	0.22	22.43	0.06
L/P/S1	86.58	86.78	78.53	36.08	33.17
L/P/S2	89.95	89.70	79.01	39.98	37.40
L/P/S3	92.48	92.63	79.18	42.90	41.50
L/P/S4	93.57	93.60	78.89	45.83	44.05
L/P/S5	93.12	94.58	76.46	45.83	44.04
L/P/S6	87.92	96.53	60.30	40.95	38.05
L/P/S7	65.01	102.38	21.71	31.20	22.88
L/P/S8	31.78	106.28	5.26	26.33	9.97
L/P/S9	11.15	108.23	1.40	26.33	3.51
L/P/S10	3.40	109.20	0.41	27.30	1.11

The TCPs for Lt/Post/Sup deviations experienced a right shift from the 6 mm deviation on that increased in magnitude with increasing deviations. The TCPs for the Rt/Ant/Inf deviations experience a small right shift for the 6 mm deviation and larger right shifts with slight increases in magnitude for the remainder deviations. The bladder NTCPs experienced a right shift for Lt/Post/Sup deviations and a small left shift for Rt/Ant/Inf deviations. The rectum NTCPs experienced a left shift that decreased in magnitude with larger shifts in the Lt/Post/Sup deviations. For Rt/Ant/Inf deviations rectum NTCPs experienced a shift right that increased with magnitude with larger shifts.

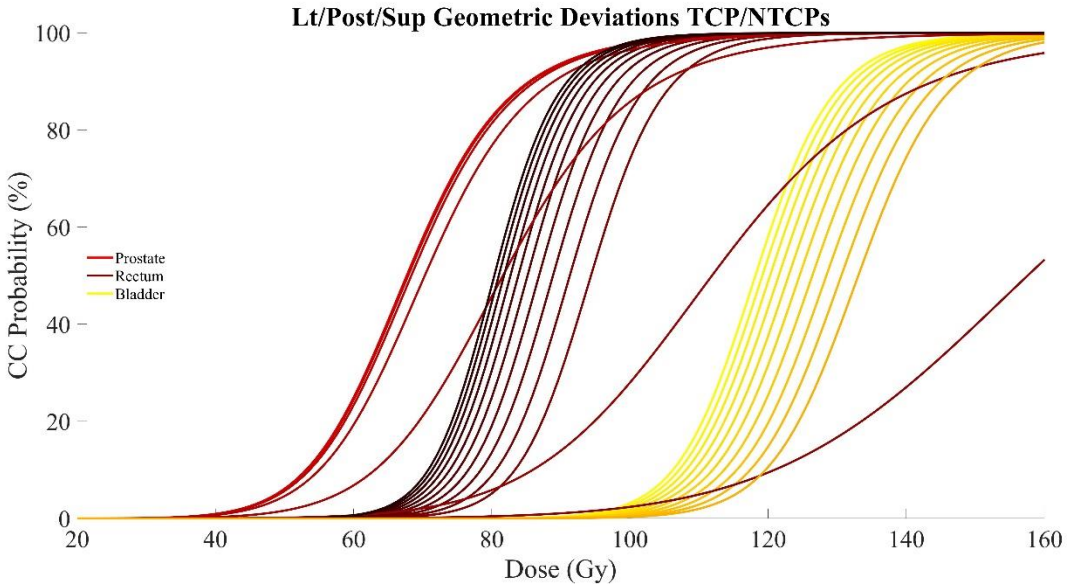

Figure 69. TCPs and NTCPs calculated for geometric deviations shifted to the patients left, posteriorly and superiorly in 1 mm increments.

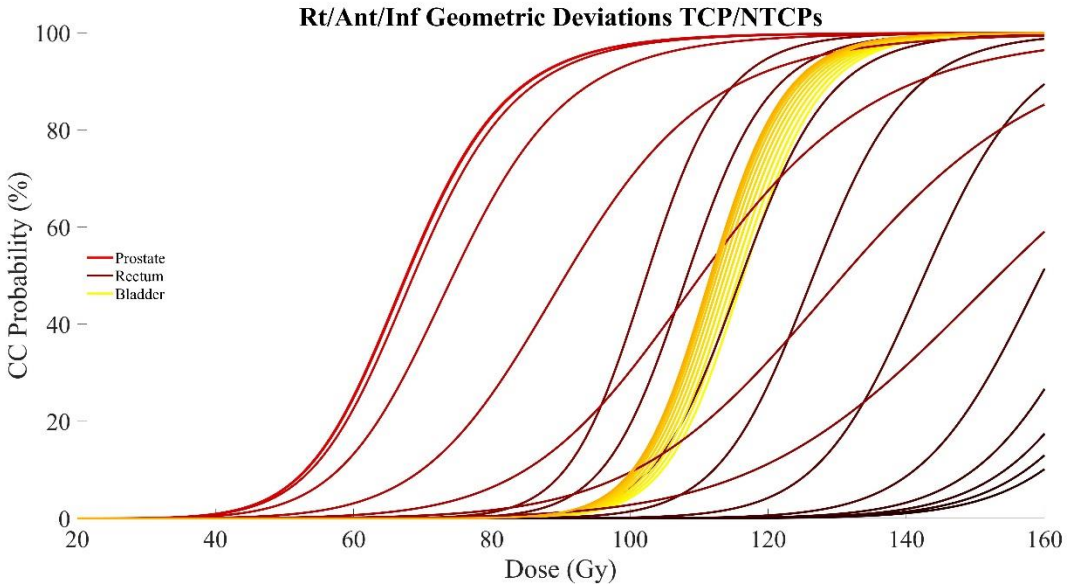

Figure 70. TCPs and NTCPs calculated for geometric deviations shifted to the patients right, anteriorly and inferiorly in 1 mm increments.

Table 29. TCP and NTCP metrics calculated from Left/Posterior/Superior and Right/Anterior/Inferior geometric deviations.

	Prostate CTV		Bladder		Rectum	
	50% Dose	80/20 Slope	50% Dose	80/20 Slope	50% Dose	80/20 Slope
R/A/I1	67.76	2.49	118.46	3.16	94.09	3.42
R/A/I2	67.76	2.49	119.44	3.16	91.16	3.57
R/A/I3	67.76	2.49	120.41	3.16	89.21	3.73
R/A/I4	67.76	2.49	121.39	3.16	87.26	3.73
R/A/I5	67.76	2.49	123.34	3.04	85.31	3.91
R/A/I6	68.74	2.49	124.31	3.04	83.36	3.73
R/A/I7	70.69	2.34	126.26	3.04	82.39	3.91
R/A/I8	81.41	1.91	128.21	2.93	81.41	3.91
R/A/I9	111.64	1.39	130.16	2.93	81.41	3.91
R/A/I10	157.46	0.00	133.09	2.83	80.44	3.91
L/P/S1	67.76	2.49	116.51	3.28	102.86	3.16
L/P/S2	67.76	2.49	115.54	3.28	108.71	3.04
L/P/S3	67.76	2.49	114.56	3.42	116.51	2.83
L/P/S4	67.76	2.49	114.56	3.28	126.26	2.65
L/P/S5	68.74	2.41	113.59	3.28	142.84	2.34
L/P/S6	74.59	2.16	113.59	3.42	159.41	2.05
L/P/S7	91.16	1.71	112.61	3.28	169.16	1.95
L/P/S8	110.66	1.41	112.61	3.42	174.04	0.00
L/P/S9	131.14	1.19	111.64	3.42	177.94	0.00
L/P/S10	153.56	0.00	111.64	3.28	180.86	0.00

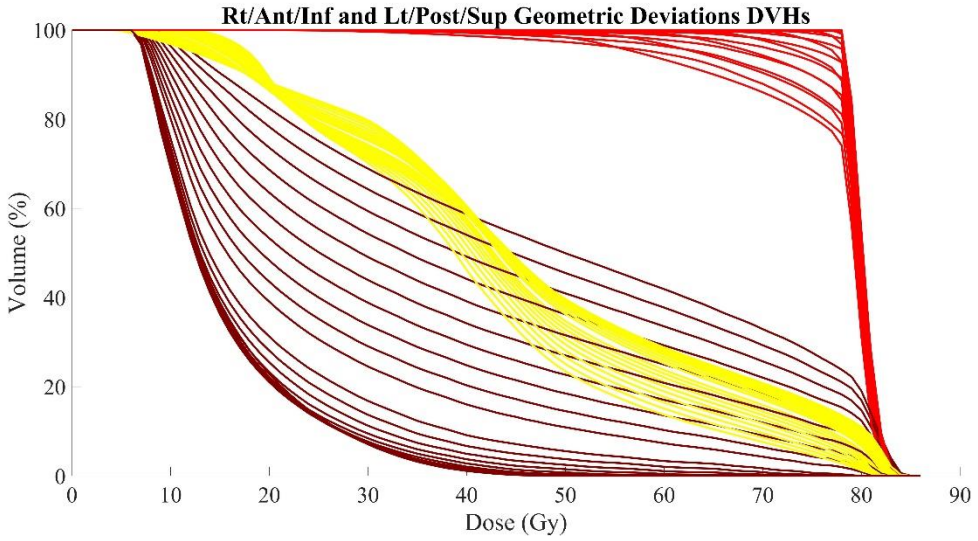

Figure 71. DVHs for Rt/Ant/Inf and Lt/Post/Sup geometric deviations.

Right, posterior, and inferior (Rt/Post/Inf) and left, anterior, and superior (Lt/Ant/Sup) geometric deviations evaluations followed. Lt/Ant/Sup deviations are denoted with dashed lines while Rt/Post/Inf deviations are denoted with dashed and dotted lines. The Lt/Ant/Sup deviation

PRQs experienced a reversal in behavior from the 4 mm deviation on. The Rt/Post/Inf deviations PRQ max values decreased from 79.08 % to 26.88 %. Lt/Ant/Sup deviations PRQ max values increased from 86.76 % to 90.03 % then fell to 1.09 %. The dose that Rt/Post/Inf deviations PRQ max values occurred at decreased from 81.90 Gy to 75.08 Gy then increased for the last deviation to 76.05 Gy. The dose at which the max occurred for Lt/Ant/Sup deviations fluctuated between 86.78 Gy and 90.68 Gy: please refer to Table 30 for specific values. The PRQ values at the prescription dose decreased for Rt/Post/Inf deviations from 76.36 % to 26.17 %. Lt/Ant/Sup deviation PRQ values at the prescription dose slightly increased for the first 3 mm (78.50 % to 78.92 %) and decreased to 0.59 %. The FWHM decreased for Rt/Post/Inf deviations beginning at 30.23 Gy and ending at 20.48 Gy by the 10 mm deviation. The FWHM decreased for Lt/Ant/Sup deviations increased from 36.08 Gy to 39.00 Gy for the first 3 mm then decreased to 22.43 Gy by the 10 mm deviation. The AUC followed similar behavior decreasing from 26.29 kGy% to 6.40 kGy% for Rt/Post/Inf deviations and began at 32.99 kGy% rising to 36.41 kGy% before falling to 0.30 kGy% for Lt/Ant/Sup deviations.

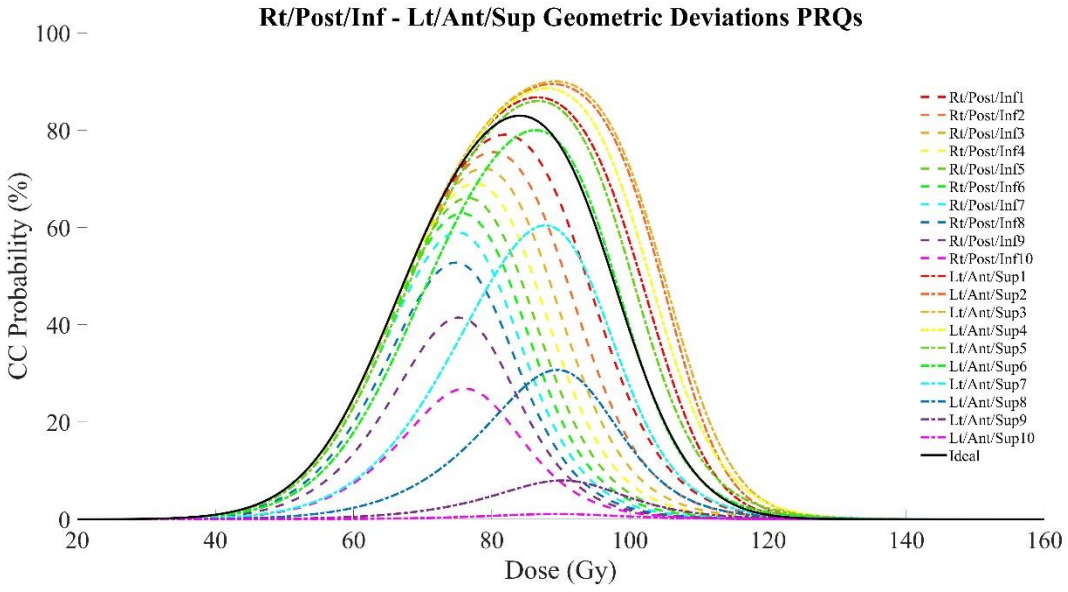

Figure 72. PRQs calculated for geometric deviations in the Right/Posterior/Inferior and Left/Anterior/Superior directions in 1mm increments.

Table 30. PRQ metrics for geometric deviations in the Right/Posterior/Inferior and Left/Anterior/Superior directions in 1 mm increments.

	Max	Dose @ Max	Rx Dose	FWHM	AUC
R/P/I1	79.08	81.90	76.36	30.23	26.29
R/P/I2	75.51	79.95	74.49	28.28	23.73
R/P/I3	72.16	78.98	72.02	26.33	21.60
R/P/I4	69.04	78.00	69.04	25.35	19.84
R/P/I5	66.04	77.03	65.49	24.38	18.31
R/P/I6	62.90	76.05	61.31	23.40	16.87
R/P/I7	59.04	75.08	56.29	23.40	15.33
R/P/I8	52.80	75.08	49.62	21.45	13.25
R/P/I9	41.48	75.08	39.39	20.48	10.05
R/P/I10	26.88	76.05	26.17	20.48	6.40
L/A/S1	86.76	86.78	78.50	36.08	32.99
L/A/S2	89.49	88.73	78.88	39.00	35.70
L/A/S3	90.03	88.73	78.92	39.00	36.41
L/A/S4	88.61	87.75	78.49	37.05	34.59
L/A/S5	86.00	86.78	76.65	34.13	31.62
L/A/S6	79.97	86.78	69.37	31.20	26.95
L/A/S7	60.45	87.75	44.16	25.35	17.62
L/A/S8	30.72	89.70	17.28	22.43	8.08
L/A/S9	7.98	90.68	3.98	21.45	2.12
L/A/S10	1.09	89.70	0.59	22.43	0.30

The TCPs for Rt/Post/Inf geometric deviations began shifting right at the 7 mm deviation and increased in magnitude with larger deviations. Lt/Ant/Sup deviation TCPs began shifting left with the 5 mm deviation and increased in magnitude with larger deviations. The bladder NTCPs for Rt/Post/Inf geometric deviations shifted right with an eventual decrease in slope. The bladder NTCPs had a shift to the left that decreased in magnitudes with larger deviations and had a slight increase in slope for Lt/Ant/Sup geometric deviations. Rt/Post/Inf geometric deviations rectum NTCPs shifted left decreasing in magnitude with larger deviations. Lt/Ant/Sup geometric deviations rectum NTCPs had a large shift right increasing in magnitude with larger deviations and eventually decreasing in slope.

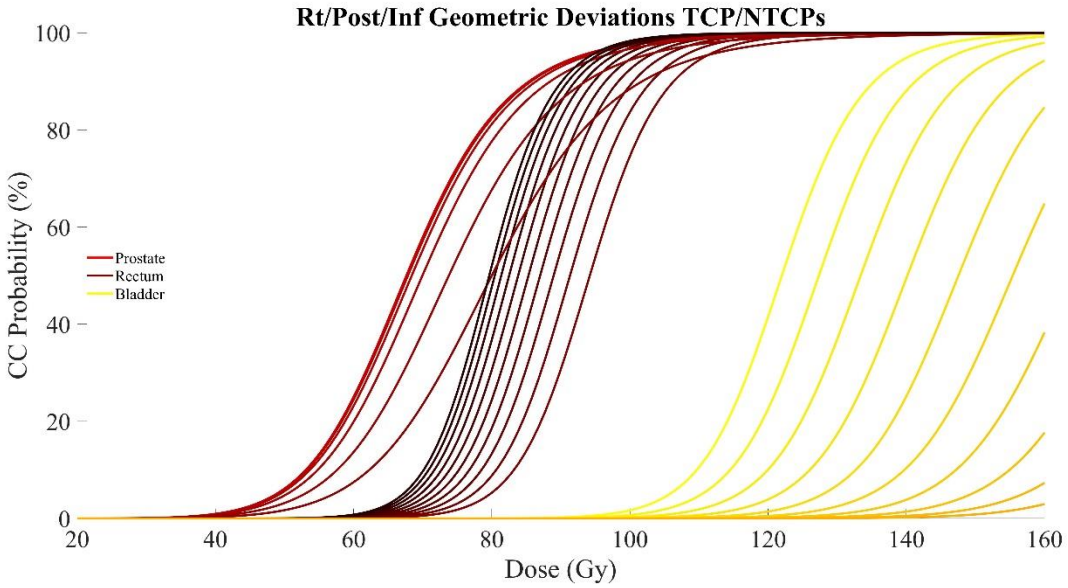

Figure 73. TCPs and NTCPs calculated for geometric deviations shifted to the patients right, posteriorly and inferiorly in 1 mm increments.

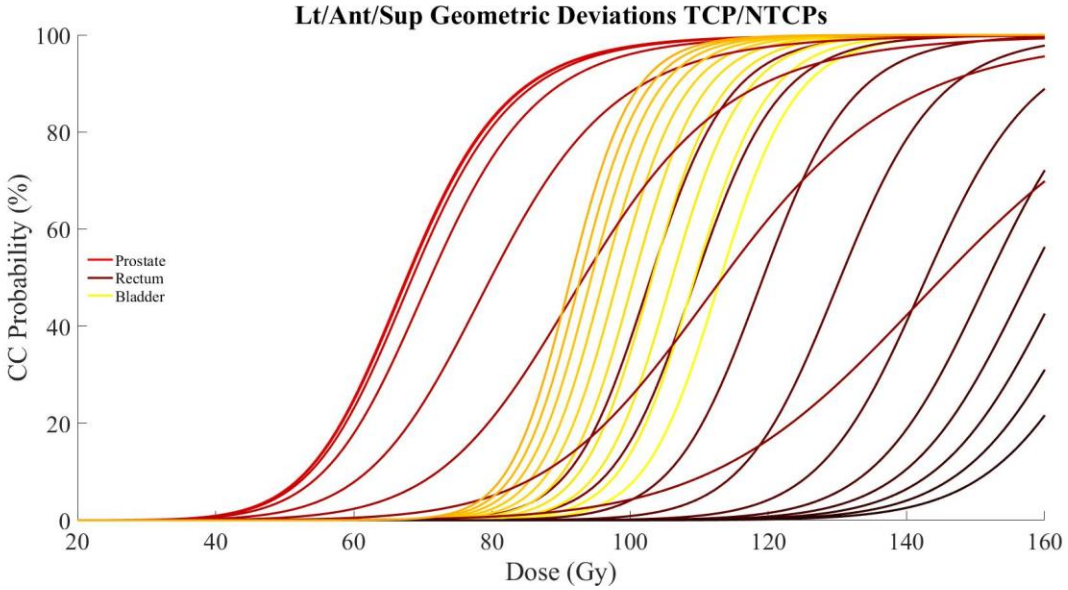

Figure 74. TCPs and NTCPs calculated for geometric deviations shifted to the patients left, anteriorly and superiorly in 1 mm increments.

Table 31. TCP and NTCP metrics calculated from Right/Posterior/Inferior and Left/Anterior/Superior geometric deviations.

	Prostate CTV		Bladder		Rectum	
	50% Dose	80/20 Slope	50% Dose	80/20 Slope	50% Dose	80/20 Slope
R/P/I1	67.76	2.49	122.36	3.16	94.09	3.42
R/P/I2	67.76	2.49	127.24	3.04	91.16	3.57
R/P/I3	67.76	2.49	133.09	2.93	89.21	3.57
R/P/I4	67.76	2.49	139.91	2.74	87.26	3.73
R/P/I5	67.76	2.49	147.71	2.65	85.31	3.91
R/P/I6	67.76	2.49	155.51	2.49	83.36	3.73
R/P/I7	68.74	2.49	163.31	2.28	82.39	3.91
R/P/I8	69.71	2.41	172.09	2.16	81.41	3.91
R/P/I9	73.61	2.22	180.86	0.00	80.44	3.91
R/P/I10	80.44	2.00	189.64	0.00	79.46	3.91
L/A/S1	67.76	2.49	113.59	3.42	102.86	3.16
L/A/S2	67.76	2.49	109.69	3.42	109.69	3.04
L/A/S3	67.76	2.49	105.79	3.57	119.44	2.83
L/A/S4	67.76	2.49	102.86	3.73	130.16	2.56
L/A/S5	68.74	2.49	100.91	3.73	142.84	2.28
L/A/S6	70.69	2.34	97.99	3.91	151.61	2.16
L/A/S7	79.46	2.00	96.04	3.91	157.46	2.10
L/A/S8	93.11	1.71	94.09	3.91	162.34	2.00
L/A/S9	113.59	1.37	93.11	4.10	167.21	1.95
L/A/S10	144.79	1.07	91.16	4.10	172.09	1.91

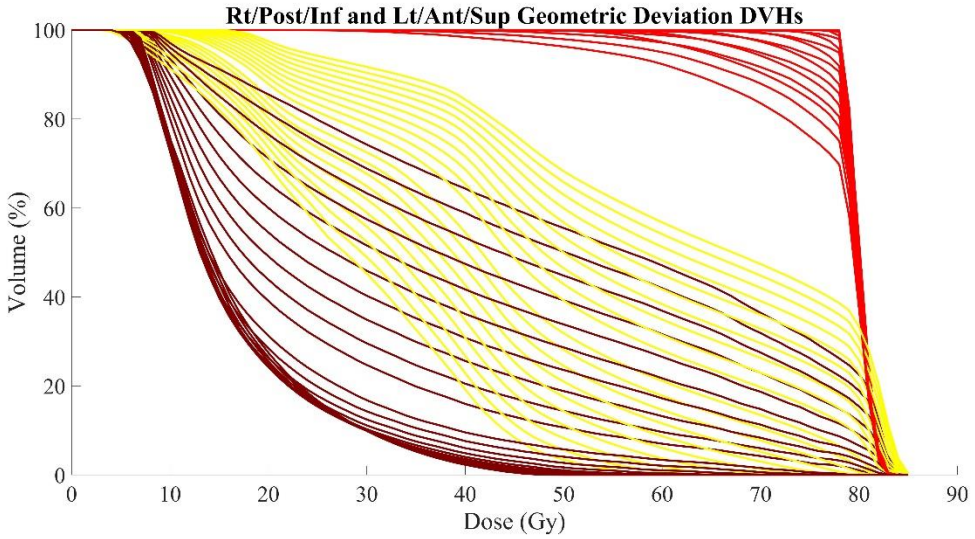

Figure 75. DVHs for Rt/Post/Inf and Lt/Ant/Sup geometric deviations.

Left, Posterior, and Inferior (Lt/Post/Inf) deviations and Right, Anterior, and Superior (Rt/Ant/Sup) deviations were next evaluated. Dashed lines represent Lt/Post/Inf PRQs and dashed and dotted lines represent Rt/Ant/Sup PRQs. Rt/Ant/Sup PRQs experienced a reversal in behavior

from the 4 mm deviation on. Lt/Post/Inf PRQ max values decreased from 78.92 % to 22.23 %. Rt/Ant/Sup PRQ max values increased for the first 3 (86.73% to 90.14 %) then decreased to 0.62 %. The dose the PRQ max occurred at decreased from 81.90 Gy to 75.08 Gy then increased to 76.05 % for the last Lt/Post/Inf geometric deviation. Rt/Ant/Sup deviations values for the dose the max occurred fluctuated: please see Table 32 for specifics. PRQ values at the prescription dose decreased for Lt/Post/Inf deviations from 76.27 % to 21.77 %. Rt/Ant/Sup deviations PRQ values at the prescription dose rose from 78.51 % to 78.90 % before falling to 0.31 %. The FWHM for Lt/Post/Inf deviations decreased from 30.23 Gy to 20.48 Gy. The Rt/Ant/Sup deviation PRQ FWHMs increased from 36.08 Gy to 39.00 Gy then decreased to 22.43 Gy. The AUC decreased for Lt/Post/Inf PRQs falling from 26.15 kGy% to 5.31 kGy%. The AUC for Rt/Ant/Sup PRQs first increased (32.98 kGy% to 36.52 kGy%) then decreased to 0.18 kGy%.

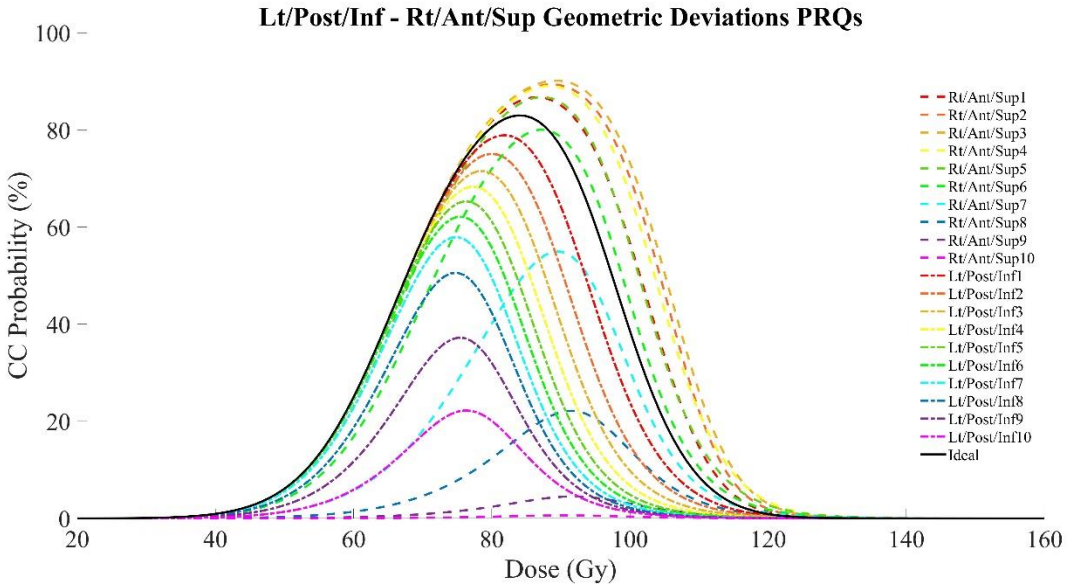

Figure 76. PRQs calculated for geometric deviations in the Left/Posterior/Inferior and Right/Anterior/Superior directions in 1mm increments.

Table 32. PRQ metrics for geometric deviations in the Left/Posterior/Inferior and Right/Anterior/Superior directions in 1 mm increments.

	Max	Dose @ Max	Rx Dose	FWHM	AUC
R/A/S1	86.73	86.78	78.51	36.08	32.98
R/A/S2	89.38	88.73	78.87	39.00	35.61
R/A/S3	90.14	89.70	78.90	39.00	36.52
R/A/S4	89.06	88.73	78.47	38.03	35.19
R/A/S5	86.74	87.75	76.70	35.10	32.55
R/A/S6	80.02	86.78	67.53	31.20	27.37
R/A/S7	54.99	89.70	35.28	25.35	15.91
R/A/S8	22.17	91.65	10.39	22.43	5.91
R/A/S9	4.53	91.65	2.00	22.43	1.24
R/A/S10	0.62	90.68	0.31	22.43	0.18
L/P/I1	78.92	81.90	76.27	30.23	26.15
L/P/I2	75.08	79.95	74.20	28.28	23.43
L/P/I3	71.51	78.98	71.49	26.33	21.23
L/P/I4	68.33	77.03	68.23	25.35	19.45
L/P/I5	65.30	76.05	64.45	24.38	17.93
L/P/I6	62.13	75.08	60.18	23.40	16.54
L/P/I7	57.94	75.08	54.77	22.43	14.92
L/P/I8	50.57	75.08	47.34	21.45	12.57
L/P/I9	37.21	75.08	35.51	20.48	8.96
L/P/I10	22.23	76.05	21.77	20.48	5.31

Rt/Ant/Sup geometric deviation TCPs experienced a large shift right beginning with the 5 mm deviation increasing in magnitude and decreasing in slope with larger deviations. Lt/Post/Inf deviations TCPs experienced a smaller shift right beginning with the 7 mm deviation increasing in magnitude and decreasing in slope with larger deviations. The bladder NTCPs for Rt/Ant/Sup deviations shifted left decreasing in magnitude and increasing in slope with larger deviations. The bladder NTCPs for Lt/Post/Inf deviations had a large shift right increasing in magnitude and decreasing in slope with larger deviations. Rt/Ant/Sup deviation rectum NTCPs experienced a right shift increasing in magnitude and decreasing in slope with larger deviations. Lt/Post/Inf deviation rectum NTCPs experienced a smaller left shift decreasing in magnitude and increasing in slope with larger deviations.

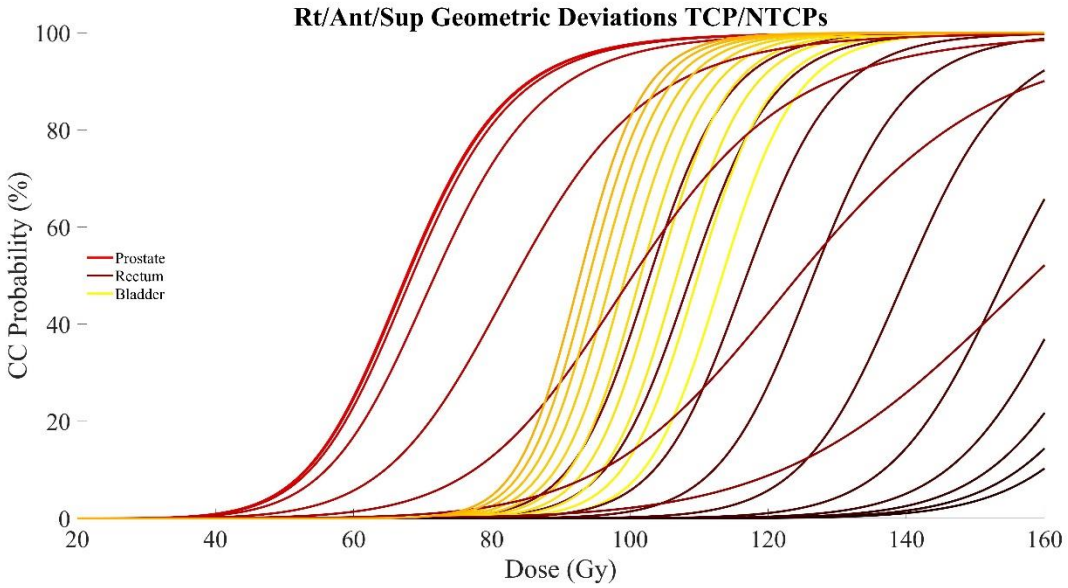

Figure 77. TCPs and NTCPs calculated for geometric deviations shifted to the patients right, anteriorly and superiorly in 1 mm increments.

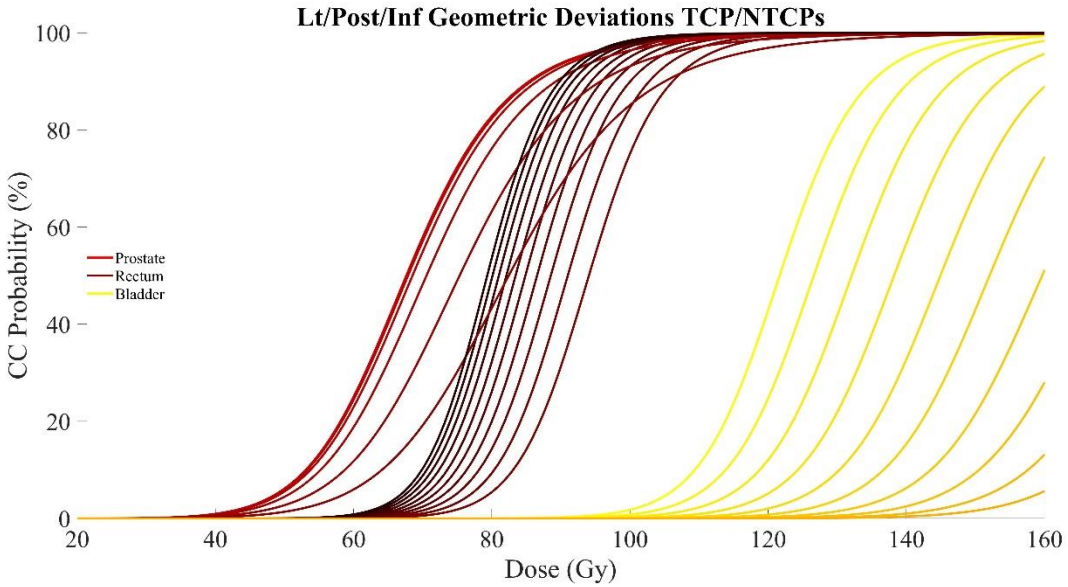

Figure 78. TCPs and NTCPs calculated for geometric deviations shifted to the patients left, posteriorly and inferiorly in 1 mm increments.

Table 33. TCP and NTCP metrics calculated from Right/Anterior/Superior and Left/Posterior/Inferior geometric deviations.

	Prostate CTV		Bladder		Rectum	
	50% Dose	80/20 Slope	50% Dose	80/20 Slope	50% Dose	80/20 Slope
R/A/S1	67.76	2.49	113.59	3.28	102.86	3.16
R/A/S2	67.76	2.49	109.69	3.42	108.71	3.04
R/A/S3	67.76	2.49	106.76	3.57	116.51	2.83
R/A/S4	67.76	2.49	103.84	3.57	126.26	2.56
R/A/S5	68.74	2.49	101.89	3.73	139.91	2.41
R/A/S6	71.66	2.28	98.96	3.73	154.54	2.16
R/A/S7	83.36	1.91	97.01	3.73	165.26	2.00
R/A/S8	100.91	1.55	96.04	3.91	172.09	1.91
R/A/S9	124.31	1.26	94.09	3.91	176.96	0.00
R/A/S10	158.44	0.00	93.11	4.10	180.86	0.00
L/P/I1	67.76	2.49	121.39	3.16	94.09	3.57
L/P/I2	67.76	2.49	126.26	2.93	91.16	3.57
L/P/I3	67.76	2.49	132.11	2.83	88.24	3.73
L/P/I4	67.76	2.49	137.96	2.74	86.29	3.73
L/P/I5	67.76	2.49	144.79	2.65	85.31	3.73
L/P/I6	67.76	2.49	151.61	2.49	83.36	3.91
L/P/I7	68.74	2.49	159.41	2.41	82.39	3.91
L/P/I8	70.69	2.34	167.21	2.28	81.41	3.91
L/P/I9	75.56	2.16	175.01	2.16	80.44	3.91
L/P/I10	82.39	1.95	183.79	0.00	79.46	3.91

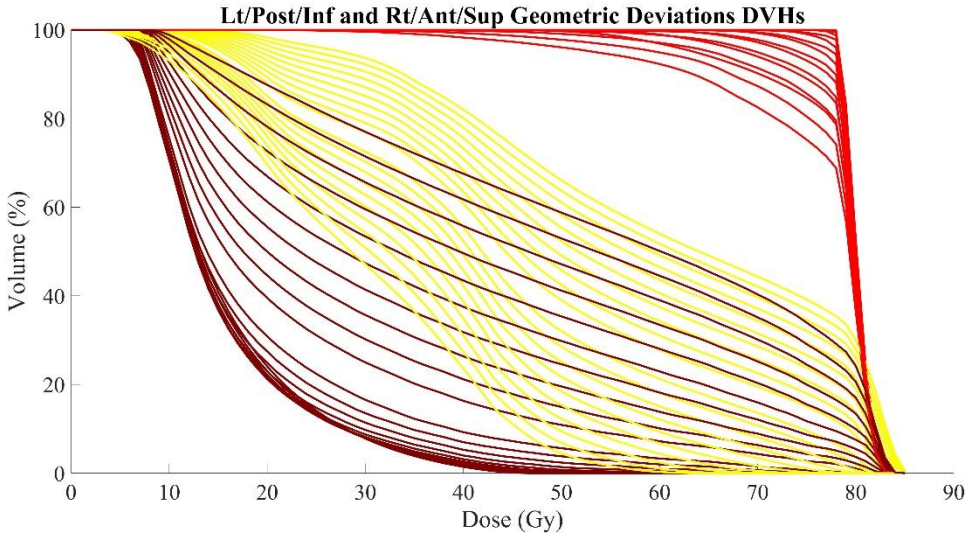

Figure 79. DVHs for Lt/Post/Inf and Rt/Ant/Sup geometric deviations.

Next geometric deviations in the left and anterior (Lt/Ant) direction, and right and posterior (Rt/Post) direction were evaluated. Lt/Ant deviations are indicated by dashed lines and Rt/Post deviations are represented by dashed and dotted lines. Lt/Ant deviation PRQs experienced a

reversal in behavior from the 4 mm deviation on. Lt/Ant deviation PRQ max values rose from the first 3 shifts (86.69 % to 91.31 %) then decreased to 12.20 %. Rt/Post deviation PRQ max values decreased from 79.25 % to 46.61 %. The dose the max occurred at decreased for Rt/Post deviations (81.90 Gy to 77.03 Gy). The dose the max occurred for Lt/Ant deviations fluctuated: please see Table 34 for quantitative specifics. The dose the max occurred at decreased for Rt/Post deviations from 81.90 Gy to 74.10 Gy. Lt/Ant deviations PRQ values at the prescription dose increased for the first three deviations (78.51 % to 79.10 %) then decreased to 4.24 %. The PRQ values at the prescription dose decreased from 76.40 % to 42.55 % for Rt/Post geometric deviations. The FWHM for Lt/Ant deviation PRQs increased from 36.08 Gy to 39.98 Gy then decreased to 22.43 Gy. The FWHM for Rt/Post deviation PRQs decreased from 30.23 Gy to 20.48 Gy. The AUC for Lt/Ant deviation PRQs increased for the first three deviations (33.10 kGy% to 38.47 kGy%) then decreased to 3.37 kGy%. The AUC for Rt/Post deviation PRQs decreased from 26.39 kGy% to 11.33 kGy%.

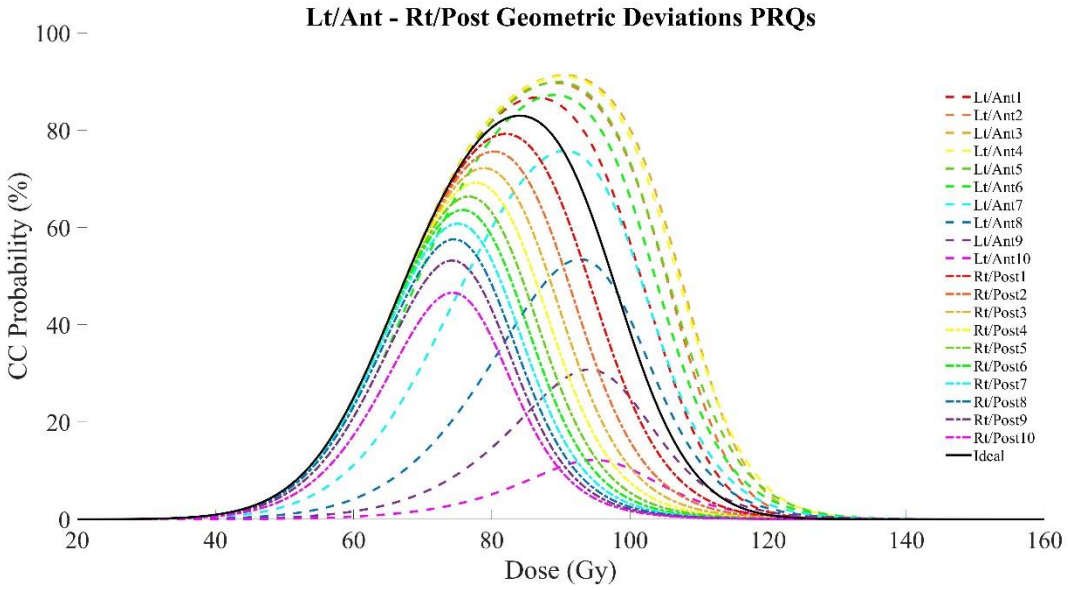

Figure 80. PRQs calculated for geometric deviations in the Right/Posterior and Left/Anterior directions in 1 mm increments.

Table 34. PRQ metrics for geometric deviations in the Right/Posterior and Left/Anterior directions in 1 mm increments.

	Max	Dose @ Max	Rx Dose	FWHM	AUC
L/A1	86.69	86.78	78.51	36.08	33.10
L/A2	89.73	88.73	78.94	39.00	36.50
L/A3	91.31	90.68	79.10	39.98	38.64
L/A4	91.09	90.68	78.93	39.98	38.47
L/A5	89.94	89.70	78.06	39.00	36.82
L/A6	87.23	88.73	74.21	36.08	33.79
L/A7	75.79	90.68	54.62	31.20	25.87
L/A8	53.49	92.63	27.77	26.33	15.89
L/A9	30.77	94.58	12.29	23.40	8.53
L/A10	12.20	94.58	4.24	22.43	3.37
R/P1	79.25	81.90	76.40	30.23	26.39
R/P2	75.61	79.95	74.52	29.25	23.78
R/P3	72.24	78.98	72.07	26.33	21.63
R/P4	69.20	78.00	69.20	26.33	19.92
R/P5	66.35	77.03	65.87	24.38	18.45
R/P6	63.61	76.05	62.16	23.40	17.16
R/P7	60.82	75.08	58.13	23.40	15.96
R/P8	57.55	74.10	53.76	22.43	14.73
R/P9	53.23	74.10	48.78	21.45	13.27
R/P10	46.61	74.10	42.55	20.48	11.33

The Lt/Ant geometric deviation TCPs experienced a shift right beginning at the 6 mm deviation increasing in magnitude and decreasing in slope with larger deviations. The Rt/Post geometric deviation TCPs experienced a small right shift beginning at the 8 mm deviation increasing in magnitude and decreasing in slope with larger deviations. The bladder NTCPs for Lt/Ant deviations experienced a shift left that decreased in magnitude and increased in slope with larger deviations. For Rt/Post deviations the bladder NTCPs experienced a shift right that increased in magnitude and decreased in slope with larger deviations. The Lt/Ant deviations rectum NTCPs experience a right shift decreasing in slope with larger deviations. The Rt/Post deviation rectum NTCPs shifted left decreasing in magnitude and increasing in slope with larger deviations.

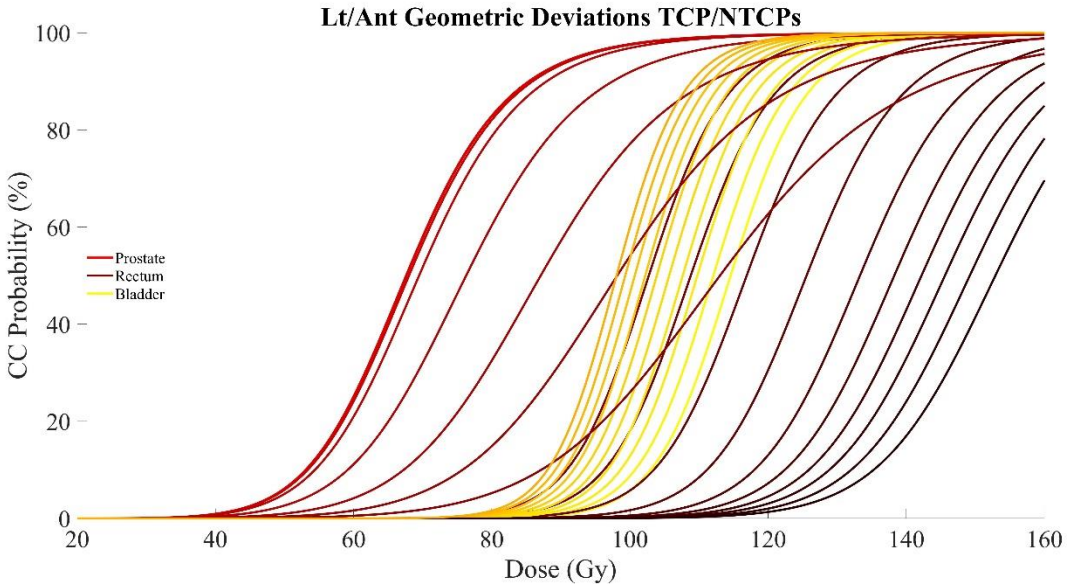

Figure 81. TCPs and NTCPs calculated for left and anterior geometric deviations in 1 mm increments.

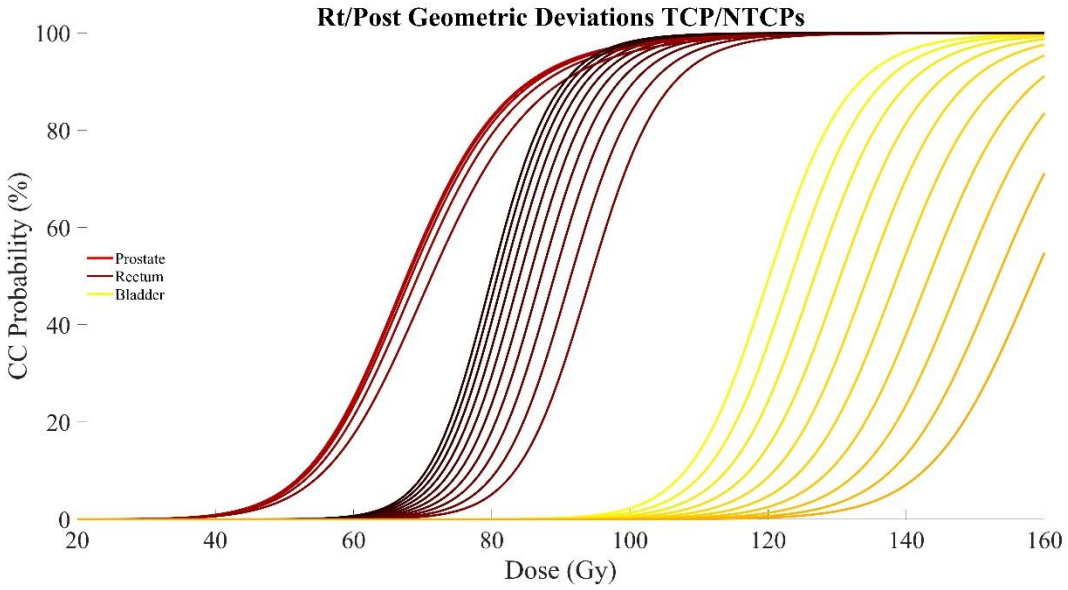

Figure 82. TCPs and NTCPs calculated for right and posterior geometric deviations in 1 mm increments.

Table 35. TCP and NTCP metrics calculated from Left/Anterior and Right/Posterior geometric deviations.

	Prostate CTV		Bladder		Rectum	
	50% Dose	80/20 Slope	50% Dose	80/20 Slope	50% Dose	80/20 Slope
L/A1	67.76	2.49	114.56	3.28	102.86	3.28
L/A2	67.76	2.49	111.64	3.42	108.71	3.04
L/A3	67.76	2.49	109.69	3.42	116.51	2.83
L/A4	67.76	2.49	107.74	3.57	125.29	2.65
L/A5	67.76	2.41	105.79	3.57	133.09	2.49
L/A6	69.71	2.34	103.84	3.57	137.96	2.41
L/A7	76.54	2.05	101.89	3.73	141.86	2.34
L/A8	87.26	1.78	100.91	3.73	145.76	2.28
L/A9	97.99	1.58	98.96	3.73	149.66	2.22
L/A10	112.61	1.39	97.99	3.91	152.59	2.16
R/P1	67.76	2.49	120.41	3.16	94.09	3.42
R/P2	67.76	2.49	123.34	3.04	91.16	3.57
R/P3	67.76	2.49	126.26	2.93	89.21	3.57
R/P4	67.76	2.49	130.16	2.93	87.26	3.57
R/P5	67.76	2.49	134.06	2.83	85.31	3.73
R/P6	67.76	2.49	138.94	2.74	84.34	3.91
R/P7	67.76	2.49	142.84	2.65	82.39	3.73
R/P8	68.74	2.49	147.71	2.56	81.41	3.91
R/P9	69.71	2.41	153.56	2.49	80.44	4.10
R/P10	71.66	2.34	158.44	2.41	80.44	4.10

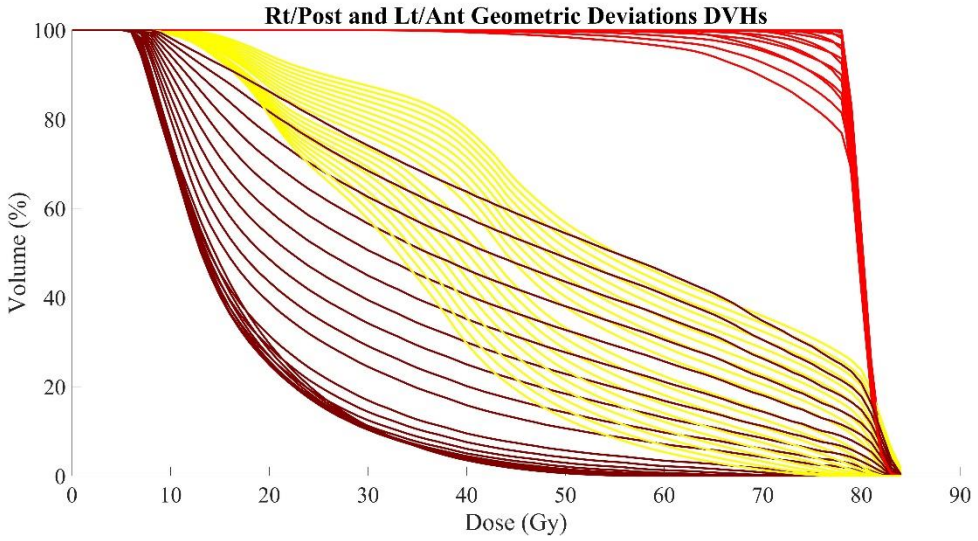

Figure 83. DVHs for Rt/Post and Lt/Ant geometric deviations.

Next the left and inferior (Lt/Inf) deviations and right and superior (Rt/Sup) deviations were evaluated. Dashed lines represent Lt/Inf deviation PRQs while dashed and dotted lines represent Rt/Sup deviation PRQs. The Lt/Inf deviations PRQ max values decreased from 82.67 %

to 76.11 %. PRQ max values decreased for Rt/Sup deviations as well from 83.05 % to 8.69 % with the majority of the decrease occurring during the last three deviations. The dose the max occurred at for Lt/Inf deviations decreased from 83.55 Gy to 81.90 Gy. For Rt/Sup deviations the dose the max occurred at increased from 83.85 Gy to 95.55 Gy with the majority of the increase occurring during the last three deviations. There was a slight decrease in the PRQ values at the prescription dose; Lt/Inf deviations decreased from 77.64 % to 73.26 % while Rt/Sup deviations decreased from 77.71 % to 2.99 % with the majority of the decreases occurring during the last three deviations. The FWHM decreased for Lt/Inf deviations from 33.15 Gy to 29.25 Gy while the Rt/Sup deviations FWHM decreased from 33.15 Gy to 22.43 Gy with the majority of the decreases occurring during the last three deviations. The AUC decreased for Lt/Inf from 29.27 kGy% to 24.63 kGy%. For Rt/Sup deviations the AUC decreased from 29.48 kGy% to 2.28 kGy% with the majority of the decreases occurring during the last three deviations.

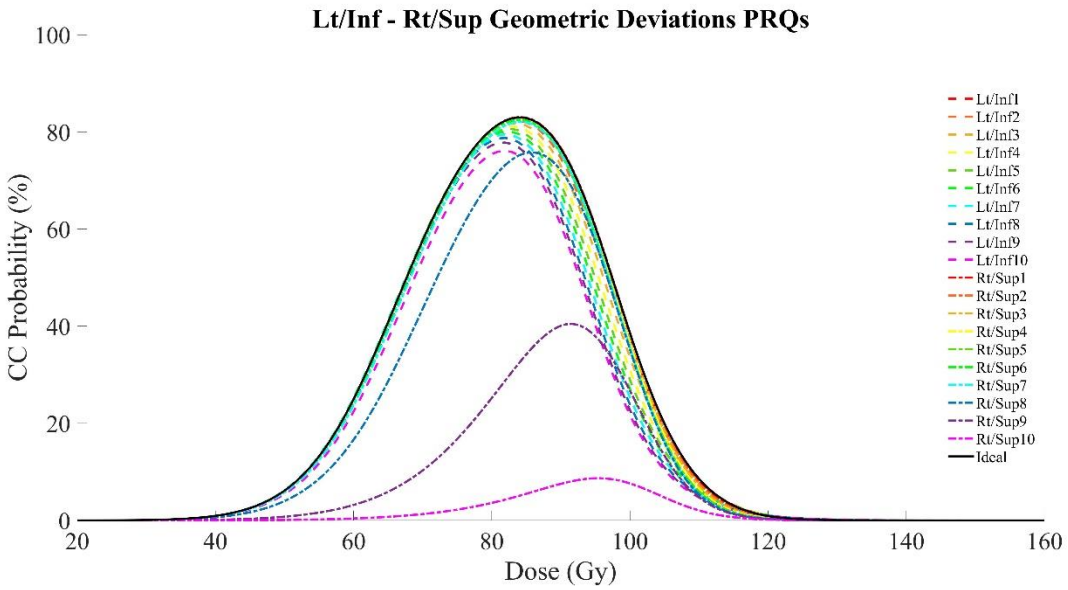

Figure 84. PRQs calculated for geometric deviations in the Left/Inferior and Right/Superior directions in 1 mm increments.

Table 36. PRQ metrics for geometric deviations in the Left/Inferior and Right/Superior directions in 1 mm increments.

	Max	Dose @ Max	Rx Dose	FWHM	AUC
L/I1	82.67	83.85	77.64	33.15	29.27
L/I2	82.30	83.85	77.57	33.15	29.00
L/I3	81.79	82.88	77.49	32.18	28.59
L/I4	81.17	82.88	77.33	32.18	28.04
L/I5	80.61	82.88	77.18	31.20	27.59
L/I6	80.06	81.90	76.98	31.20	27.14
L/I7	79.47	81.90	76.66	30.23	26.67
L/I8	78.77	81.90	76.17	30.23	26.18
L/I9	77.80	81.90	75.22	30.23	25.57
L/I10	76.11	81.90	73.26	29.25	24.63
R/S1	83.05	83.85	77.71	33.15	29.48
R/S2	82.97	83.85	77.67	33.15	29.31
R/S3	82.93	83.85	77.65	33.15	29.18
R/S4	82.76	83.85	77.58	33.15	28.93
R/S5	82.58	83.85	77.46	33.15	28.69
R/S6	82.50	83.85	77.26	33.15	28.58
R/S7	82.07	83.85	76.40	32.18	28.27
R/S8	75.81	85.80	66.07	30.23	24.80
R/S9	40.48	91.65	21.64	23.40	11.15
R/S10	8.69	95.55	2.99	22.43	2.28

The TCPs for Lt/Inf deviations were effectively unchanged for the first 9 deviations then had a small right shift with decreased slope. Rt/Sup deviation TCPs experienced larger right shifts decreasing in slope for the last 3 deviations. The bladder NTCPs for Lt/Inf deviations experience a right shift increasing in magnitude and decreasing in slope with larger deviations. Rt/Sup deviation bladder NTCPs experience a left shift decreasing in magnitude and increasing in slope with larger deviations. Rectum NTCPs for Lt/Inf deviations experienced a shift left while Rt/Sup deviation rectum NTCPs experienced a small shift right.

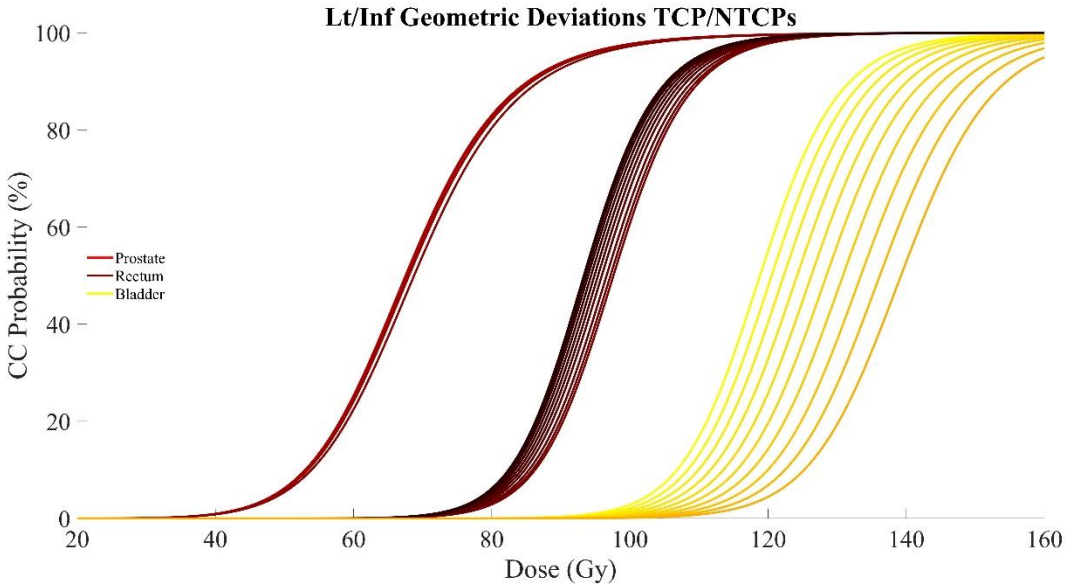

Figure 85. TCPs and NTCPs calculated for left and superior geometric deviations in 1 mm increments.

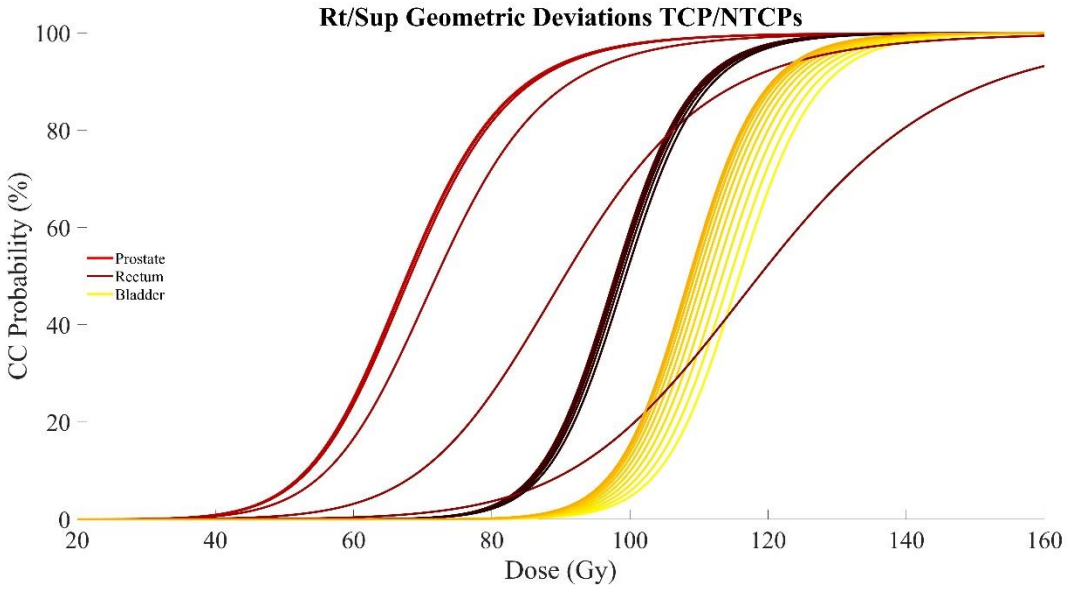

Figure 86. TCPs and NTCPs calculated for right and inferior geometric deviations in 1 mm increments.

Table 37. TCP and NTCP metrics calculated from Left/Inferior and Right/Superior geometric deviations.

	Prostate CTV		Bladder		Rectum	
	50% Dose	80/20 Slope	50% Dose	80/20 Slope	50% Dose	80/20 Slope
L/I1	67.76	2.49	118.46	3.16	97.99	3.42
L/I2	67.76	2.49	120.41	3.16	97.01	3.42
L/I3	67.76	2.49	122.36	3.04	97.01	3.42
L/I4	67.76	2.49	124.31	3.04	96.04	3.28
L/I5	67.76	2.49	126.26	3.04	95.06	3.42
L/I6	67.76	2.49	128.21	2.93	95.06	3.42
L/I7	67.76	2.49	131.14	2.93	94.09	3.42
L/I8	67.76	2.49	133.09	2.93	94.09	3.57
L/I9	67.76	2.41	136.01	2.74	94.09	3.42
L/I10	68.74	2.41	138.94	2.74	93.11	3.42
R/S1	67.76	2.49	115.54	3.28	97.99	3.28
R/S2	67.76	2.49	114.56	3.28	97.99	3.28
R/S3	67.76	2.49	113.59	3.28	97.99	3.28
R/S4	67.76	2.49	112.61	3.42	97.99	3.28
R/S5	67.76	2.49	111.64	3.42	97.99	3.28
R/S6	67.76	2.49	110.66	3.42	97.99	3.28
R/S7	67.76	2.41	109.69	3.42	97.99	3.28
R/S8	71.66	2.28	109.69	3.42	97.99	3.42
R/S9	90.19	1.71	108.71	3.42	98.96	3.28
R/S10	118.46	1.30	108.71	3.57	98.96	3.28

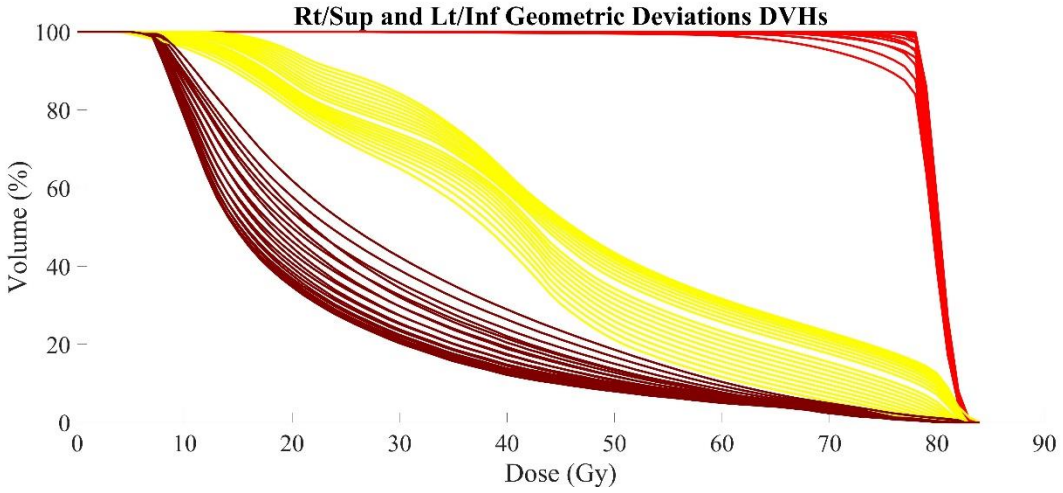

Figure 87. DVHs for Rt/Sup and Lt/Inf geometric deviations.

The next set of geometric deviations evaluations performed were in the anterior and inferior (Ant/Inf) directions and in the posterior and superior (Post/Sup) directions. Ant/Inf PRQs are denoted by dashed lines while Post/Sup PRQs are denoted by dashed and dotted lines. The Ant/Inf deviation PRQs experienced a reversal in behavior from the 6 mm deviation on. The PRQ max

values for Ant/Inf deviations increased for the first 4 deviations from 86.53 % to 93.20 % then decreased to 5.74 %. The PRQ max values for Post/Sup deviations decreased from 79.28 % to 1.53 %. The dose the max occurred at increased for Ant/Inf deviations from 86.78 Gy to 105.30 Gy. For Post/Sup deviations the dose the PRQ max occurred at fluctuated: please see Table 38 for quantitative specifics. The PRQ value at the prescription dose for Ant/Inf deviations increased for the first 3 deviation from 78.52 % to 79.19 % then decreased to 0.89 %. For Post/Sup deviations the PRQ value at the prescription dose decreased from 76.39 % to 1.52 %. The FWHMs for Ant/Inf deviations increased from 36.08 Gy to 44.85 Gy for the first 5 deviations then decreased to 25.35 Gy. Post/Sup deviations FWHMs decreased from 30.23 Gy to 21.45 Gy except for the last deviation where it increased to 22.43 Gy. The AUC increased from 33.11 kGy% to 43.25 kGy% for the first four Ant/Inf deviations then decreased to 1.78 kGy%. The AUC for Post/Sup deviations decreased from 26.36 kGy% to 0.42 kGy%.

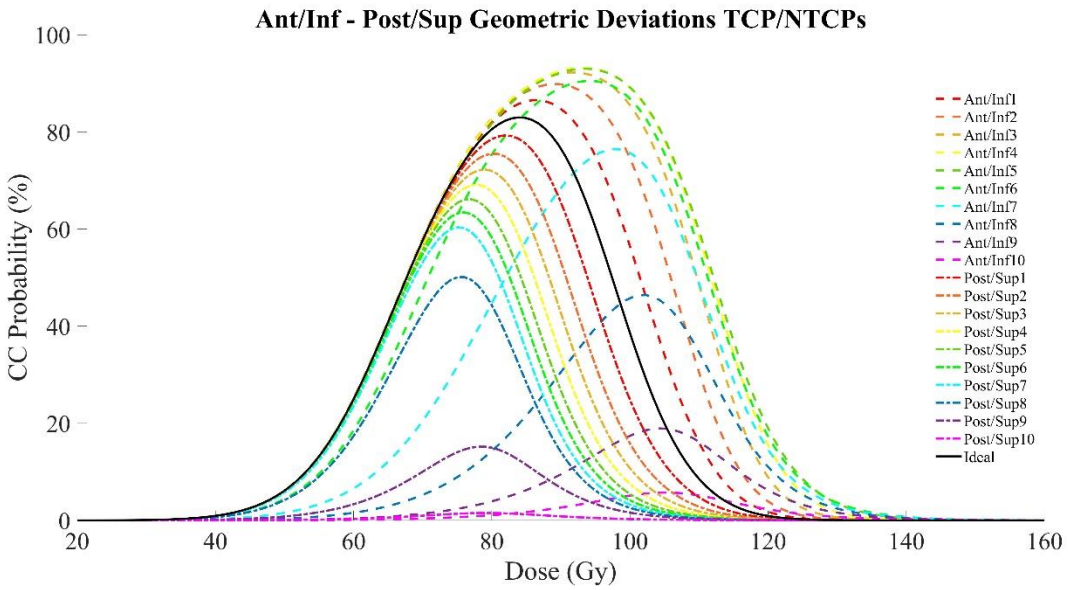

Figure 88. PRQs calculated for geometric deviations in the Anterior/Inferior and Posterior/Superior directions in 1 mm increments.

Table 38. PRQ metrics for geometric deviations in the Anterior/Inferior and Posterior/Superior directions in 1 mm increments.

	Max	Dose @ Max	Rx Dose	FWHM	AUC
A/I1	86.53	86.78	78.52	36.08	33.11
A/I2	89.84	88.73	79.00	39.98	37.20
A/I3	92.24	91.65	79.19	42.90	40.89
A/I4	93.20	93.60	79.03	44.85	43.01
A/I5	93.01	93.60	77.85	44.85	43.25
A/I6	90.50	94.58	70.80	41.93	40.01
A/I7	76.43	97.50	39.41	34.13	28.50
A/I8	46.39	102.38	11.91	27.30	14.66
A/I9	18.94	104.33	3.23	25.35	5.73
A/I10	5.74	105.30	0.89	25.35	1.78
P/S1	79.28	81.90	76.39	30.23	26.36
P/S2	75.52	79.95	74.43	28.28	23.68
P/S3	72.26	78.98	72.06	26.33	21.62
P/S4	69.12	78.00	69.12	26.33	19.86
P/S5	66.15	77.03	65.69	24.38	18.35
P/S6	63.44	76.05	62.10	23.40	17.09
P/S7	60.36	75.08	58.01	23.40	15.82
P/S8	50.09	76.05	48.38	22.43	12.64
P/S9	15.18	78.98	15.18	21.45	3.80
P/S10	1.53	78.98	1.52	22.43	0.42

Ant/Inf deviation TCPs experienced a shift right beginning at the 6 mm deviation increasing in magnitude and decreasing in slope with larger deviations. Post/Sup deviation TCPs experienced a shift right beginning at the 8 mm deviation increasing in magnitude and decreasing in slope with larger deviations. The bladder NTCPs for Ant/Inf deviations shifted left while Post/Sup bladder NTCPs had a larger shift right. Rectum NTCPs for Ant/Inf deviations experienced a larger shift right increasing in magnitude and decreasing in slope with larger deviations. Post/Sup deviations rectum NTCPs experience a left shift decreasing in magnitude and increasing in slope with larger deviations.

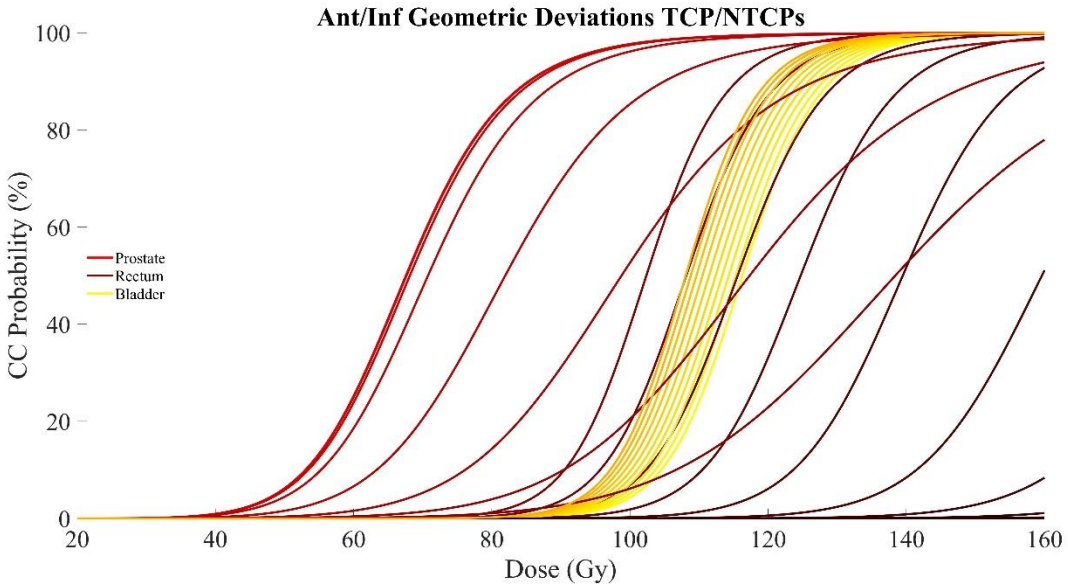

Figure 89. TCPs and NTCPs calculated for anterior and inferior geometric deviations in 1 mm increments.

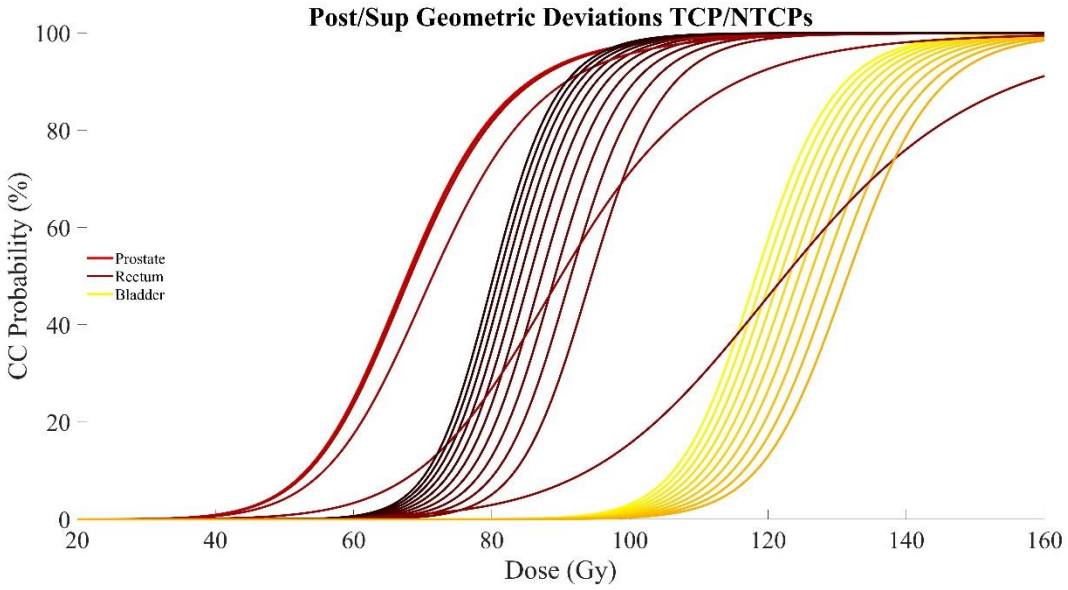

Figure 90. TCPs and NTCPs calculated for posterior and superior geometric deviations in 1 mm increments.

Table 39. TCP and NTCP metrics calculated from Anterior/Inferior and Posterior/Superior geometric deviations.

	Prostate CTV		Bladder		Rectum	
	50% Dose	80/20 Slope	50% Dose	80/20 Slope	50% Dose	80/20 Slope
A/I1	67.76	2.49	116.51	3.28	102.86	3.16
A/I2	67.76	2.49	115.54	3.28	107.74	3.04
A/I3	67.76	2.49	114.56	3.28	115.54	2.83
A/I4	67.76	2.49	113.59	3.28	124.31	2.65
A/I5	67.76	2.41	112.61	3.28	139.91	2.34
A/I6	70.69	2.28	111.64	3.42	159.41	2.10
A/I7	82.39	1.91	110.66	3.42	182.81	0.00
A/I8	98.96	1.58	109.69	3.57	0.00	0.00
A/I9	117.49	1.32	108.71	3.57	0.00	0.00
A/I10	137.96	1.12	107.74	3.42	0.00	0.00
P/S1	67.76	2.49	118.46	3.28	94.09	3.42
P/S2	67.76	2.49	119.44	3.28	91.16	3.57
P/S3	67.76	2.49	120.41	3.16	89.21	3.57
P/S4	67.76	2.49	121.39	3.16	87.26	3.57
P/S5	67.76	2.49	123.34	3.04	85.31	3.73
P/S6	67.76	2.49	124.31	3.04	84.34	3.91
P/S7	67.76	2.41	126.26	3.04	83.36	3.91
P/S8	71.66	2.28	128.21	2.93	82.39	3.91
P/S9	90.19	1.75	129.19	2.93	81.41	3.91
P/S10	122.36	1.26	131.14	2.93	80.44	3.91

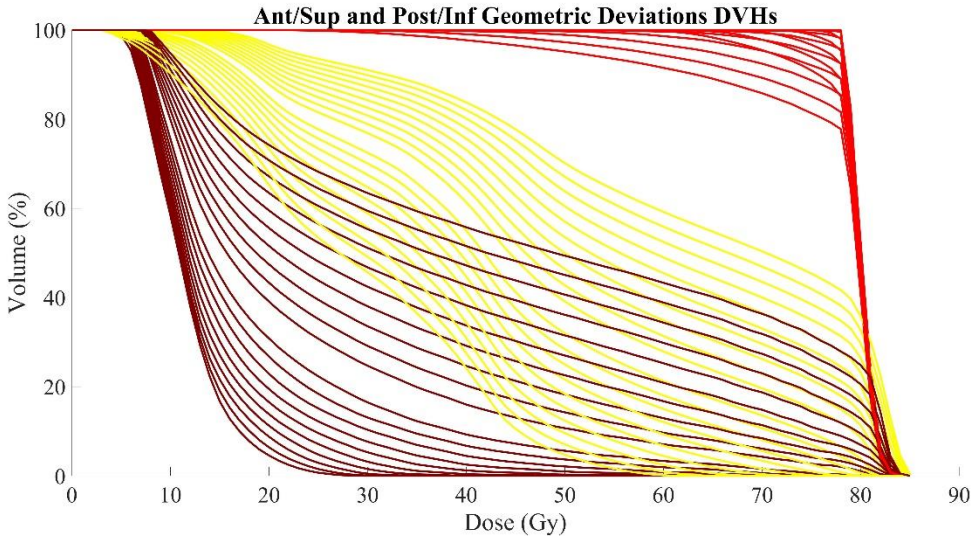

Figure 91. DVHs for Ant/Sup and Post/Inf geometric deviations.

Left and posterior (Lt/Post) geometric deviations and right and anterior (Rt/Ant) deviations evaluations followed. Lt/Post deviations PRQs are represented by dashed lines while Rt/Ant deviations PRQs are represented by dashed and dotted lines. The Rt/Ant deviation PRQs

experienced a reversal in behavior from the 5 mm deviation on. The PRQ max values for Lt/Post deviations decreased from 79.13 % to 46.71 %. The PRQ max values for Rt/Ant deviations increased for the first 4 deviations from 86.73 % to 91.61 % before decreasing 6.04 %. The dose the max occurred at for Lt/Post deviations decreased from 81.90 Gy to 74.10 Gy. The dose the max occurred at for Rt/Ant increased from 86.78 Gy to 97.50 Gy. The PRQ value at the prescription dose for Lt/Post deviations decreased from 76.35 % to 42.10 %. For Rt/Ant deviations the prescription dose PRQ value increased for the first 3 deviations (78.52 % to 79.07 %) then decreased to 1.66 %. The FWHMs decreased for Lt/Post deviations from 30.23 Gy to 20.48 Gy. The FWHMs for Rt/Ant deviations increased for the first 3 deviations (36.08 Gy to 40.59 Gy) then decreased to 24.38 Gy. The AUC for Lt/Post deviations decreased from 26.29 kGy% to 11.32 kGy%. The AUC for Rt/Ant deviations increased for the first 4 (33.17 kGy% to 39.55 kGy%) then decreased to 1.74 kGy%.

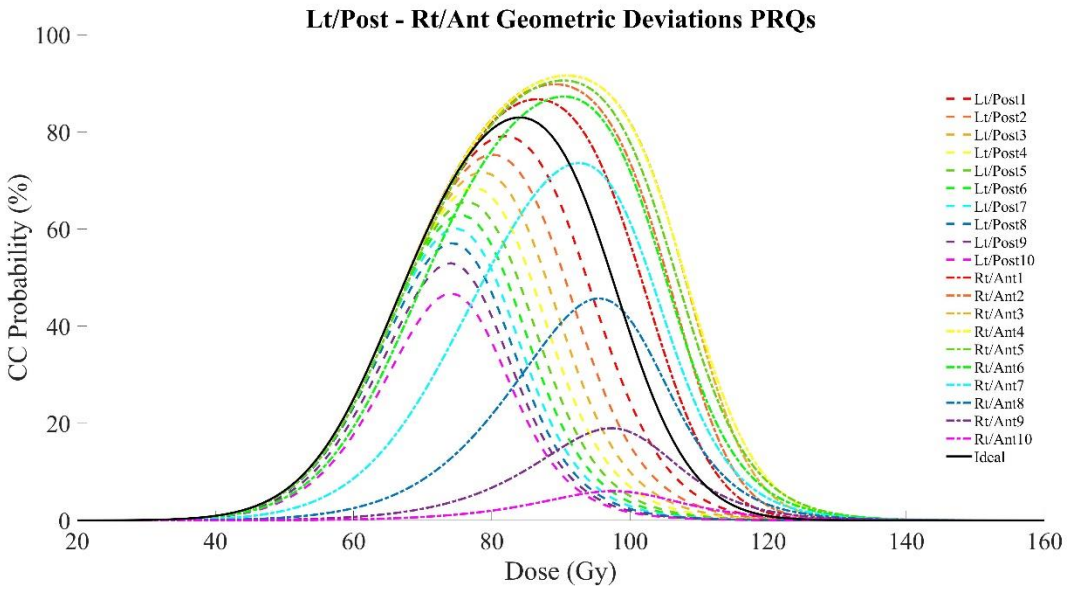

Figure 92. PRQs calculated for geometric deviation in Left/Posterior and Right/Anterior directions in 1 mm increments.

Table 40. PRQ metrics for geometric deviation in Left/Posterior and Right/Anterior directions in 1 mm increments.

	Max	Dose @ Max	Rx Dose	FWHM	AUC
L/P1	79.13	81.90	76.35	30.23	26.29
L/P2	75.31	79.95	74.32	28.28	23.56
L/P3	71.65	78.98	71.58	26.33	21.29
L/P4	68.46	77.03	68.41	25.35	19.53
L/P5	65.54	76.05	64.81	24.38	18.06
L/P6	62.79	75.08	60.96	23.40	16.80
L/P7	60.06	75.08	56.82	22.43	15.64
L/P8	57.07	74.10	52.63	22.43	14.51
L/P9	52.97	74.10	47.89	21.45	13.14
L/P10	46.71	74.10	42.10	20.48	11.32
R/A1	86.73	86.78	78.52	36.08	33.17
R/A2	89.81	88.73	78.94	39.98	36.71
R/A3	91.59	90.68	79.07	40.95	39.23
R/A4	91.61	90.68	78.85	40.95	39.55
R/A5	90.59	90.68	77.77	39.98	38.14
R/A6	87.29	90.68	71.82	37.05	34.49
R/A7	73.61	92.63	47.22	30.23	25.15
R/A8	45.73	95.55	18.37	25.35	13.49
R/A9	18.99	97.50	5.56	23.40	5.36
R/A10	6.04	97.50	1.66	24.38	1.74

TCPs for Lt/Post deviations experienced a small shift right beginning at the 8 mm deviation with a slight decrease in slope. TCPs for Rt/Ant deviations experienced a larger shift right beginning at the 6 mm deviation increasing in magnitude and decreasing in slope with larger deviations. Lt/Post deviations bladder NTCPs experienced a shift right that increased in magnitude and decreasing in slope. Rt/Ant deviations bladder NTCPs experienced a small shift left decreasing in magnitude and increasing in slope with larger deviations. Rectum NTCPs for Lt/Post deviations experienced a left shift decreasing in magnitude and increasing in slope with larger deviations. Rt/Ant deviations rectum NTCPs experienced a larger right shift increasing in magnitude and decreasing in slope with larger deviations.

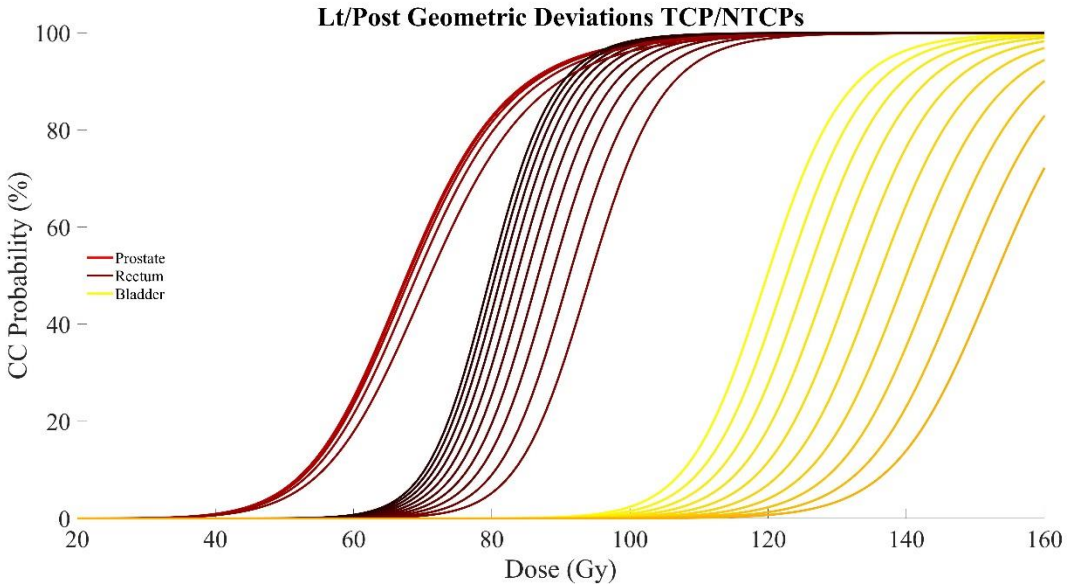

Figure 93. TCPs and NTCPs calculated for left and posterior geometric deviations in 1 mm increments.

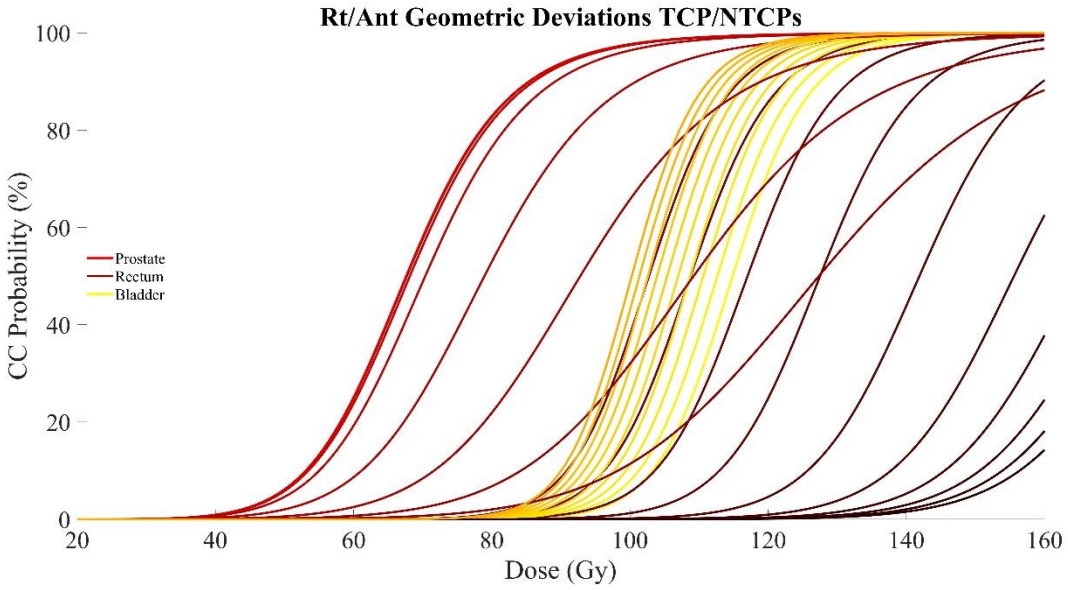

Figure 94. TCPs and NTCPs calculated for right and anterior geometric deviations in 1 mm increments.

Table 41. TCP and NTCP metrics calculated from Left/Posterior and Right/Anterior geometric deviations.

	Prostate CTV		Bladder		Rectum	
	50% Dose	80/20 Slope	50% Dose	80/20 Slope	50% Dose	80/20 Slope
L/P1	67.76	2.49	119.44	3.16	94.09	3.42
L/P2	67.76	2.49	122.36	3.16	91.16	3.57
L/P3	67.76	2.49	125.29	2.93	88.24	3.73
L/P4	67.76	2.49	129.19	2.93	86.29	3.73
L/P5	67.76	2.49	132.11	2.93	85.31	3.73
L/P6	67.76	2.49	136.01	2.83	83.36	3.73
L/P7	67.76	2.49	139.91	2.74	82.39	3.91
L/P8	68.74	2.41	143.81	2.56	81.41	3.91
L/P9	68.74	2.41	148.69	2.56	80.44	3.91
L/P10	70.69	2.34	152.59	2.41	79.46	4.10
R/A1	67.76	2.49	114.56	3.28	102.86	3.28
R/A2	67.76	2.49	112.61	3.28	108.71	3.04
R/A3	67.76	2.49	110.66	3.42	117.49	2.83
R/A4	67.76	2.49	108.71	3.57	127.24	2.56
R/A5	67.76	2.41	106.76	3.57	141.86	2.34
R/A6	70.69	2.34	105.79	3.57	155.51	2.16
R/A7	78.49	2.00	103.84	3.57	164.29	2.00
R/A8	93.11	1.67	102.86	3.73	170.14	1.95
R/A9	109.69	1.44	100.91	3.73	174.04	0.00
R/A10	127.24	1.22	99.94	3.73	176.96	0.00

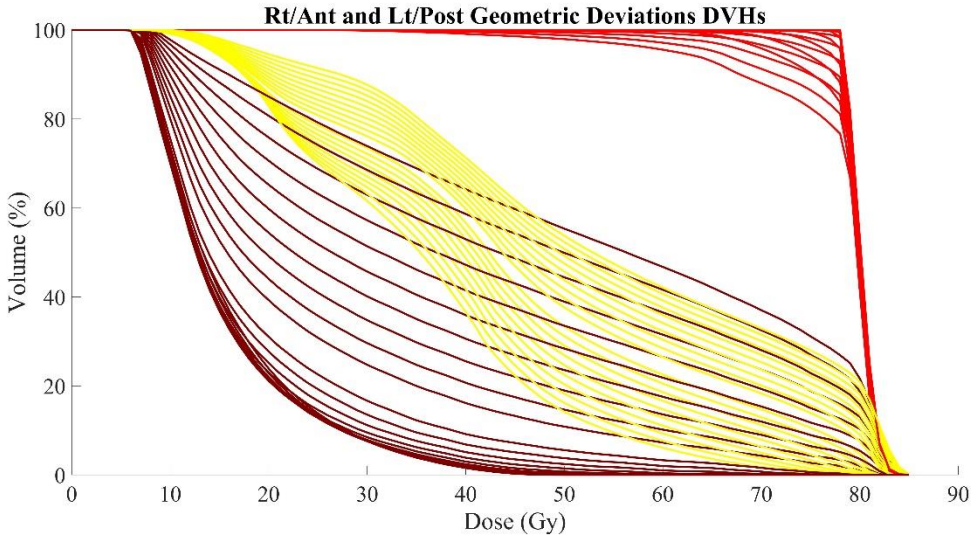

Figure 95. DVHs for Lt/Post and Rt/Ant geometric deviations.

Next deviations applied in the left and superior (Lt/Sup) and right and inferior (Rt/Inf) directions were evaluated. Dashed lines denoted the Lt/Sup deviation PRQS while dashed and dotted lined denote the Rt/Inf deviations. The Lt/Sup deviation PRQ max values decreased from

83.01 % to 10.48 % with the majority of the decrease occurring in the last three deviations. The PRQs max values for Rt/Inf averaged 82.83 ± 0.25 %. For Lt/Sup deviations the dose the max occurred at increased from 83.85 Gy to 94.58 Gy with the majority of the increase occurring in the last three deviations. Rt/Inf deviations dose that the max occurred at averaged 84.05 ± 0.41 %.t The PRQ value at the prescription dose for Lt/Sup deviations decreased from 77.70 % to 3.69 % with the majority of the decrease occurring in the last three deviations. Rt/Inf deviations PRQ value at the prescription dose fluctuated: please see Table 42 for quantitative specifics. The FWHMs for Lt/Sup deviations PRQs decreased from 33.15 Gy to 22.43 Gy with the majority of the decreasing occurring in the last three deviations. The FWHMs for Rt/Inf deviations was 33.15 Gy for deviations except the 8 mm deviation where the FWHM was 34.13 Gy. The AUC for Lt/Ant deviations decreased from 29.42 kGy% to 2.70 kGy% with the majority of the decrease occurring in the last three deviations. For Rt/Inf deviations the AUC increased from 29.45 kGy% to 30.19 kGy% but decreased on the last deviation to 29.80 kGy%.

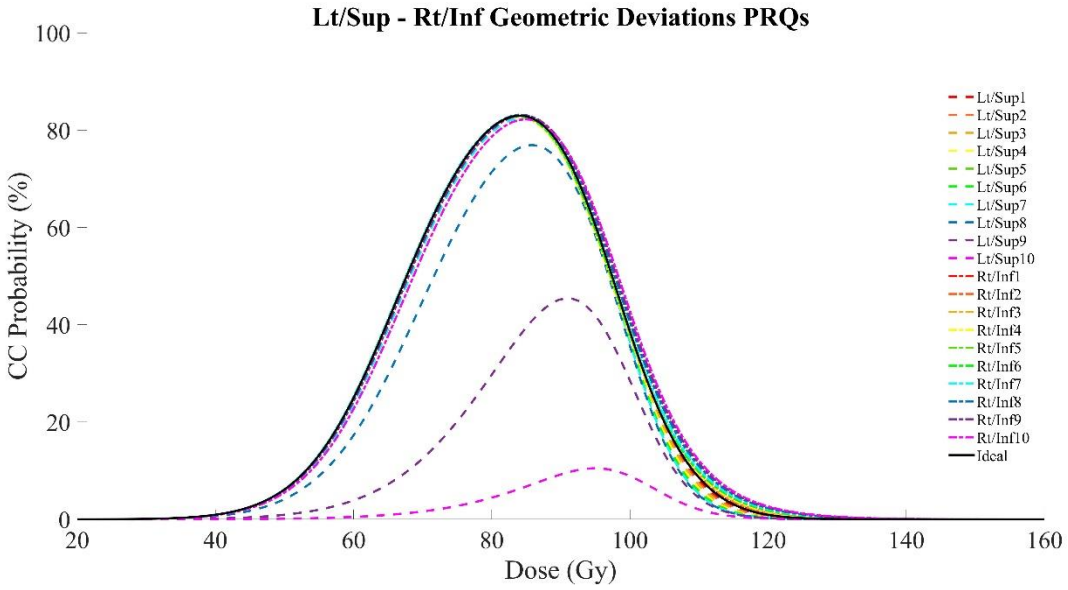

Figure 96. PRQs calculated for geometric deviations in the Left/Superior and Right/Inferior directions in 1 mm increments.

Table 42. PRQ metrics for geometric deviations in the Left/Superior and Right/Inferior directions in 1 mm increments.

	Max	Dose @ Max	Rx Dose	FWHM	AUC
L/S1	83.01	83.85	77.69	33.15	29.42
L/S2	83.01	83.85	77.68	33.15	29.31
L/S3	83.09	83.85	77.70	33.15	29.27
L/S4	83.00	83.85	77.66	33.15	29.06
L/S5	82.91	83.85	77.57	33.15	28.88
L/S6	82.91	83.85	77.36	32.18	28.81
L/S7	82.45	84.83	76.50	32.18	28.44
L/S8	76.95	85.80	67.38	30.23	25.25
L/S9	45.43	90.68	25.72	24.38	12.57
L/S10	10.48	94.58	3.69	22.43	2.70
R/I1	82.84	83.85	77.69	33.15	29.45
R/I2	82.83	83.85	77.73	33.15	29.52
R/I3	82.77	83.85	77.75	33.15	29.52
R/I4	82.70	83.85	77.76	33.15	29.50
R/I5	82.84	83.85	77.84	33.15	29.68
R/I6	82.92	83.85	77.89	33.15	29.79
R/I7	83.01	83.85	77.88	33.15	29.92
R/I8	83.17	83.85	77.74	34.13	30.18
R/I9	83.01	84.83	77.11	33.15	30.19
R/I10	82.24	84.83	75.42	33.15	29.80

TCPs for Lt/Sup deviations experienced a larger shift right beginning at the 8 mm deviation increasing in magnitude and decreasing in slope with larger deviations. Rt/Inf deviations TCPs experienced a small change on the last deviation with a small shift right. Lt/Sup deviations bladder NTCPs experienced a left shift decreasing in magnitude and increasing in slope with larger deviations. Rt/Inf bladder NTCPs experienced a right shift increasing in magnitude and decreasing in slope with larger deviations. Rectum NTCPs for Lt/Sup deviations experienced a small shift right with an even smaller shift right for Rt/Inf deviations rectum NTCPs.

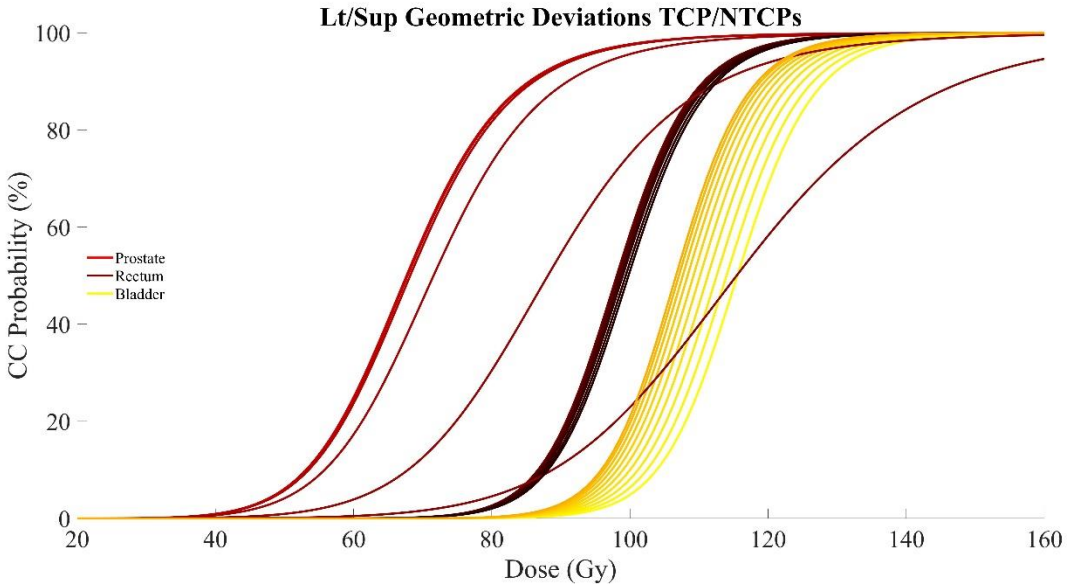

Figure 97. TCPs and NTCPs calculated for left and superior geometric deviations in 1 mm increments.

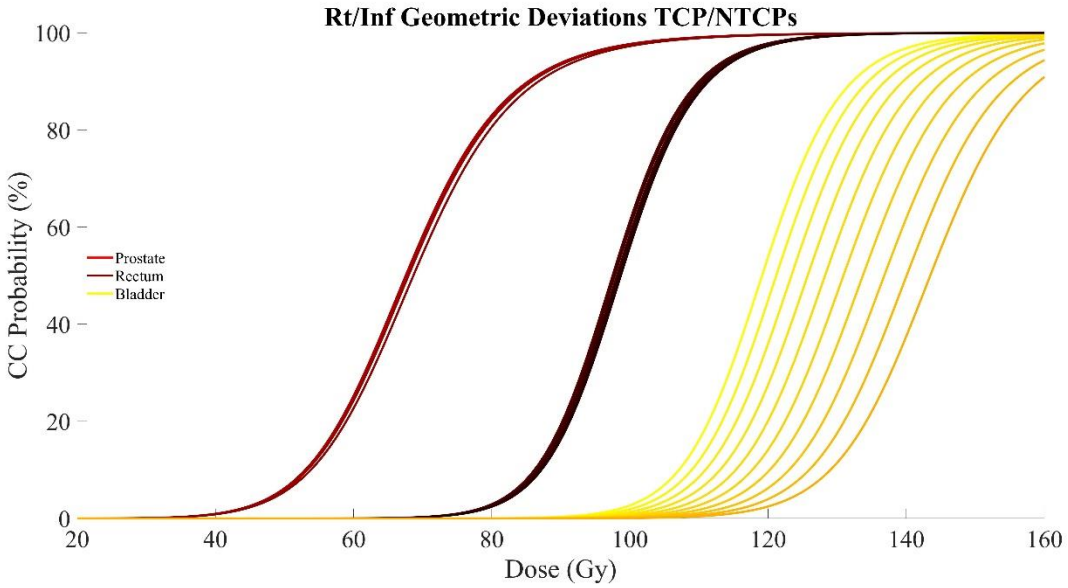

Figure 98. TCPs and NTCPs calculated for right and inferior geometric deviations in 1 mm increments.

Table 43. TCP and NTCP metrics calculated from Left/Superior and Right/Inferior geometric deviations.

	Prostate CTV		Bladder		Rectum	
	50% Dose	80/20 Slope	50% Dose	80/20 Slope	50% Dose	80/20 Slope
L/S1	67.76	2.49	115.54	3.28	97.99	3.28
L/S2	67.76	2.49	113.59	3.42	97.99	3.28
L/S3	67.76	2.49	112.61	3.28	97.99	3.42
L/S4	67.76	2.49	111.64	3.42	97.99	3.42
L/S5	67.76	2.49	109.69	3.42	97.99	3.42
L/S6	67.76	2.49	109.69	3.42	98.96	3.28
L/S7	67.76	2.41	108.71	3.42	98.96	3.28
L/S8	71.66	2.28	107.74	3.57	98.96	3.28
L/S9	88.24	1.75	106.76	3.57	98.96	3.28
L/S10	115.54	1.35	106.76	3.57	99.94	3.28
R/I1	67.76	2.49	119.44	3.16	97.99	3.28
R/I2	67.76	2.49	121.39	3.16	97.99	3.28
R/I3	67.76	2.49	123.34	3.04	97.99	3.42
R/I4	67.76	2.49	125.29	2.93	97.01	3.42
R/I5	67.76	2.49	128.21	3.04	97.99	3.42
R/I6	67.76	2.49	131.14	2.93	97.99	3.28
R/I7	67.76	2.49	134.06	2.83	97.99	3.28
R/I8	67.76	2.49	136.99	2.83	97.99	3.28
R/I9	67.76	2.41	139.91	2.74	97.99	3.42
R/I10	68.74	2.41	143.81	2.65	98.96	3.28

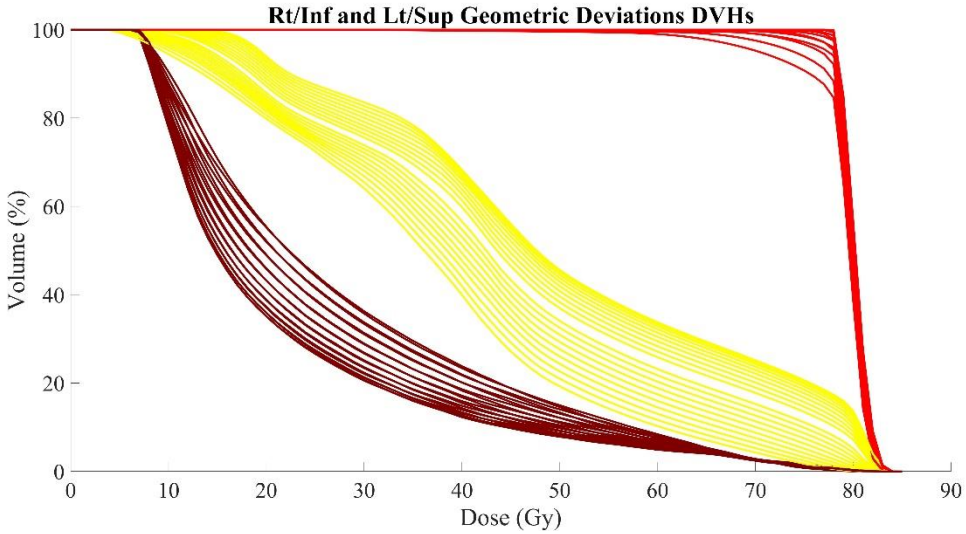

Figure 99. DVHs for Lt/Sup and Rt/Inf geometric deviations.

The final geometric deviations evaluated were shifts applied in the anterior and superior directions (Ant/Sup) and posterior and inferior (Post/Inf) directions. Dashed line represents the Ant/Sup deviation PRQs while dashed and dotted lines represented the Post/Inf deviations PRQs.

The Ant/Sup deviation PRQs experienced a reversal in behavior from the 4 mm deviation on. Ant/Sup deviations PRQ max values increased for the first 3 deviations from 86.76 % to 90.06 % then decreased to 0.55 %. The PRQ max values for Post/Inf deviations decreased from 79.03 % to 43.97 %. For Ant/Sup deviations the dose the max occurred at fluctuated: please see Table 44 for quantitative specifics. The dose the max occurred at for Post/Inf deviations decreased from 81.90 Gy to 74.10 Gy. The PRQ value at the prescription dose for Ant/Sup deviations slightly increased for the first 3 deviations from 78.50 % to 78.91 % then decreased to 0.33 %. The PRQ value at the prescription dose for Post/Inf deviations decreased from 76.33 % to 39.14 %. For Ant/Sup deviations the FWHMs increased for the first 3 deviations from 36.08 Gy to 39.00 Gy then decreased to 22.43 Gy. The FWHMs for Post/Inf deviations decreased from 30.23 Gy to 20.48 Gy. The AUC for Ant/Sup deviations increased for the first 3 deviations from 33.00 kGy% to 36.44 kGy% then decreased to 0.15 kGy%. The AUC decreased for Post/Inf deviations from 26.24 kGy% to 10.53 kGy%.

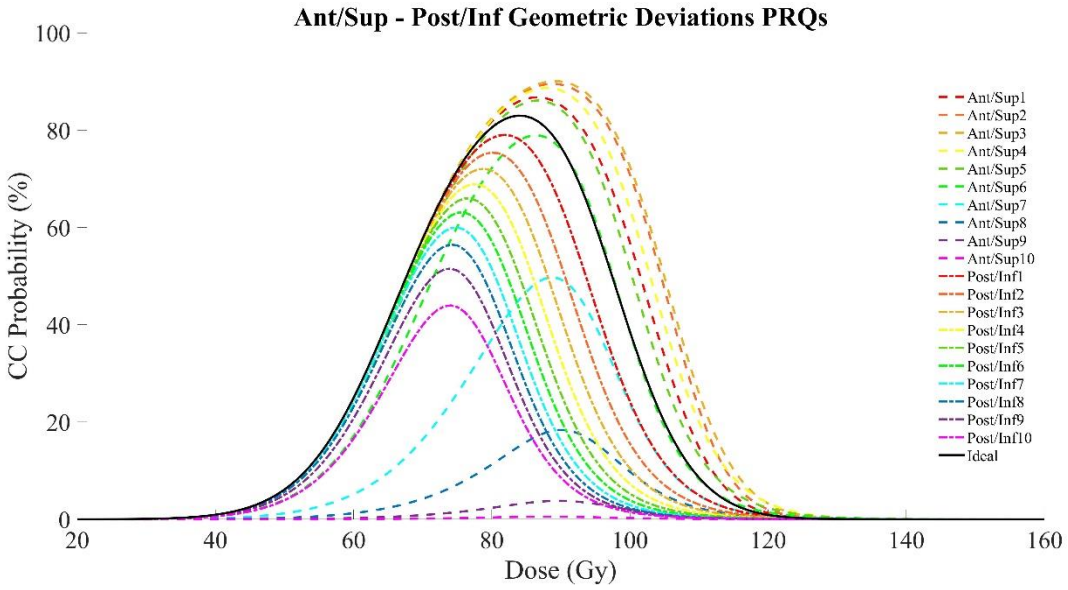

Figure 100. PRQs calculated for geometric deviations in the Anterior/Superior and Posterior/Inferior directions in 1 mm increments.

Table 44. PRQ metrics for geometric deviations in the Anterior/Superior and Posterior/Inferior directions in 1 mm increments.

	Max	Dose @ Max	Rx Dose	FWHM	AUC
A/S1	86.76	86.78	78.50	36.08	33.00
A/S2	89.52	88.73	78.87	39.00	35.76
A/S3	90.06	89.70	78.91	39.00	36.44
A/S4	88.69	87.75	78.51	37.05	34.69
A/S5	86.11	86.78	76.86	34.13	31.72
A/S6	78.94	86.78	67.93	30.23	26.35
A/S7	49.74	88.73	32.51	24.38	13.90
A/S8	18.37	89.70	9.48	22.43	4.81
A/S9	3.80	89.70	1.98	22.43	1.02
A/S10	0.55	87.75	0.33	22.43	0.15
P/I1	79.03	81.90	76.33	30.23	26.24
P/I2	75.38	79.95	74.40	28.28	23.63
P/I3	72.06	78.98	71.94	26.33	21.54
P/I4	68.87	78.00	68.87	25.35	19.76
P/I5	65.94	76.05	65.38	24.38	18.27
P/I6	63.06	76.05	61.38	24.38	16.92
P/I7	59.99	75.08	56.76	22.43	15.61
P/I8	56.49	74.10	51.86	21.45	14.30
P/I9	51.54	74.10	46.16	21.45	12.69
P/I10	43.97	74.10	39.14	20.48	10.53

Ant/Sup deviations TCPs experienced a shift right beginning at the 5 mm deviation increasing in magnitude and decreasing in slope with larger deviations. The Post/Inf deviations TCPs experience a small shift right beginning at the 8 mm deviation. The bladder NTCPs for Ant/Sup deviations experienced a left shift decreasing in magnitude and increasing in slope with larger deviations. For Post/Inf deviations bladder NTCPs experienced a right shift increasing in magnitude and decreeing in slope with larger deviations. The rectum NTCPs for Ant/Sup deviation experienced a larger right shift increasing in magnitude and decreasing in slope with larger deviations. Post/Inf deviations rectum NTCPs experience a left shift decreasing in magnitude and increasing in slope with larger deviations.

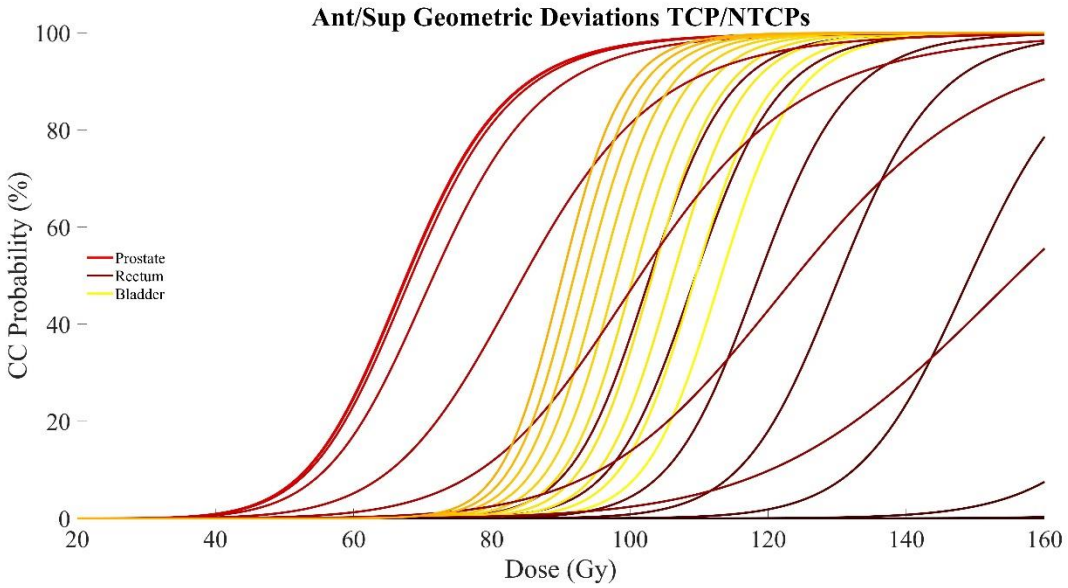

Figure 101. TCPs and NTCPs calculated for anterior and superior geometric deviations in 1 mm increments.

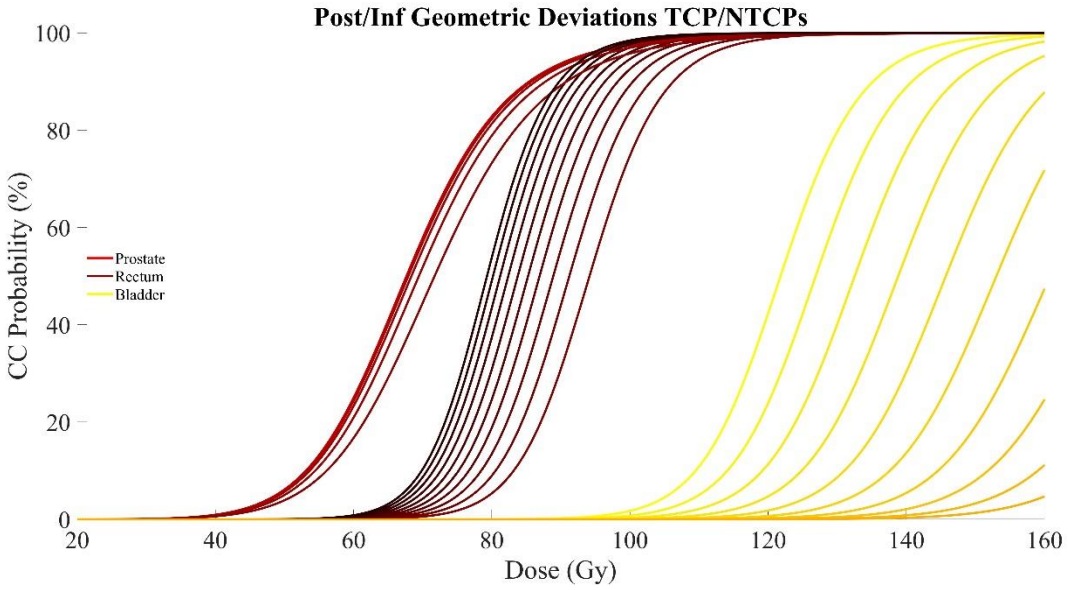

Figure 102. TCPs and NTCPs calculated for posterior and inferior geometric deviations in 1 mm increments.

Table 45. TCP and NTCP metrics calculated from Anterior/Superior and Posterior/Inferior geometric deviations.

	Prostate CTV		Bladder		Rectum	
	50% Dose	80/20 Slope	50% Dose	80/20 Slope	50% Dose	80/20 Slope
A/S1	67.76	2.49	113.59	3.42	102.86	3.16
A/S2	67.76	2.49	109.69	3.42	109.69	3.04
A/S3	67.76	2.49	105.79	3.42	118.46	2.74
A/S4	67.76	2.49	102.86	3.73	130.16	2.56
A/S5	68.74	2.49	100.91	3.73	149.66	2.22
A/S6	71.66	2.28	97.99	3.91	183.79	0.00
A/S7	84.34	1.86	96.04	3.91	0.00	0.00
A/S8	101.89	1.55	94.09	4.10	0.00	0.00
A/S9	124.31	1.26	92.14	4.10	0.00	0.00
A/S10	155.51	0.00	90.19	4.32	0.00	0.00
P/I1	67.76	2.49	121.39	3.16	94.09	3.42
P/I2	67.76	2.49	127.24	3.04	91.16	3.57
P/I3	67.76	2.49	132.11	2.93	89.21	3.57
P/I4	67.76	2.49	138.94	2.74	87.26	3.73
P/I5	67.76	2.49	145.76	2.65	85.31	3.91
P/I6	67.76	2.49	152.59	2.49	83.36	3.73
P/I7	67.76	2.49	160.39	2.34	82.39	3.91
P/I8	68.74	2.49	169.16	2.22	81.41	3.91
P/I9	69.71	2.34	176.96	0.00	80.44	3.91
P/I10	71.66	2.28	184.76	0.00	79.46	3.91

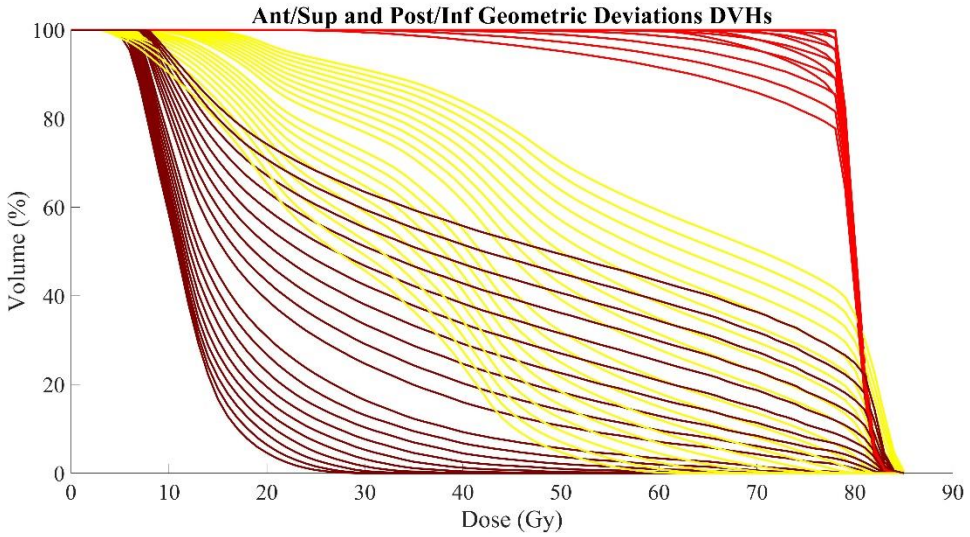

Figure 103. DVHs for Ant/Sup and Post/Inf geometric deviations.

3.2 Radiation Therapy Quality vs. Time Relationship

With the library of PRQs generated estimating quality vs. time relationships can begin. Three interpretations were generated for general and specific tasks to demonstrate approaches

individuals or clinics could take to understand the progression quantitatively of their radiotherapy process. Minus and plus percentages of the prescription dose PRQs were omitted for the quality vs. time relationship portion leaving a library of 325 PRQs for sampling. PRQs were first grouped into sets defined by the magnitude of their deviations. Expansions, contractions, and geometric offsets of 1 mm were grouped together and so forth. Figure 104 displays the average PRQs for each set of deviations plotted with one another. As deviations decreased the average PRQs increased in peak, value at the prescription dose, FWHM and AUC. The dose that the peaks occur at fluctuates and will be discussed later in 4.1.3 PRQ Behavior.

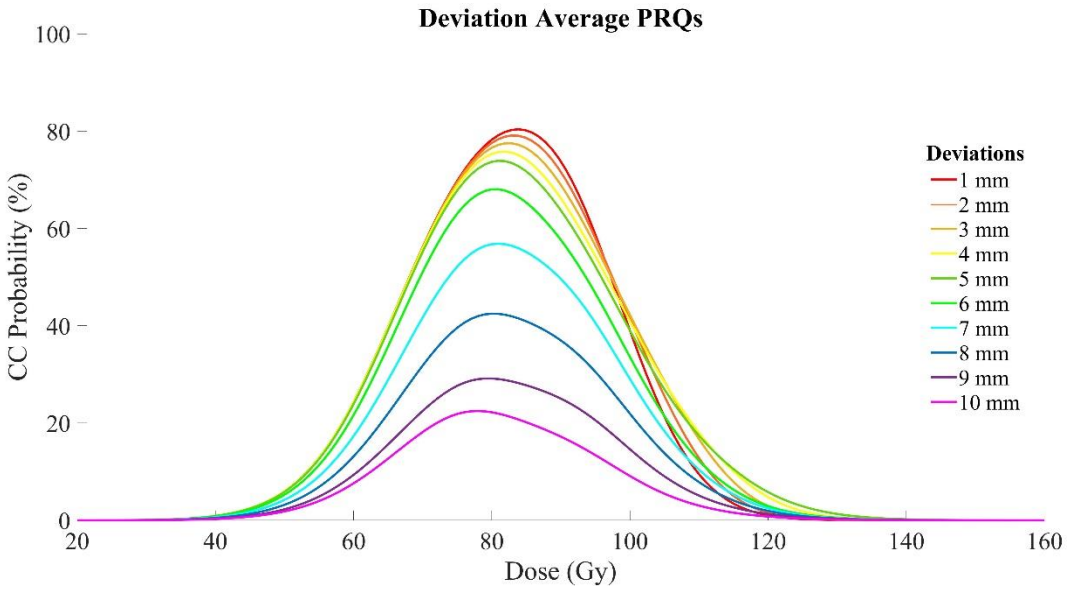

Figure 104. Plot for the average PRQ for a set of deviations as PRQs are grouped by their deviation magnitudes.

The control and complication probability ranges that PRQs fell into are displayed in Figure 105. 15 % (49 PRQs) had a max value less than 50 %. 29 % (95 PRQs) had a max value higher than the ideal plan or 82.99 %. 58% (187 PRQs) had a max value between 70-90 %. Only 12 PRQs had a max value between 20-40 %.

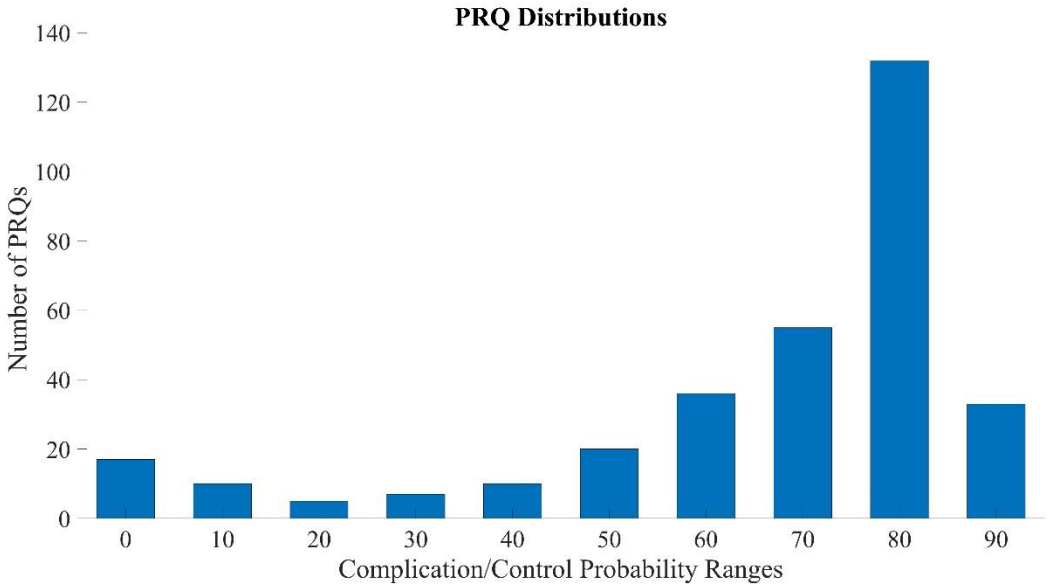

Figure 105. Distribution as PRQs are sorted based on the number of PRQs (y axis) within a range of complication/control probabilities (x axis).

This established the library of PRQs to be sampled from when determining the progression of quality from any given sequence of events in radiotherapy.

3.2.1 Generalized Tasks

The first interpretation of the quality vs. time relationship grouped the general tasks with the deviation average PRQs. With 5 general tasks and 10 deviation average PRQ sets, two sets were assigned to each general task. Larger deviations were coordinated with earlier tasks then the average of each set was calculated. Consult was represented by the 9-10 mm deviation PRQs average, simulation was represented by the 7-8 mm deviation PRQs average, treatment planning was represented by the 5-6 mm deviation PRQs average, plan review was represented by the 3-4 mm deviation PRQs average, and treatment was represented by the 1-2 mm deviation PRQs average. This corresponded to a PRQ max value of 25.78 % for consult, 49.65 % for simulation, 70.98 % for treatment planning, 76.64 % for plan review, and 79.71 % for treatment. As treatment continues and eventually is completed after several weeks, it is assumed that the quality continues to increase to the ideal PRQ max value of 82.99 %. While the ideal PRQ max value was not the largest for this study, it could be assumed that this value could increase to larger values with the completion of treatment. As discussed in 4.1.3 PRQ Behavior however, the largest PRQs occur with contracted volumes from the normal tissues. These are more indicative of the absence of

normal tissues or incomplete volumes. The peak of the average PRQs associated with general tasks was then assumed to occur after a work week for each task or 40 hours as seen in Figure 106.

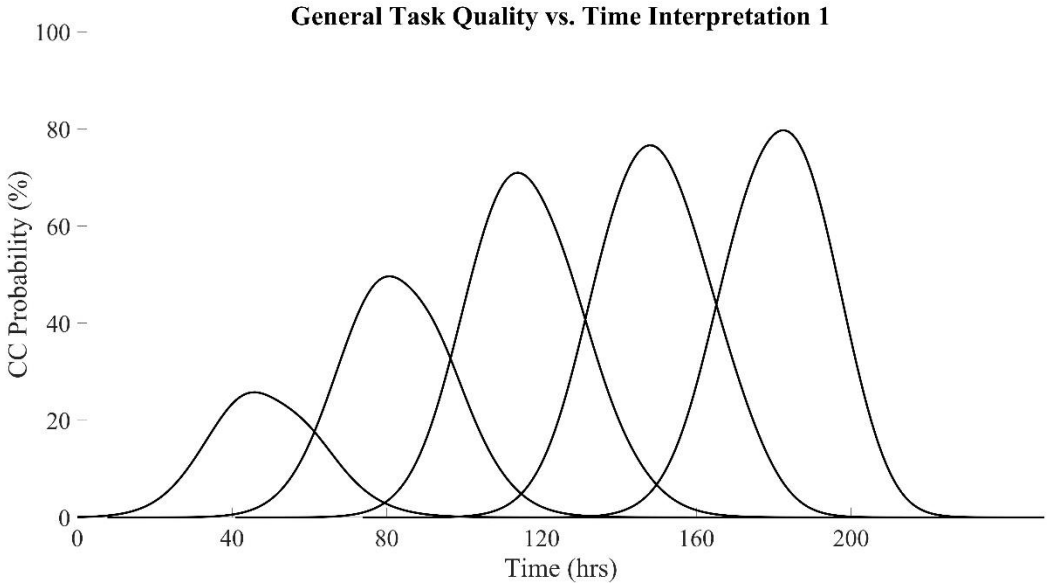

Figure 106. Quality vs Time interpretation one with each generalized task PRQ being calculated with two deviation magnitude PRQ averages. Consult is represented by 9-10 mm deviation PRQ averages. Simulation is represented by 7-8 mm deviation PRQ average. Treatment Planning is represented by 5-6 mm deviation PRQ averages. Plan review is represented by 3-4 mm deviation PRQ averages. Treatment is represented by 1-2 mm deviation magnitude PRQ averages.

The second interpretation of quality vs. time relationship assumes that larger increases in quality occur during treatment planning. General tasks were then assigned the following PRQs: consult was represented by the 10 mm deviation PRQs average, simulation was represented by the 9 mm deviation PRQs average, treatment planning was represented by the 5-8 mm deviation PRQs average, plan preview was represented by the 3-4 mm deviation PRQs average, and treatment was represented by the 1-2 mm deviation PRQs average. This corresponded to a PRQ max value of 22.47 % for consult, 29.15 % for simulation, 60.32 % for treatment planning, 76.64 % for plan review, and 79.71 % for treatment. Figure 107 displays the quality vs. time relationship for the second interpretation. As treatment continues and eventually is completed after several weeks, it is assumed that the quality would continue to increase to the PRQ max value of a specified sequence of events.

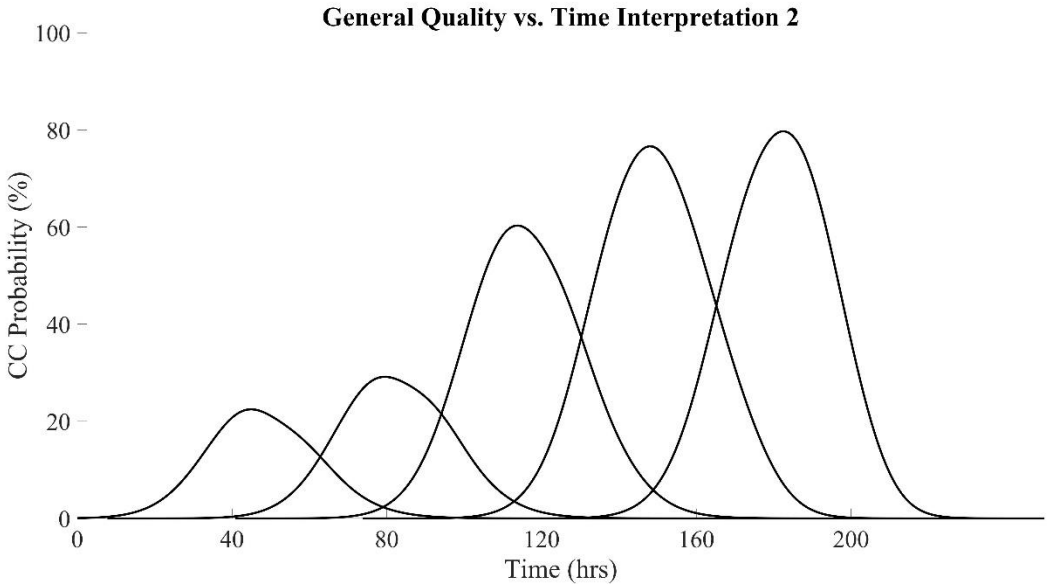

Figure 107. Quality vs. Time interpretation two with each generalized task being calculated by assigning various deviation magnitude PRQ averages. Consult is represented by 10 mm deviation PRQ average. Simulation is represented by 9 mm deviation PRQ average. Treatment Planning is represented by 5-8 mm deviation PRQ averages. Plan review is represented by 3-4 mm deviation PRQ averages. Treatment is represented by 1-2 mm deviation magnitude PRQ averages.

The third interpretation of the quality vs. time relationship assumed an equal weighed increase in quality for general tasks. Instead of using averages of PRQs, single PRQs were selected to represent the increase in quality. The library of PRQs was arranged in order of ascending max values for easier sampling. General tasks were coordinate with PRQs that reached control and complication probabilities of specified values, or achieved max values, in 15 % increments. Consult was represented by a PRQ with a 15 % max value, simulation was represented by a PRQ with 30 % max value, treatment planning was represented by a PRQ with a 45 % max value, plan review was represented by a PRQ with a 60 % max value, and treatment was represented with a PRQ with s 75 % max value. Figure 108 displays the quality vs. time relationship for the third interpretation. As treatment continues and eventually is completed after several weeks, it is assumed that the quality would continue to increase to the PRQ max value of a specified sequence of events.

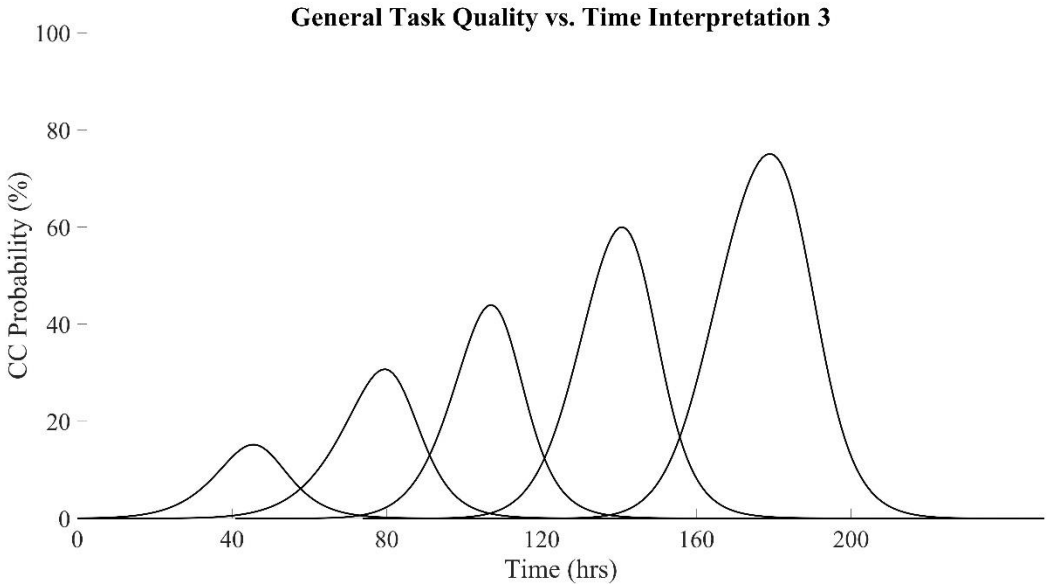

Figure 108. Quality vs. Time interpretation three with each generalized task being calculated by assigning various deviation PRQ percentages. Consult is represented by a 15 % PRQ. Simulation is represented by a 30 % PRQ. Treatment Planning is represented by a 45 % PRQ. Plan review is represented by a 60 % PRQ. Treatment is represented by a 75 % PRQ.

These three interpretations for quality vs. time relationships demonstrate how a clinic can define their unique increase in quality for radiotherapy as tasks are completed.

3.2.2 Specific Tasks

Specific task quality vs time relationships were generated for the three interpretations outlined for the general tasks. PRQs were selected from the library related to the general task PRQs sampled and associated. For interpretation one, PRQs sampled to represent specific tasks within consult were selected from the range of PRQs with max values between 0.00 % and 25.78 %, PRQs with max values between 25.78 % and 49.65 % represent simulation specific tasks and so forth. An evenly distributed approach was employed when selecting PRQs for specific tasks within a general task. There were less options for PRQ selection in the lower quality PRQs limiting the ability to evenly distribute the quality increases for consult and simulation.

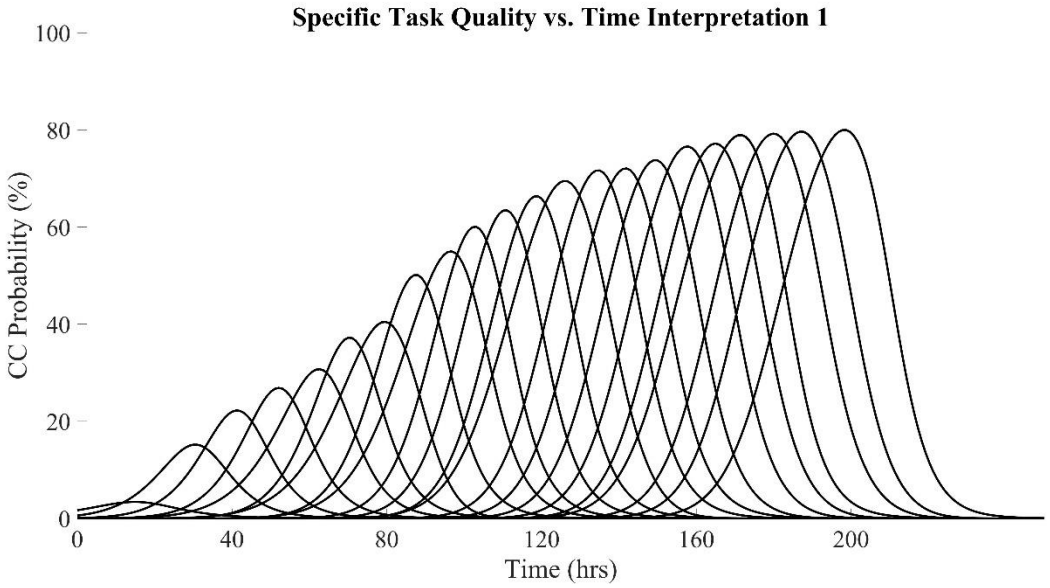

Figure 109. Quality vs. Time interpretation one for specific tasks.

Figure 109 displays the quality vs. time relationship for PRQs selected for specific tasks in interpretation one. During this interpretation the majority of the quality increase occurs during the first two weeks of the course of treatment. Figure 110 displays the second interpretation of the quality vs time relationship. Here the majority of the quality increase occurs during the third and fourth week of the course of treatment. During this interpretation it was assumed that the majority of the quality increase occurred during the treatment planning portion.

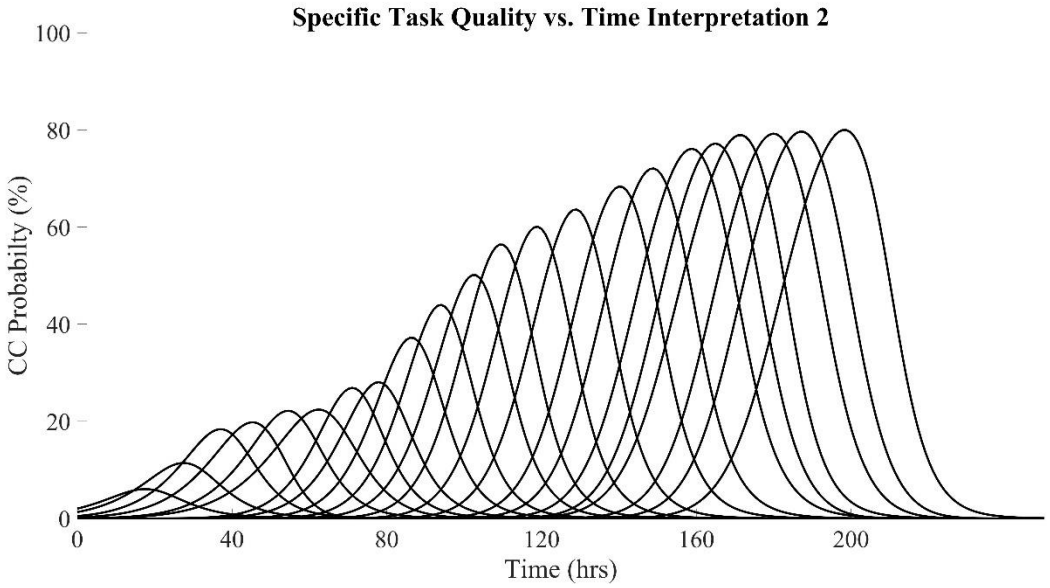

Figure 110. Quality vs. Time interpretation two for specific tasks.

Figure 111 displays the third interpretation for specific task quality vs. time relationships. For this interpretation focus was placed on selecting percentages of quality to represent tasks as opposed to associating deviation average PRQs with tasks. This interpretation emphasized an equal weighted distribution for all tasks (general and specific) with the PRQs sampled. For the 22 specific tasks identified and the 83.00 % PRQ max for the ideal each task correlated to an approximant increase in quality of 4 % per task.

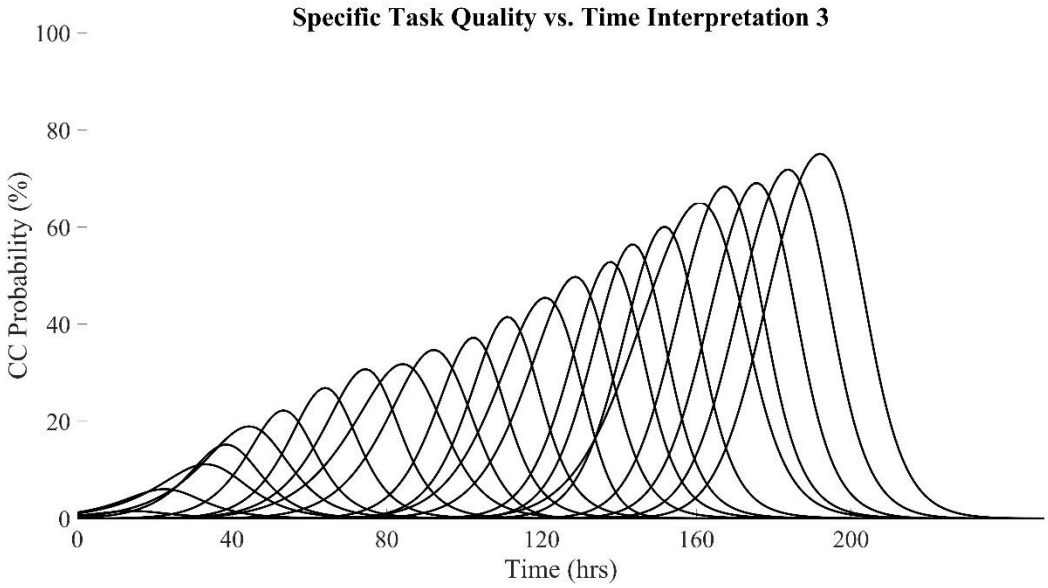

Figure 111. Quality vs. Time interpretation three for specific tasks.

3.2.3 Quality vs. Time Relationships

The three interpretations described above demonstrate the ability to sample a possible PRQ for any given task over time. Depending on the preference of an individual or clinic, variation can occur in how appropriate selections from the PRQ library relate to the tasks in a given process. Viewing the PRQ library in totality can provide insight into the decisions used to sample PRQs for task relation and meaningful quality vs. time relationship plots. Figure 112 and Figure 113 display graphs of the entire PRQ library that were created in 2 and 3 dimensions. PRQs for both were plotted in ascending order of PRQ max values. Similar plots could be created based on all PRQ metrics and combinations of them. For this study focus was placed on the max value that was calculated for all deviations. In total 325 PRQs were used for sampling of the 345 created and those are included in the figures below. Minus and plus dose deviation PRQs were omitted as discussed later. For the 2D plot each PRQ was plotted with a 39 Gy offset (half the prescription dose) to better coordinate where the peaks appear on the plot. There is a steep rise in control and complication probabilities at the beginning of the curve due to the under sampling of low complication free tumor control probabilities. A portion of near constant PRQ max values occurs around 83 % or close to the ideal max value. There are also the appearances of various trend lines that occur as PRQ functions overlap. This gives rise to multiple trends lines that are plotted within this one graph.

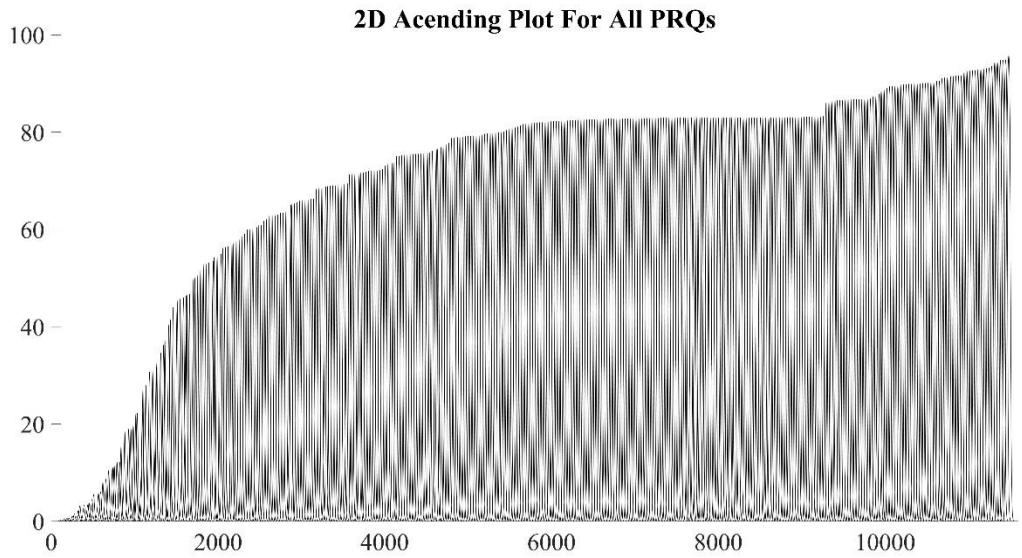

Figure 112. 2D Plot of all calculated PRQs plotted in ascending order.

Figure 113 displays the 3D plot of the PRQ library created in ascending order. The z-axis (into the page) is the PRQ number (#) with the y-axis being the control and complication probability (%) and the x-axis being dose (Gy). This provides the best reference for the relationships of how quality increases with decreases in deviations. Specifically, the variation of the dose the PRQ max occurs at can be viewed with ease in Figure 113. This plot provides an overall informative reference for the range of complication free tumor control probabilities created by applying deviations to a plan and the metrics incorporated with each PRQ. The shift in the dose the max occurs at can be seen clearly as a curve in the PRQs on the right side and the numerous PRQs on the left with larger values for the dose the max occurs at. Groups of similar PRQs from different deviations cause the appearance of thicker lines to form at certain probabilities.

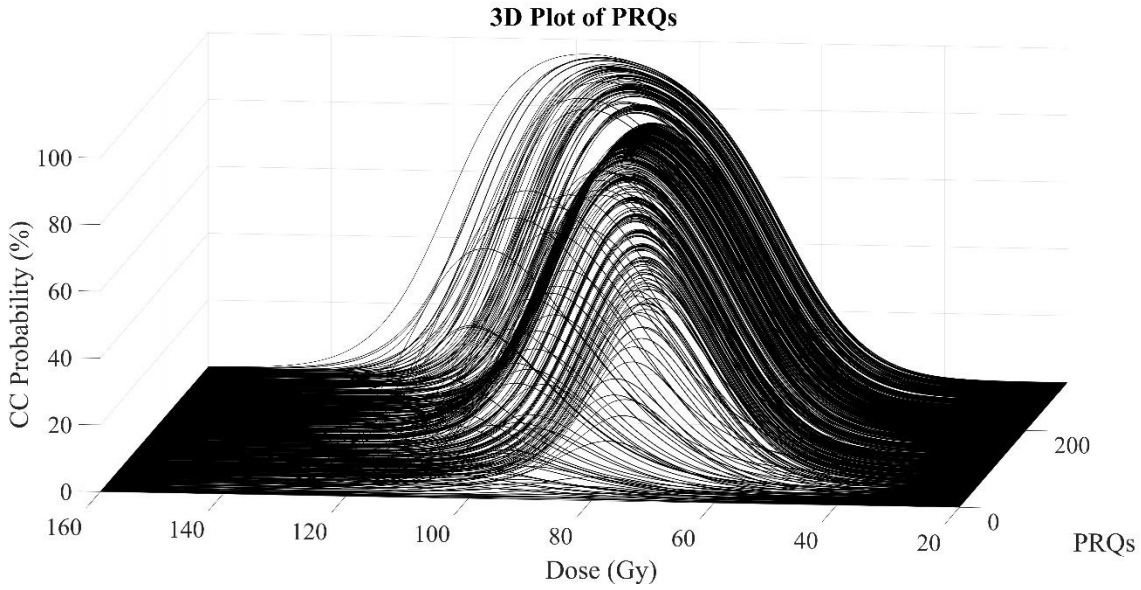

Figure 113. 3D Plot of all calculated PRQs plotted in ascending order.

SEC operate within this range of PRQs creating the realm in which treatments exist. Any deviations that could occur will produce PRQs within this domain and range.

4. DISCUSSION

The sensitivity of complication free tumor control probabilities allows a thorough means of evaluating how deviations in treatment parameters alter the doses tissues receive. Only using up to 10 mm delineation or geometric deviations, a wide range of PRQs was generated varying in max value from 0.22 % to 95.70 %. Pockets appear within this range given specific circumstances where numerous deviations produce similar PRQs. For instance, geometric deviations including an anterior or posterior component produce comparable PRQs for various deviation increments evaluated. This can be seen in Figure 113 and Figure 120 in section 4.1.3 PRQ Behavior with the 2D plot of all PRQs where the appearance of thick black lines occur. This demonstrates the concept of deviations from various scenarios producing similar results. To better understand the PRQs that could be generated given specific scenarios one must evaluate the behavior of the doses tissues receive or the behavior of the DVHs, TCPs, and NTCPs.

4.1 Initial Analysis

Complication free tumor control probability functions behavior can be seen in the results for the various deviations in Chapter 3 Results. Similarly, TCP, NTCP, and DVH behaviors are also observed as variations are applied to an “ideal” plan with their plots following the complication free tumor control probabilities (PRQs). The dynamic behavior observed in DVHs, TCPs, NTCPs, and PRQs provides valuable insight into the physical means in which actions from tasks in the radiotherapy process physically alter dose to tissues. The domain and range possibilities can be estimated from this study’s data set to understand how fluctuations occur in the DVHs, TCPs, NTCPs, and PRQs as deviation scenarios alter doses to tissues.

4.1.1 DVH Behavior

Figure 114 displays all prostate CTV DVHs. Figure 115 displays all bladder DVHs. Figure 116 displays all rectum DVHs. As deviations were evaluated boundary conditions for all structures DVHs can be estimated. Three regions are used here to describe the DVHs based on the behavior observed. Drawing a line from the upper left corner to the bottom right corner of the DVH graphs defines these regions. The first region is the bottom left of the graphs, the second is the area around the line splitting the graph and the third is the upper right of the graphs. Deviations applied will cause normal tissue DVHs to fluctuate between the first and second region while tumor DVHs

would fluctuate in the third region. Unacceptable DVHs for normal tissues begin to occur as DVHs shift towards the third region or begin to have large sections above the drawn line. Depending on the sensitivity of the normal tissue in question an appropriate DVH varies between the first and second region. As tumor DVHs begin to encroach in any manner towards the second region they become unacceptable as the tumor does not receive the prescription dose increasing the chance of not being eradicated.

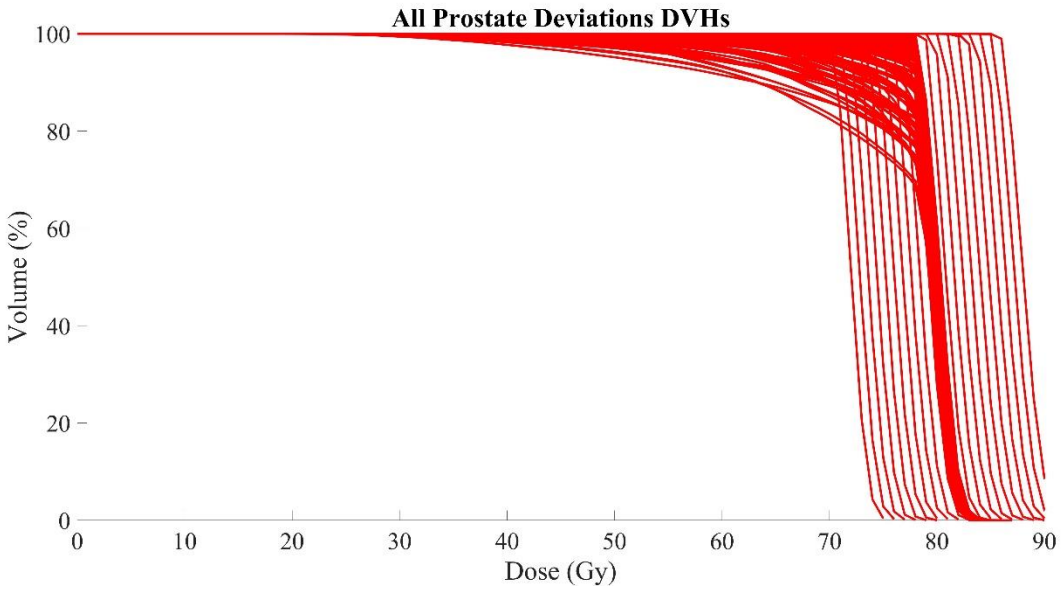

Figure 114. DVHs for all prostate CTV deviations that were evaluated.

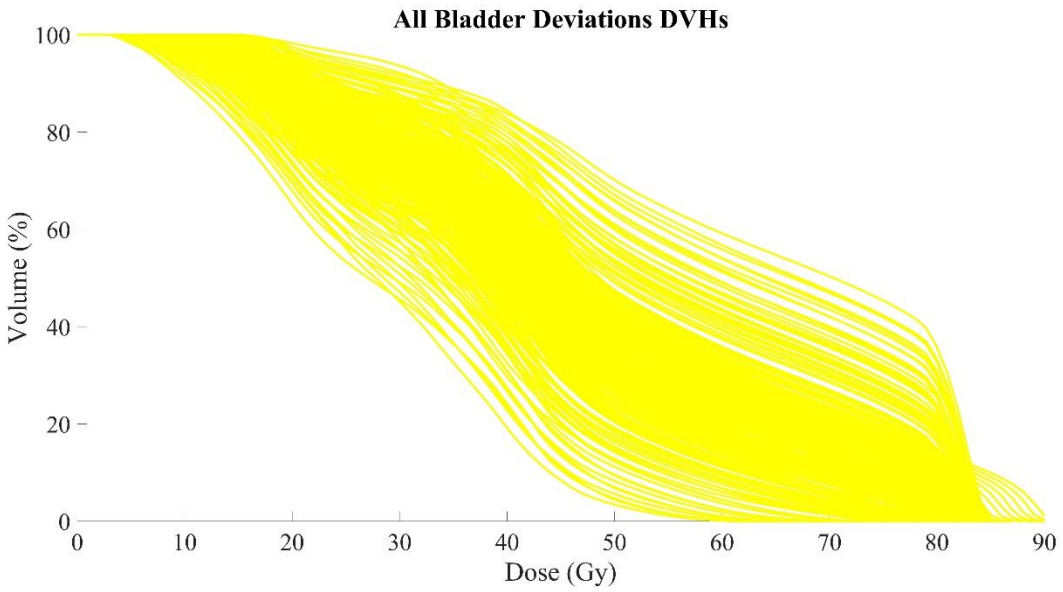

Figure 115. DVHs for all bladder deviations that were evaluated.

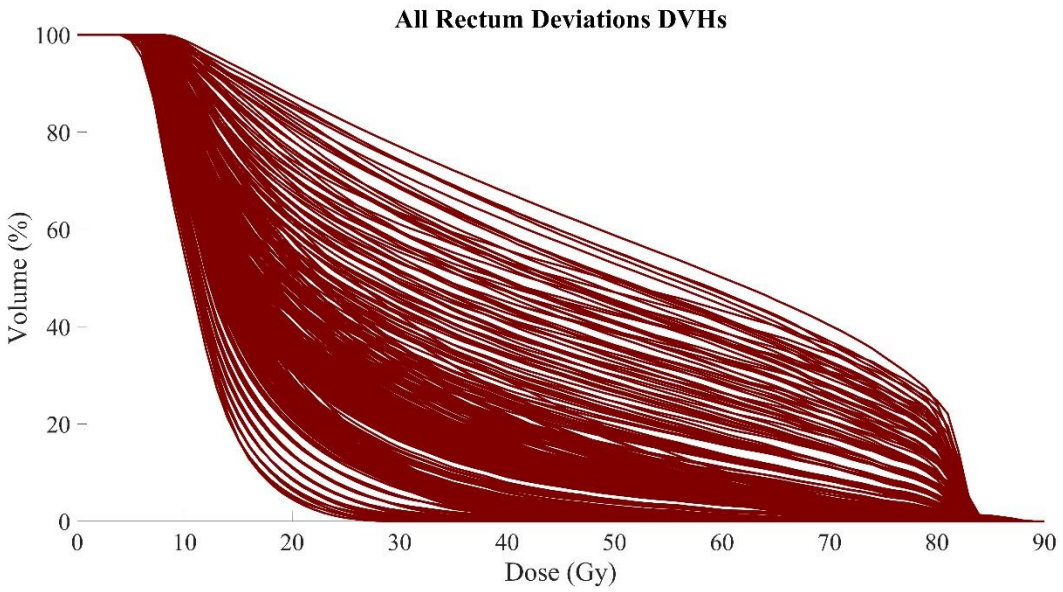

Figure 116. DVHs for all rectum deviations that were evaluated.

In the case evaluated for this study the “ideal” rectum DVH operated in the first region, the “ideal” bladder DVH operated in the second region and the “ideal” prostate CTV DVH operated in the third region. Deviations that increased rectal dose began to push the rectum DVHs into the second region while decreases further pushed the DVHs to the lower left corner of the graph. The bladder deviations that decreased bladder dose pushed the DVHs toward the first region and

deviations that increased bladder dose pushed the DVHs toward the third region. Deviations that decreased prostate CTV dose had their DVHs pulled toward the second region which only occurred with larger deviations. Additional combinations of deviations that could be calculated will produce similar DVHs within these regions outlined for each structure. By continually creating plans to account for possible deviations and combinations of deviations, DVHs can be generated for any scenario to fill out the empty space on the graph for each structure and encapsulate these possibilities. Hypothetically if plans with all possible combinations of deviations were created a complete PRQ library could be established. At some point however creating plans for scenarios with large deviations will not produce meaningful or usable information. There is a limit to the extent of deviations needed to create a full PRQ library. This is related to the catastrophic limit and is discussed in section 4.1.4 Quality vs. Time Relationships.

As actions are performed or as tasks are completed, doses to structures are altered. As mentioned earlier actions or tasks either indirectly or directly affect the dosimetric and geometric components of a treatment plan by either providing information for or physically altering a treatment parameter. These actions, outlined in the radiotherapy process, cause large or small volumes of tissues to experience a change in the dose they are receiving. Understanding how an action then changes a tissue's DVH can then be extrapolated out to the overall effect on the quality or the control and complication probabilities. For instance, completing actions related to delimiting structures to their ideals would see of flow of normal tissue DVH's towards the lower left corner, or a flow in the direction moving from the second to the first region, while the prostate CTV DVHs would flow into the upper right corner or in the third region. Imaging for patient setup actions would decrease geometric deviations and normal tissue DVHs would once again flow in the direction moving from the second to first region while the prostate CTV DVH would flow into the corner of the third region. As DVHs flow back and forth between the first, second, and third regions as actions are performed and deviations are minimized, the TCPs and NTCPs change as well.

4.1.2 TCP and NTCP Behavior

Initial review of TCP and NTCP plots show the dynamic behavior of delineated structures for applied delineation and geometric deviations. Figure 117 displays all prostate CTV TCPs. For the prostate CTV, as the dose is removed from increasing volumes of the tumor the curves shift

right and eventually decrease in slope. Of the deviations evaluated, deviations larger than 5 mm are necessary to cause measurable change in prostate CTV TCPs. This of course is related to the definition of Planning Target Volume (PTV) and the rationale used in treatment methodologies in radiation therapy to account for uncertainties and ensure the tumor will receive the prescribed dose. For this case the margin was a 6.5 mm symmetrical expansion with exceptions for areas pushing into surrounding normal tissues, most notably the posterior portion due to the rectum. Differences in the TCP begin to be seen as deviations approach this margin. The 5 mm geometric deviations applied in the anterior directions, either solely or in combination with other translational directions, cause slight changes seen visibly in the TCP plots. This either causes the line to appear thicker (Ant, Lt/Ant/Inf, Lt/Ant, Ant/Inf, Rt/Ant, CTV expansion) or in some cases even causes the plotted line to appear as its own curve (Rt/Ant/Inf, Lt/Ant/Sup, Rt/Ant/Sup, Ant/Sup, CTV expansion). From 6 mm on for geometric deviations the TCPs begin to experience larger shifts to the right and large decreases in slope. For delineation deviations the 6 mm deviation TCP shifts right and continues to fall to the right with increased deviations.

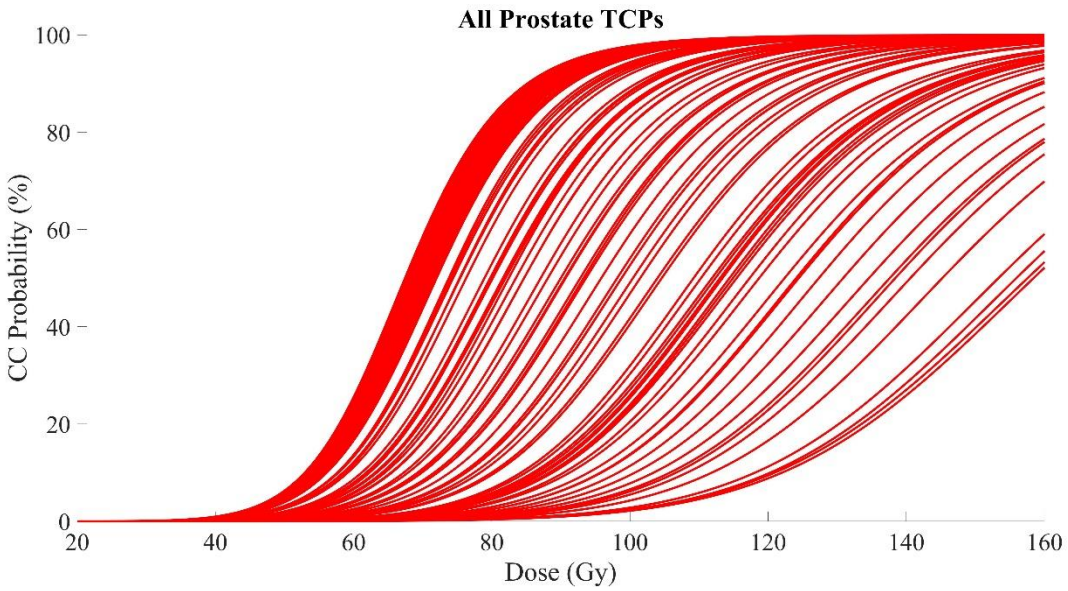

Figure 117. Plot consisting of all prostate CTV TCPs calculated for applied deviations.

From these evaluations a domain and range can be identified for TCP functions that can occur from the numerous hypothetical scenarios plausibly generated. The contractions of the CTV cause the TCPs to be unchanged meaning these TCPs are a left side limit for the TCP for the given

plan. A plan in which CTV contractions cause the TCPs to experience a shift left would establish the left side limit more notable with smaller margins used for a given PTV. Prostate CTV deviations that cause larger portions of the CTV be outside of and away from PTV, or the prescription dose points in the dose cloud, create the TCPs on right side of Figure 117. For the range of deviations evaluated, the right side limit is set by the 10 mm deviations. Combination of delineation and/or geometric deviations for the most part will produce TCPs inside these ranges. Some combinations, such as an underdrawn prostate CTV with a 10 mm geometric deviation, will produce TCPs father right on the graph. These however will produce PRQs equal to zero and will be excluded from this study and analysis. The catastrophic region is defined as deviations in the range that produce PRQs equal to zero. This is discussed more thoroughly in the following section on 4.1.4 Quality vs. Time Relationships and the catastrophic limit.

Figure 118 displays all bladder NTCPs while Figure 119 displays all rectum NTCPs. For normal tissues, delineation expansions cause NTCPs to shift right and contractions cause NTCPs to shift left. This is due to the normal tissues receiving more dose as they are expanded into the PTV and receiving less dose as they are contracted away from the PTV. With larger right shifts NTCPs also experienced a decrease in slope with larger left shifts NTCPs experiencing a slight increase in slope. Shifts right, or scenarios that decreased dose to a normal tissue, generally had larger magnitude shifts than their counterpart left shifts. Typically, as a NTCP shifted left the magnitude of the shift would decrease while right shifts magnitudes would increase with larger deviations. Geometric deviations with a posterior component cause rectum NTCPs to shift left and bladder NTCPs right. Geometric deviations with an anterior component cause the bladder NTCP to shift left and the rectum NTCPs to shift right.

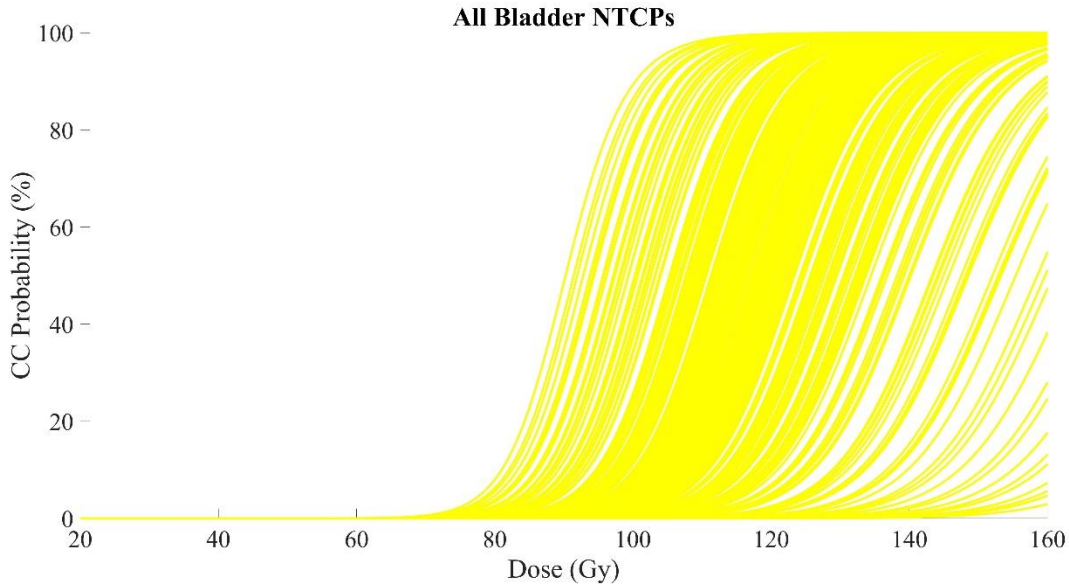

Figure 118. Plot consisting of all bladder NTCPs calculated for applied deviations.

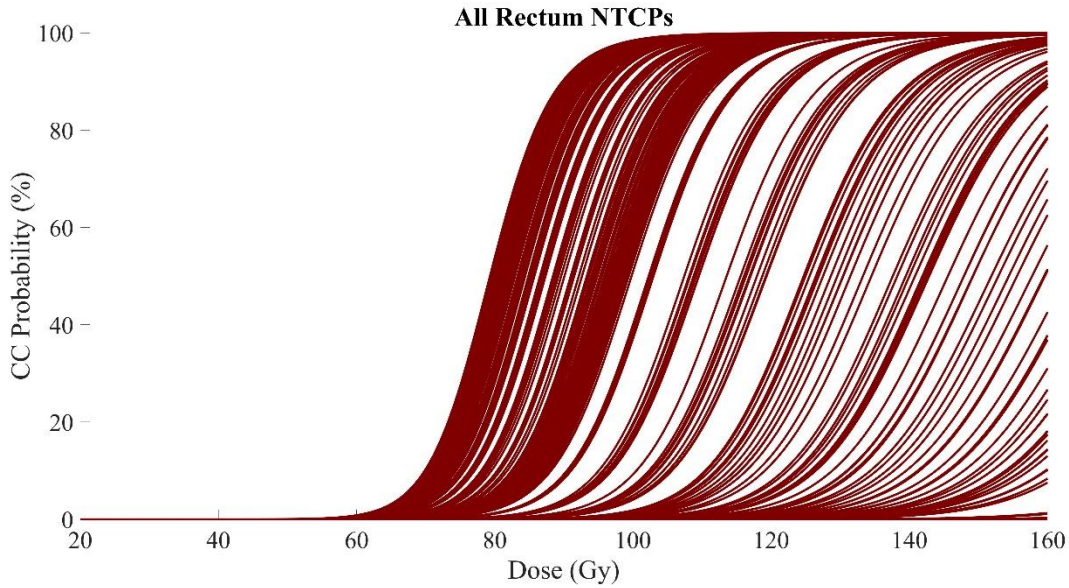

Figure 119. Plot consisting of all rectum NTCPs calculated for applied deviations.

The bladder NTCPs left side limits are generated by anterior geometric deviations. Delineation deviations have little effect on bladder NTCPs. The right side limits are generated by the posterior geometric deviations. For the rectum NTCPs the left side limits come from the posterior deviations and the right side limits from the anterior deviations. As described before combinations of deviations will produce NTCPs within these boundaries. The left side of the

NTCPs represents the main area of interest as deviations that cause these NTCPs are related to larger doses to the normal tissues. The right side becomes important when balancing dose to the tumor and normal tissues. The distance between the furthest left NTCP and furthest right NTCP provides information on the quality of the plan. This indicates a level of optimization as a larger distance implies one normal tissue is being overdosed while another is receiving very little dose. This is best seen in Figure 58 displaying the posterior geometric deviation TCPs and NTCPs graph. The 10 mm deviation NTCPs have the largest distance between them as dose has been shifted into the rectum and away from the bladder. There is a relationship between this distance and the sensitivities of the tissues. Data currently exist for the distances between normal tissue NTCPs from approved and treated plans. This relationship can then be quantified and used to further optimize the planning process.

4.1.3 PRQ Behavior

Figure 120 displays a 2D plot of all PRQs from delineation and geometric deviations plotted together. The left side of the PRQs is defined by scenarios where deviations maintained prescription doses for the tumor. As the tumor begins to lose dose, the left side of a PRQ shifts right and the max decreases, as can be seen with the numerous PRQs in the central portion and right side of the graph. The right side of the PRQs is defined by scenarios where the deviations minimize the normal tissues doses as well as maintain tumor prescription doses. The right side shifts left and the max decreases with scenarios where deviations increase doses to normal tissues. The peak then is a representation of how well any scenarios deviations maintains tumor dose and minimizes normal tissues doses. The peaks, or dose the max occurs at, vary back and forth depending on the deviation scenario. Of the centrally located PRQs, those with peaks on the left have their loss of quality dominated by high normal tissue doses while ones with peaks on the right have their loss of quality dominated by low tumor doses.

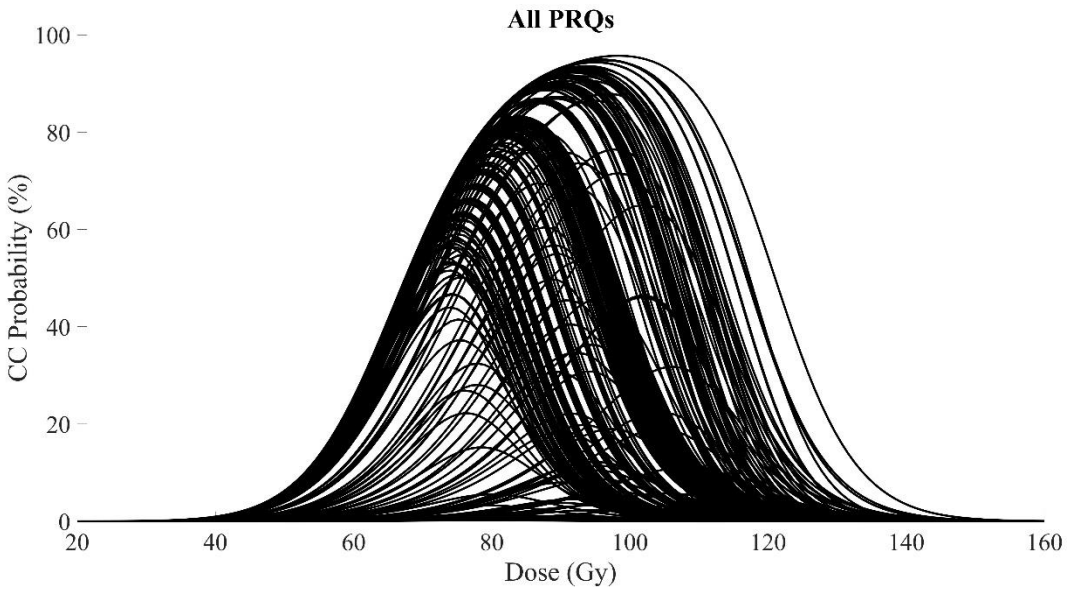

Figure 120. All PRQs plotted on the same graph.

These establish the boundary conditions for which the radiotherapy process operates for this prostate CTV IMRT plan. Any given sequence of events (SOE), or SEC, will produce a probability function inside these limits. Combinations of deviations will produce similar PRQs that essentially collapse to zero at a faster rate than single deviations. For example, a geometric deviation in the posterior direction and a delineation deviation of the rectum in the anterior direction will cause large volumes of the rectum to be irradiated, growing in magnitude with larger deviations. There are situations in which a geometric deviation and delineation deviation cancel each other out, but this would still produce a PRQ within this range.

The appearance of thick black lines on the left as PRQs collapse is related to increases in rectal doses. By expanding the rectum into the PTV or having a geometric offset shifting the rectum into the PTV, similar decreases occur in different deviation scenarios and manifest on the left side of the graph. Around 80 Gy a distinct curve can be viewed when tracing the peaks of the PRQs. Starting around the ideal (82.99 % or near the thickest black line) rectum dominated PRQs peaks shift left then begin shifting right around 50 %. The shift back to the right occurs with geometric deviations large enough to remove the tumor outside of the PTV decreasing its dose. Similar behavior is observed with anterior geometric deviations and PRQs of the right side of the

graph where bladder dose dominates the PRQ but it is not as distinct. Left sided PRQs are correlated with the more sensitive normal tissues. The main contributor to the collapse in PRQs on the right side comes from the tumor losing dose.

It was observed that 34.2 % (111/325) of PRQs were larger than the ideal PRQ, or the initial treatment plan PRQ, meaning that more optimal scenarios provide better avoidance of normal tissues while still maintain appropriate tumor coverage. 9.23 % (30/325) of these PRQs came from the contraction deviations calculated and may not be realistic as typically individuals are trained to be conservative in volume contour estimates. Contractions deviations were stopped at 5 mm because these contours are unreasonably small for the tissue's volume. These contractions however created the largest PRQs and increases the dose the max occurs at. A relationship exists then as to a limit that the dose the max occurs at can vary from the prescription dose. Situations with large PRQs and larger doses at which the max occurs have a relationship with smaller volumes. This can be an indicator to a clinic that volumes are under drawn or possibly not all normal tissue contours have been completed. In these cases, larger PRQs are more of an indicator that something is incorrect as opposed to an extremely well designed and executed treatment plan.

Figure 113 displayed all PRQs plotted in ascending order in 3D providing valuable information to the possibilities of treatment quality. As tasks are completed, deviations are minimized, and one essentially climbs the peaks of the PRQs tracing out a path. The sequence of events (SOE) is correlated with this path. As tasks are completed, PRQs are sampled related to appropriate representative deviations and viewing each PRQ sampled as a frame in a movie one can watch the quality increase. A movie was created with each frame being the PRQ plotted in ascending order. As PRQs increased (tasks being completed minimizing deviations) the peak of the PRQs fluctuate from right to left. This is indicative of the balancing act of getting dose to the tumor and minimizing dose to the normal structures. As the plots shift to the right dose to the tumor is low and as they shift left doses to normal tissues are too high.

It is here that as one traces out the peaks of PRQs viewed in ascending order that an interesting behavior is observed. As the peaks shift left and right while increasing in max value a relationship to damped harmonic oscillation can be seen. Thus, a complex process can be understood in terms of damped harmonic oscillation with the amplitude representative of

deviations amplitudes. Incidents, poor performance or new information learned would create larger deviations which would then start the damped harmonic oscillation process again. Over long periods of time a signal can be generated then consisting of a series of damped harmonic oscillations related to the tasks performed and the performance of those tasks. Such a signal is a massive step towards real time monitoring of quality in a complex process.

4.1.4 Quality vs. Time Relationships

Figure 113 is the main result from this work and displays the PRQs plotted in ascending order or the PRQ library used to estimate quality vs. time relationships. This is the most informative graph to provide a sense of the how quality varies for the complex process of radiation therapy for prostate IMRT plans. At low control and complication probabilities the peaks shift along the dose axis between 70 Gy to 110 Gy. This is related to the overdosing of normal tissues and under dosing the tumor from certain deviations. Less dose to the tumor produces the PRQs with a higher dose values that the max occurs at while more dose to the normal tissues produces PRQs with max values occurring closer to the prescription dose. Taking any individual PRQ then, one can assess the types of doses that delineated structures are receiving based the graphs and PRQ metrics.

As tasks are completed a distinct SOE is defined while PRQs are sampled to represent progress to the final PRQ achieved. Figures 121-123 show 3D plots for all PRQs with the specific task interpretations of quality vs. time PRQs highlighted in red. As tasks are defined and deviations linked to those tasks, PRQs are sampled. This demonstrates how a clinic achieves their quality for treatments or how the clinic jumps from peak to peak while actions ideally decrease deviations to provide the best treatment possible. A question arises then as to the means for generating a meaningful PRQ library.

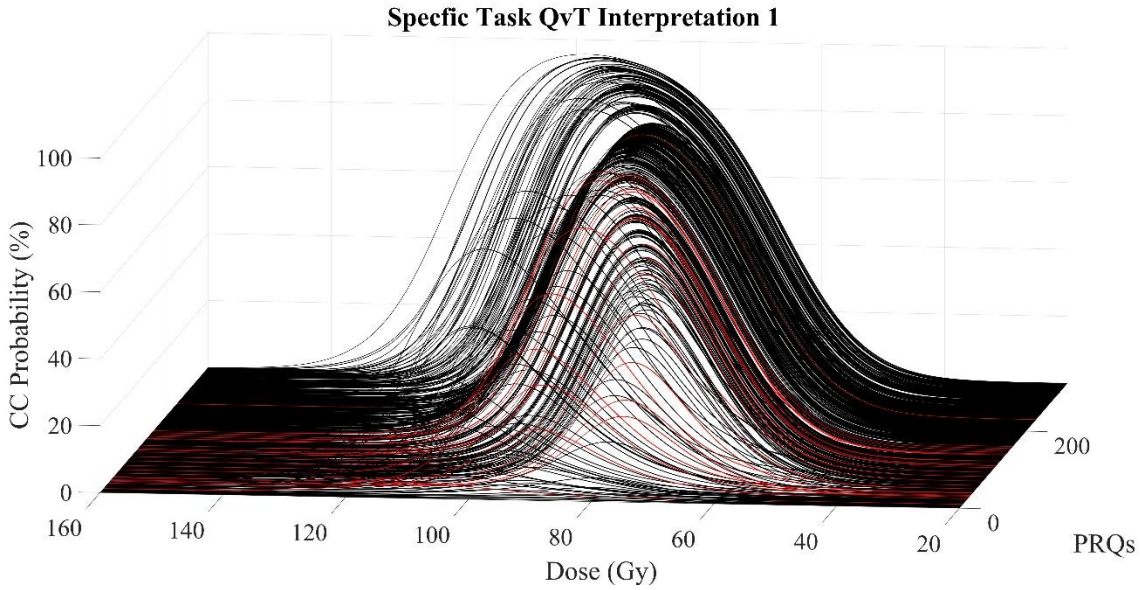

Figure 121. 3D Plot consisting of all PRQs with the PRQs sampled for specific tasks in interpretation 1 highlighted in red.

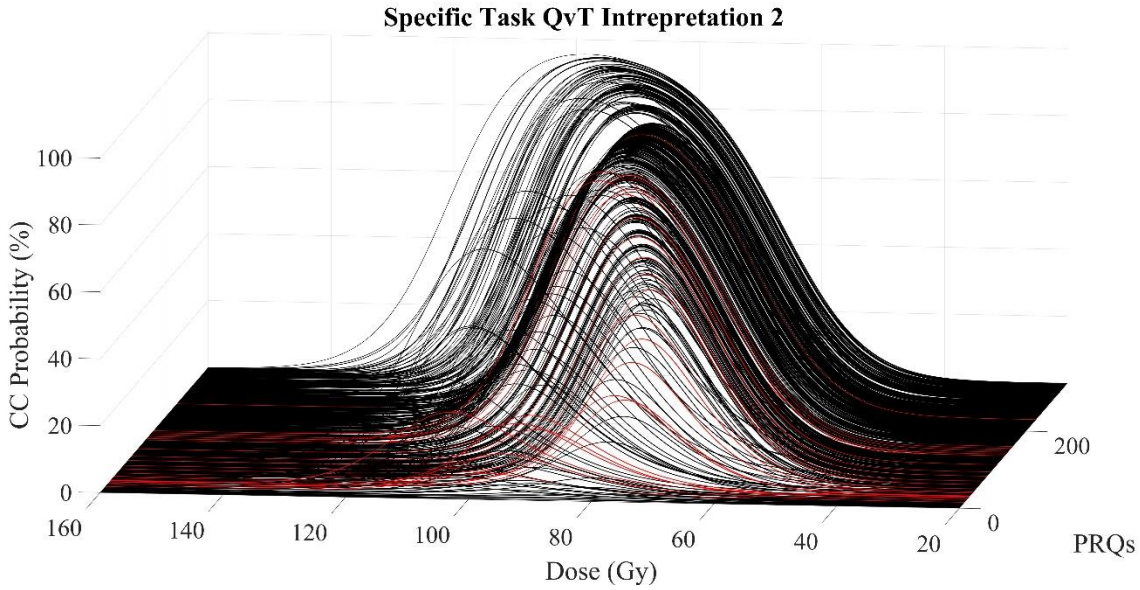

Figure 122. 3D Plot consisting of all PRQs with the PRQs sampled for specific tasks in interpretation 2 highlighted in red.

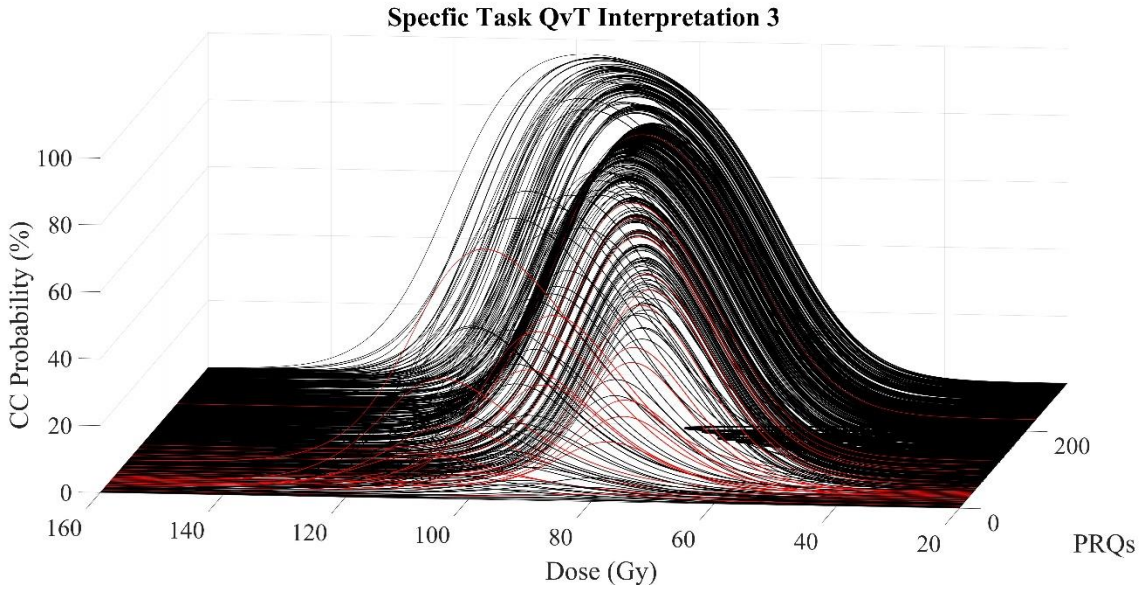

Figure 123. 3D Plot consisting of all PRQs with the PRQs sampled for specific tasks in interpretation 3 highlighted in red.

An assumption will be made that any course of treatment would not be provided in any manner without providing the chance of a benefit to the patient. This means that some tasks must be completed and that deviations at this point are in the range that will produce a non-zero PRQ or a measurable entity. While errors and accidents can cause deviations that will produce PRQs equal to zero, safety structures exist to prevent this leading to the field of quality and safety. When evaluating the quality of radiotherapy, the main region of interest contains scenarios and actions that produce measurable PRQs and the region where the PRQs begin to approach zero.

This lends to an explanation for the scenarios and actions that produce PRQs equal to zero as there are many. The scenarios and actions that produce PRQs equal to zero are considered catastrophic events or catastrophic errors; doses to tissues in this region cause severe complications, death from the disease, or the ultimate catastrophic error of patient death from a radiation overdose. This becomes the definition of the catastrophic region; Sequences of events in which the magnitude of their deviations produces PRQs equal to zero. For this study the catastrophic region is likely around deviations of 12-15 mm as at this point essentially all PRQ calculations will be zero.

Practically speaking, however, determining the area where PRQs began to approach zero is of more relevance, or essentially determining the range of deviations that began to produce near

zero PRQs. Quality and safety practices are intended to prevent catastrophic events, and safety structures are designed to provide indicators or warnings before such events occur. Understanding the scenarios and deviations that cause these provides increased value to the radiotherapy safety sciences. This area will be referred to as the catastrophic limit, or the range of deviations that produce a specific amount of PRQs below a certain value. The catastrophic limit then defines the region of deviations that begin to produce a rise in quality, or a measurable entity to begin tracking how quality varies. Operating in the catastrophic region is contrary to the goal of radiation therapy, or any complex process for that matter, and understanding when this limit is being approached is necessary for identifying undesired operations or determining that a benefit is not being provided to a patient in radiotherapy.

For this study there are numerous PRQs that approach zero within the 10 mm deviation range evaluated. While low PRQs are under sampled keep in mind that only generalized deviations were investigated. Combinations of deviations within the 10 mm deviation range would produce an increased number of low PRQs to sample from. As seen with the amount of PRQs in the 70-90 % range, combination deviations would produce similar results for low PRQs. This 10 mm deviation range is effective then in capturing the behavior of PRQs and provides a realistic estimate for the catastrophic limit for this case. This creates a deviation set that produces a meaningful PRQ library to sample from for quality vs. time relationships. There is logic and rational used to determine the amount and types of deviation needed. Future studies will benefit from the types of deviations sets generated and used depending on the type of evaluations desired.

As deviation sets are created, PRQ libraries are generated to link with SOE. An additional step is needed to determine how PRQs will be sampled, their links to deviations, and relations to the tasks in the process. Defining the quality vs. time relationship then becomes a normalization problem. With a SOE set and a PRQ deviation set, the rates that PRQs increased as SOEs are completed must be determined. Depending on the amount of time a given task takes and the proposed increase in quality for that task, or the decrease in deviations, a clinic can appropriately map the increase inequality for their inherent operation. This is related to the variables of a function described earlier in section 2.2.2 and 2.2.3. An analogy is that the PRQ library forms a mountain of quality that must be climbed in order to treat a patient successfully. As the procedure progresses

the mountain is ascended and one now tracks how fast the mountain is ascended as well as the final peak reached. The majority of future work is based on this concept, or evaluating the rates that clinics achieve higher quality of treatments with their specific procedures.

4.2 Verification and Validation Analysis

The simple deviations that were applied with a favorable patient geometry allows verification of the meaningful information gained due to the change in PRQs observed. Deviations were chosen to be realistic possibilities based on errors that could and have occurred. As seen with the catastrophic limit and region, a large portion of scenarios will produce results that are not quantitative in that their PRQ is equal to zero. The magnitude of deviations investigated was sufficient to produce a range of PRQs that reach the catastrophic limit, allowing the measurement of realistic scenarios to assess routine operations as well as track a path into the catastrophic region.

4.2.1 Delineation Variations

For the tumor, delineation contractions should have little to no effect on the outcome of the treatment. This is due to the PTV being the planning delineation used to account for possible errors or uncertainties in the treatment course, ensuring the tumor will receive the prescribed dose. As the volume contracts, there is still a fairly homogenous dose distribution in the region providing the prescribed dose. In Figure 48 this is demonstrated by the need to magnify the graph in order to visualize the difference. Here differences in PRQs mainly stem from the inhomogeneities in the dose distribution, or hot and cold spots. Depending on the location of these inhomogeneities in relation to the contraction deviations, the PRQ will be affected accordingly. In this case the hot spots are located on periphery of the tumor, so as the volume shrinks there is a slight decrease in PRQ as the average dose per unit volume decreases.

As the tumor is expanded, a change in PRQ should occur as the volume begins to exceed the PTV. The margin for the PTV in general was 6.5 mm excluding adjacent normal tissues. The edges of the PTV begin to experience larger dose gradients meaning if the tumor volume did extend to this area the tumor edges would receive doses less than the prescription. In Figure 47 it can be seen that when the tumor volume is expanded the PRQ begins to decrease. For each additional mm the volume is expanded there is a large decrease in PRQ which is expected as significant tumor

volumes are not receiving doses even close to the prescription dose in some cases. The same effect is observed in Figure 47 in which the TCP begins to shift right at the 6 mm deviation expansion.

The bladder is a less sensitive tissue in comparison to the rectum and the patient geometry favors the bladder for this case as it has less surface area adjacent to the tumor then the rectum. Refer to Figure 31 for visual reference. With bladder contractions and expansions there is little to no effect on the PRQs. When viewing the geometry this can be expected as relatively small volumes begin receiving dose as deviations increase. The NTCPs for the bladder have small changes with each deviation in comparison to all NTCPs observed and the bladder NTCPs are already to the far right of Figure 32 and Figure 33 for the ideal plan. The proximal bladder delineation deviations in themselves serve as a validation by demonstrating that the bladder is still sensitive to changes in dose from deviations. In this case there is a noticeable change on the right side of the PRQ. Due to the low dose the bladder received in this case the NTCPs provide the best refence for the deviations effect.

The rectum is a more sensitive tissue and has a larger portion of its volume adjacent to the tumor. Small deviations cause large changes in the doses to those adjacent rectal volumes. Rectal contractions cause less does to the adjacent volumes and increase the PRQs as indicated by the NTCPs large right shift. This is expected since as the rectum moves away from the tumor it should receive less dose and a lower complication probability. Rectal expansions did the opposite and caused the adjacent volumes to receive more dose. This lead to decreases in PRQs and left shifts of the rectal NTCPs as large volume of the rectum are now receiving prescription doses. The proximal rectal contractions and expansions behaved in a similar manner. The lowest control and complication probabilities occurred with the largest proximal rectum expansion PRQs. This is as expected as expansion only in the proximal direction adds less volume to the overall rectal volume but still receives the same doses as the isotopically expanded rectum. The proximal expansion contour then has a large dose per volume increasing the probability of complication.

4.2.2 Geometrics Variations

This case was chosen due to the patient geometry which makes it favorable for verification with geometric deviations. The three structures used in evaluation are relatively well aligned on the same axis (±y, anterior/posterior, or longitudinal axis). Motion in this axis limits variables that

could affect the doses to tissues. Posterior motion increases dose to the rectum, which is the more sensitive tissue, and anterior motion increases dose to the bladder or the less sensitive tissue. The PTV is not a complete isotropic expansion of the CTV either and this can be used to further validate that large motions in the inhomogeneous directions should be seen in the results. Referring to Figure 16 it can be seen that the posterior margin is smaller than others, the superior margin larger and that the volume of the tumor is posteriorly weighted.

Left and right motion has little effect on the PRQs. In these scenarios dose is not increasing in normal tissues and large portions of the tumor still receive the prescription dose 10 mm out as can be seen scrolling through the CT slices. There is little change in PRQs with inferior motion which has the larger margin between the PTV and CTV on the superior side of the tumor. Superior motion has little effect on the PRQs until the 8 mm deviation. It is here that the PRQ begins to drop. This is expected as large portions of the bottom of the tumor began to lose prescription dose at these deviations.

Anterior and posterior motion cause large changes in PRQs as seen in Figure 56. As deviations in the posterior direction increase the PRQs steadily decreases. The bladder continues to lose dose with each deviation while the rectum has a large portion of the prescription dose shifted into it as seen in the subsequent DVHs and NTCPs. Due to the posteriorly weighted volume of the tumor at the 10 mm deviation the tumor volume still receives a large dose with a slight dip at the end of the DVH. This can be seen in the posterior deviation PRQs as the left side experiences little change and the majority of the decrease comes from overdosing the rectum.

Anterior deviations PRQs initially increase before beginning to decrease. This is due to the rectum being the more sensitive structure. This is best observed in Figure 57 where there is a crossover of the bladder and rectum NTCPs that occurs with the 3 mm deviation. In this figure it is seen that the bladder continues to receive higher dose while the rectum dose continues to decrease which is expected. This further validates that the PRQ is accurately representing the treatment plan as a whole by including information from all delineated structures. At 6 mm the tumor also begins to lose considerable dose. The posterior margin for the tumor was smaller than the rest due to the proximity of the rectum and as anterior shifts increase large portions of the tumor volume begin to lose dose. This is seen in anterior deviation PRQs as the left sides shift

right and the PRQs collapse around 98 Gy. This is expected as anterior motion in this case is more sensitive due to the reduced margin of the posteriorly weighted tumor volume.

From here deviations that have a geometric component in any direction experience similar behavior as seen in their PRQs, TCPs, NTCPs, and DVHs. For geometric deviations that include all directions numerous PRQs fall below 20 % as the consequences of the scenario increases dose to a normal tissue while simultaneously losing dose to the tumor. This constitutes the PRQs in the middle of the plots. As discussed earlier, PRQs with a left side farther to the right are indicative of the tumor losing dose, the further right the less dose the tumor is receiving. This is the case for the smallest PRQs observed in this study's deviation set that occurred. This involved an anterior component that in combination with another direction or directions significantly shifts the dose distribution away from the majority of the tumor and into a normal tissue (bladder). Here the posterior portion of the tumor receives little dose and the majority of the prescription dose in the dose distribution has been shifted into the bladder. Even though the bladder is more resistant it still receives such larger doses that the collapse of the PRQ functions in these scenarios is the greatest. Reviewing all geometric deviations, the directions in which the shifts are occurring match with the expected effects in dose that both the tumor and normal tissues experience from the offsets.

4.2.3 Radiation Biology Parameter Variation

There are many interpretations and varieties of radiobiological parameters that can be used depending on the criteria used for selecting endpoints and survival. These include matching population studies to cellular cultures, patient sample selections, statistical model selection, determining normal tissue endpoints and most important to this work, the effect of process uncertainties[55,57–60,64–73]. Several of the research goals proposed from QUNATEC aim to address these issues and provide a framework for researcher to achieve better reproducibility with their results. By varying the radiobiological parameters, the behavior of complication free tumor control probabilities can be verified to represent the intrinsic nature of the dose distributions impact. Changes in the size, shape, and location of PRQs are dependent then on the justification used when choosing radiobiological parameters. Three studies were selected that had variations in the parameters used to demonstrate that similar behavior in the PRQs are observed and results are inherent to the dose distributions caused by deviations.

The first study proposed a range of values to be used for the structure model parameter relating to volume a[59]. Two verification tests where done using the lowest and highest values for each structure. For prostate a = -7 and -15, for bladder a = 12 and 4, and for rectum a = 8 and 3. The larger values are indicative of more sensitivity in normal tissues and tumor control probability is less sensitive to cold spots. The delineation deviations for all structures and geometric deviations in the anterior and posterior direction were evaluated as seen in Figure 27 and Figure 56. The ideal PRQ using the original parameters is plotted for reference in black. It can be seen that overall the PRQs are smaller with large a values for each structure which is expected as more weight is being placed on the normal tissues doses due to the larger values. The bladder and rectum values are much closer together, meaning their sensitives are more similar due to volume effects. In this case the bladder has the higher value making its overall volume more sensitive meaning its PRQs should experience large magnitude changes compared to the rectum. This is seen in both the delineation and geometric deviations.

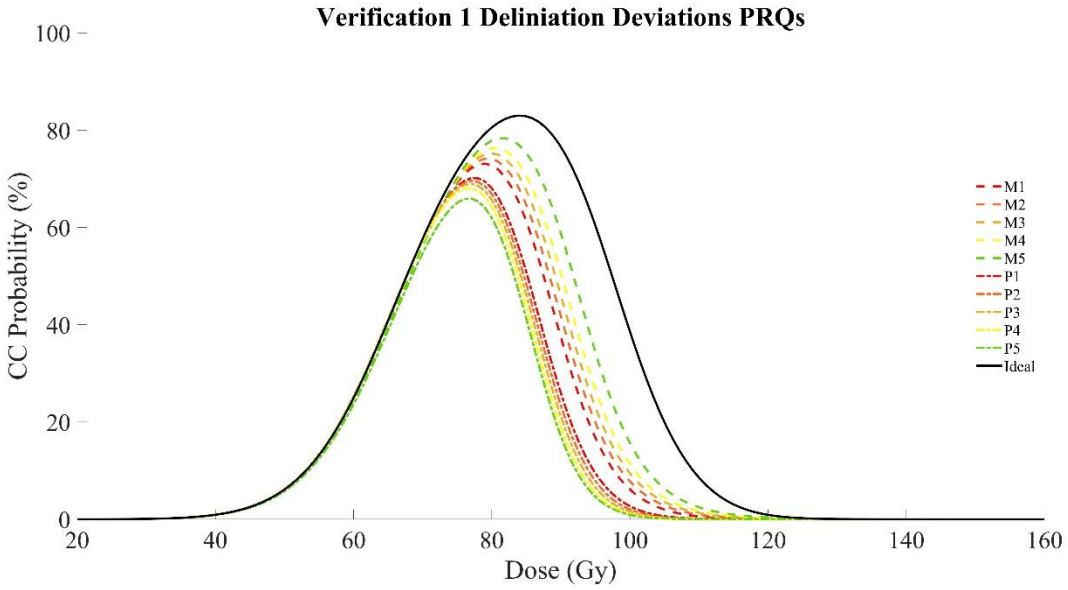

Figure 124. Delineation Deviations PRQs for the first verification test using alternate radiobiological parameters.

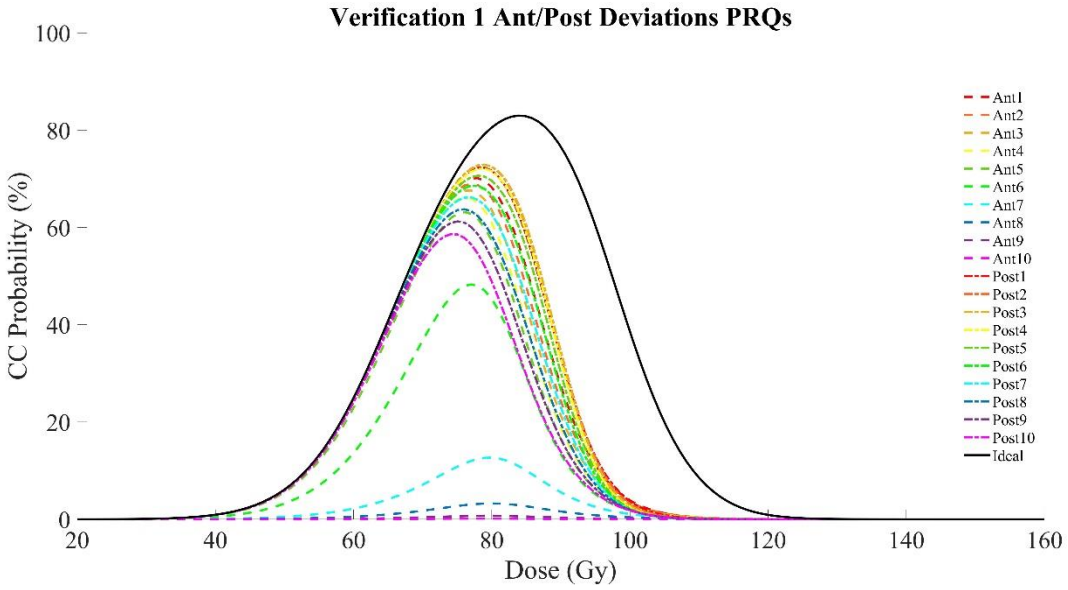

Figure 125. Anterior and Posterior Deviations PRQs for the first verification test using alternate radiobiological parameters.

The second verification test used the lower values that where proposed and the subsequent delineation and geometric deviations PRQs plots are displayed below. With lower values normal tissues volumes are less sensitive to radiation and tumors control probability is more sensitive to cold spots. It can be seen that the overall PRQs are larger than the ideal as expected. Once again the bladder and rectum values are almost equal meaning they are relatively similar in sensitivity. In both verification tests the anterior geometric deviations effectively crash towards the center of the plot, demonstrating that loss of dose to the tumor is being captured and represented.

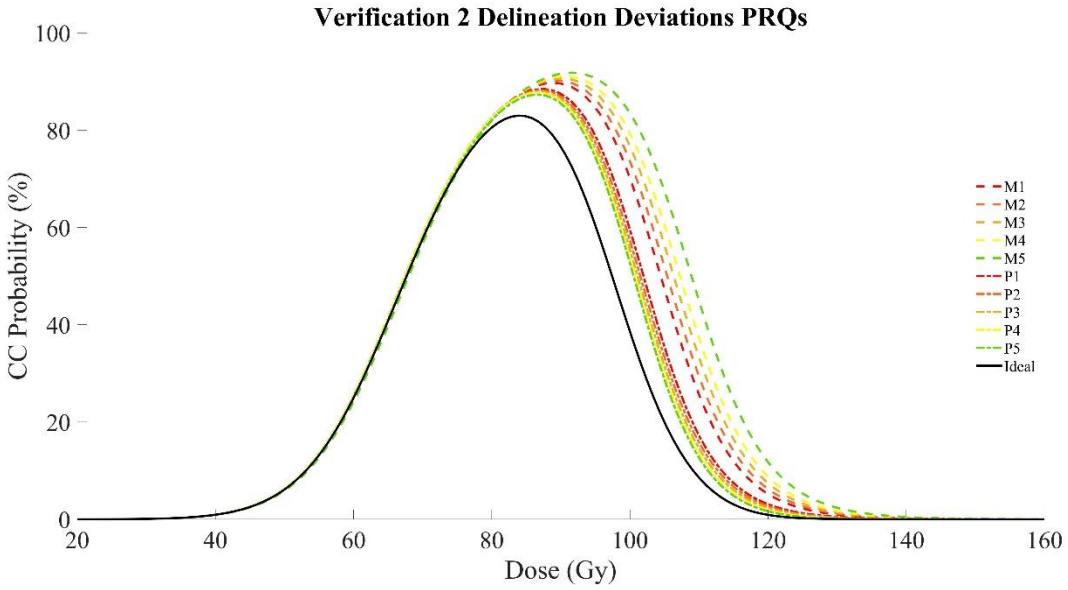

Figure 126. Delineation Deviations PRQs for the second verification test using alternate radiobiological parameters.

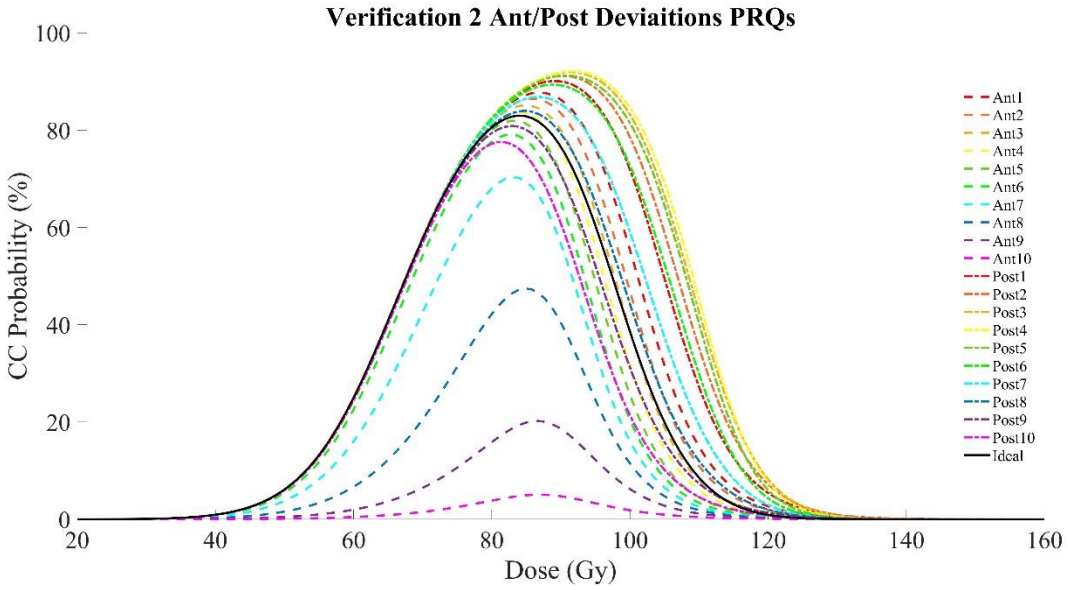

Figure 127. Anterior and Posterior Deviations PRQs for the second verification test using alternate radiobiological parameters.

The third verification test used varied most radiobiological parameters being displayed in Table 46[66]. The PRQs with this verification test have different shapes differentiating for the stereotypical gaussian curves. The behavior observed however is the same from delineation and geometric deviations. With anterior geometric deviations the PRQ crash still occurs beginning at the 6 mm deviation due to the loss of tumor dose. Here it will be noted that for anterior deviations

all verifications experience at first an increase in the PRQs then a decrease. This is due to the rectum losing dose before bladder dose increases to the point of dominating the right side of the PRQs.

Table 46. Radiobiological parameters used for verification test 3.

	Radiobiological Parameters				
	a	γ_{50}	TCD_{50}	TD_{50}	α/β
Prostate	-13	2.2	67.5	–	1.5
Rectum	8.33	2.66	–	80	5.4
Bladder	2	3.6	–	80	7.5

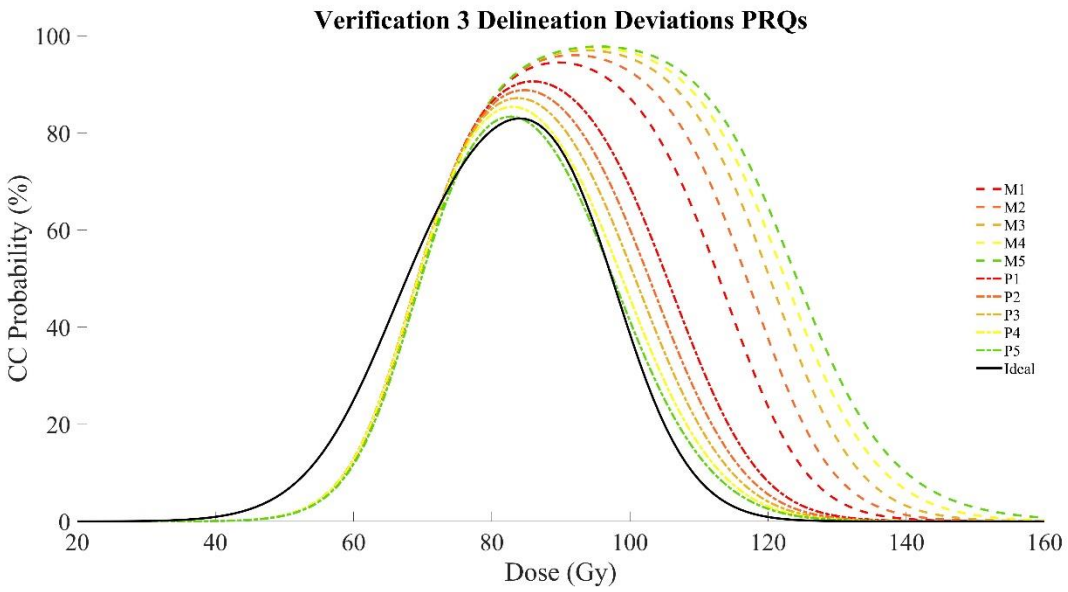

Figure 128. Delineation Deviations PRQs for the third verification test using alternate radiobiological parameters.

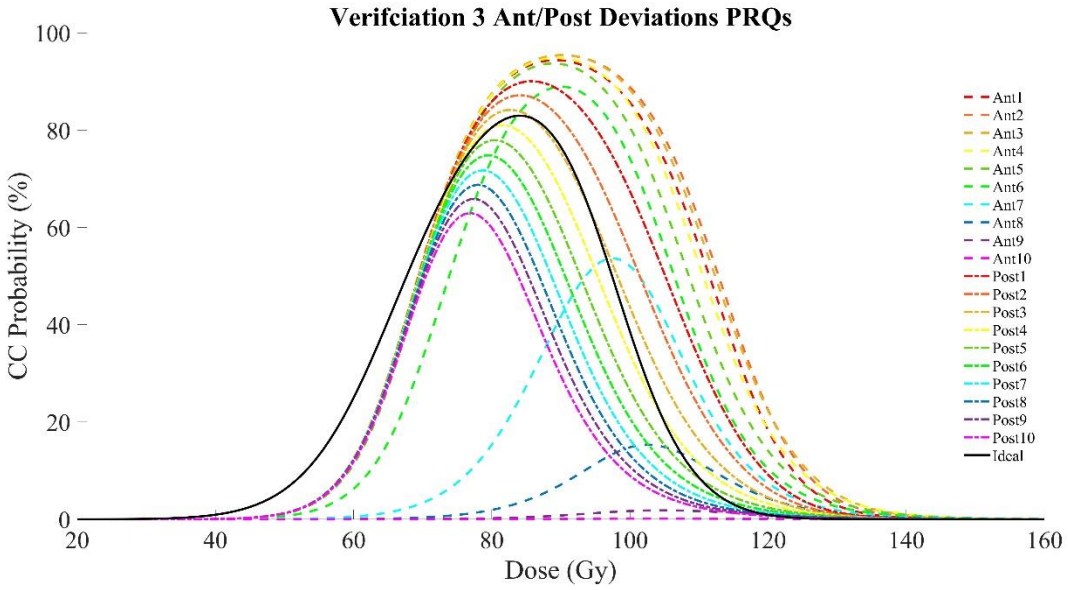

Figure 129. Anterior and Posterior Deviations PRQs for the third verification test using alternate radiobiological parameters.

The next verification test used the parameters displayed in Table 47[67]. This publication incorporated a wildly different value for the TCD_{50} from that seen in other literature. This produced a function with an early steep rise with a flat top near 100 % control/complication probability as seen in Figure 130 and Figure 131. Essentially the function is a bloated gaussian function. This is expected as the low value for TCD_{50} means the probability for controlling the tumor will be achieved at low doses. Despite the wildly different function however, similar behavior is observed as seen with all other PRQs.

Table 47. Radiobiological parameters used for verification test 4.

	Radiobiological Parameters				
	a	γ_{50}	TCD_{50}	TD_{50}	α/β
Prostate	-10	1	28.34	–	1.2
Rectum	8.33	4	–	80	3.9
Bladder	2	4	–	80	8

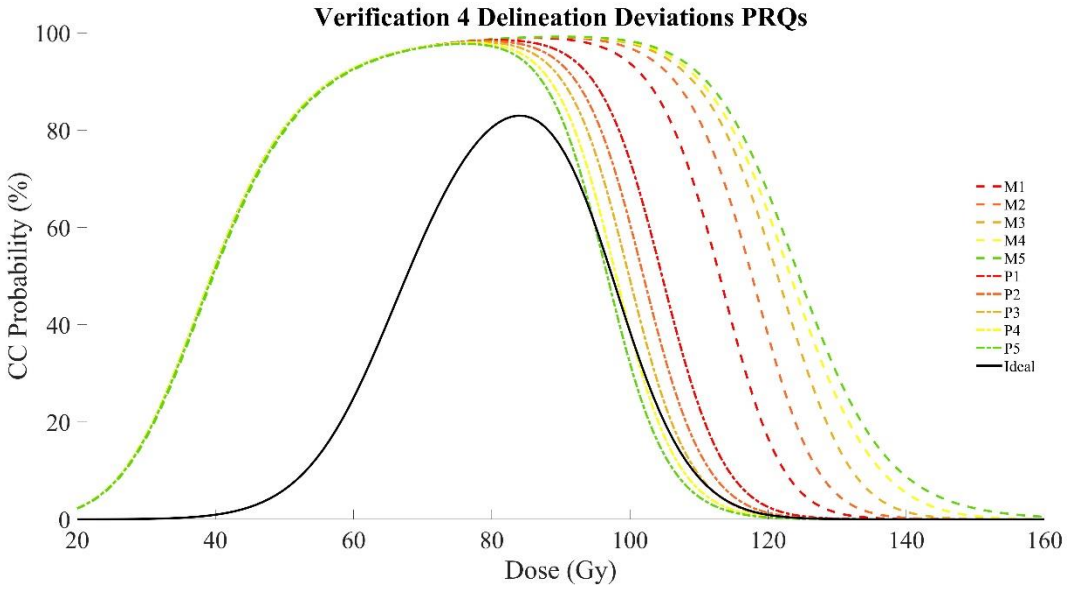

Figure 130. Delineation Deviations PRQs for the fourth verification test using alternate radiobiological parameters.

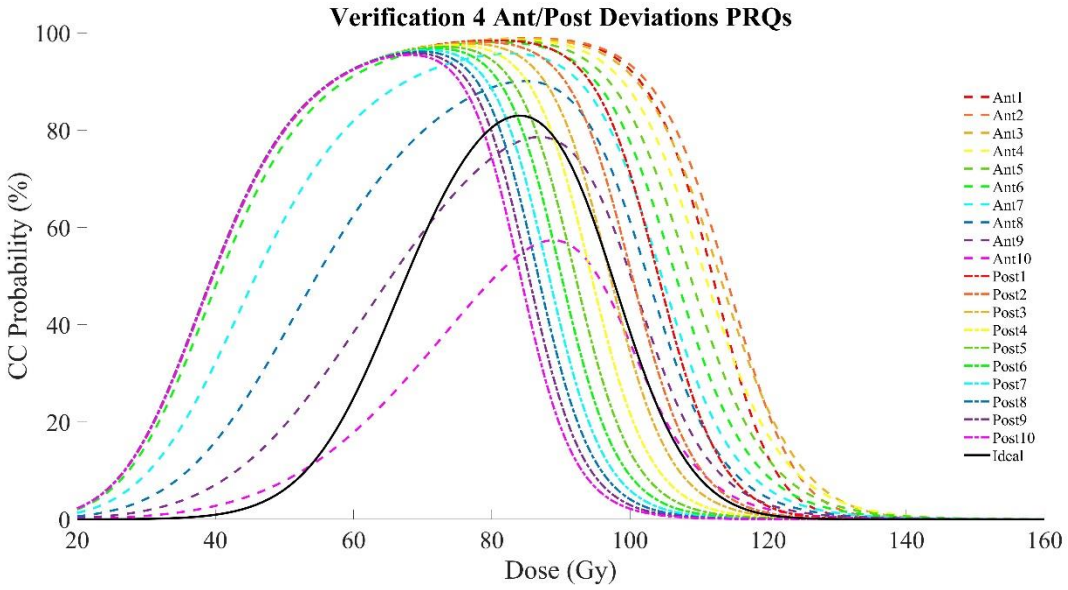

Figure 131. Anterior and Posterior Deviations PRQs for the fourth verification test using alternate radiobiological parameters.

The final verification test that was run simply varied the treatment parameters by 20 %. Figure 132 and Figure 133 display PRQs for delineation deviations of all structures and geometric deviations in the anterior and posterior direction when the parameters were increased by 20 %. The main difference is that all PRQs are shifted to the right with their peaks occurring at larger doses with a slightly larger value than the ideal. PRQs still steadily decrease for posterior geometric

deviations and anterior deviations begin to collapse on the left side at the 6 mm deviation due to loss of tumor dose.

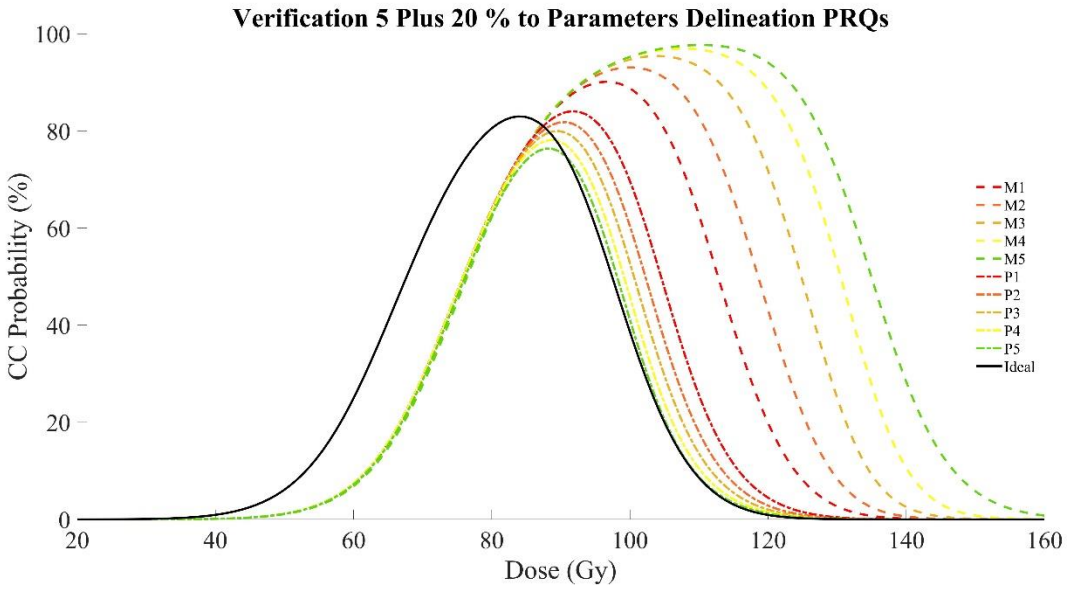

Figure 132. Delineation Deviation PRQs for the fifth verification test that increases parameters by 20 %.

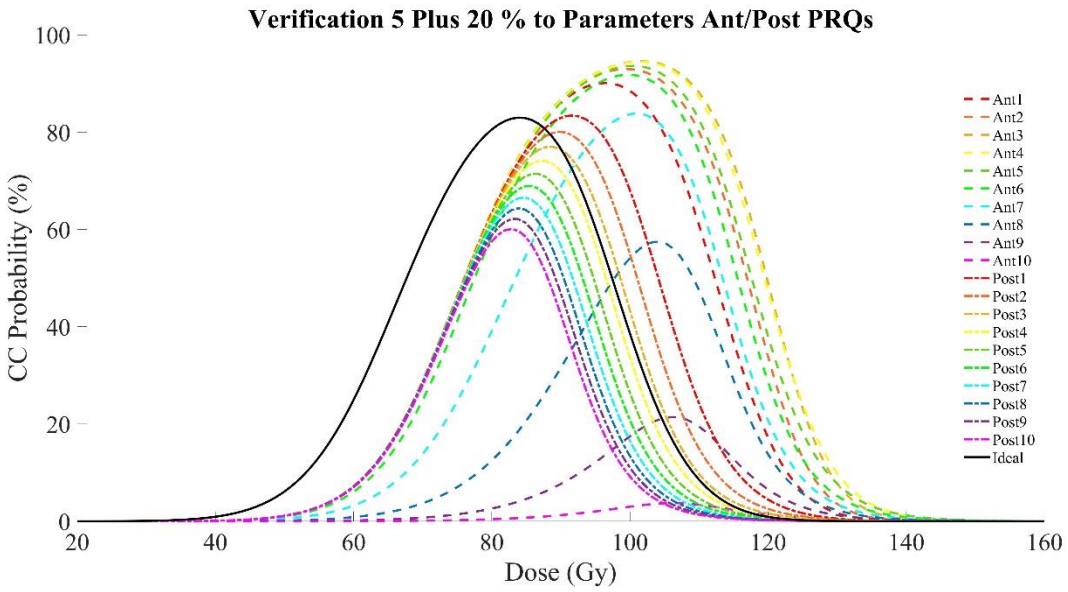

Figure 133. Anterior and posterior deviation PRQs for the fifth verification test that increased parameters by 20 %.

Figure 134 and Figure 135 display PRQs for delineation and geometric deviations when the parameters were decreased by 20 %. For the decrease in parameters the PRQs are shifted to

the left with their peaks decreasing in value. Similar behavior is observed as seen with all PRQs that have been generated.

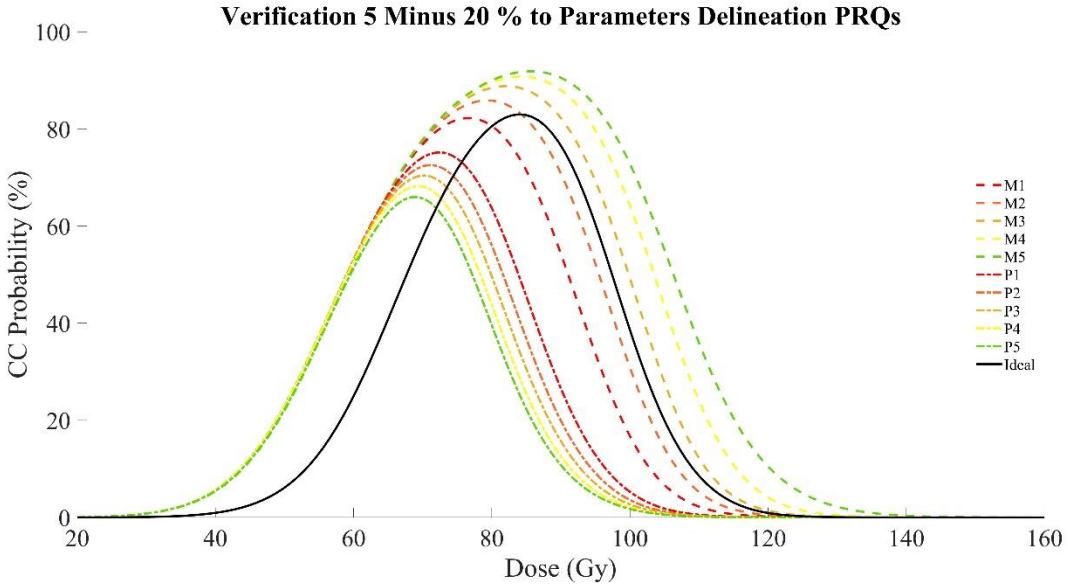

Figure 134. Delineation Deviation PRQs for the fifth verification test that decreased parameters by 20 %.

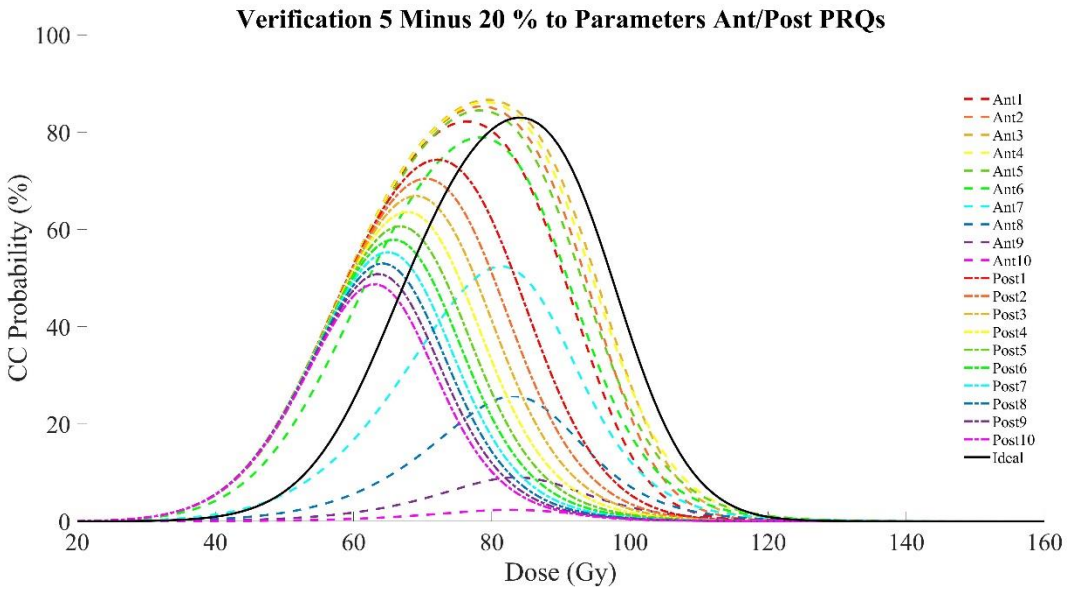

Figure 135. Anterior and posterior deviation PRQs for the fifth verification test that decreased parameters by 20 %.

4.3 Potential Applications

With the ability to quantitatively evaluate a treatment plan and track its progress through the process, many immediate applications and future projects are presented. It provides the ability

to directly correlate devices, equipment and process steps to a relative quantitative measurement to understand their overall effect on possible patient outcomes. It allows a means to measure past incidents and monitor current practices with a few simple metrics. By creating generalized tasks and generalized deviations, clinics with different detailed methods of performing their processes can compare results consistently with complication free tumor control probabilities. Setting standards for the field can be determined based on quantitative evaluations of the methods and actions used to complete treatment courses as opposed to expert consensus. Being able to trace actions to their effect on the overall quality leads to the ability to build more accurate and precise models for the response of tissues to radiation and the methods to deliver therapeutic doses.

4.3.1 Device, Equipment, and Process Evaluations

The complexity of radiation therapy has continued to significantly change over the past three decades[29,30,74–90]. As much as radiation therapy has changed in that time, the future will continue to see innovations and evolutions of the tools and methods used to treat cancer patients. With this comes increased complexities and changes in radiotherapy procedures. This presents a problem: technological advances are changing the way patients are treated faster than the field can fully understand these new technologies and develop appropriate methods for incorporating them into the clinical routine[91]. The result is that the implementation of devices surpasses the development of adequate protocols and procedures for these technologies let alone their impact on the final quality of treatment. Attention has been brought to incidents that have occurred in radiotherapy and the medical physics profession resulting from the use of new technologies implemented clinically[24,25,92]. The field still lacks a tool to quantitatively evaluate the impact new devices, equipment and procedures have if not used or performed optimally.

One example comes from what is now a fundamental device used in most treatments; the multi-leaf collimator. The multi-leaf collimator had a patent filed in 1987[93], and publications on appropriate use continued through the 1990's[77,94–98]. It was not until 2001 that a formal report was published to assist the radiation therapy community with acquisition, testing, commissioning, daily use and quality assurance of this device that was already being used across the country[99]. Another example occurs with IMRT, which is also now a fundamental component of modern day treatments. IMRT publications on its uses began emerging the in late 1990's[100–104] and similarly

the formal report for tools and techniques for the use of IMRT was published in 2011[105]. Task Group (TG) reports published by the American Associate of Physicists in Medicine (AAPM) provide guidance for installation, commissioning and ongoing quality assurance for devices, equipment and special procedures in radiation therapy[17,35,56,99,105–114] but are often lacking in procedural details. These have proven to have deficiencies and recently Medical Physics Practice Guidelines (MPPG) have been released to further aid device and equipment usage as well as procedure performances techniques[51,115–123]. These come with a disclaimer however, contrary to the nature of having reports to guide procedures and practices, and there is still no means to validate the effects on patient outcomes from imperfect use of devices, equipment or procedures. Systematic methods are needed to allow the evaluation of new technologies to quantitatively demonstrate the extent that risks are mitigated and the quality of treatments being achieved.

By building SEC the specific places in procedures where devices and equipment are used are identified. Quantitative data can now be generated to demonstrate how a malfunction or misuse of devices, equipment or procedures changes the complication free tumor control probability and hence treatment quality. Quantitative data can be gathered to determine normal means of operations to help guide what constitutes an unacceptable malfunctioning or misused device, equipment or procedure. There are data currently available in clinics related to the shifts applied after cone beam computer tomographic (CBCT) scans for the final setup for patient prostate treatments. A clinic's average shifts then would correlate to the final setup task in the generalized task for treatment providing a deviation decrease by that amount. Hypothetically say the clinic has an average of a 1 mm shift in the anterior and posterior direction. If there were no other deviations that occurred, this would be the change in the PRQs for the 1 mm geometric deviation complication free tumor control to the ideal complication free tumor control. If there are other deviations, or if devices and equipment uncertainties become incorporated into the result, the actual deviations that occur at that point no longer match ideals and the effects can quantitatively be compared to the ideal decrease that should have occurred.

Reviewing the results for geometric deviations in the anterior and posterior directions, if a SOE occurs in which the deviations are within tolerance (± 1 mm) this gives a 3.75 % change in the quality of radiotherapy treatment. Recognize however that the posterior 1 mm deviation quality

is less than the ideal while the anterior deviation is greater than the ideal quality. If a clinic is shifting their patients from an anterior direction to the origin for whatever reason, they are actually losing quality for this case. This leads to the possibility of a 7.5 % decrease in the quality of treatment achievable based alone on geometric deviations in the posterior direction occurring within tolerance. Now assume a scenario with a CBCT resolution of ± 1 mm incorporated into the above that is off in the posterior direction, and the patient is setup an additional mm in the posterior direction. The final setup task in the general task of treatment now has a 7 % decrease from the ideal. Actions and tasks related to ensuring the final setup shifts and CBCT are operating properly within the process create unique SOEs that can be identified, stored and used for future evaluations.

Within clinics there are many examples as described above where a plethora of data already exists in the various databases that are currently used in radiation medicine. Similarly applying this methodology to all devices, equipment and procedures to quantitatively demonstrate the extent that they affect quality within given tolerances can be accomplished, let alone for scenarios with out of tolerance occurrences. Future work is required to evaluate the data that is currently stored. Implementations of new devices, equipment, or procedures can be evaluated quantitatively then assessed as to their projected improvements to the radiotherapy process. This continues to aid the quality and safety agenda in a systematic fashion to identify and mitigate undesired events from occurring.

4.3.2 Incident Learning Systems Examples

The amount of hypothetical scenarios that can occur leading to a given PRQ can be overwhelming to generate. Incident learning systems, or past examples, are one of the best places to begin narrowing down the scenarios that should be generated and evaluated. These of course represent situations that have occurred and there is plenty of value to understanding the impact they had, quantitatively. These examples provide the basis for marking SOEs related to unacceptable performances during a process providing guidance for future monitoring of processes.

Initially an example is treated as a single event that affects the quality vs. time relationship at a certain point or specific task. For severe incidents this would be representative of a PRQ equal to zero or an increase in deviations of a magnitude leading to the catastrophic region. One example

coming from the New York Times[24,25,92] articles almost a decade ago involves the jaws being left open during an SRS treatment. Without knowing the exact details, quality vs. times plots can be generated for this event. It can be assumed that during the treatment is when the event occurred. The last PRQ on each of the three generalized tasks for quality vs. relationship plots in section 3.2.1 would be zero or the function collapses completely. For the specific task quality vs time relationship plots it can be assumed the event occurred during the specific task of delivery, or the second to last PRQ. The last two PRQs for the quality vs. time plots in section 3.2.2 would then be zero or the plot has a sharp drop to zero. This would also be displayed on a 3D plot where once again the PRQs continue to increase until dropping to zero at the second to last specific task plotted.

It can be argued that the specific task in which the event occurred was not delivery and was another specific task during treatment. Similar methodology follows. If the specific task was the pre-treatment preparation task instead, the 18th PRQ in the quality vs. time plots in section 3.2.2 would then drop to zero as well as the 18th PRQ in a 3D plot. The quality would continue to rise until having a steep drop to zero over the course of time the specific task takes. Even though the event did not occur during the other generalized tasks, an evaluation can still be completed using the same methodology for tasks that involve setting jaw positions. Some obvious examples are during the review of the TPS parameters task during plan review, the plan setup task during treatment planning, or achieving plan objectives during treatment planning. Each of these tasks has the potential for the jaws to be left open or verification of the jaw positions to be unacceptable. This would cause the quality vs time plots to crash to zero at these specific task points. If specific tasks are linked to the jaw positions, it can be argued that those points are also possibilities for where the quality drops to zero.

Pretend now that the event occurred during treatment planning, but the jaw positions error was discovered and corrected during plan review. The quality vs. time plot would experience a sharp drop to zero then a steep rise back up to the quality achieved with the correct jaw positions. At whatever specific task was determined to have caused the error, the quality vs time plot would crash to zero until rising again during the review of the TPS parameters task. In the same way if the error occurred during the pre-treatment preparation task but was discovered during the final setup or delivery, the quality vs. time plot would decrease and increase at those points respectively.

This example is of a severe incident however that operates in the catastrophic region. Such events are rare, but this does demonstrate how the quality vs. time relationship behaves due to a catastrophic event. There are plenty of events lacking in severity that occur frequently which can provide valuable information with more immediate use. Events with minor errors or near misses are the best examples. In these cases, there are not as drastic of changes in quality vs. time relationships and errors can be seen propagated through the entire system over time. In the first two interpretations of quality vs. time, the quality is directly linked to the magnitude of deviations occurring at any given task. If an event occurred that caused a 1 mm posterior deviation, all points past that would have their quality decreased by this amount. By the end of the course of treatment instead of the deviations decreasing from 1 mm to zero for the last tasks, the deviations would actually decrease from 2 mm to 1 mm giving a 3.75 % decrease in quality from the ideal.

If multiple events occur causing deviations this can also be tracked. Assume that at the half way point of the process the 1 mm posterior deviation error occurred. From this point on the quality is decreased by 3.75 % from the ideal for each point. Assume another event then occurs three quarters of the way through the process that also causes a 1 mm posterior deviation. From this point on the quality is now decreased by 7.5 % than the ideal and after all tasks are completed the final quality reaches 75.51 % as opposed to 82.99 %. This also allows evaluation of strategies and methods used to detect and prevent errors. Instead of the second error occurring, if the first error was detected three quarters of the way through the process the quality at this point would increase an additional 3.75 % as now a tasks was completed to decreases the posterior deviation. While these are simple examples the methodology can be extrapolated out for numerous errors that cause deviations or tasks that catch and fix said errors. As incidents, events, and normal process operations are evaluated, quantitative information becomes available to provide improved decision support for efficiency and resource allocation needs in the clinic.

4.3.3 Improving Models for Patient Outcomes

As departments begin to quantitatively evaluate their devices, equipment, processes and incident examples, an easy cross comparison is now achievable using the methodology outlined in this work. The creation of generic tasks at several levels allows departments to group their procedures into the generalized and specific tasks. Complication free tumor control probabilities

allow the quantitative comparison of these results to better understand procedural performance on patient quality. This allows a systematic approach to scientifically evaluate successes and failures when incorporating new devices, equipment and procedures.

For this study only three structures were used to demonstrate the proof of concept. An interesting observation is made from this as constructing more realistic models requires additional structures to be included. With small deviations the dose cloud mainly affects the three structures used in this study. With larger deviations however, specifically in multiple directions, the dose cloud is substantially directed towards other organs and tissues that are unaccounted for. These organs and tissues are now receiving considerable doses in these situations and will have a large contribution to the decrease in quality.

Moving forward, including as many organs as possible as well as a surrogate organ to represent all tissues unaccounted for provides the most realistic results. Delineating a surrogate organ is not complicated and most planning software allows this to be done with ease. A body contour can outline the entirety of tissues and simply subtracting all delineated tissues (in this case prostate CTV, bladder and rectum) from the body will create a structure to provide dosimetric statistics. At this point in time dummy variables for the radiobiological parameters could be estimated to best account for the response of tissues that have not been robustly studied and how to combine numerous tissues together in a meaningful way. This would be best achieved by running iterations on the parameters for such a structure to optimize the collapse of the PRQ to a more central location. This may also lead to more peaks centered at the prescription dose as more dependence on all normal tissues is included pushing the peaks down and shifting them to the left. This is what is seen as bladder and rectum doses were increased and decreased. As both were contracted the peaks increased and shifted right and when expanded the peaks decreased and shifted left.

The radiobiological parameters used in this study were developed to represent population based outcomes matched with cellular culture studies. While they represent population data well, they may not be acceptable for individual patient evaluations. The verification and validation section demonstrated that changes in parameters created PRQs that exhibit similar behavior. Any given patient may have changes in their parameters analogous to the five different verification tests

performed. This works methodology still allows a quantitative result to be acquired for evaluation. Currently determining these parameters is not possible but several areas of research are working towards this[124–131]. Patient demographic factors such as genetics, environmental impacts, and patient lifestyles will affect these parameters. As knowledge is increased into these factors relationships on radiobiological parameters, appropriate values can be used to fully optimize patient specific treatments.

While refining radiobiological parameters to represent individual patients is important, uncertainties in devices, equipment and process performances also impact patient outcomes. Currently poor outcomes related to sub optimal performances are included in the risk percentages used for patient outcomes. A patient experiencing rectal complications will be categorized in the percent of patients that experience complications. As is seen with anterior and posterior deviations, this complication could be due to geometric deviations instead. Risks patients face from treatments can be further refined to provide more accurate analyses. Specifically, adaptive radiotherapy will provide results on delineation and geometric uncertainties to demonstrate what final doses to tissues actually ended up being. Reexamining clinical studies with adaptive radiotherapy studies and complication free tumor control probabilities will further refine the risks associated with courses of treatment.

Last, optimizing procedural performance can be accomplished using complication free tumor control probabilities. The results of this work demonstrate that a higher quality of treatment was achievable for the case evaluated. Using the current practices and dose statistics, this went unnoticed and the plan was approved for treatment. This type of evaluation provides additional knowledge for the intrinsic nature of the plan and allows insight into the effects that performance deviations can have on treatment. Patient specific instructions for setup and delivery can help minimize situations that decrease the quality of treatment. Incorporating these into the current practice can further increase the quality of treatments provide to patients.

5. CONCULSION

Complication free tumor control probabilities can be used to quantitatively represent a given radiation therapy treatment relatively. By varying treatment parameters, quantitative functions can be generated to represent possible outcomes from non-ideal treatments. These outcomes are linked to all tasks involved over a full course of treatment based on the estimated treatment parameter variations that could occur. As the radiation therapy process progresses, its quality can be tracked as deviations are identified, realistically or hypothetically. This can be used to evaluate devices, equipment and process performance to provide decision support for resource allocation in clinical practices. This establishes a systematic mechanism for comparison across the field of radiation oncology to demonstrate the effectiveness of strategies implemented in a reproducible manner.

5.1 Research Objectives Review

Both research objectives outlined in section 1.3 were achieved with a high level of success. The first objective investigated how treatment parameter deviations affect complication free tumor control probabilities to be used for creating a PRQ library to represent the range of quality for a given treatment course. Initially it was hypothesized that PRQs would not be highly sensitive to the deviations proposed. This raised concern that measurable differences in PRQs might not be achievable with small deviations and that the overall magnitude of deviations proposed would not possess enough variation to provide meaningful interpretations of quality vs. time relationships for a course of radiation therapy. Extra steps were anticipated to deal with this issue by creating additional, unrealistic plans in an attempt to force the PRQs to smaller values that could represent earlier stages of the radiotherapy treatment process. This was unnecessary though as the PRQs were highly sensitive to deviations as demonstrated in the results section. This improves the robustness of this work in that a single plan was evaluated as opposed to multiple plans and approaches evaluated with their results stitched together to form the PRQ library. The most important aspect of this relates to the unchanged multileaf collimator sequences and configurations that have come to dominate modern day radiotherapy treatment deliveries[105]. By using the same multileaf collimator sequence and configuration, the actual variation in treatment quality that could occur given a proposed treatment plan has been defined.

The deviations used in this study provided significant value in understanding the potential quality of treatments, but improvements could have been made. Reviewing the PRQs presented in the results section, it is clear that the bladder has the smallest contribution to the overall complication free tumor control probabilities. While there is much ambiguity in the radiobiological parameters for the bladder, the variation in inter and intra fractional volume, and the corresponding endpoints related to these two[57,61], this work could have been enhanced by using parameters that increased the bladders contribution to complication free tumor control probabilities. Situations that increase bladder doses are undesirable even if their effects do not lead to minor or severe complications. A primary goal of radiation therapy is to avoid dose to normal tissue and constructing a model that identifies increases in doses to them has more practical applications. When evaluating the quality of a treatment then, identifying increases in normal tissue doses regardless of the severity of complication is necessary when attempting to quantify the results. The linear no threshold model provides the justification for this[29].

While the deviations that were evaluated provided a sufficient PRQ library to understand treatment quality variations, PRQs with max values below 50 % complication free tumor control were under sampled. This was due to the simplistic nature of the deviations proposed. Additional types of deviations could have been included to provide a more homogenous distribution of PRQs. Combinations of delineation and geometric deviations are very practical and represent realistic scenarios that currently occur during courses of treatment. It is easy to image situations where the volume of a normal tissue is underdrawn, and a geometric offset occurs in the same direction as the unaccounted for tissue. This results in smaller deviation magnitudes producing larger decreases in PRQs. Creating more anisotropic delineation deviations is also more practical to represent realistic clinical practices[61,62,132]. These include contractions and expansions in various directions as well as non-uniform contractions and expansions. Due to the large variability of contours in general, extensive amounts of delineation deviations and their corresponding PRQs possess immediate applicability to quantifying the quality of treatment courses.

This study used a logistic model with population based radiobiological parameters that best represent the normal tissues and low to intermediate risk disease for prostate cancer treatments. The reality is that these values do not directly correlate between population data and any specific

patient. Further improvement to identify variation in treatment quality, specific on an induvial patient level, could be established by using multiple values for these parameters. As seen in section 4.2.3, a variety of radiobiological parameters were used for verification and validation purposes[59,66,67]. In Figures 124-135, it can be seen that the ideal PRQ from this study produced a PRQ centrally located compared to the PRQs created with the variant radiobiological parameters used for verification and validation. This can be expected as the values chosen best represent population data creating "average" values. In section 4.2.3 however, all structure delineations and anterior/posterior deviations were the only deviation sets evaluated. A more complete PRQ library can be created by evaluating all proposed deviations with incremental changes in radiobiological parameters. Parameters for all structures can be varied in equal amounts, individual structure parameters can be varied independently, and random variations of parameters within specified ranges could be used to generate additional PRQs.

With the above mentioned additional PRQs that could be generated, quality vs. time relationships can be further expanded upon. The second research objective was more open ended serving as a proof of concept, however its major limitation was the size of the PRQ library to sample from. In this work several interpretations that clinics could use to understand the increase in quality as tasks are performed and completed were presented in section 3.2. A more homogenous distribution of PRQs allows better sampling providing more precise and accurate association of lower level specific tasks with PRQs earlier in the process. This also enables additional lower hierarchies to be defined for specific tasks which can be associated with unique PRQs. The radiotherapy process for this work was categorized into 22 tasks. Defining another 2 hierarchal levels, assuming four additional tasks for the defined specific tasks in this study, would create 88 and 352 highly specific tasks, respectively. Once again, this increases the precision and accuracy of quality vs. time relationships and the association with highly specific tasks to realistic PRQs.

The second objective for this study focused on an assumption that tasks were performed in order and completed ideally with the first attempt. This generated quality vs. time relationships that continually increased over time. The reality however is that variations in quality will occur thorough out the entire process and tasks will be performed out of order or repeated. Any task performed could decrease the quality compared to the previous task(s). With a limited PRQ library

to sample from, the iterative nature of the radiation therapy complex process is difficult to model in detail. A broader PRQ library with the amount of PRQs much greater than the defined tasks provides the ability to expand on these possibilities generating accurate models for quality vs. time relationships with more sophisticated sequence of event chains. Most of the future work stemming from this dissertation is related to these concepts: modeling increased sets of deviations creating enhanced PRQ libraries, continually defining lower lever hierarchal tasks outlining the immaculate details of the radiotherapy complex process and associating the two to increase the knowledge and understanding as to how specific actions at any point in time affect the quality of a course of treatment.

5.2 Future Work

The results from this study provide a framework for expanding the quality and safety agenda for radiation therapy in a quantitative manner. Potential applications and future studies have already been mentioned and alluded to, but a more detailed outline for direct steps to be taken moving forward will encompass the remainder of this work. An estimated chronological progression of the research to follow based on the analyses and conclusions from the results is presented below.

To begin, it is recognized that creating realistic analyses of treatment courses are desirable. This will be achieved using this framework by developing methods to model deviations to a greater degree and including all tissues receiving dose to determine complication free tumor control probabilities. The purpose for these is to establish more homogenous PRQ distributions for any given treatment plan that represents all possible scenarios related to uncertainties and errors that could occur. The initial work for modeling deviations to a greater degree is discussed in generating anisotropic and non-uniform delineations and geometric offsets. Current software enables these with ease, however, further mechanisms require development to include models representing device, equipment and procedural specific deviations and their effects on treatment parameters. Current work in adaptive radiotherapy and an extensive literate review of delineation and geometric errors currently experienced will help guide the development of mechanisms to incorporate more detailed deviations.

The inclusion of all tissues in the PRQ calculation can also be accomplished in the near future. While there are limited tissues with robust analyses determining appropriate radiobiological parameters, the use of surrogate structures provides the ability to account for all other tissues that do receive dose. Significant work is required to determine appropriate radiobiological parameters for all tissues and accounting for them in some manner begins this process. Adherence to the linear no threshold model once again provides justification for this approach. Although physiological endpoints related to dose are unknown for these types of tissues, including some relationship to complication probabilities must occur as any dose received by normal tissues has the potential to produce a stochastic response in due time. Furthermore, this is a novel idea and the contribution that all tissues receiving dose have on treatment outcomes has been largely neglected with focused placed on tissues receiving large doses. Preventing minor complications in the future will depend on including analyses of all tissues receiving dose.

This study focused on a prostate IMRT technique. Future studies will benefit the field by performing this type of analysis for all types of treatment techniques and modalities. These include plans with a single field, dual fields, 4 fields, and multiple fields with static collimation. Additionally, dynamic collimation for the above mentioned plans and field arrangements can be evaluated to demonstrate quantitatively the effect deviations have on the quality of treatments given specific techniques. Expanding this framework to all diseases types is only natural and will require additional analyses to determine appropriate catastrophic regions and catastrophic limits for each case. It is recognized that technological advances and process improvements have resulted in higher quality treatments over the years, but the opportunity to directly link quantitative specifics to these advances is now available for retrospective analyses for all avenues of radiotherapy. This provides a quantitative systematic mechanism to evaluate the strategies used over the years to improve the quality of treatments based on their effects to diseased and normal tissues. With extensive PRQ libraries generated and retrospective analysis completed, more precise and accurate deviational decreases with tasks are completed can follow. This leads to improved models for quality vs. time relationships. Eventually however, applying the results of ideal quality vs. time relationships in real time are desired.

As defined tasks are completed information is acquired, stored, and associations with quality vs. time relationships can be determined. The majority of this future work will occur with thorough evaluations of data that are currently collected and stored in radiation therapy and correlating them to defined tasks. Currently, analysis of data stored in radiation therapy is deficient compared to the magnitude of data collected. Multiple databases exist for patient management systems, treatment machines, treatment planning systems, additional devices, equipment, and quality assurance practices. All data that are stored already possess relationships with one another through database management systems theory with keys, super keys, unique keys and so forth. These keys provided unique identifies to correlate data with the tasks defined throughout the process, corresponding treatment parameters and hence quality vs. time relationships. As tasks are completed in real time, numerous elements in the database are populated. By scanning or querying the databases, it can be determined when tasks are completed and an appropriate PRQ can be sampled to represent the theoretical quality at any moment.

Several opportunities for future work have been presented here with the potential for more stemming from expansions of this work's ideas and their results. As stated at the beginning of the introduction, radiation therapy continues to reconsider its approaches to quality, safety and procedural management as new information is learned and new tools developed. In the future there is no doubt that approaches will continue to be reconsidered as new problems and issues emerge. The emergence of such will require new individuals to develop sophisticated methods to address those issues further increasing the quality and safety of radiation therapy. With that, the author would like to thank the reader for making it to the end of this manuscript. The first step in improving quality and safety in any field, at any time, is to make an effort to do so.

APPENDICIES

Appendix A: Sequence of Events for Radiation Therapy

Consult

$C_{AA}\backslash E\backslash A\backslash 1\ldots N \rightarrow C_{AA}\backslash E\backslash B\backslash 1\ldots N \rightarrow C_{AA}\backslash E\backslash C\backslash 1\ldots N \rightarrow$

$C_{AA}\backslash A\backslash A\backslash 1\ldots N \rightarrow C_{RN}\backslash A\backslash A\backslash 1\ldots N \rightarrow C_{MD}\backslash A\backslash A\backslash 1\ldots N \rightarrow C_{MD}\backslash A\backslash B\backslash 1\ldots N \rightarrow C_{MD}\backslash A\backslash C\backslash 1\ldots N \rightarrow C_{MD}\backslash A\backslash D\backslash 1\ldots N \rightarrow$

$C_{MD}\backslash B\backslash A\backslash 1\ldots N \rightarrow C_{MD}\backslash B\backslash B\backslash 1\ldots N \rightarrow C_{MD}\backslash B\backslash C\backslash 1\ldots N \rightarrow C_{MD}\backslash B\backslash D\backslash 1\ldots N \rightarrow$

$C_{MD}\backslash C\backslash A\backslash 1\ldots N \rightarrow C_{MD}\backslash C\backslash B\backslash 1\ldots N \rightarrow C_{MD}\backslash C\backslash C\backslash 1\ldots N \rightarrow C_{MD}\backslash C\backslash D\backslash 1\ldots N \rightarrow$

$C_{MD}\backslash D\backslash A\backslash 1\ldots N \rightarrow C_{MD}\backslash D\backslash B\backslash 1\ldots N \rightarrow C_{MD}\backslash D\backslash C\backslash 1\ldots N \rightarrow C_{MD}\backslash D\backslash D\backslash 1\ldots N \rightarrow$

Simulation

$S_{AA}\backslash E\backslash A\backslash 1\ldots N \rightarrow S_{AA}\backslash E\backslash B\backslash 1\ldots N \rightarrow S_{AA}\backslash E\backslash C\backslash 1\ldots N \rightarrow$

$S_{RTT}\backslash A\backslash A\backslash 1\ldots N \rightarrow S_{RTT}\backslash A\backslash B\backslash 1\ldots N \rightarrow S_{RTT}\backslash A\backslash C\backslash 1\ldots N \rightarrow S_{RTT}\backslash A\backslash D\backslash 1\ldots N \rightarrow S_{RTT}\backslash A\backslash E\backslash 1\ldots N \rightarrow S_{RTT}\backslash E\backslash A\backslash 1\ldots N \rightarrow S_{RTT}\backslash E\backslash C\backslash 1\ldots N \rightarrow$

$S_{RTT}\backslash B\backslash A\backslash 1\ldots N \rightarrow S_{RTT}\backslash B\backslash B\backslash 1\ldots N \rightarrow S_{RTT}\backslash B\backslash C\backslash 1\ldots N \rightarrow S_{RTT}\backslash B\backslash D\backslash 1\ldots N \rightarrow S_{RTT}\backslash E\backslash A\backslash 1\ldots N \rightarrow S_{RTT}\backslash E\backslash B\backslash 1\ldots N \rightarrow S_{RTT}\backslash E\backslash C\backslash 1\ldots N \rightarrow$

$S_{RTT}\backslash C\backslash A\backslash 1\ldots N \rightarrow S_{RTT}\backslash C\backslash B\backslash 1\ldots N \rightarrow S_{RTT}\backslash C\backslash C\backslash 1\ldots N \rightarrow S_{RTT}\backslash C\backslash D\backslash 1\ldots N \rightarrow S_{RTT}\backslash E\backslash A\backslash 1\ldots N \rightarrow S_{RTT}\backslash E\backslash B\backslash 1\ldots N \rightarrow S_{RTT}\backslash E\backslash C\backslash 1\ldots N \rightarrow$

$S_{RTT}\backslash D\backslash A\backslash 1\ldots N \rightarrow S_{RTT}\backslash D\backslash B\backslash 1\ldots N \rightarrow S_{RTT}\backslash D\backslash C\backslash 1\ldots N \rightarrow S_{RTT}\backslash E\backslash A\backslash 1\ldots N \rightarrow S_{RTT}\backslash E\backslash B\backslash 1\ldots N \rightarrow S_{RTT}\backslash E\backslash C\backslash 1\ldots N \rightarrow$

Tx Planning

$TP_{CMD}\backslash A\backslash A\backslash 1\ldots N \rightarrow TP_{CMD}\backslash A\backslash B\backslash 1\ldots N \rightarrow TP_{CMD}\backslash A\backslash C\backslash 1\ldots N \rightarrow TP_{CMD}\backslash A\backslash D\backslash 1\ldots N \rightarrow$

$TP_{CMD}\backslash B\backslash A\backslash 1\ldots N \rightarrow TP_{CMD}\backslash B\backslash B\backslash 1\ldots N \rightarrow TP_{MD}\backslash B\backslash C\backslash 1\ldots N \rightarrow TP_{CMD}\backslash B\backslash C\backslash 1\ldots N \rightarrow TP_{CMD}\backslash B\backslash D\backslash 1\ldots N \rightarrow$

$TP_{CMD}\backslash C\backslash A\backslash 1\ldots N \rightarrow TP_{CMD}\backslash C\backslash B\backslash 1\ldots N \rightarrow TP_{CMD}\backslash C\backslash C\backslash 1\ldots N \rightarrow TP_{CMD}\backslash C\backslash D\backslash 1\ldots N \rightarrow TP_{MD}\backslash C\backslash C\backslash 1\ldots N \rightarrow TP_{MD}\backslash C\backslash D\backslash 1\ldots N \rightarrow$

TP_{CMD}\D\A\1…N → TP_{CMD}\D\B\1…N → TP_{CMD}\D\C\1…N → TP_{CMD}\D\D\1…N →

TP_{CMD}\E\A\1…N → TP_{CMD}\E\B\1…N → TP_{CMD}\E\C\1…N → TP_{CMD}\E\D\1…N →

Plan Review

PR_{MD1}\A\A\1…N → PR_{MD1}\A\B\1…N → PR_{MD1}\A\C\1…N → PR_{MD1}\A\D\1…N →

PR_{MD2}\A\A\1…N → PR_{MD2}\A\B\1…N → PR_{MD2}\A\C\1…N → PR_{MD2}\A\D\1…N →

PR_{RTT}\A\A\1…N → PR_{RTT}\A\B\1…N → PR_{RTT}\A\C\1…N → PR_{RTT}\A\D\1…N →

PR_{QMP}\A\A\1…N → PR_{QMP}\A\B\1…N → PR_{QMP}\A\C\1…N → PR_{QMP}\A\D\1…N →

PR_{QMP}\B\A\1…N → PR_{QMP}\B\B\1…N → PR_{QMP}\B\C\1…N → PR_{QMP}\B\D\1…N →

PR_{QMP}\C\A\1…N → PR_{QMP}\C\B\1…N → PR_{QMP}\C\C\1…N → PR_{QMP}\C\D\1…N →

PR_{QMP}\D\A\1…N → PR_{QMP}\D\B\1…N → PR_{QMP}\D\C\1…N → PR_{QMP}\D\D\1…N →

Treatment

T_{AA}\F\A\1…N → T_{AA}\F\B\1…N → T_{AA}\F\C\1…N → T_{RTT}\F\A\1…N → T_{RTT}\A\C\1…N →

T_{RTT}\A\A\1…N → T_{RTT}\A\B\1…N → T_{RTT}\A\C\1…N → T_{RTT}\F\A\1…N → T_{RTT}\A\C\1…N →

T_{RTT}\B\A\1…N → T_{RTT}\B\B\1…N → T_{RTT}\B\C\1…N → T_{RTT}\B\D\1…N →

T_{RTT}\C\A\1…N → T_{RTT}\C\B\1…N → T_{RTT}\C\C\1…N → T_{RTT}\C\D\1…N → T_{QMP}\C\B\1…N → T_{QMP}\C\C\1…N → T_{QMP}\C\D\1…N → T_{MD}\C\B\1…N → T_{MD}\C\C\1…N → T_{MD}\C\D\1…N →

T_{RTT}\D\A\1…N → T_{RTT}\D\B\1…N → T_{QMP}\D\B\1…N → T_{MD}\D\B\1…N → T_{RTT}\D\C\1…N →

T_{RTT}\E\A\1…N → T_{RTT}\E\B\1…N → T_{RTT}\E\C\1…N → T_{RTT}\E\D\1…N

Appendix B: Radiation Therapy Control Loops

Consult

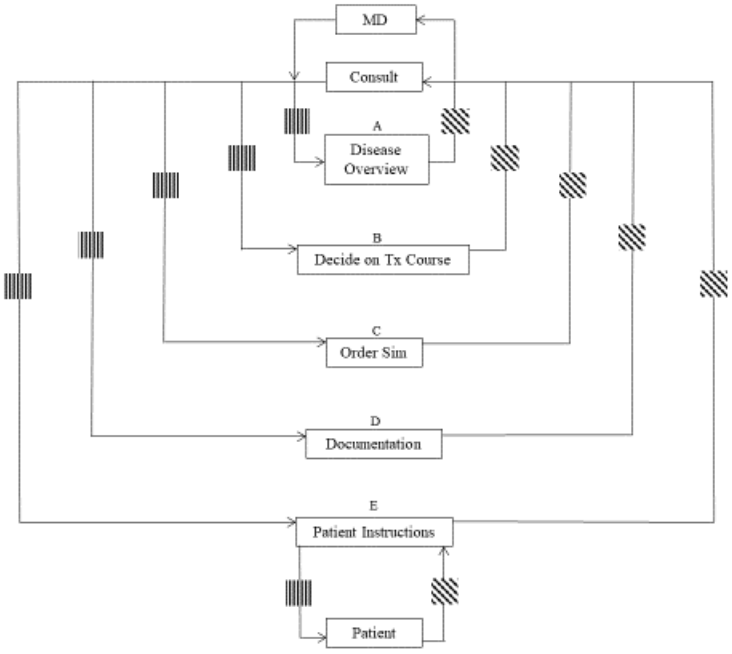

Appendix B Figure 1. Control Loop for the Physicians specific tasks in the Consult general task

Simulation

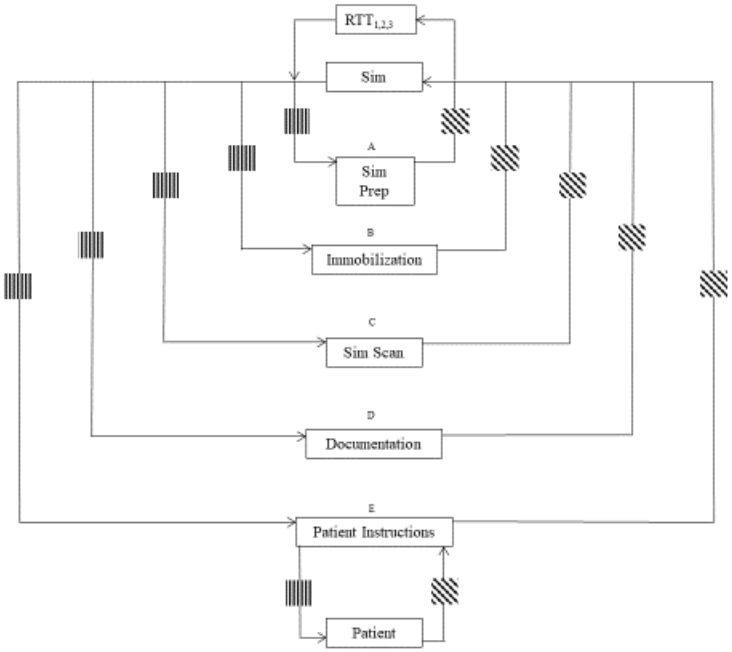

Appendix B Figure 2. Control Loop for the Radiation Therapist specific tasks in the Simulation general task.

Treatment Planning

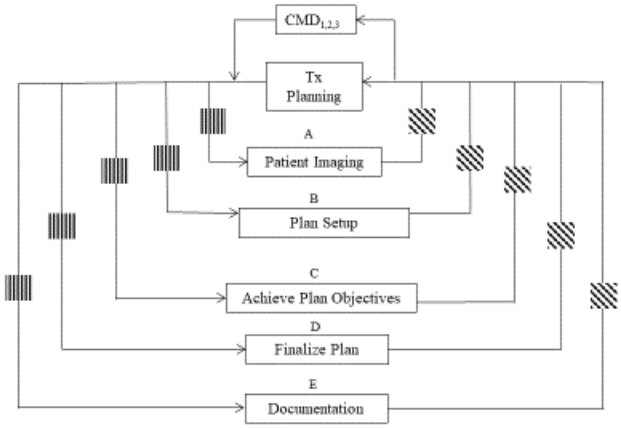

Appendix B Figure 3. Control Loop for the Certified Dosimetrist specific tasks in the Treatment Planning general task.

Plan Review

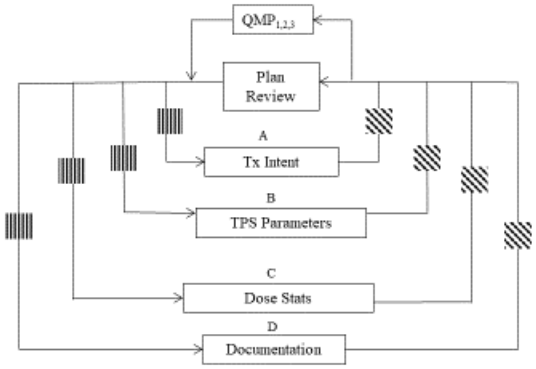

Appendix B Figure 4. Control Loop for the Qualified Medical Physicists specific tasks in the Plan Review general task.

Treatment

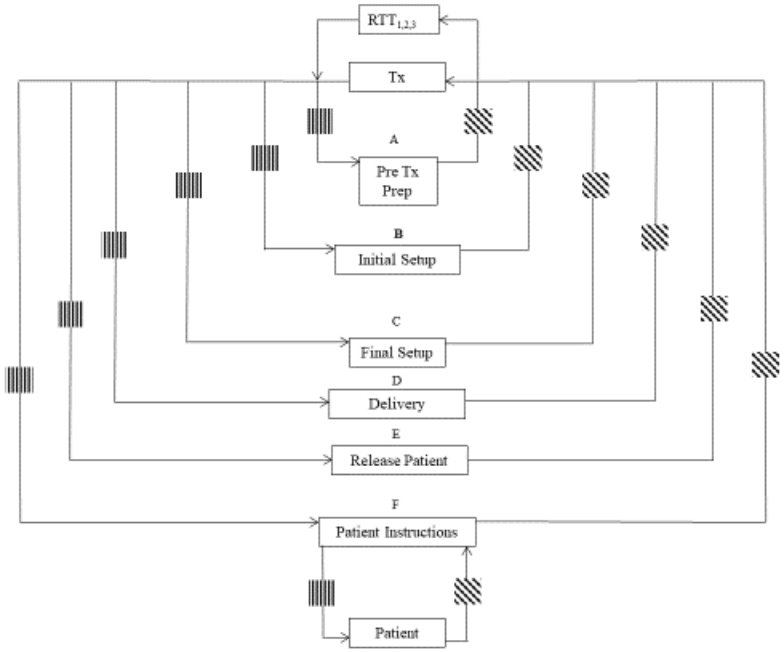

Appendix B Figure 5. Control Loop for the Radiation Therapists specific tasks in the Treatment general task.

REFERENCES

1. Bohmer R. Designing Care: Aligning the Nature and Management of Health Care. In: Boston, MA: Havard Business Press; 2009.

2. Kohn LT, Corrigan JM, Donaldson MS. *To Err Is Human: Building a Safer Health System*. Vol 21. Washington, D.C.: National Academy Press; 2000. doi:10.1017/S095026880100509X

3. Kapur A, Potters L. Six sigma tools for a patient safety-oriented, quality-checklist driven radiation medicine department. *Pract Radiat Oncol*. 2012;2(2):86-96. doi:10.1016/j.prro.2011.06.010

4. Potters L, Kapur A. Implementation of a "No Fly" safety culture in a multicenter radiation medicine department. *Pract Radiat Oncol*. 2012;2(1):18-26. doi:10.1016/j.prro.2011.04.010

5. Leape L, Berwick D. Five Years After To Err Is Human: What Have We Learned? *J Am Med Assoc*. 2005;293(19):2384-2390. doi:10.1177/004057364900600101

6. Malin JL, Schneider EC, Epstein AM, Adams J, Emanuel EJ, Kahn KL. Results of the National Initiative for Cancer Care Quality: how can we improve the quality of cancer care in the United States? *J Clin Oncol*. 2006;24(4):626-634. doi:10.1200/JCO.2005.03.3365

7. Moran JM, Fraass BA. Introduction: Quality, Technology, and Outcomes in Radiation Oncology. *Semin Radiat Oncol*. 2012;22(1):1-2. doi:10.1016/j.semradonc.2011.10.001

8. Oldenhof MT, van Leeuwen JF, Nauta MJ, et al. Consistency of FMEA used in the validation of analytical procedures. *J Pharm Biomed Anal*. 2011;54(3):592-595. doi:10.1016/j.jpba.2010.09.024

9. Rose C, Stovall E, Ganz P, Desch C, Hewitt M. Cancer Quality Alliance: Blueprint for a better cancer care system. *CA Cancer J Clin*. 2008;58(5):266-292. doi:10.3322/CA.2008.0012

10. Siochi RA, Stern RL, Balter P, et al. Information technology resource management in radiation oncology. *J Appl Clin Med Phys*. 2009;10(4):3116.

11. Sundararaman S, Babbo AE, Brown JA, Doss R. Improving patient safety in the radiation oncology setting through crew resource management. *Pract Radiat Oncol*. 2014;4(4):e181-e188. doi:10.1016/j.prro.2013.09.003

12. Terezakis S, Pronovost P, Harris K, DeWeese T, Ford E. Safety Strategies in an Acaemic Radiation Oncology Department and Recommendations for Action. *Jt Comm J Qual Patient Saf*. 2011;37(7):291-299.

13. Richardson W, Berwick D, Bisgard JC, et al. *Crossing the Quality Chasm: A New Health System for the 21st Century*. Vol 323. Washington, D.C.: National Academy Press; 2001. doi:10.1136/bmj.323.7322.1192

14. WHO. Radiotherapy risk profile. *Who*. 2008. http://www.who.int/patientsafety/activities/technical/radiotherapy_risk_profile.pdf.

15. Wilson JF, Owen J. Quality research in radiation oncology: a self-improvement initiative 30 years ahead of its time? *J Am Coll Radiol*. 2005;2(12):1001-1007. doi:10.1016/j.jacr.2005.06.009

16. Huq MS, Fraass BA, Dunscombe PB, et al. A Method for Evaluating Quality Assurance Needs in Radiation Therapy. *Int J Radiat Oncol Biol Phys*. 2008;71(1):S170-S173. doi:10.1016/j.ijrobp.2007.06.081

17. Huq MS, Fraass BA, Dunscombe PB, et al. THE REPORT OF TASK GROUP 100 OF THE AAPM : APPLICATION OF RISK ANALYSIS METHODS TO RADIATION THERAPY QUALITY. *Med Phys*. 2015.

18. Donabedian A. The quality of care. How can it be assessed? *J Am Med Assoc*. 1988;260(12):1743-1748. doi:10.1001/jama.260.12.1743

19. Hayman J. Measuring the quality of care in radiation oncology. *Semin Radiat Oncol*. 2008;18(3):201-206. doi:10.1016/j.semradonc.2008.01.008

20. Hayman J. Treatment Summaries in Radiation Oncology and Their Role in Improving Patients' Quality of Care: Past, Present, and Future. *J Oncol Pract*. 2009;5(3):108-109. doi:10.1200/JOP.0934404

21. Hendee WR. Safety and accountability in healthcare from past to present. *Int J Radiat Oncol Biol Phys*. 2008;71(1 Suppl):S157-61. doi:10.1016/j.ijrobp.2007.04.096

22. Hohnen P, Hasle P. Making work environment auditable - A "critical case" study of certified occupational health and safety management systems in Denmark. *Saf Sci*. 2011;49(7):1022-1029. doi:10.1016/j.ssci.2010.12.005

23. Drupsteen L, Groeneweg J, Zwetsloot GIJM, Drupsteen L. Critical Steps in Learning From Incidents : Using Learning Potential in the Process From Reporting an Incident to Accident Prevention. *Int J Occup Saf Ergon*. 2013;19:63-77. doi:10.1080/10803548.2013.11076966

24. Bogdanich W. Radiation Offers New Cures, and Ways to Do Harm. *New York Times*. 2010:1-18.

25. Bogdanich W. As Technology Surges, Radiation Safeguards Lag. *New York Times*. 2010:1-13.

26. Attix F. *Introduction to Radiological Physics and Radiation Dosimetry*. New York: John Wiley & Sons, Inc; 1986.

27. Bentel G. *Radiation Therapy Planning*. Second. (Wonsiewicz M, Navrozov M, eds.). New York: McGraw-Hill; 1996.

28. Cherry S, Sorenson J, Phelps M. *Physics in Nuclear Medicine*. Third. (Ross A, ed.).

Philadelphia: Saunders; 2003.

29. Hall E, Giaccia A. *Radiobiology for the Radiologist*. Seventh ed. Philadelphia: Lippincott Williams & Wilkins; 2012.

30. Khan FM. *The Physics of Radiation Therapy*. Fourth edi. Philadelphia: Lippincott Williams & Wilkins; 2009.

31. Johns H, Cunningham J. *The Physics of Radiology*. Fourth. (Books T, ed.). Springfield, Illinois: Thomas, CHarles C; 1983.

32. Washington C, Leaver D. *Principles and Practice of Radiation Therapy*. 4th ed. St. Louis: Elsevier Health Sciences; 2015.

33. Bushberg J, Seibert JA, Leidholdt E, Boone J. *The Essential Physics of Medical Imaging*. Third. (Mitchell C, ed.). Philadelphia: Lippincott Williams & Wilkins; 2012.

34. McRobbie D, Moore E, Graves M, Prince M. *MRI: From Picture to Proton*. Second. (Press CU, ed.). New York: Cambridge University Press; 2007.

35. Fraass B, Doppke K, Hunt M, et al. American Association of Physicists in Medicine Radiation Therapy Committee Task Group 53: quality assurance for clinical radiotherapy treatment planning. *Med Phys*. 1998;25(10):1773-1829. doi:10.1118/1.598373

36. Zwetsloot G, Aaltonen M, Wybo JL, Saari J, Kines P, Beeck R Op De. The case for research into the zero accident vision. *Saf Sci*. 2013;58:41-48. doi:10.1016/j.ssci.2013.01.026

37. Renn O. *Risk Governance: Coping with Uncertainty in a Complex World*. London: Earthscan; 2008.

38. Adams JGU. Risk homeostasis and the purpose of safety regulation. *Ergonomics*. 1988;31(4):407-428. doi:10.1080/00140138808966688

39. Loewenstein GF, Weber EU, Hsee CK, Welch N. Risk as feelings. *Psychol Bull*. 2001;127(2):267-286. doi:10.1037/0033-2909.127.2.267

40. Rasmussen J. Risk management in a dynamic society: A modelling problem. *Saf Sci*. 1997;27(2-3):183-213. doi:10.1016/S0925-7535(97)00052-0

41. Rasmussen & Warner, F. J. Human Error and the Problem of Causality in Analysis of Accidents [and Discussion]. *Philos Trans R Soc Landon*. 1990;12(327):449-462.

42. Walton R. From Control to Commitment in the Workplace. *Havard Buisness Rev*. 1985;63 (2)(March):77-84.

43. Heinrich H. *Industrial Accident Prevention: A Scientific Approach*. McGraw-Hill Book Company, inc.; 1931.

44. Reason J. Human error: models and management. *Bmj*. 2000;320(7237):768-770. doi:10.1136/bmj.320.7237.768

45. Leveson NG. *Engineering a Safer World: Systems Thinking Applied to Safety*. Cambridge, MA; 2011. http://medcontent.metapress.com/index/A65RM03P4874243N.pdf.

46. Carroll JS. Organizational Learning Activities in High-Hazard Industries: the Logics Underlying Self-Analysis. *J Manag Stud*. 1998;35(6):699-717. doi:10.1111/1467-6486.00116

47. Perrow C. *Normal Accidents: Living with High-Risk Technologies*. New York: Basic Books; 1984.

48. Perrow C. The Limits of Safety: The Enhancement of a Theory of Accidents. *J Contingencies Cris Manag*. 1994;2(4):212-220. doi:10.1111/j.1468-5973.1994.tb00046.x

49. Renn O. Precaution and Ecological Risk. In: *Encyclopedia of Ecology*. vol. 5. Oxford: Elsevier; 2008:2909-2916.

50. Weinberg G. *An Introduction to General Systems Thinking*. 25 Anv edi. New York: Dorset House Publishing Company, Incorporated; 1975.

51. Feynman R, Gottlieb M, Leighton R. *Tips On Physics: A Problem-Solving Supplement to the Feynman Lectures on Physics*. (Black A, ed.). San Francisco, CA: Pearson: Addison Wesley; 2006.

52. Leveson NG. *Safeware: System Safety and Computers*. Boston: Addison Wesley; 1995.

53. Taguchi G. *Introduction to Quality Engineering*. Tokyo: Asian Productivity Organization; 1988.

54. Gay HA, Niemierko A. TECHNICAL NOTE A free program for calculating EUD-based NTCP and TCP in external beam radiotherapy. 2019;(2007). doi:10.1016/j.ejmp.2007.07.001

55. Emami B, Lyman J, Brown A, et al. Tolerance of Normal Tissue to Therapeutic Irradiation. *Int J Radiat Oncol Biol Phys*. 1991;21(1):109-122.

56. Li XA, Alber M, Deasy JO, et al. *The Use and QA of Biologically Related Models for Treatment Planning Report of AAPM Task Group 166*.; 2012.

57. Burman C, Kutcher G, Emami B, Goitein M. FItting of Normal Tissue Tolerance Data to an Analytic Function. *Int J Radiat Oncol Biol Phys*. 1991;21:123-135.

58. Cheung R, Tucker SL, Lee AK, et al. Dose-response characteristics of low- and intermediate-risk prostate cancer treated with external beam radiotherapy. *Int J Radiat Oncol Biol Phys*. 2005;61(4):993-1002. doi:10.1016/j.ijrobp.2004.07.723

59. Trofimov A, Nguyen PL, Coen JJ, et al. Radiotherapy Treatment of Early-Stage Prostate Cancer with IMRT and Protons: A Treatment Planning Comparison. *Int J Radiat Oncol Biol Phys*. 2007;69(2):444-453. doi:10.1016/j.ijrobp.2007.03.018

60. Snyder M, Joiner MC, Konski A, Bossenberger T, Burmeister J. Dose escalation in prostate

cancer using intensity modulated neutron radiotherapy. *Radiother Oncol*. 2011;99(2):201-206. doi:10.1016/j.radonc.2011.05.019

61. Viswanathan AN, Yorke ED, Marks LB, Eifel PJ, Shipley WU. Radiation Dose-Volume Effects of the Urinary Bladder. *Int J Radiat Oncol Biol Phys*. 2010;76(3 SUPPL.):116-122. doi:10.1016/j.ijrobp.2009.02.090

62. Michalski JM, Gay H, Jackson A, Tucker SL, Deasy JO. Radiation Dose-Volume Effects in Radiation-Induced Rectal Injury. *Int J Radiat Oncol Biol Phys*. 2010;76(3 SUPPL.):123-129. doi:10.1016/j.ijrobp.2009.03.078

63. Boyer AL, Schultheiss T. Effects of dosimetric and clinical uncertainty on complication-free local tumor control. *Radiother Oncol*. 1988;11(1):65-71. doi:10.1016/0167-8140(88)90046-1

64. Sanchez-Nieto B, Nahum AE. the Delta-Tcp Concept : a Clinically Useful Measure of. *Radiat Oncol*. 1999;44(2):369-380.

65. Marks LB, Yorke ED, Jackson A, et al. Use of Normal Tissue Complication Probability Models in the Clinic. *Int J Radiat Oncol Biol Phys*. 2010;76(3 SUPPL.). doi:10.1016/j.ijrobp.2009.07.1754

66. Kim KH, Chung JB, Suh TS, et al. Dosimetric and radiobiological comparison in different dose calculation grid sizes between Acuros XB and anisotropic analytical algorithm for prostate VMAT. *PLoS One*. 2018;13(11):e0207232. doi:10.1371/journal.pone.0207232

67. Rana S, Cheng C. Radiobiological impact of planning techniques for prostate cancer in terms of tumor control probability and normal tissue complication probability. *Ann Med Health Sci Res*. 2014;4(2):167. doi:10.4103/2141-9248.129023

68. Selvaraj J, Uzan J, Baker C, Nahum A. Loss of local control due to tumor displacement as a function of margin size, dose-response slope, and number of fractions. *Med Phys*. 2013;40(4). doi:10.1118/1.4795131

69. Gulliford SL, Partridge M, Sydes MR, Webb S, Evans PM, Dearnaley DP. Parameters for the Lyman Kutcher Burman (LKB) model of Normal Tissue Complication Probability (NTCP) for specific rectal complications observed in clinical practise. *Radiother Oncol*. 2012;102(3):347-351. doi:10.1016/j.radonc.2011.10.022

70. Bentzen SM, Constine LS, Deasy JO, et al. Quantitative Analyses of Normal Tissue Effects in the Clinic (QUANTEC): An Introduction to the Scientific Issues. *Int J Radiat Oncol Biol Phys*. 2010;76(3 SUPPL.):3-9. doi:10.1016/j.ijrobp.2009.09.040

71. Bentzen SM, Parliament M, Deasy JO, et al. Biomarkers and Surrogate Endpoints for Normal-Tissue Effects of Radiation Therapy: The Importance of Dose-Volume Effects. *Int J Radiat Oncol Biol Phys*. 2010;76(3 SUPPL.):145-150. doi:10.1016/j.ijrobp.2009.08.076

72. Wu Q, Djajaputra D, Liu HH, Dong L, Mohan R, Wu Y. Dose sculpting with generalized equivalent uniform dose. *Med Phys*. 2005;32(5):1387-1396. doi:10.1118/1.1897464

73. Nahum AE, Uzan J. (Radio)biological optimization of external-beam radiotherapy. *Comput Math Methods Med*. 2012;2012. doi:10.1155/2012/329214

74. Thor M, Apte A, Deasy J, Muren L. Statistical simulations to estimate motion-inclusive dose-volume histograms for prediction of rectal morbidity following radiotherapy. *Acta Oncol (Madr)*. 2013;52(July 2012):666-675. doi:http://dx.doi.org/10.3109/0284186X.2012.720382

75. Sukumar P, Padmanaban S, Jeevanandam P, Syam Kumar S a, Nagarajan V. A study on dosimetric properties of electronic portal imaging device and its use as a quality assurance tool in Volumetric Modulated Arc Therapy. *Reports Pract Oncol Radiother J Gt Cancer Cent Poznań Polish Soc Radiat Oncol*. 2011;16(6):248-255. doi:10.1016/j.rpor.2011.08.001

76. Nyflot MJ, Cao N, Meyer J, Ford EC. Improved accuracy for noncoplanar radiotherapy : an EPID-based method for submillimeter alignment of linear accelerator table rotation with MV isocenter. *J Appl Clin Med Phys*. 2014;15(2):151-159. doi:10.1120/jacmp.v15i2.4682

77. LoSasso T, Chui CS, Ling CC. Physical and dosimetric aspects of a multileaf collimation system used in the dynamic mode for implementing intensity modulated radiotherapy. *Med Phys*. 1998;25(10):1919-1927. doi:10.1118/1.598381

78. Grządziel A, Smolińska B, Rutkowski R, Ślosarek K. EPID dosimetry – configuration and pre-treatment IMRT verification. *Reports Pract Oncol Radiother*. 2007;12(6):307-312. doi:10.1016/S1507-1367(10)60069-7

79. De Neve W, De Gersem W, Madani I. Rational Use of Intensity-Modulated Radiation Therapy: The Importance of Clinical Outcome. *Semin Radiat Oncol*. 2012;22(1):40-49. doi:10.1016/j.semradonc.2011.09.003

80. Cai YC, Ge Y, Bernard D, Turian J, Chu JCH. Detection of electron beam energy variations using a computed radiography system. *J Appl Clin Med Phys*. 2009;10(4):2911. http://www.ncbi.nlm.nih.gov/pubmed/19918220.

81. Bujold A, Craig T, Jaffray D, Dawson L a. Image-Guided Radiotherapy: Has It Influenced Patient Outcomes? *Semin Radiat Oncol*. 2012;22(1):50-61. doi:10.1016/j.semradonc.2011.09.001

82. Andersen ES, Muren LP, Sørensen TS, et al. Bladder dose accumulation based on a biomechanical deformable image registration algorithm in volumetric modulated arc therapy for prostate cancer. *Phys Med Biol*. 2012;57(21):7089-7100. doi:10.1088/0031-9155/57/21/7089

83. Fraass BA. The Impact of Treatment Complexity and Computer-control Delivery Technology on Treatment Delivery Errors. *Int J Radiat Oncol Biol Phys*. 1998;41(5):959-970.

84. Marks LB, Light KL, Hubbs JL, et al. The Impact of Advanced Technologies on Treatment

Deviations in Radiation Treatment Delivery. *Int J Radiat Oncol Biol Phys*. 2007;69(5):1579-1586. doi:10.1016/j.ijrobp.2007.08.017

85. Amols HI. New technologies in radiation therapy: ensuring patient safety, radiation safety and regulatory issues in radiation oncology. *Health Phys*. 2008;95(5):658-665. doi:10.1097/01.HP.0000326334.64242.46

86. Huang G, Medlam G, Lee J, et al. Error in the delivery of radiation therapy: Results of a quality assurance review. *Int J Radiat Oncol Biol Phys*. 2005;61(5):1590-1595. doi:10.1016/j.ijrobp.2004.10.017

87. Zelefsky MJ, Kollmeier M, Cox B, et al. Improved clinical outcomes with high-dose image guided radiotherapy compared with non-IGRT for the treatment of clinically localized prostate cancer. *Int J Radiat Oncol Biol Phys*. 2012;84(1):125-129. doi:10.1016/j.ijrobp.2011.11.047

88. Van Esch A, Depuydt T, Huyskens DP. The use of an aSi-based EPID for routine absolute dosimetric pre-treatment verification of dynamic IMRT fields. *Radiother Oncol*. 2004;71(2):223-234. doi:10.1016/j.radonc.2004.02.018

89. Trott KR, Doerr W, Facoetti A, et al. Biological mechanisms of normal tissue damage: Importance for the design of NTCP models. *Radiother Oncol*. 2012;105(1):79-85. doi:10.1016/j.radonc.2012.05.008

90. Thor M, Petersen JBB, Bentzen L, Høyer M, Muren LP. Deformable image registration for contour propagation from CT to cone-beam CT scans in radiotherapy of prostate cancer. *Acta Oncol (Madr)*. 2011;50(6):918-925. doi:10.3109/0284186X.2011.577806

91. Fraass BA, Moran JM. Quality, Technology and Outcomes: Evolution and Evaluation of New Treatments and/or New Technology. *Semin Radiat Oncol*. 2012;22(1):3-10. doi:10.1016/j.semradonc.2011.09.009

92. Bogdanich W, Rebelo K. A pinpoint beam strays invisibly, harming instead of healing. *New York Times*. http://www.nytimes.com/2010/12/29/health/29radiation.html. Published December 28, 2010.

93. Nunan C. Multileaf collimator and compensator for radiotherapy machines. 1989.

94. Källman P, Lind B, Eklöf A, Brahme A. Shaping of arbitrary dose distributions by dynamic multileaf collimation. *Phys Med Biol*. 1988;33(11):1291-1300. http://www.ncbi.nlm.nih.gov/pubmed/3231672.

95. Bortfeld T, Kahler DL, Waldron TJ, Boyer AL. X-ray field compensation with multileaf collimators. *Int J Radiat Oncol Biol Phys*. 1994;28(3):723-730. doi:10.1016/0360-3016(94)90200-3

96. Stein J, Bortfeld T, Dörschel B, Schlegel W. Dynamic X-ray compensation for conformal radiotherapy by means of. *Radiother Oncol*. 1994;32:163-173. doi:10.1016/0167-8140(94)90103-1

97. Burman C, Chui CS, Kutcher G, et al. Planning, delivery, and quality assurance of intensity-modulated radiotherapy using dynamic multileaf collimator: a strategy for large-scale implementation for the treatment of carcinoma of the prostate. *Int J Radiat Oncol Biol Phys*. 1997;39(4):863-873. doi:S0360-3016(97)00458-6 [pii]

98. Boyer a L, Yu CX. Intensity-modulated radiation therapy with dynamic multileaf collimators. *Semin Radiat Oncol*. 1999;9(1):48-59. doi:10.1016/S1053-4296(99)80054-X

99. Boyer A, Biggs P, Galvin J, et al. Basic Applications of Multileaf Collimators. *Med Phys*. 2001;(72):56. doi:10.1002/0471671746.ch4

100. Low DA, Mutic S. Abutment region dosimetry for sequential arc IMRT delivery. *Phys Med Biol*. 1997;42:1465-1470.

101. Zelefsky MJ, Fuks Z, Happersett L, et al. Clinical experience with intensity modulated radiation therapy (IMRT) in prostate cancer. *Radiother Oncol*. 2000;55(3):241-249. doi:10.1016/S0167-8140(99)00100-0

102. Chao KSC, Ozyigit G, Tran BN, Cengiz M, Dempsey JF, Low D a. Patterns of failure in patients receiving definitive and postoperative IMRT for head-and-neck cancer. *Int J Radiat Oncol Biol Phys*. 2003;55(2):312-321. doi:10.1016/S0360-3016(02)03940-8

103. Hall EJ, Wuu C-S. Radiation-induced second cancers: the impact of 3D-CRT and IMRT. *Int J Radiat Oncol*. 2003;56(1):83-88. doi:10.1016/S0360-3016(03)00073-7

104. Low DA, Mutic S. A commercial IMRT Treatment Planning Dose Calculation Algorith. *Radiat Oncol*. 1998;41(4):921-927.

105. Low DA, Moran JM, Dempsey JF, Dong L, Oldham M. Dosimetry tools and techniques for IMRT. *Med Phys*. 2011;38(3):1313-1338. doi:10.1118/1.3514120

106. Das IJ, Cheng C-W, Watts RJ, et al. Accelerator beam data commissioning equipment and procedures: Report of the TG-106 of the Therapy Physics Committee of the AAPM. *Med Phys*. 2008;35(9):4186-4215. doi:10.1118/1.2969070

107. Klein EE, Hanley J, Bayouth J, et al. Task Group 142 report: quality assurance of medical accelerators. *Med Phys*. 2009;36(9):4197-4212. doi:10.1118/1.3190392

108. Yin F-F, Wong J, Balter J, et al. *The Role of In-Room KV X-Ray Imaging for Patient Setup and Target Localization Report of AAPM Task Group 104*.; 2009.

109. Nath R, Biggs PJ, Bova FJ, et al. AAPM code of practice for radiotherapy accelerators: report of AAPM Radiation Therapy Task Group No. 45. *Med Phys*. 1994;21(7):1093-1121. doi:10.1118/1.597398

110. Herman MG, Balter JM, Jaffray D a, et al. Clinical use of electronic portal imaging: report of AAPM Radiation Therapy Committee Task Group 58. *Med Phys*. 2001;28(5):712-737. doi:10.1118/1.1368128

111. Mutic S, Palta JR, Butker EK, et al. Quality assurance for computed-tomography simulators and the computed-tomography-simulation process: report of the AAPM Radiation Therapy Committee Task Group No. 66. *Med Phys*. 2003;30(66):2762-2792. doi:10.1118/1.1609271

112. Keall PJ, Mageras GS, Balter JM, et al. The management of respiratory motion in radiation oncology report of AAPM Task Group 76. *Med Phys*. 2006;33(10):3874-3900. doi:10.1118/1.2349696

113. Murphy MJ, Balter J, Balter S, et al. The management of imaging dose during image-guided radiotherapy: report of the AAPM Task Group 75. *Med Phys*. 2007;34(10):4041-4063. doi:10.1118/1.2775667

114. Chiu-Tsao S-T, Schaart DR, Soares CG, Nath R. Dose calculation formalisms and consensus dosimetry parameters for intravascular brachytherapy dosimetry: recommendations of the AAPM Therapy Physics Committee Task Group No. 149. *Med Phys*. 2007;34(11):4126-4157. doi:10.1118/1.2767184

115. Clements JB, Baird CT, de Boer SF, et al. AAPM medical physics practice guideline 10.a.: Scope of practice for clinical medical physics. *J Appl Clin Med Phys*. 2018;19(6):11-25. doi:10.1002/acm2.12469

116. Fontenot JD, Alkhatib H, Garrett JA, et al. AAPM Medical Physics Practice Guideline 2.a: Commissioning and quality assurance of X-ray-based image-guided radiotherapy systems. *J Appl Clin Med Phys*. 2014;15(1):3-13. doi:10.1120/jacmp.v15i1.4528

117. Gress DA, Dickinson RL, Erwin WD, et al. AAPM medical physics practice guideline 6.a.: Performance characteristics of radiation dose index monitoring systems. *J Appl Clin Med Phys*. 2017;18(4):12-22. doi:10.1002/acm2.12089

118. Halvorsen PH, Cirino E, Das IJ, et al. AAPM-RSS Medical Physics Practice Guideline 9.a. for SRS-SBRT. *J Appl Clin Med Phys*. 2017;18(5):10-21. doi:10.1002/acm2.12146

119. Seibert JA, Clements JB, Halvorsen PH, et al. AAPM medical physics practice guideline 3.a: Levels of supervision for medical physicists in clinical training. *J Appl Clin Med Phys*. 2015;16(3):30-36. doi:10.1120/jacmp.v16i3.5291

120. Smilowitz JB, Das IJ, Feygelman V, et al. AAPM Medical Physics Practice Guideline 5.a.: Commissioning and QA of Treatment Planning Dose Calculations - Megavoltage Photon and Electron Beams. *J Appl Clin Med Phys*. 2015;16(5):14-34. doi:10.1120/jacmp.v16i5.5768

121. Smith K, Balter P, Duhon J, et al. AAPM medical physics practice guideline 8.a.: Linear accelerator performance tests. *J Appl Clin Med Phys*. 2017;18(4):23-39. doi:10.1002/acm2.12080

122. Cody DD, Fisher T, Gress DA, et al. AAPM Medical Physics Practice Guideline 1 . a : CT Protocol Management and Review Practice Guideline.

123. de los Santos LEF, Evans S, Ford EC, et al. Medical Physics Practice Guideline 4.a:

Development, implementation, use and maintenance of safety checklists. *J Appl Clin Med Phys*. 2015;16(3):37-59. doi:10.1120/jacmp.v16i3.5431

124. Boero IJ, Paravati AJ, Xu B, et al. Importance of radiation oncologist experience Among patients with head-and-neck cancer treated with intensity-modulated radiation therapy. *J Clin Oncol*. 2016;34(7):684-690. doi:10.1200/JCO.2015.63.9898

125. Gupta S, Tao L, Murphy JD, et al. Race/Ethnicity-, Socioeconomic Status-, and Anatomic Subsite-Specific Risks for Gastric Cancer. *Gastroenterology*. 2019;156(1):59-62.e4. doi:10.1053/j.gastro.2018.09.045

126. Gillespie EF, Matsuno RK, Xu B, et al. Geographic Disparity in the Use of Hypofractionated Radiation Therapy Among Elderly Women Undergoing Breast Conservation for Invasive Breast Cancer. *Int J Radiat Oncol Biol Phys*. 2016;96(2):251-258. doi:10.1016/j.ijrobp.2016.05.006

127. Ha D, Kerr J, Ries AL, Fuster MM, Lippman SM, Murphy JD. *A Model-Based Cost-Effectiveness Analysis of an Exercise Program for Lung Cancer Survivors Following Curative-Intent Treatment*.; 2019. doi:10.1097/phm.0000000000001281

128. Lopez Ramos C, Brandel MG, Steinberg JA, et al. The impact of traveling distance and hospital volume on post-surgical outcomes for patients with glioblastoma. *J Neurooncol*. 2019;141(1):159-166. doi:10.1007/s11060-018-03022-w

129. Bryant AK, Banegas MP, Martinez ME, Mell LK, Murphy JD. Trends in radiation therapy among cancer survivors in the United States, 2000-2030. *Cancer Epidemiol Biomarkers Prev*. 2017;26(6):963-970. doi:10.1158/1055-9965.EPI-16-1023

130. Coe TM, Fero KE, Fanta PT, et al. Population-Based Epidemiology and Mortality of Small Malignant Gastrointestinal Stromal Tumors in the USA. *J Gastrointest Surg*. 2016;20(6):1132-1140. doi:10.1007/s11605-016-3134-y

131. Murphy JD, Sandler D, White AJ, O'Brien KM. Severe acne and risk of breast cancer. *Breast Cancer Res Treat*. 2019;177(2):487-495. doi:10.1007/s10549-019-05302-z

132. Roach M, Nam J, Gagliardi G, El Naqa I, Deasy JO, Marks LB. Radiation Dose-Volume Effects and the Penile Bulb. *Int J Radiat Oncol Biol Phys*. 2010;76(3 SUPPL.). doi:10.1016/j.ijrobp.2009.04.094